





S First Author 1978-2005 Scheer Schupp Shafer Smith Stroup Stuart Sung Swalen Hupfer Ringsdorf van wagene...

View Arrange By Action Share Edit Tags

Search

	Name	Date Modified	Size
NCE_WITHO...	 Scheer 1995 Intelli...terials Education.pdf	Feb 10, 2006, 9:17 PM	570 KB
	 Scheer 1995 Repor...shape memory .pdf	Nov 10, 2018, 2:31 PM	1 MB
rop	 Schupp Hupfer 198...genen ringsdorf.pdf	Jun 4, 2006, 5:10 PM	1.6 MB
ly Files	 Shafer 2005 Weather in West.pdf	May 13, 2006, 2:47 PM	219 KB
downloads	 Smith 1975 Polyme...n Hill Hibbs Kim.pdf	Oct 31, 2017, 6:13 PM	868 KB
ad Drive	 Smith 1982 Contac...Angles bowman .pdf	Apr 3, 2006, 11:16 AM	1.8 MB
ications	 Smith 1982 Oxidati...e doyle gregonis.pdf	Jun 4, 2006, 6:13 PM	1.4 MB
ktop	 Smith 2001 Creatin...inecense Conf 2001	Jan 5, 2018, 10:32 AM	579 KB
uments	 Stroup 1992 Elasticity Map Preprint.pdf	Apr 3, 2006, 11:46 AM	1.1 MB
oh's MacBook	 Stroup 1993 SFM Preprint.pdf	Apr 3, 2006, 11:36 AM	1.1 MB
	 Stroup 1995 Polym...lady Radmacher.pdf	Nov 11, 2018, 9:30 PM	495 KB
	 Stroup Pungor __ AF...lymer Lea Hlady.pdf	Nov 11, 2018, 1:52 PM	2 MB
	 Stuart 1994 Albumi...lished deceased.pdf	Nov 11, 2018, 9:25 PM	2.7 MB
	 Sung 1978 Note Wa...gregonis russell.pdf	Jun 4, 2006, 6:18 PM	501 KB
	 Sung 1981 NMR H...MA gregonis jhon.pdf	Oct 12, 2006, 8:04 PM	1.3 MB
	 Sung 1981 NMR PHEMA.pdf	Jul 7, 2006, 10:00 PM	2.1 MB
	 Sung 1984 Water S...a jhon gregonis .pdf	Jun 4, 2006, 6:26 PM	1.4 MB
	 Swalen 87 Report...sraelachvili rabolt .pdf	Jun 4, 2006, 6:49 PM	8.8 MB

# Applying "Intelligent" Materials to Materials Education

R. J. SCHEER

*Protein Solutions, Inc., 350 West 800 North, Suite 218, Salt Lake City, UT 84103*

J. D. ANDRADE\*

*University of Utah, 2480 MEB, Salt Lake City, UT 84112*

**ABSTRACT:** A very large number of science and engineering courses taught in colleges and universities today do not involve laboratories. Although good instructors incorporate class demonstrations, hands-on homework, and various teaching aids, including computer simulations, the fact is that students in such courses often accept key concepts and experimental results without discovering them for themselves. The only partial solution to this problem has been increasing use of class demonstrations and computer simulations.

We feel strongly that many complex concepts can be observed and assimilated through experimentation with properly designed materials. We propose the development of materials and specimens designed specifically for *education purposes*.

"Intelligent" and "communicative" materials are ideal for this purpose. Specimens which respond in an observable fashion to new environments and situations provided by the student/experimenter provide a far more effective materials science and engineering experience than readouts and data generated by complex and expensive machines, particularly in an introductory course. Modern materials can be designed to literally communicate with the observer. Although some such materials can be obtained from commercial and research sources and are suitable for experiencing and learning certain materials phenomena and behavior, there has been no concerted effort to develop materials specifically for education application.

We are embarked on a project to develop a series of explorations we call the Labless Labs® utilizing various degrees and levels of intelligence in materials. It is expected that such Labless Labs® would be complementary to textbooks and computer simulations and would be used to provide a *reality* for students in courses and other learning situations where access to a *laboratory* is non-existent or limited. Our initial project will center around a Labless Lab® for Polymer Science.

## BACKGROUND AND RATIONALE

UNDERGRADUATE students in many science and engineering courses in the United States have little or no laboratory experience in such courses. The labless science and engineering course has become a very common feature in higher education. Although outstanding instructors attempt to overcome this deficiency with the use of classroom demonstrations, discovery-based homework assignments, class projects, and computer simulations, many instructors may not have the time or inclination to utilize these tools, particularly in relatively large lecture environments. Labs are also not generally available for correspondence, distance learning, or TV/video courses. We feel there is a need for *small, inexpensive, completely self contained laboratories* which can supplement existing textbooks.

The several hundred undergraduate engineering programs in the country nearly all teach a course in materials science, most with a significant polymer component, and many of them teach a separate course in polymer materials. In addition,

advanced high school chemistry or physics courses often include a significant polymer materials component. There are on the order of 40,000 introductory materials science texts sold annually in the U.S. and Canada [1,2]. The National Science Teachers Association has a high school supplement text for polymer science which is very popular with high school teachers throughout the country.

Although many of these texts come with instructions for experiments and demonstrations, in reality these are rarely performed due to the difficulty in obtaining the materials in a timely and inexpensive fashion.

The Exploratorium, an interactive, hands-on science museum in San Francisco, and Klutz Press in Palo Alto, California, recently teamed up to produce a volume called *The Explorabook*, in which a range of hands-on, discovery-based experiments were incorporated into a small inexpensive book [3]. *The Explorabook* is the largest selling children's science book in the United States today. In Great Britain, the Science Museum of London teamed up with Watts Books to publish another popular interactive book called *The Most Amazing Pop-Up Science Book*, in which several hands-on explorations center around basic science

\*Author to whom correspondence should be addressed.

concepts [4]. These demonstrate the need for challenging scientific materials by the general public. That need is also present in higher education.

The recent Project 2061 report of the American Association for the Advancement of Science (AAAS) states [5]:

For teachers to be able to bring all students to the level of understanding and skill proposed in this report, they will need a new generation of books and other instructional tools. . . . Textbooks and other teaching materials in current use are—to put it starkly—simply not up to the job.

Although there has been major soul searching and even restructuring of education throughout the nation and a growing emphasis on hands-on, discovery, experiential activities, this renaissance has not yet significantly penetrated higher education. Science and engineering education in many institutions is still highly didactic in nature, relying on computer simulation and visualization to provide an "experimental" experience for students. There are two major problems with this approach:

1. Motivation—students know that there is a difference between virtual reality and real reality.
2. Students otherwise excellently prepared for college and university work often lack experience in dealing with simple tools, in working with their hands, and in making simple common sense observations and deductions.

This is due to two major features of our society:

1. There is no need for major segments of the society to learn how to use simple tools or to do simple technical manipulations with their hands. We are a service oriented society—nearly everything is done for us. We have a whole generation of students, and even many of their parents, who lack simple tool utilization and basic observational skills.

We have seen and taught university undergraduates with A — grade point averages who literally do not know the difference between a Phillips head and a slot head screwdriver, or what a crescent wrench is. We have the same problem in graduate school—particularly with students from the Orient whose background is largely based on theory and problem-solving in the absence of hands-on or experimental experience.

2. The public education system in this country, up until very recently, has not emphasized experiential, common sense, hands-on approaches to situations and problems. As indicated earlier, that situation is of course changing and is changing very rapidly, but the college age generation that has been through that system needs help.

Another important area of education is the field of distance learning [6–9]. There is great interest in making our educational system available inexpensively to a much wider segment of society. Through the new national information infrastructure there will be a proliferation of courses and even full degree programs available via our televisions and

computer terminals. The Public Broadcasting Service (PBS) has developed a new program called "Going the Distance". It will let students complete an associate of arts degree by watching courses on television, and is scheduled to start the fall of 1994 at 60 colleges served by 22 PBS stations [6]. Several states, including Utah, are strongly committed to the development of distance learning for secondary and post-secondary education. Governor Mike Leavitt, Utah, has stated: "I challenge you to make education an activity that is not bound by buildings, place, or space". We call this "Education and Science without Walls". Although there is much that can be done in these arenas with excellent lecturers and presenters, with outstanding video segments, and with computer activities and virtual reality simulations, the bottom line is the same as discussed briefly above. Without actual hands-on, experiential, *real reality* experience, the topics and concepts presented will never be fully internalized—will never become "common sense" for the individuals involved. A Labless Lab® approach to such real reality will facilitate such internalization, such experience, and such learning.

## POLYMERIC MATERIALS

Plastic and polymeric materials are ubiquitous in modern society. A significant fraction of chemists, physicists, and engineers work in polymer related industries or utilize polymers in scientific and engineering activities. Polymer materials are unique because of their macromolecular nature. Large molecular weight molecules behave, in general, very differently from low molecular weight molecules and molecular or atomic solids. Many of the rules of thumb learned in elementary physics and chemistry appear to not apply in the case of polymeric materials.

Most students come into polymer courses with various concepts and preconceptions which lead them to conclude that the behavior and properties of polymers are counter intuitive. It is therefore important that they fully discover and observe the properties and behavior of polymeric materials for themselves.

It is appropriate to begin our Labless Lab® effort with polymeric materials because they are readily available for a wide variety of applications and because they exhibit a range of phenomena which are very easy to observe, experience, and discover.

There is considerable interest in effective polymer education [10]. The American Chemical Society (ACS) Division of Chemical Education often includes polymer related articles in its *Journal of Chemical Education* [11,12] and in its sessions at the American Chemical Society annual meetings. The ACS also has a Polymer Education Committee, as does the Society of Plastic Engineers (SPE). Polymer education is also of interest to the American Institute of Chemical Engineers (AIChE) and the Materials Research Society (MRS). There is a Polymer Education Center at the

University of Wisconsin, Steven's Point and a Polymer Education Newsletter [10]. The Institute for Chemical Education at the Department of Chemistry at the University of Wisconsin, Madison, is also active in providing a variety of educational materials for discovery based chemistry and polymer education [13].

These activities are all helpful and indeed have greatly stimulated this project. However, the typical instructor, particularly in relatively large enrollment classes, often does not have the time or the inclination to assemble the materials, components, and equipment necessary to put together an effective discovery laboratory, particularly if the

class is a lecture only course, which is typical for many introductory material science and polymer science courses.

### "COMMUNICATIVE" MATERIALS

"Communicative" materials are those which alter their properties or characteristics when subjected to a perturbation by the observer. The material's response to the perturbation is readily observed without recourse to any instruments or apparatus. The observer's own senses are sufficient. There are, of course, many examples from com-

Table 1. Major topics in a one quarter (10 weeks) undergraduate course, *Introduction to Polymer Science and Polymeric Materials (MSE 519, University of Utah)* [16].

Topic	Key Concepts	Conventional Materials/Methods	Communicative Materials
Polymer applications	Wide range of properties and compositions	Examples from consumer products and engineering devices and machines	None
Macro molecules	High molecular weights, packing, entanglement	Individual examples	MW gradient comonomer gradient
Polymerization and copolymerization	Properties = $f$ (composition, molecular weight)	Individual examples	MW gradient comonomer gradient
Morphology and structure	Packing, ordering, melting	Individual examples, molecular simulation	Crystallization, annealing, ordering as $f(T, t)$ , composition gradient
Block copolymers	Phase separation, incompatibility	Blends, diblock-triblock—copolymers	Blend gradient
Solubility and solutions	Solution interactions and thermodynamics	Individual examples—MW, polarity, temp.	Temp. gradient—LCST composition gradient
$T$ - $t$ effects	$T$ - $t$ superposition; effect of properties on $T$ and $t$	Specific examples	$T_g$ gradient/ composition gradient
Cross-linking	Networks, elasticity, viscoelasticity	Individual examples	Cross-link gradient; mechanical response
Additives	Plasticization	PVC-plasticizer—individual samples	Plasticizer gradient, $T_g$ gradient
Surface properties	Wetting/surface modifi.	Individual examples	Wetting gradients, capillarity
Processing	Fiber formation, film molding	Thermoplastic, thermoset, $T$ and processing	$T_g$ gradient, cross-link gradient composition gradient
Adhesives	Adhesion/surface properties	Hi and low energy polymers, contact angle, peel tests	Surface property gradient
Electrical fields	Conductivity, ionization, solubility	Mainly conductive polymers	Ionogenic polymers and biopolymers; electrically responsive polymers; $T_g$ gradient; LCST
Biopolymers	Structural proteins	Silk, collagen	Polypeptide gradients
Environmental issues	Cost, energy, solid waste, biodegradation	Specific examples, classes, stability	Composition/ morphology gradients; stability



mon, everyday practice: the change in color or optical density of a liquid crystal thermometer or a liquid crystal based computer screen; the change in hardness/softness and other mechanical properties of polymers due to changes in temperature; the polymerization or setting up of glues, adhesives, and caulks; the elasticity and extension of rubber bands; etc. Although these are all useful, there are many opportunities for enhancing the educational content of polymeric materials through the design and development of materials which can be used to directly experience key concepts and phenomena (Table I).

Table I presents key concepts and topics in a typical introductory polymer science course, together with a set of Labless Lab<sup>®</sup> experiments.

Materials, polymers included, are usually developed for commercial application and for meeting some particular consumer or industrial need. We are *developing materials specifically for science education*. With these special materials the student can *directly observe* physical and chemical parameters and materials behavior. This is possible by utilizing *gradient materials* for example [14]. We have been utilizing gradient surfaces for many years in our study of the surface properties and biocompatibility of medical polymers [15-17]. We are now using these surfaces in biomaterials courses [18], because integration of materials and devices with surrounding tissues and the biocompatibility of materials and devices tends to be a strong function of the surface properties of the materials (surface free energy, polarity, hydrophobicity, charge density, roughness, and surface dynamics). These properties play important roles in various biocompatibility situations [19,20].

Gradients are used in particular areas of research. For example, biochemists commonly use gels with a gradient in cross link density, thereby developing a gradient in porosity. This is widely used in electrophoresis for protein analysis and separation [21]. Polyelectrolyte gradient gels are used in electric fields to produce a gradient in pH, which allows the separation of macromolecules on the basis of net charge [21]. Gradients in surface to volume ratio have been used to study concentration and mass transport dependent effects [22,23].

What does one do with these novel and unique polymer samples for science education? Table I presents a typical topic outline for an Introduction to Polymer Materials course. This represents Materials Science and Engineering 519, the required polymer course for Materials Science majors at the University of Utah [24]. This is the first and last polymer materials course for those students who do not go on into the polymer science track.

The first column in Table I presents the general topic, followed by a column of commercial or conventional polymer examples, followed by a column of the special materials we are developing. The table indicates how the new materials, as well as existing materials, are used by students to discover and observe various material concepts, properties, and behavior.

## PROJECT RESULTS

### Temperature Gradient Device

We tested several designs of temperature gradient devices. The heat sources were semiconductor resistors powered by an adjustable power supply. The heating substrates were aluminum plates machined to varying geometries. Surface temperatures were recorded using thermocouples, an infrared detector, and thermochromic liquid crystals (TLCs).

This device produces a surface temperature gradient from a hot end of 60°C to a cool end of 30°C over a distance of approximately 8 centimeters. Our intent was to generate a linear gradient using a single heat source and a nonlinear heat sink. For a uniform geometry with a single heat source the temperature decreases with the log of the distance from the heat source [25].

$$T \approx \ln(d)$$

where

$T$  = temperature

$d$  = distance from heat source

By adjusting the heating substrate's geometry, the temperature decrease was flattened to approach a linear gradient. During several trials, data taken from the aluminum surface after heating with 0.7 watts of power indicated a steady-state temperature of 60°C directly above the heat source, a temperature of 45°C a distance of 4 cm from the heat source and a temperature of 30°C at a distance of 8 cm from the heat source. The ambient temperature was 24°C. The geometry used is shown in Figure 1.

Explorations developed for the temperature gradient include temperature dependent behavior of polymers such as solubility, rigidity, hardness, and stress/strain relaxation.

### Homopolymer $T_g$

We selected several common homopolymers with  $T_g$ s in the range of -120°C to 105°C. They are low density

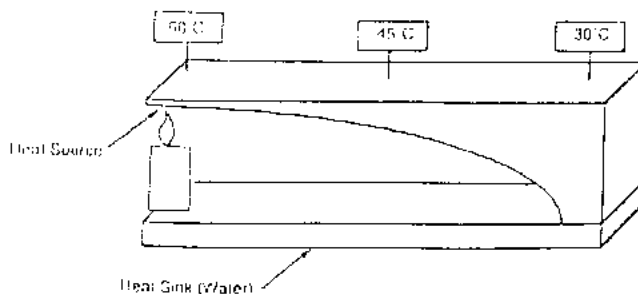


Figure 1. Schematic of temperature gradient profile geometry. The high temperature end is the narrow cross section portion with the heat source. The low temperature end is the wide cross section with the water serving as a large heat sink.

### Cross-Link Gradient

We evaluated several methods to produce cross-link gradient polymers. Cross-link density gradient polymers are routinely formed and utilized in electrophoresis studies at the University of Utah's Center for Biopolymers. Our studies of the acrylamide gel with a cross-link gradient show that this gradient will demonstrate the effect of cross-linking on mechanical properties without requiring sophisticated laboratory equipment other than human tactile senses.

Cross-link gradients can be formed in another way. Photocrosslinking occurs in three polymer system types: (a) those bearing functional groups which crosslink themselves under photoirradiation; (b) those mixed with crosslinkers; and (c) those polymerized in the presence of di- and poly-functional monomers. In an effort to decrease the risk of contact with small molecules (monomers and crosslinkers) we will develop a system utilizing the first of these systems, polymer chains which themselves contain crosslinking groups [30-32].

Two methods of creating a *gradient* system are considered, (a) nonuniform distribution of crosslinkable groups and (b) nonuniform light irradiation. Also, so that light energy will be available uniformly to all portions of the polymer the geometry should be that of a thin film. (See Figure 4.)

Likely systems include polyethylene, polyvinyl alcohol, polystyrene and other systems with carbon-carbon double bonds.

Explorations for this system will include crosslinking several polymer samples using light chemical means. The student can feel the effect that crosslinking has on the mechanical properties of polymers.

### Copolymer Gradients

We are using methacrylate homopolymers of varying alkyl chain length to demonstrate the effect of side chain length or internal plasticization on  $T_g$  and thus on the physical and mechanical properties [33]. Two comonomer gradients were produced by pouring one type of partially cured

monomer into a second partially cured monomer of lesser density. Two different gradient systems were prepared and evaluated: polymethyl methacrylate/polyhexyl methacrylate (PMMA/PHMA) and polymethyl methacrylate/polyhydroxyethyl methacrylate (PMMA/PHEMA). The PMMA/PHMA gradients exhibited a gradient in stiffness at room temperature (23°C); the PMMA end with a  $T_g$  of 105°C was rigid and the PHMA end with a  $T_g$  of -35°C was soft. This gradient demonstrates the effect of sidechain bulk and mobility on the backbone chain stiffness and bulk polymer stiffness. The PMMA/PHEMA gradients exhibited a water absorption gradient. At equilibrium in water, the PMMA end kept its original shape and was rigid and collapsed while the PHEMA end swelled and became flexible. This gradient demonstrates the effect of sidechain hydrophilicity and hydrophobicity on water absorption, as well as the effect of small molecules on the flexibility and stiffness of a polymer.

Further efforts in this area will center around creating a more uniform gradient and simplifying the mixing procedure. Probable procedures include mixing the monomers with a gradient pumping system. (See Figure 5.) This system of generating a gradient will produce a more uniform and linear gradient of materials properties. After speaking with a representative of Gilson, Inc. (maker of several lines of peristaltic pumps), it was suggested that we use computer control to develop a reproducible pattern of gradient gels. We agree and intend to develop a program to incrementally adjust pumping rates to produce the most useful and observable gradient properties.

Explorations utilizing these samples include water uptake and stiffness measurements, similar to the characterization studies performed for the evaluation of these polymer gradients. Neither of these explorations involve sophisticated equipment other than the human senses of sight and touch. They plainly demonstrate the effect of sidechain chemistry on the mechanical and chemical behavior of the polymer system.

### Ionic/Temperature Responsive Polymers

Hydrophilic polymer gels absorb water and swell; hydrophobic polymer gels expel water and collapse. By reversibly switching a polymer's characteristics from hydrophilic to hydrophobic we can control the amount of water uptake. Research to utilize this phenomenon for drug delivery is ongoing at the Center for Controlled Chemical Delivery at the University of Utah's Research Park. In consultation with the Center, we are developing a polymer system that demonstrates the effect of hydrophilicity and hydrophobicity on water absorption. Currently, we are concentrating on systems which utilize switching in response to changes in temperature, electric field, pH, and water ion content.

Polymer gel networks which form as the result of hydrogen bonding can be disturbed with the use of an electric

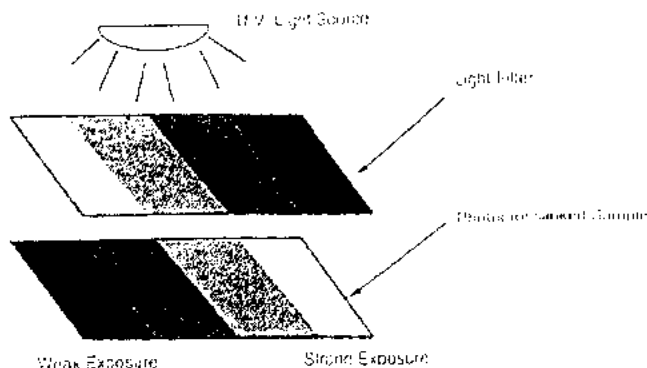


Figure 4. Depiction of nonuniform light irradiation for induction of gradient in crosslink density.

polyethylene (LDPE), high density polyethylene (HDPE), polypropylene (PP), 15% plasticized polyvinyl chloride (PVC), polyethylene terephthalate (PETE), polystyrene (PS), and unplasticized PVC.

The homopolymers that were chosen for the Labless Lab<sup>®</sup> are listed in Table 2.

These were chosen based on their glass transition temperatures and use as common packaging materials [26-28]. Students are thus able to compare common packaging materials with those samples included in the kit.

Samples of these polymers were placed on the temperature gradient device described above to demonstrate the change in properties when a polymer is heated above its  $T_g$ . (See Figure 2.)

In explorations of this type, the student can see and feel the change in material properties with temperature. The glass transition temperature is particularly evident and will be different for each polymer studied.

### Plasticizer Gradient

We successfully refined a technique which directly demonstrates the effect of low molecular weight molecules on the mechanical behavior of polymeric materials. Several techniques for DOP (di-octylphthalate) plasticizer extraction of 35% plasticized PVC were tested. Long strips of extruded PVC with a 35% by weight DOP plasticizer were treated in a methanol extraction bath. The strips were suspended in a flask which was closed except for a small inlet tube for the addition of the methanol solvent. Methanol, which dissolves DOP but not PVC, was added to the flask while stirring. The net effect was that the bottom of the plasticized PVC was immersed in methanol for 72 hours, while the top of the plasticized PVC was never exposed to methanol. These techniques were based on preliminary work performed by Mike Goodwin [29]. (See Figure 3.)

After drying the samples to remove residual methanol, the strips were subjected to a series of mechanical tests to measure their relative hardness and rigidity. During examination of the samples we used drape tests as well as indentation testing to determine the effects of the plasticizer on

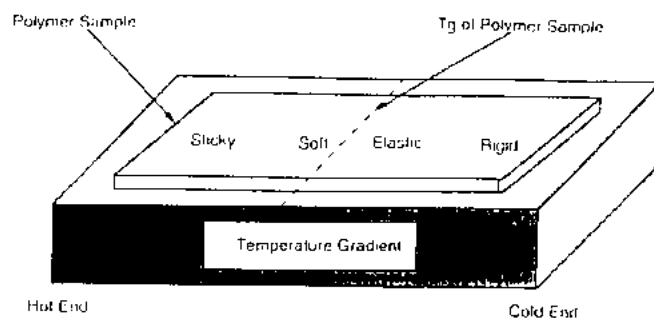


Figure 2. Schematic explaining the mechanical behavior of a generic polymer sample placed on the temperature gradient device. This exploration will demonstrate the different thermal behaviors of various common polymers, as well as show the range of mechanical properties near a polymer's  $T_g$ .

the mechanical properties of the polymer. Other tests included placing the samples, or pieces of them, on a uniform temperature portion of the temperature gradient. The softening temperature of each portion of the gradient samples was determined and related to the amount of plasticizer present in the samples. These explorations demonstrated that higher concentrations of plasticizer led to lower stiffness and hardness, as well as lower glass transition temperatures than the PVC with lower concentrations of plasticizer. Again, without sophisticated equipment, the student can study the effects of low molecular weight compounds on the mechanical and thermal behavior of a polymer.

These gradients demonstrate an observable difference in polymer stiffness and elasticity. Several different experiments were performed using these samples. We utilized a "droop" test, where the sample was held rigidly along its gradient edge and thin sections of the strip were cut and allowed to drape under the force of gravity. Using this method, the sample droops more where a larger concentration of plasticizer is present and less where the sample is more rigid with less plasticizer.

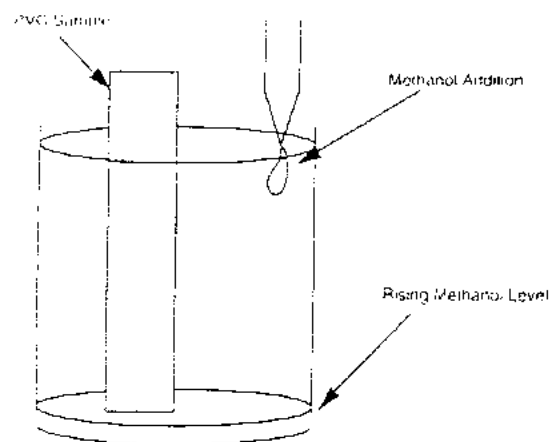
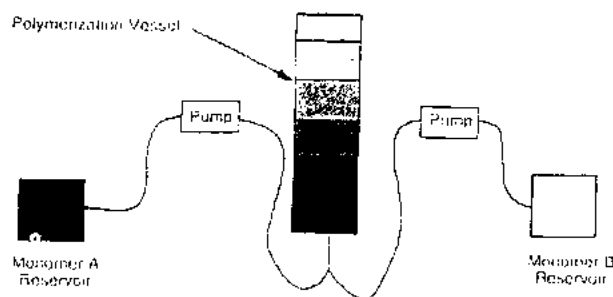


Figure 3. Schematic of the DOP extraction procedure. Methanol is slowly added over a period of three days until it reaches the top of the sample. The bottom of the sample is in methanol for 72 hours, the top is in methanol for 0 hours.

Table 2. List of common homopolymers, their  $T_g$  and source.

Polymer	Glass Transition Temperature	Common Source
Low density polyethylene	-120°C	Lawn bags
Polypropylene	-20°C	Yogurt containers
High density polyethylene	-20°C	Milk jugs
Polyethylene terephthalate	70°C	Soft drink bottles
15% plasticized polyvinyl chloride	60°C	Credit cards
Unplasticized polyvinyl chloride	105°C	Sewer pipes
Polystyrene	100°C	Compact disc cases



**Figure 5.** Schematic of proposed monomer pumping system. The pump for monomer "B" will begin transferring the less dense fluid, slowly pump "A" will begin to transfer the more dense monomer. During final stages only pump "A" is transferring monomer.

field. An example of this phenomena is described by Sung Wan Kim et al. They describe how the network polymer of Poly(ethyloxazoline) (PEOx) and Poly(methacrylic acid) (PMAA), which are held together with hydrogen bonding below a pH of 5.0 and released from their hydrogen bonding above pH 5.4, dissolves under the influence of an electric current [34–36].

Poly(*N*-isopropylacrylamide) (PiPAAm) exhibits obvious hydration-dehydration changes in water in response to relatively small changes in temperature. PiPAAm exhibits a lower critical solution temperature (LCST) near 32°C [37–40]. This behavior is shown schematically in Figure 6. This is best demonstrated by dissolving a fraction of a gram of PiPAAm in several milliliters of water and placing a few drops in each well on a row of culture plates. When this row is placed along a temperature gradient, the higher temperature wells will cloud as the polymer precipitates out of solution. (See Figure 7.)

Explorations for these polymer samples include studying the effects of temperature, pH, and electric field on polymer swelling and solubility. By studying how each of these environmental factors affects the polymer, hypotheses can be made regarding why changes in outside conditions affect the chemistry of the polymer chain.

### Surface Property Gradient

The gradient surface is one in which a distinct surface property is varied continuously from one end of the sample to the other [41]. Wettability gradients were generated on

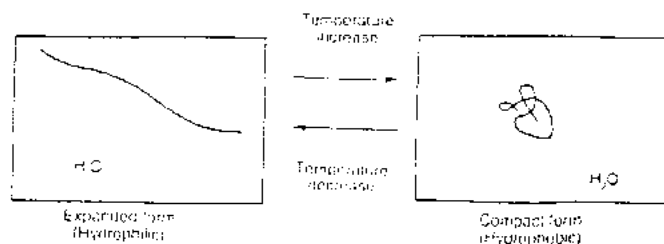


**Figure 6.** Temperature-responsive hydration-dehydration changes for poly (*N*-isopropylacrylamide) in aqueous media.

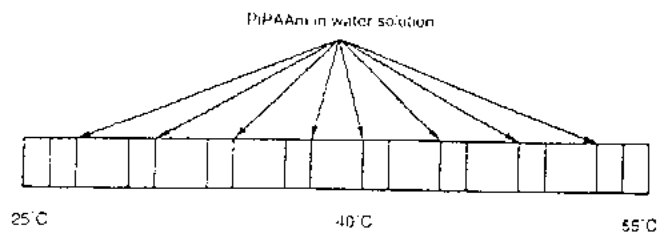


**Figure 7.** Behavior of PiPAAm(aq) over a range of temperatures. Darkened fields represent wells containing solution at different degrees of cloudiness.

samples of polystyrene using an oxygen plasma field [42–45]. The gradients were formed by placing a plasma barrier/mask along one half of the polystyrene surface and plasma treating the entire sample for 20 seconds. Because the oxygen plasma is a gas, some of it will travel under the mask and generate polar groups across the surface for a small distance [43]. (See Figure 8.) The schematic representation of the intended treatment result is shown in Figure 9. During wettability measurements the treated end was completely wetted with a thin film of water, and the untreated end allowed water to bead up considerably. Other measures of wettability included a capillary effect along the length of the treated surfaces. The treated end allowed water to wick up approximately two centimeters while the untreated end only allowed the water to wick up approximately 0.5 centimeters. These samples demonstrate dipole-dipole bonding and the difference between bulk and surface properties of a material.

The treated end, with more polar surface groups, demonstrates a lower contact angle with water than the untreated end showing mostly nonpolar surface groups. When drops of water are placed on the surface, they behave as shown in Figure 10.

Explorations performed with this sample center around observable differences between the ends of the gradient sample. After using the water droplet test and a capillarity test to measure wettability, we are confident that the student can witness on their own the differences in wettability and calculate the ratios of hydrophobic/hydrophilic groups on the polymer surface.

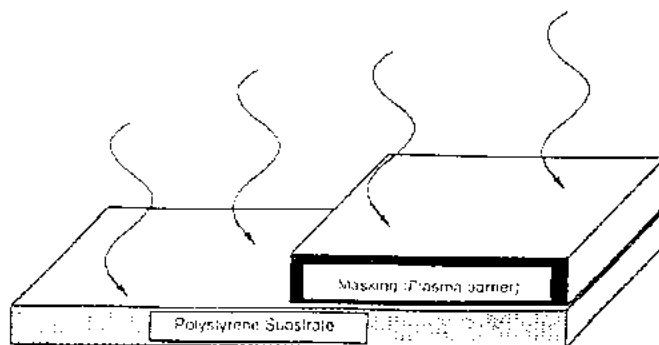


**Figure 8.** Schematic of polystyrene substrate with masking barrier to prevent surface modification from the plasma treatment.

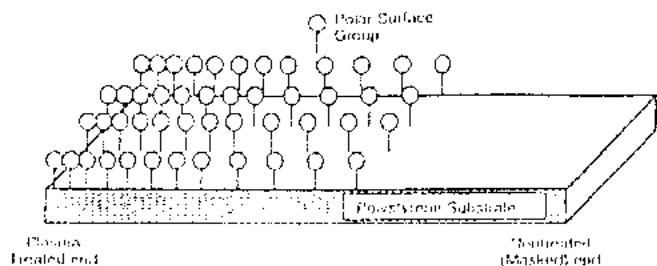


Figure 9. Descriptive image of hydrophobic polystyrene surface with new polar hydrophilic surface groups after  $O_2$  plasma treatment.

## CONCLUSION/SUMMARY

A Labless Lab<sup>®</sup> for polymer materials is well on its way to becoming a real reality. Preliminary versions are being tested in a course at the University of Utah. A field test version keyed to several major textbooks in polymer science and engineering should be available by summer, 1995. Limited commercial distribution is expected in early 1996.

The goal is to develop a Labless Lab<sup>®</sup> in polymer materials which could be made available in classroom quantities with prices comparable to those of existing textbooks, i.e., in the \$40–\$60 range per unit. It is anticipated that there will be two such products, an introductory polymer materials version and a more advanced version.

We are interested in learning of additional materials and phenomena which could be incorporated into the Labless Lab<sup>®</sup> in a very inexpensive manner. Labless Labs<sup>®</sup> in other appropriate science and engineering courses are also under development.

The Labless Lab<sup>®</sup> is a registered trademark of Protein Solutions, Inc., Salt Lake City, Utah.

## ACKNOWLEDGEMENTS

This material is based upon work supported by the National Science Foundation under SBIR award number III-9361652. Any opinions, findings and conclusions or recommendations expressed in this publication are those of the

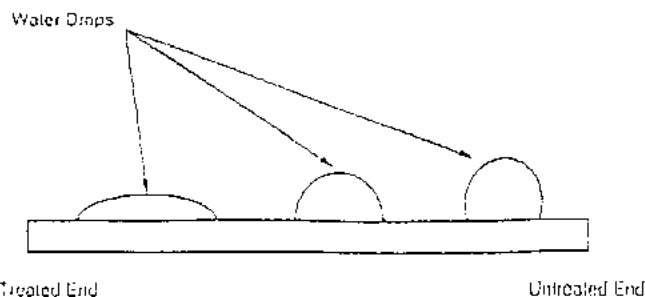


Figure 10. Schematic of water drops on polystyrene plasma treated gradient surface.

author and Protein Solutions, Inc. and do not necessarily reflect the views of the National Science Foundation.

Our initial work in this area was funded at the University of Utah by a small grant from the American Chemical Society's Division of Polymer Chemistry, Polymer Education Program. The application of the concept to a basic polymer materials science course at the University of Utah was funded by the University of Utah Teaching Committee Grant. Most of the existing work on the project is focused at Protein Solutions, Inc. in Salt Lake City, a science education products company, and funded by a small business innovation research (SBIR) grant from the National Science Foundation. J. D. Andrade acknowledges discussions on these topics with K. Caldwell, W. Callister, L. Feng, V. Hlady, and T. Matsuda.

## REFERENCES

- Deanin, R. B. and R. R. Martin. 1994. "Survey of Polymer Education in U.S. Colleges and Universities", Preprints, *Polymer Sci. and Engrg.* (ACS), pp. 45–56.
- Callister, W. 1991. *Materials Science & Engineering an Introduction*, 2nd Ed. Wiley: Personal Communication.
1991. *Explorabook*. Palo Alto, CA: Klutz Press.
- Young, J. 1994. *The Most Amazing Pop-Up Science Book*. London: Watts Books.
- Rutherford, J. 1988. *Project 2061: Science for All Americans*. Washington, DC: American Association for the Advancement of Science, p. 14.
- Toby Levine Communications, Inc. Bethesda, Maryland. 1994. *Going the Distance: A Handbook for Developing Distance Degree Programs Using Television Courses and Telecommunications Technologies*. Annenberg/CPIB Project and PBS Adult Learning Service, Corporation for Public Broadcasting and Public Broadcasting Service.
- Watkins, B. T. 1994. "Uniting North Dakota", *Chronicle of Higher Ed.*, A17 (August 10).
- Frans, J. 1994. "The Academic Potential of Distance Learning", 3:53.
- Bennett, J. G. 1994. "The Need for Continuing Education", *Chemical and Engineering News*, (July 11):36.
- Droske, J. 1993. *Polyed Information Center and Polymer Education Newsletter*, Dept. of Chemistry, University of Wisconsin-SP, Stevens Point, WI 54481.
- Seymour, R. B. 1982. "Recommended ACS Syllabus for Introductory Courses in Polymer Chemistry", *J. Chem. Educ.*, 59:652.
- Mathias, L. J. 1983. "The Lab for Intro. Polymer Courses", *J. Chem. Educ.*, 60:990.
- Institute for Chemical Education, Dept. of Chemistry, University of Wisconsin-Madison, 1101 University Ave., Madison, WI 53706-1396.
- Hoffman, A. S. 1991. "Environmentally Sensitive Polymers and Hydrogels 'Smart' Biomaterials", *MRS Bulletin*, (September):42–46.
- Hlady, V. 1988. "Hydrophobicity Gradient on Silica Surfaces", *Colloids and Surfaces*, 33:185–190.
- Golander, C. G. 1989. "... Surfaces with a Hydrophobicity Gradient", *Colloids and Surfaces*, 34.
- Lee, J. H. 1991. "Wettability Gradient Surfaces Prepared by Corona Discharge", *Trans. Soc. for Biomaterials*, 17:133.
- Andrade, J. D. and H. B. Lee. 1992. "Surface Property Gradients for Biomaterials Education", *Abstracts, Fall Meeting of Biomed. Engrg. Soc.*, 3.
- Andrade, J. D., ed. 1976. *Hydrogels for Medical and Related Applications*, ACS Symp. Series 31. American Chemical Society.
- Andrade, J. D., ed. 1985. *Surface and Interfacial Aspects of Biomedical Polymers*, Vol. 1. Plenum, especially Chapters 2,3.

21. Ho, C-H., V. Hlady, G. Nyquist, J. D. Andrade and K. Caldwell. 1991. "Proteins Studied by High-Resolution Two-Dimensional Gel Electrophoresis", *J. Biomed. Materials Research*, 25:423-441.
22. Vroman, L. and A. Adams. 1986. "Proteins in Narrow Spaces" (Lens on Slide Gradient Method), *J. Colloid Interface Sci.*, 111.
23. Elwing, H. 1991. "Lens on Surface", *J. Biomat. Sci. Polymer Ed.*, 3:7-16.
24. Andrade, J. D. Syllabus for MSE 519, *Introduction to Polymeric Materials*, Univ. of Utah.
25. White, F. M. 1988. *Heat and Mass Transfer*. MA: Addison-Wesley Publishing Company.
26. Billmeyer, F. W. 1984. *Textbook of Polymer Science*. NY: John Wiley and Sons.
27. Garbassi, F., M. Morra and E. Occhiello. 1994. *Polymer Surfaces: From Science to Technology*. NY: John Wiley and Sons.
28. Young, R. J. 1981. *Introduction to Polymers*. NY: Chapman and Hall.
29. Goodwin, M. 1994. BSc Thesis. University of Utah, Department of Materials Science and Engineering.
30. Allan, N. S. 1982. *Developments in Polymer Photochemistry*. NJ: Applied Science Publishers.
31. Ranby, B. and J. F. Rabek. 1975. *Photodegradation, Photo-Oxidation and Photostabilization of Polymers*. NY: John Wiley and Sons.
32. Roffney, C. G. 1982. *Photopolymerization of Coatings*. NY: John Wiley and Sons.
33. Larsen, R. 1994. BSc Thesis. University of Utah, Department of Materials Science and Engineering.
34. Shiga, T., Y. Hirose, A. Okada and T. Kurauchi. 1992. "Bending of Poly(Vinyl Alcohol)-Poly(Sodium Acrylate) Composite Hydrogel in Electric Fields", *J. App. Poly. Sci.*, 44:249-253.
35. Tanaka, T., I. Nishio, S. T. Sun and S. Ueno-Nishio. 1992. "Collapse of Gels in an Electric Field", *Science*, 218(October 29):467-469.
36. Matsuo, E. S. and T. Tanaka. 1992. "Patterns in Shrinking Gels", *Nature*, 358(August 6):482-485.
37. Tanaka, T. 1981. "Gels", *Scientific American*, 249:124-138.
38. Bae, Y. H., T. Okano and S. W. Kim. 1990. "Temperature Dependence of Swelling of Crosslinked Poly(N,N'-alkyl substituted acrylamides) in Water", *J. Poly. Sci.*, 28B:923-936.
39. Okano, T., Y. H. Bae, H. Jacobs and S. W. Kim. 1990. "Thermally On-Off Switching Polymers for Drug Permeation and Release", *J. Controlled Release*, 11:255-265.
40. Fujishige, S., K. Kubota and I. Ando. 1989. "Phase Transition of Aqueous Solutions of Poly(N-isopropylacrylamide) and Poly(N-isopropylmethacrylamide)", *J. Phys. Chem.*, 93:3311-3313.
41. Elwing, H. and C. G. Golander. 1990. "Gradients in Chemical Composition", *Adv. Colloid Interface Sci.*, 32:317-339.
42. Elwing, H., S. Welin, A. Askendal, U. Nilsson and I. Lundström. 1987. "A Wettability Gradient Method for Studies of Macromolecular Interactions at the Liquid/Solid Interface", *J. of Colloid and Interface Science*, 119:203-210.
43. Gölander, C-G., Y-S. Lin, V. Hlady and J. D. Andrade. 1990. "Wetting and Plasma-Protein Adsorption Studies Using Surfaces with a Hydrophobicity Gradient", *Colloids and Surfaces*, 49:289-302.



# INCORPORATING "INTELLIGENT" MATERIALS INTO SCIENCE EDUCATION

Robert J. Scheer, Ph.D.  
Research Scientist  
Protein Solutions, Inc.  
Salt Lake City, Utah

**Key Words:** Polymers, Plastics, Science, Education, Intelligent materials

**Prerequisite Knowledge:** Basic chemistry and physics

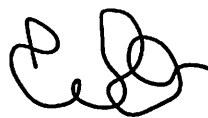
**Objective:** To learn the fundamentals of polymer science/engineering through hands-on explorations.

## Outline

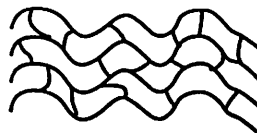
- I. Handout of materials for exercises in polymeric and materials sciences.
  - A. DOP plasticizer gradient of poly(vinyl chloride)
  - B. Shape memory polymer, poly(norbornene)
  - C. Surface wettability gradient, polystyrene
  - D. Temperature responsive polymer, poly(N-isopropyl acrylamide)
  - E. Ion concentration responsive polymer, sodium polyacrylate
- II. Review of basic concepts and themes covered in introductory polymer/materials class (1-7)
- III. Rational and philosophy for the intelligent materials lab (8-10)
  - A. Provide "real reality" in the classroom (8)
  - B. Easily assimilated format
  - C. Provide a lab where one does not exist due to cost or logistics (9,10)
  - D. Free up instructor time for class preparation and student interaction
- VI. "Do the lab"

# Basic Concepts and Themes in Polymer Science and Engineering (1-7)

**Molecular Weight and Distribution**



**Thermoset/Thermoplastic**



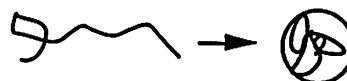
**Steric Hindrances/Side Groups**



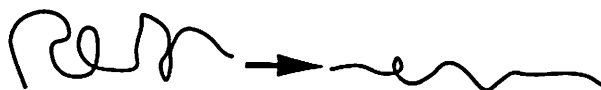
**Polymerization**



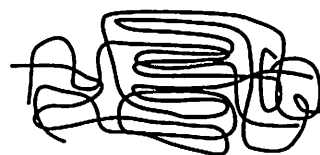
**Intermolecular Forces/Cohesive Energy Density**



**Entropy/Elasticity**



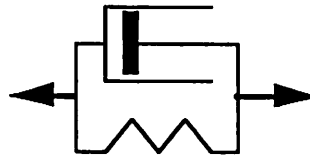
**Morphology/Crystallinity**



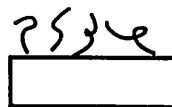
**Temperature Transitions**



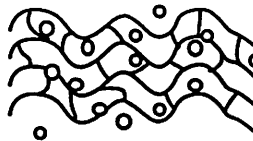
**Viscoelasticity**



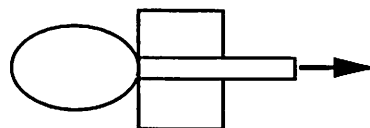
**Surface versus Bulk Properties**



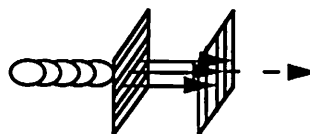
**Modifiers/Additives**



**Processing/Fabrication**



**Optical Properties**



**Time-Temperature Superposition**



# Cross reference grid of Material System with Introductory Polymer Concepts

Material System and Concept	Heat Shrink	Temperature Responsive Polymer	Ionic Responsive Polymer	Tg Homopolymers	Heat Shrink Material	Composites	Surface Gradient	Voight-Maxwell Models	Shape Memory Polymer	Elastomer	Polymerization Procedure	Spherulite Gradient	Crosslink Gradient	Plasticizer Gradient	Copolymer gradient
Molecular Weight and Distribution											X	X	X		
Morphology(Crystallinity)					X				X	X		X			
Intermolecular Forces	X	X		X	X			X	X	X			X	X	X
Cohesive Energy Density/Solubility		X	X											X	
Polymerization											X		X		X
Thermoset/Thermoplastic	X							X		X		X	X		
Glass Transition	X			X				X	X			X	X	X	X
Time-Temp Superposition/Viscosity								X				X			
Entropy	X								X	X		X			
Stearic Hindrance		X	X	X	X			X	X				X		X
Macromolecular Effects		X	X					X	X	X		X	X	X	
Surface/Bulk Properties							X								
Processing			X	X	X						X	X		X	
Additives/Fillers						X					X			X	
Optical Properties		X	X									X			

## Rational and Philosophy

Most students come into polymer courses with various concepts and preconceptions which lead them to conclude that the behavior and properties of polymers are counter-intuitive. It is therefore important that they fully discover and observe the properties and behavior of polymeric materials for themselves.

A very large number of science and engineering courses taught in colleges and universities today do not involve laboratories. Although good instructors incorporate class demonstrations, hands-on homework, and various teaching aids, including computer simulations, the fact is that students in such courses often accept key concepts and experimental results without discovering them for themselves. The only partial solution to this problem has been increasing the use of class demonstrations and computer simulations.

We are developing a set of inexpensive and convenient hands-on discovery based experiments which the students can perform for themselves. The laboratory, although packaged like a textbook, will contain within it all of the materials, equipment, and information needed to directly discover and experience key concepts related to polymer materials.

The experiments are based on:

- 1) actual materials commonly utilized in consumer products, and
- 2) a set of specially developed materials which the students can utilize to directly see and experience complex concepts (8).

In both cases, the experiments and observations will utilize only the students' senses for transduction and detection.

Another important area of education which this research will impact is the growing field of distance learning. The Public Broadcasting Service (PBS) has developed a new program called "Going the Distance." In the PBS's definitive guide to distance learning, *Going the Distance* (9), major issues related to developing a distance learning program are discussed. The guide points out special needs of the laboratory sciences and distance learning. Others have addressed distance learning (9,10), and currently several states, including Utah, are strongly committed to the development of distance learning for secondary and post-secondary education.

Uniqueness: The difference between our proposed laboratory explorations and those of other, more common exercises is two-fold. The primary difference is in the required detection devices; our laboratories require the human perceptions of both sight and touch, others often require costly (though not more sophisticated) detection equipment. This is the very difference which allows the Labless Lab™ to be used outside the classroom. The secondary difference is the use of "intelligent materials" as teaching devices (8). The students can utilize these materials to directly see complex polymer concepts.

# Plasticizer Gradient (PVC)

Observation #1:

Draping

Stiffness/Compliance §13.2 (1)

Additives §15.7, p.329

Low M.W. Components §8.2, p.157

Molecular Weight Distributions §9.3, p.187

Viscoelasticity §13.5, §12.2

Observation #2:

Indentation

Hardness §13.2

Elasticity §13.2

Viscoelasticity §13.5., §12.2.

Observation #3:

Molding

Viscoelasticity §13.5, §12.2

Glass Transition §12.10

Long Molecule Mobility §10.3 p. 217, §10.4, p.217

Time-Temp. Relationship §13.14, p.298

Processing

Intermolecular Forces §13.15, p.301



# Shape Memory Polymer (polynorbornene)

## Observation #1:

Comparison of mechanical properties at room temperature and at  $T > T_g$

Glass Transition §12.10

Elasticity §13.2

Intermolecular Forces §13.15, p. 301

## Observation #2:

Mold polymer when  $T > T_g$  and cool, does it hold its shape?

Intermolecular Forces §8.14, p.177

Glass Transition §12.10

## Observation #3:

Reheat above  $T_g$

Molecular Mobility §12.1

Glass Transition §12.10

Intermolecular Forces §8.14, p.177

## Surface Wettability Gradient (polystyrene)

Observation #1:

Sessile Drop Test

Intermolecular Forces §8.14, p.177

Surface and Bulk properties §

Observation #2:

Peel Test

Intermolecular Forces §8.14, p.177

Surface and Bulk properties §

Observation #3:

Capillarity Test

Intermolecular Forces §8.14, p.177

Surface and Bulk properties §

# Temperature Responsive Polymer (poly(N,isopropylacrylamide))

## Observation #1:

Dry material properties  
compared to solution properties

Intermolecular Forces §8.14, p.177

Solubility and Concentration §8.14, p.177

Side Groups §15.6, p.327

## Observation #2:

Effect of different temperatures  
on solution properties

Intermolecular Forces §8.14, p.177

Solubility and C.E.D. §8.14, p.177

Optical properties §

Side Groups §15.6, p.327

## Observation #3:

Reversibility – Heating and Cooling

Solubility and C.E.D. §8.14, p.177

Intermolecular Forces §8.14, p.177

# Ionic Responsive Polymer (sodium polyacrylate)

## Observation #1:

Dry material properties  
compared to  
Hydrated gel material properties

Crosslinking §15.13, p.345

Elasticity §13.2

Morphology §11.8

## Observation #2:

Affect of different solutions  
(saline, sugar water, food coloring)

Intermolecular Forces §8.14, p.177

Solubility and Concentration §8.14, p.177

Side Groups §15.6, p.327

## Observation #3:

Reversibility – Heat, Agitation

Molecular Mobility §12.1

Intermolecular Forces §8.14, p.177

## Observation #4:

Solution Properties

Viscosity §9.13, p.207

Molecular Weight §9.2, p.187

Cohesive Energy Density §8.14, p.177

## References

1. Cowie, J.M.G.: *Polymers: Chemistry and Physics of Modern Materials*. Chapman and Hall, 1991.
2. Billmeyer, F.W.: *Textbook of Polymer Science*. John Wiley and Sons, 1984.
3. Young, R.J.: *Introduction to Polymers*. Chapman and Hall, 1981.
4. Cambell, I.M.: *Introduction to Synthetic Polymers*. Oxford University Press, 1994.
5. Rodriguez, F.: *Principles of Polymer Systems*. McGraw-Hill, 1982.
6. Carraher, C.: *Polymer Chemistry*. Dekker, 1992.
7. Seymour, R.B.: Recommended ACS Syllabus for Introductory Courses in Polymer Chemistry. *J. Chem. Educ.*, vol. 59, 1982, p. 652.
8. Andrade, J.D.; and Scheer, R.J.: Applying 'Intelligent' Materials for Materials Education: The Labless Lab™. *Proceedings of the Second International Conference on Intelligent Materials*. C.A. Rogers, and Williams, G.G., eds. Technomic, 1994.
9. Toby Levine Communications, Inc. Bethesda, Maryland. *Going the Distance: A Handbook for Developing Distance Degree Programs Using Television Courses and Telecommunications Technologies*. Annenberg/CPB Project and PBS Adult Learning Service, Corporation for Public Broadcasting and Public Broadcasting Service. 1994.
10. Watkins, B.T. "Uniting North Dakota." *The Chronicle of Higher Education*. Aug. 10, 1994, p. A17.

## Surface characterization of functional poly(diacetylene) and poly(butadiene) mono- and multilayers<sup>\*)</sup>

H. Schupp, B. Hupfer, R. A. Van Wagenen<sup>\*)</sup>, J. D. Andrade<sup>\*)</sup>, and H. Ringsdorf

Institut für Organische Chemie, Johannes Gutenberg-Universität, Mainz, (Federal Republic of Germany)  
and

<sup>\*)</sup> College of Engineering, Dept. of Bioengineering, University of Utah, Salt Lake City, Utah (USA)

LP

**Abstract:** The surface properties of Langmuir-Blodgett mono- and multilayers of a variety of amphiphilic poly(diacetylene)s and poly(butadiene)s were investigated by contact angle, streaming potential  $\zeta$ , ellipsometry, and X-ray photoelectron spectroscopic (XPS) measurements. Captive air and octane angles varied between approximately 60° and 105° for hydrophobic x-layers and 31° to 46° for hydrophilic surfaces depending on the particular head group, whereas advancing angles determined via the vertical plate method are considerably higher. Negative streaming potentials were obtained for all surfaces. Positively charged monolayers yielded less negative  $\zeta$ -potential values (–28 mV) than negatively charged (–52 mV) or hydrophobic (–50 mV) layers. Ellipsometry measurements yielded an average layer thickness of  $27 \pm 6$  Å for 3 to 11 layers. X-ray photoelectron spectroscopy results qualitatively confirmed the expected composition. All of the samples, which were handled and stored in air after deposition and polymerization, were surface oxidized.

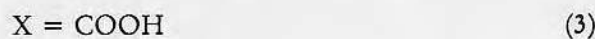
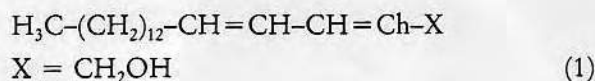
**Key words:** Contact angle, streaming potential, ellipsometry, photoelectron spectroscopy, Langmuir-Blodgett multilayers, poly(diacetylene)s, poly(butadiene)s.

### Introduction

The bilayer type lipid membrane, which surrounds all living cells, has a variety of functions which are necessary in order to sustain life. For studying specific properties of the very complex biomembranes simple membrane models have been developed such as lipid monolayers at the gas-water interface [1], planar bilayer lipid membranes [2] or spherical liposomes (vesicles) [3]. One of the shortcomings of these membrane models is their low long-term stability, which is mainly due to the lack of the stabilizing proteins present in biomembranes. Since a defined stabilization via protein incorporation into model membranes is very difficult, different methods for stabilizing model membranes have been investigated. E. g. the incorporation of cholesterol into the membrane of vesicles [4] leads to a prolonged lifetime of these vesicles in vitro as well as in vivo. Another approach has been developed by Khorana et al. [5], who linked lipids carrying photoactivable groups to proteins incorporated in model membranes. In addition,

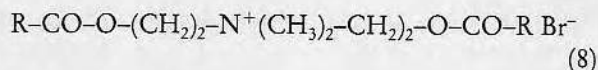
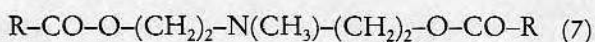
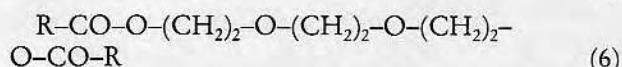
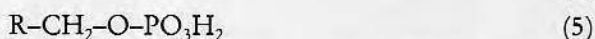
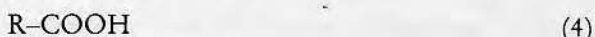
a variety of authors recently described the build up of stable model membranes, which can be obtained by the polyreaction of lipids bearing polymerizable groups in mono- and multilayers [6], bilayer lipid membranes [7], and vesicles [8], where acryloylic, methacryloylic, butadienic, allylic, as well as diacetylenic moieties were used as polymerizable units.

Since the head groups of most of the polymerizable lipids do not correspond to the naturally occurring ones, for any application of polymerized vesicles in vivo e. g. as drug carriers [3] or as synthetic cell models (which could be of potential use as antitumor agents on a molecular level [8i]) information about the surface properties of the synthetic vesicle forming compounds is necessary. For this reason the present investigation concerns with the surface properties of a number of butadienic and diacetylenic lipids (1)–(8).



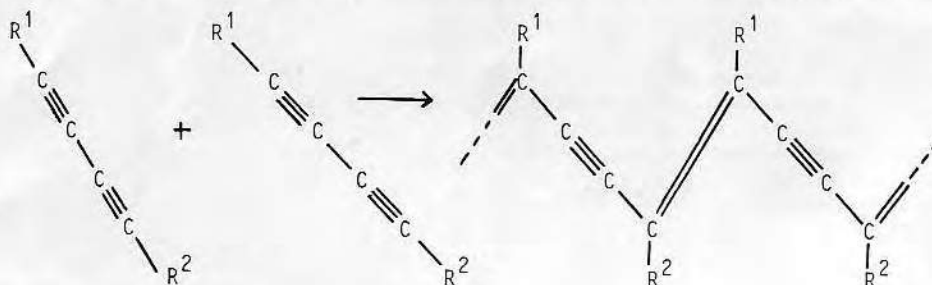
<sup>\*)</sup> Dedicated to Prof. Dr. F. H. Müller.



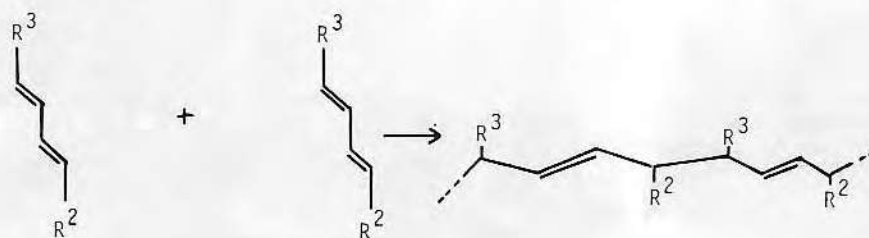


where  $\text{R} = \text{H}_3\text{C-(CH}_2\text{)}_{12}\text{-C}\equiv\text{C-C}\equiv\text{C-(CH}_2\text{)}_8$ .

Diacetylenic derivatives yield totally rigid, conjugated, blue or red colored polymer backbones [6c],



whereas 1,4-disubstituted butadienes polymerize in monolayers and vesicles to form more flexible 1,4-trans-polybutadienes [6g]:



Polydiacetylene mono and multilayers have so far been characterized by X-ray measurements [6c, 9], UV [6c, 10], and resonance Raman spectroscopy [11], as well as by electron microscopy [6c]. Very little is known about their surface properties such as surface potential, contact angles or photoelectron spectroscopy [12], although oriented polymer layers are an ideal system for such investigations.

Layers of amphiphilic compounds such as diacetylene carbonic acid (4) can usually be built up by the Blodgett technique in three kinds of orientations [1], i. e. in *x*- or *y*-layers yielding a hydrophobic surface, or in *z*-layers yielding a hydrophilic surface. So besides the possibility to orient all the monomers as *x*- or *y*-layers — in a *z*-layer orientation the functionalities can be varied from negatively charged surfaces (3), (4), (5) to neutral (1), (2), (6), a chargeable (7), and finally to a positively charged system (8).

## Experimental part

The syntheses of the monomers have been described elsewhere [6f, 6g, 7d]. The following materials were used as solid substrates:

For contact angle measurements: cleaned (see below) microscope coverslips ( $2,4 \times 6$  cm); for streaming potentials: cleaned microscope slides ( $2,5 \times 7,5$  cm). All the glass substrates were cleaned in „Microclean“ detergent solution at  $40^\circ\text{C}$ , rinsed with distilled water, then treated with dichromate-sulfuric acid at  $80^\circ\text{C}$  for 15 minutes, rinsed with filtered distilled water and ethanol and decreased in a freon TF/ethanol azeotrope vapor. For ellipsometry: Chromium vapor deposited on clean glass in a  $10^{-5}$  torr vacuum system. Only the cadmium salt of compound (4) was used for ellipsometry studies. Details of the deposition of mono- and multilayers of Cd salts of diacetylene carbonic acids on solid substrates have been described in the literature [6c]. *x*-layers of (3) and (4) were obtained at  $2^\circ\text{C}$  and  $20^\circ\text{C}$  subphase temperature, respectively, under a constant surface pressure of  $10 \text{ mN}\cdot\text{m}^{-1}$  using a Langmuir trough with a movable barrier, a dipping rate of  $5 \text{ mm}\cdot\text{min}^{-1}$  and a  $1\cdot 10^{-3}$  molar solution of  $\text{CdCl}_2$  in doubly distilled water (pH 5,5) as subphase. For the transfer of all compounds in a *z*-layer like orientation, the monomers were polymerized via UV-light ( $2 \text{ mW}\cdot\text{cm}^{-2}$ , 254 nm) as monolayers at the nitrogen-water interface [6b] at  $10^\circ\text{C}$  and a constant surface pressure of  $10 \text{ mN}\cdot\text{m}^{-1}$ . Cleaned microscope slides and coverslips were dipped through the polymer monolayers parallel to the water surface, inverted under water and lifted up to the air in an area of the trough not covered with a monolayer. The homogeneity of these films was checked by contact angle measurements.

For static contact angle determinations the captive air and octane methods were used [13]. From height and diameter of the air and octane bubbles the contact angles could be estimated [14]. Dynamic

contact angles were measured by the vertical plate method. The general principles of this technique are discussed in [14–17]. In the present work, a Scotts mechanical testing machine (GCA/Precision Scientific, Chicago, Illinois, USA) was used as a movable carriage. A Cahn electrobalance, which was connected with a plotter, was used as wetting balance so that contact angle hysteresis was automatically recorded. Dynamic advancing and receding angles could be directly determined from the diagrams [16–17].

The details of flat plate streaming potential measurements have been described [20]. Streaming electrolyte was 0.01 M KCl solution buffered to pH 7.4 via  $2 \cdot 10^{-4}$  M  $\text{KH}_2\text{PO}_4$  and  $9 \cdot 10^{-4}$  M  $\text{Na}_2\text{HPO}_4$ . The samples were stored in electrolyte solution for 16 hours prior to measurements. Zeta potentials were determined with a program written for a Texas Instruments (TI 59) calculator.

Thickness measurements were obtained from mono- and multilayers deposited on chromium-coated glass. A Rudolph Research RR 2000 laser ellipsometer (6328 Å) was used.  $\Delta$  and  $\Psi$  were measured at different positions for each of the chrome-coated samples before and after monolayer deposition, using a refractive index of  $n_f = 1.52$  and  $K_f = 0.12$  [12]. Cr film optical constants were measured as  $n_s = 2.81 \pm 0.23$  and  $k_s = 1.56 \pm 0.33$  at 6328 Å [12].

Substrate optical constants were calculated from standard equations [19] having the measured  $\Delta$  and  $\Psi$  values. Film thicknesses were calculated using standard equation [19] by comparing  $n$  and  $k$  values for the film and the  $n$  and  $k$  values for the Cr substrate.

X-ray photoelectron spectra (XPS) were obtained with a Hewlett-Packard 5950 B instrument with monochromatic  $\text{AlK}\alpha_{1,2}$  (1487 eV) X-rays. X-ray power was 800 watts at the anode. Sample charging was compensated by use of an electron flood gun, although the sample films were semiconductive. Wide scans (0–1000 eV) and high resolution narrow scans (20 eV) were determined. Ambient temperature was employed.

## Results and discussion

### X-ray photoelectron spectroscopy

A detailed examination of the expected composition of the samples prepared for XPS analysis shows that the major component is carbon. As these samples were deposited on glass substrates, generally only one layer thick, considerable show through of the underlying glass substrate was evident in the spectra. Thus, the oxygen peaks from the samples could not be readily analyzed because of the overwhelming influence of the oxygen from the glass substrate. In those samples which contain nitrogen, refer to table 1, the concentration is roughly one part nitrogen to 50 parts carbon. In the case of the sample with a quaternized nitrogen, the counterion is bromine with a comparable concentration. In the case of the sample with phosphate terminal groups, the concentration is one part phosphorus to 26 parts of carbon. The XPS spectra did show the qualitative presence of bromine, nitrogen, and phosphorus in those samples for which they were expected. These elements were not detected in the other samples examined (table 1). Because of time and resource limitations in this study, sufficient instrument time

Table 1. Approximate elemental ratios of monolayers containing specific functional groups

Monolayer functional group	Br	P	N	C
–COOH	0	0	0	26
–OH	0	0	0	18
–O–PO <sub>3</sub> H <sub>2</sub>	0	1	0	26
N–CH <sub>3</sub>	0	0	1	57
N <sup>+</sup> CH <sub>3</sub>	1	0	1	58
–O C–C	0	0	0	58
–O				

was not available to do a thorough analysis of the bromine, phosphorus, and nitrogen constituents.

In previous studies with unsaturated hydrocarbon polymers, surface oxidation begins to become apparent in XPS spectra after four hours exposure to atmospheric conditions [17]. Those results were confirmed in this study because all of the samples were examined several months after they were produced and all showed extensive surface oxidation with the C-1s and O-1s features comparable to those observed previously in oxidized polybutadiene [17].

### Contact angle analysis

The degree of surface oxidation complicates the streaming potential and contact angle analysis. Advancing and receding water contact angles in oxidized polybutadienes have shown that, although the advancing angle decreases only slightly after long term storage in air, the receding angle shows a substantial decrease from about 70 to 40 degrees after one week storage in air [17]. The contact angle data (table 2) for hydrophobic monolayers of the poly(diacetylenes) (4), (5) and (8) do not differ very much from each other – the nature of the head group does not seem to have an effect on these contact angles. The same is the case for the butadienes (2) and (3). A relatively big difference, however, can be observed for mono- and multilayers of poly-(4): three layers of this acid are more hydrophobic than one. This may be due to glass-water interactions, since water is known to penetrate very easily through a monolayer. Three layers shield the glass better than one does and the result is a more hydrophobic surface.

The ellipsometry data (table 4) suggest that a single layer may be somewhat expanded or thicker than expected. As expected the advancing  $\theta$  values are

Table 2. Contact angles of oriented, functional polymer layers

Compound	Orientation	No. of layers	$\theta_{\text{air}}^{\text{a)}}$	$\theta_{\text{rec}}^{\text{b)}}$	$\theta_{\text{adv}}^{\text{b)}}$
glass	—	—	—	23.0	56.0
poly-(3)	<i>x</i>	1	61.4	49.6	88.8
poly-(4)	<i>z</i>	1	31.1	—	—
poly-(4)	<i>x</i>	1	57.5	48.3	86.1
poly-(4)	<i>x</i>	3	64.0	62.2	88.2
poly-(2)	<i>x</i>	1	60.6	48.5	85.3
poly-(5)	<i>x</i>	1	55.5	—	—
poly-(8)	<i>x</i>	1	60.5	40.0	95.9
poly-(8)	<i>z</i>	1	42.3	—	—
poly-(5)	<i>z</i>	1	32.5	—	—
poly-(3)	<i>z</i>	1	46.4	—	—
poly-(2)	<i>z</i>	1	33.7	—	—
poly-(6)	<i>z</i>	1	44.0	—	—
poly-(7)	<i>z</i>	1	53.9	—	—

<sup>a)</sup> Captive bubble method, air bubble introduced at polymer-water interface.

<sup>b)</sup>  $\theta$  advancing and  $\theta$  receding determined by vertical Wilhelmy plate dynamic technique [16].

higher than the angles for the hydrated surfaces, and the static contact angles are smaller than the dynamic advancing and smaller than the dynamic receding angle data in all cases. Wilhelmy plate and captive air angles are compared in reference [18].

On the contrary, the angles of the hydrophilic surfaces show very big differences due to the different head groups. The static air angle data vary from about 32 degrees for the negatively charged to 44 degrees for the neutral poly(diacetylene) surfaces, whereas the poly(dienoic acid) (3) shows an unusually high but reproducible air angle of 46 degrees.

### Streaming potentials

The contact of any charged or chargeable surface with a polar medium, such as an aqueous electrolyte solution, leads to the formation of an electrical double layer, where ions from the solution may adsorb to the surface. Thus, it is impossible to determine the surface potential itself but only the so-called zeta potential  $\zeta$ , at the shear plane [20–23] between the layer of adsorbed ions and nonbound ions. Nevertheless,  $\zeta$  give useful information related to surface charge densities and the kind of charge on the surfaces, which may be useful parameters for estimating the biocompatibility of synthetic materials [22]. Usually zeta potential data are calculated from streaming potential values, which are obtained when an electrolyte solution forced by a pressure difference  $\Delta P$  flows through a thin capillary or flat plate cell provided with two electrodes. The zeta potential can be calculated from the streaming potential,  $E_{\text{str}}$ , by means of equation:

$$\zeta = \frac{4 \cdot \pi \cdot \eta}{\epsilon} \cdot \frac{E_{\text{str}}}{\Delta P} \cdot \frac{C}{R}$$

where  $\eta$  is the viscosity of the electrolyte,  $\epsilon$  the dielectric constant, and  $R$  the measured AC resistance of the capillary electrolyte system.  $C$  is a predetermined system constant.

Accurate measurements of  $E_{\text{str}}$  data is only possible if the fluid flow is steady, incompressible, laminar, and established. Therefore, the applicability of streaming measurements is generally limited to long capillary tubes or porous plugs of compacted particles or fibers. Recently a new method for streaming measurements has been described [20] wherein the streaming cell has a flat plate geometry. The major advantage of this method is that the flat surfaces permit the application of other surface characterization techniques. With the flat plate cell zeta potentials can be calculated from [19–22]:

$$= 8,4922 \cdot 10^8 \cdot \frac{\eta \cdot C}{\epsilon \cdot R} \cdot \frac{E_{\text{str}}}{\Delta P}$$

In addition, the surface charge density at the shear plane can be obtained from the relation

$$\sigma = \frac{2\epsilon \cdot n_i^0 \cdot k \cdot T}{\pi} \cdot \sinh \frac{Z \cdot e_0}{2kT} \cdot \zeta$$

where

$n_i^0$  = concentration of the *i*th ionic species in the bulk

$k$  = Boltzmann constant

$T$  = absolute temperature

$Z$  = valence of the ionic species

$e_0$  = electron charge

$\zeta$  = interfacial potential at the shear plane.



Table 3. Zeta potentials and surface charge densities of oriented functional polymer layers

Compound	Orientation	No. of layers	$\zeta$ (mV)	$\sigma \cdot 10^{-4}$ charges $\cdot \mu\text{m}^{-2}$	$\zeta_{\text{corr}}$ (mV) <sup>a)</sup>
glass	—	—	—57.6	2.84	—15.9
poly-(4)	<i>x</i>	1	—56.4	2.76	—14.7
poly-(4)	<i>x</i>	3	—52.4	2.50	—10.7
poly-(3)	<i>x</i>	1	—48.7	2.27	—7.0
poly-(3)	<i>z</i>	1	—50.7	2.39	—9.0
poly-(3)	<i>z</i>	1	—46.8	2.16	—5.1
poly-(5)	<i>z</i>	1	—48.0	2.23	—6.3
poly-(7)	<i>z</i>	1	—38.6	1.71	+3.2
poly-(8)	<i>z</i>	1	—31.5	1.35	+10.3
poly-(6)	<i>z</i>	1	—41.7	1.86	0

<sup>a)</sup> Normalized to the value of poly(6) taken as zero. (See text for details).

In the present work we were interested in the effect of charge of polymer monolayers on the zeta potential. It has been shown [21–24] that the addition of a small amount of charge to hydrophilic methacrylates did tend to increase absolute streaming potential values with increasing amounts of charge addition.

The data for our oriented polymer layers of the *x*- as well the *z*-type are summarized in table 3. Highly negative zeta potentials are obtained for the neutral hydrophobic *x*-layers, which are even more negative than those of the negatively charged *z*-layers (poly-(3), poly-(4), poly-(5)). Furthermore, the absolute value for one *x*-layer of poly-(4) is considerably higher than the one for three layers. Since a monolayer is only about 2.7 nm thick, this may be due to the effect of the glass substrate, which is highly negatively charged. Also, all hydrophilic surfaces exhibit negative zeta values, even if they carry positive charges (poly-(8)), for which one would expect a positive zeta value. As indicated, however,  $\zeta$  is the potential at the shear plane which is determined by specifically bound ions on the surface. If one takes, however, the value of the neutral ether-polymer, poly-(6) as a standard ( $\zeta = 0$ ) and relates all other data to this value, the effect of the glass is excluded and a nice trend can be observed (column " $\zeta_{\text{cor}}$ " in table 3):

a. As expected the ammonium salt (poly-(8)) exhibits the most positive zeta potential value.

b. The amine poly-(7), which is certainly protonized to some extent under the experimental conditions, also shows a positive zeta potential, but less positive compared to poly-(8).

c. The negatively charged as well as the hydrophobic surfaces all exhibit negative zeta potentials.

### Ellipsometry

The ellipsometry results are presented in table 4. The samples were prepared in Mainz, Germany and transported to Utah, USA in special holders, where they were examined several months after preparation. Given these variables and the errors inherent in the ellipsometry technique [19], the values are reasonable and confirm the expected thicknesses of these mono- and multilayer diacetylene films. The first layer value is higher than expected; this could be a real effect or could be due to surface contaminations and/or oxidation.

### Conclusions

Functionalized polydiacetylene and polybutadiene mono- and multilayers were characterized by X-ray

Table 4. Summary of ellipsometry results for the Cd salts of poly-(4)

Layers deposited	Measured thickness Å	Average thickness	Average thickness per layer, Å
1	39,52,62,21,18	38 ± 19	38 ± 19
3	53, 89, 69, 76, 93, 48, 57	69 ± 18	23 ± 6
5	119, 95, 95, 122, 134	113 ± 17	23 ± 3
7	193, 188, 196, 183, 213	195 ± 11	28 ± 2
9	244, 289, 296, 187, 222	248 ± 46	28 ± 5
11	383, 353, 331	356 ± 26	32 ± 3

Average of all data: 29 Å per layer.

photoelectron spectroscopy, water contact angles, streaming potential measurements in 0.01 M KCl solutions and ellipsometry. The streaming potential data correlated quite well with the functional group character and expected charge character of the functionalized surfaces. Ellipsometry confirmed the expected thickness of the films within the error limits of the technique.

Qualitative elemental analysis by the XPS technique confirmed the presence of nitrogen, phosphorus, and bromine counterion in those monolayers for which they were expected. Further interpretation of the contact angle data as well as the X-ray photoelectron spectroscopy data was complicated by the fact that these materials are susceptible to atmospheric oxidation and were significantly surface oxidized.

#### Acknowledgements

This work is partially supported by the Deutsche Forschungsgemeinschaft (SFB 41, Mainz) and by U.S. NIH grant HL 18519. The assistance of Dr. T. Doyle, Dr. L. Smith is appreciated.

#### References

1. Gaines, G. L., "Insoluble Monolayers at Liquid-Gas Interfaces". Interscience (New York 1966).
2. Tien, H. T., "Bimolecular Lipid Membranes, Theory and Practice", Dekker (New York 1974).
3. Gregoriadis, G., A. C. Allison, "Liposomes in Biological Systems", Wiley (New York 1980).
4. Gregoriadis G., in reference [3], p. 25.
5. Gupta, C. M., E. E. Costello, H. G. Khorana, Proc. Natl. Acad. Sci. U.S.A. **76**, 3139 (1979).
6. a) Naegele, D., H. Ringsdorf, J. Polym. Sci., Polym. Chem. Ed. **15**, 2821 (1977); b) Day, D. R., H. Ringsdorf, J. Polym. Sci., Polym. Lett. Ed. **16**, 205 (1978); c) Tieke, B., G. Lieser, G. Wegner, J. Polym. Sci., Polym. Chem. Ed. **17**, 1631 (1979); d) Day, D. R., H.-H. Hub, H. Ringsdorf, Isr. J. Chem. **18**, 325 (1979); e) Hupfer, B., H. Ringsdorf, H. Schupp, Makromol. Chem. **182**, 247 (1981); f) Hub, H.-H., B. Hupfer, H. Koch, H. Ringsdorf, J. Macromol. Sci.-Chem. **A15**, 701 (1981); g) Ringsdorf, H., H. Schupp, *ibid.* **A15**, 1015 (1981).
7. Benz, R., W. Praß, H. Ringsdorf, Angew. Chem., in press.
8. a) Hub, H.-H., B. Hupfer, H. Ringsdorf, ACS, Org. Coat. Plast. Chem. **42**, 2 (1980); b) Regen, S. L., B. Czech, A. Singh, J. Am. Chem. Soc. **102**, 6638 (1980); c) Johnston, D. S., S. A. Sanghera, M. Pons, D. Chapman, Biochim. Biophys. Acta **602**, 57 (1980); d) Hub, H.-H., B. Hupfer, H. Koch, H. Ringsdorf, Angew. Chem. Int. Ed. Engl. **19**, 938 (1980); e) O'Brien, D. F., T. H. Whitesides, R. T. Klingbiel, J. Polym. Sci., Polym. Lett. Ed. **19**, 95 (1981); f) Akimoto, A., K. Dorn, L. Gros, H. Ringsdorf, H. Schupp, Angew. Chem. Int. Ed. Engl. **20**, 90 (1981); g) Bader, H., H. Ringsdorf, J. Skura, *ibid.* **20**, 91 (1981); h) Koch, H., H. Ringsdorf, Makromol. Chem. **182**, 255 (1981); i) Gros, L., H. Ringsdorf, H. Schupp, Angew. Chem. Int. Ed. Engl. **20**, 305 (1981); j) Kunitake, T., N. Nakashima, K. Takarabe, M. Nagai, A. Tsuge, H. Yanagi, J. Am. Chem. Soc. **103**, 5945 (1981); k) Hupfer, B., H. Ringsdorf, ACS Sympos. Ser., in press.
9. Day, D. R., J. B. Lando, Macromolecules **13**, 1478 (1980); *ibid.* **13**, 1483 (1980).
10. Day, D. R., H. Ringsdorf, Makromol. Chem. **180**, 1059 (1979).
11. Tieke, B., D. Bloor, Makromol. Chem. **180**, 2275 (1979).
12. Hupfer, B., H. Schupp, J. D. Andrade, H. Ringsdorf, J. Electr. Spectrosc. Relat. Phenom. **23**, 103 (1981).
13. Andrade, J. D., R. N. King, D. E. Gregonis, D. L. Coleman, J. Polym. Sci., Polym. Symp. **66**, 313 (1979).
14. Neumann, A. W., R. J. Good in "Surface and Colloid Science", Vol. 11; p. 31. R. J. Good, R. R. Stromberg, eds., Plenum (New York 1979).
15. Johnson, R. E., Jr., R. H. Dettre in: "Surface and Colloid Science", Vol. 2; E. Matijevic, ed., Plenum (New York 1969).
16. Johnson, R. E., R. H. Dettre, D. A. Brandreth, J. Colloid Interface Sci. **62**, 205 (1977).
17. Smith, L., C. Doyle, D. E. Gregonis, J. D. Andrade, J. Appl. Polym. Sci., in press.
18. Gregonis, D. E., R. Hsu, D. E. Buerger, L. M. Smith, J. D. Andrade in: "Solvent-Property Relationship in Polymers", R. B. Seymour, G. A. Stahl, eds., Pergamon (1982) in press.
19. Müller, H. R., Adv. Electrochem. Electrochem. Eng. **9**, 167 (1973).
20. Van Wagenen, R. A., J. D. Andrade, J. Colloid Interface Sci. **76**, 305 (1980).
21. Van Wagenen, R. A., D. L. Coleman, R. N. King, P. Triolo, L. Brostrom, L. M. Smith, D. E. Gregonis, J. D. Andrade, J. Colloid Interface Sci., in press.
22. Sawyer, P. N., J. Electrochem. Soc. **125**, 419c (1978).
23. Van Wagenen, R. A., RhD Thesis, University of Utah (1976).
24. Coleman, D. L., PhD Thesis, University of Utah (1980).

Received December 9, 1981

#### Authors' addresses:

H. Schupp, B. Hupfer, H. Ringsdorf  
Institut für Organische Chemie  
Johannes-Gutenberg-Universität  
J.-J.-Becher-Weg 18-20  
6500 Mainz

R. A. van Wagenen, J. D. Andrade  
College of Engineering  
Department of Bioengineering  
University of Utah  
Salt Lake City  
Utah 84112 (USA)

## **Weather in the West: A new perspective to weather education in a science center.**

Jason C. Shafer

Dept. of Meteorology, University of Utah, Salt Lake City, Utah

Joseph D. Andrade

Dept. of Bioengineering, University of Utah, Salt Lake City, Utah

### **1. INTRODUCTION**

Our weather experiences are based upon what we observe where we live, work, and play. In Utah and the adjoining regions, dramatic topography creates sharp contrasts in weather and climate over short distances. For example, it can be mostly sunny in the valley, while a blizzard rages in the nearby mountains. Weather in the West will offer a unique perspective to observing, questioning, and thinking about weather at the Utah Science Center. Weather in the West will allow visitors to explore how and why the mountains, valleys, basins, and lakes of the western United States affect their weather.

The Utah Science Center (USC) will be a new center for environmental awareness and education in an objective, informal, non-threatening, and open environment. The USC sees itself as the first “third generation” science center in that it will take visitors to new levels of interactivity. The USC has three main themes: (1) You are the experiment; (2) Energy, including the flow of energy in the atmosphere; (3) Home or Planet Earth and its environments and changes. The USC will open in spring 2007 in Salt Lake City and expects

about 400,000 visitors a year ([www.utah-sciencecenter.org](http://www.utah-sciencecenter.org)).

### **2. OBJECTIVE**

Our objective is to help develop more aware, educated, empowered citizens. This will be accomplished by inspiring visitors to observe and to be curious about how weather works, with a focus on the unique weather of the western United States. This will be accomplished by offering an engaging perspective that visitors can relate their weather experiences to. Leonardo da Vinci once said, “All knowledge is based on perspective.” We feel that one of the greatest challenges to this project is providing visitors adequate perspective to connect their real world experiences so that they can have a tangible experience that is accurately connected to atmospheric principles and processes. Weather in the West exhibits will attempt to do this through a number of activities.

### **3. ACTIVITIES**

Activities in the USC will consist of main floor interactive exhibits, demonstration carts, and small “theatre” demonstrations. In addition, special supervised activities in basement laboratories will be available.

Weather in the WEST will feature three phases of development. The core concepts of Weather in the WEST and their flow interac-

---

Corresponding Author Address: Jason Shafer, Meteorology Dept. Univ. of Utah, 135 S 1460 E RM 819, Salt Lake City, UT 84112; Email: [jshafer@met.utah.edu](mailto:jshafer@met.utah.edu)



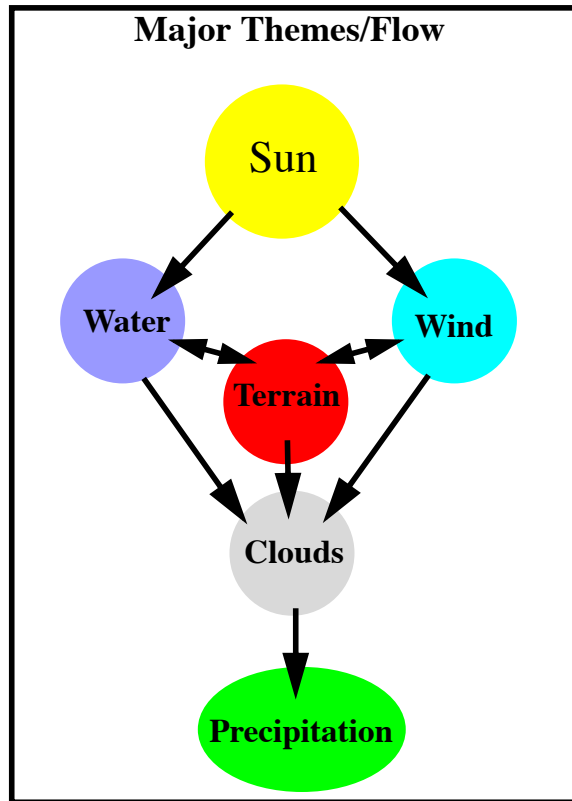


Figure 1. Major themes and flow of Weather in the West.

tions are shown in Fig. 1. We will focus largely on how and why terrain (Fig. 2) affects components of weather across the western United States. Weather in the West is being designed, funded, and developed in 3 phases. Phase I and

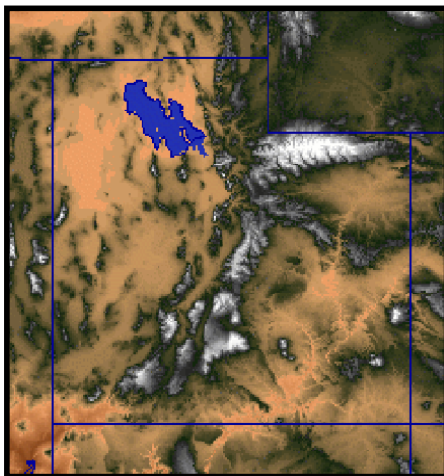


Figure 2. Complex terrain over Utah.

parts of II will be implemented upon opening; Phase II will be available 1-2 years later, and Phase III the following year.

### Phase I Activities

- *Water Tower Barometers*: Two giant water barometers will bring pressure concepts to life. Visitors will see atmospheric pressure changes in one barometer and make their own changes in another barometer.
- *Electric Atmosphere*: Lightning and thunder are created by visitors.
- *Weather Central*: A *Weather Hawk* weather station ([www.weatherhawk.com](http://www.weatherhawk.com))



Figure 3. Weather Central Exhibit of the Leonardo on Wheels traveling science center.

collects weather observations outside and transmits them to an interface on the exhibit floor. Figure 3 shows a similar set up during a recent exhibition of Leonardo on Wheels ([www.theleonardo.org/onwheels](http://www.theleonardo.org/onwheels)) the traveling portion of USC.

- *Wind power and you*: Connects the wind you can create with your power generation potential. We will create a windmill that can create electricity, using Leonardo da Vinci's windmill design. This may be combined with wind cannon.
- *Wind Cannon*: Human-powered wind cannon that allows visitors to create wind. Vis-

itors will be able visualize, feel, and measure the wind they create.

- *Pressure, wind, and mountains:* Interactive computer-based exhibit will allow visitors to explore atmospheric pressure and wind at various elevations across Utah. Instrumentation at nearby ski areas will be exploited for this purpose.
- *Explore your weather:* Interactive computer-based exhibit will allow visitors to experience weather at various locations across the western United States. This exhibit will use web cams (e.g., Fig. 5) and data from MesoWest ([www.met.utah.edu/mesowest](http://www.met.utah.edu/mesowest)) throughout the western United States.

## Phase II Activities

- *Weather Tug-of-War:* Allows two visitors to generate a pressure gradient and produce fluid flow or wind. This will be constructed from a transparent tube connecting two chambers. The visitors can modify the pressure in these chambers while an anemometer or ball value within the tube moves.
- *Mountains, winds, and clouds:* Will use pictures (e.g., Fig. 4), time-lapse videos,



Figure 4. Lenticular cloud over a cumulus over the Wasatch Mountains.

and fluid flow chambers to show how mountains can affect wind and clouds.

- *Mountains winds:* visitors will be able to explore winds created or enhanced by terrain over the western United States. This will involve short explanatory video segments along with visualization of such winds.
- *Water all around you:* This will show how much water is in the air and clouds around you. Measurements from the GPS Integrated Precipitable Water network will be exploited.
- *Water Hog:* Details people's annual consumption of water versus what falls at their home. This will be accomplished by having two transparent tubes that fill up with water. The demand and supply of water across various regions of Utah will be highlighted.

## Phase III Activities

- *Create a Cloud:* A warm cloud chamber allows visitors to create a cloud. Visitors will change the pressure and temperature of a moist chamber to produce or destroy a cloud.
- *Make it Snow:* A cold cloud chamber allows visitors to create a cloud and then make it snow. A storage freezer and video magnification will visualize the small snow flakes showing how the "Greatest Snow on Earth" is created.
- *Weather Lab:* Provides weather information for visitors to analyze and ultimately forecast their weather. It will use a series of wall-mount computer displays.
- *Can you beat the forecaster?* Visitors will make their own forecasts, and compete with each other, local meteorologists and personalities. Visitors will get to keep a print out, and a database will store visitors' numbers.
- *Natural Disaster:* Visitors will be able to create and explore avalanches, flash floods,

and other natural disasters over the western United States.

Within each of these phases, we will rotate through seasonal exhibits. For example, *Mountain Winds* may show how a cold pool/inversion develops in the winter, or how monsoon thunderstorms develop over mountains in the summer.

We will strive to connect all of these activities to something that is tangible and real to visitors' participation in these exhibits to make their experiences meaningful. For example, many of the exhibits will feature live web cameras (e.g., Fig. 5) from various locations. These images will be shown alongside nearby

images that portray the evolution of clouds during major weather events.

#### 4. SUMMARY

We feel that there is a tremendous potential for educating people about weather and their physical environment in a science center environment. Our approach to doing this involves connecting visitors' experiences to real weather in an interactive, entertaining, and mildly competitive atmosphere. We end by requesting your help with this project. We would like to share experiences and form links with other science centers and institutions. Your participation and input are especially needed in the following topics:

1. What activities could most effectively demonstrate the links between terrain and weather/climate?
2. What's the most effective way to connect one's personal weather experiences to fundamental atmospheric principles and processes?
3. Are you interested in being a partner?

Send your input to Joseph Andrade (see below) or Jason Shafer (see first page).

Joseph D. Andrade Ph.D.  
Department of Bioengineering  
University of Utah  
Utah Science Center  
c/o 949 Millcreek Way  
Salt Lake City, UT 84106

Email: [joeandrade@uofu.net](mailto:joeandrade@uofu.net)  
[www.utahsciencecenter.org](http://www.utahsciencecenter.org)

#### ACKNOWLEDGEMENTS

We thank the members of the USC Weather Team, especially Christine Watson-Mikell, Jodi Saeland, Jim Steenburgh, and

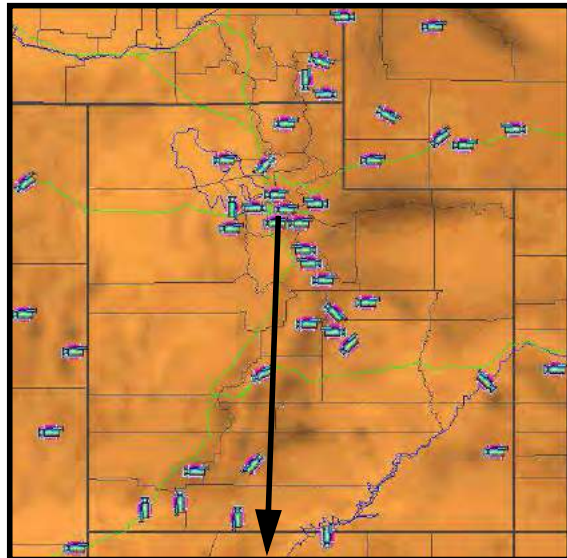


Figure 5. Web Camera map and example image

weather observations. In addition to these live images, we will likely use a suite of canned

Mike Anderson. We thank Jay Newlin at the Science Museum of Minnesota, Lis Cohen at the Museum of Science Boston, and the Mount Washington Observatory for helping our project by sharing their ideas and experiences. We also acknowledge in kind and grant support from Weather Hawk ([www.weather-hawk.com](http://www.weather-hawk.com)), Utah State Office of Education, and the Utah Energy Office.



*Polymer Preprints 16(2)(1975)*  
**Polymer Preprints 16(2)(1975)**

**GLOW DISCHARGE SURFACE TREATMENT FOR IMPROVED CELLULAR ADHESION**

by  
 Lee Smith, Douglas Hill, John Hibbs, Sun Wan Kim,  
 Joseph Andrade and Donald Lyman  
 Division of Artificial Organs  
 Salt Lake City, Utah 84112

By examining more closely cell-substrate adhesion interactions, additional insight may be gained into the phenomena of cell contact with natural and synthetic substrates. Most cellular processes occur while the cell is in some way interacting with a substrate. This interaction can be measured by several means--by the morphological changes observed in cells that spread to various degrees over a substrate surface, or by the degree of adhesion and attachment existing between the cell and substrate. Morphological changes, while perhaps the easiest to monitor, afford little in the way of quantitative insight. Adhesion is much more difficult to measure. However, if performed correctly, it can yield reproducible and quantitative information of the cell-substrate interactions.

While in vitro testing of cell substrate interactions is not perfect, it can supply knowledge, both for use in cellular biology and for applications to prosthetic devices. With the cell cloning techniques currently available, one can obtain and maintain many different types of cell lines with consistent characteristics. Although the cultured cell may be very different from the normal cell in situ, many cellular processes can still be investigated with well characterized cultured cells. Supplying a substrate with all the characteristics of normal in vivo tissue is impossible and unnecessary. Rather, the testing of synthetic polymer, metal and glass substrates--each with its own special characteristics--can easily reveal trends in biological compatibility. We can observe the change in cell-substrate interactions as a function of both cell and substrate parameters such as surface charge, wettability, chemical structure, topography and many others that may be related to the in vivo situation.

A number of techniques have been used to measure substrate-cell adhesion. In 1947 Dan attempted to measure cell adhesion quantitatively by using a jet or stream of water (1). Coman used microneedles to attempt to pull tissue cells from a substrate to investigate their adhesiveness (2).

More recently, Hochmuth, et al (3) used a rotating shear disc, similar to the one devised by Weiss, to measure the adhesion of red blood cells to synthetic substrates. Their work also illustrates the advantages of using well controlled techniques for measuring cell adhesion. Their results indicate that a minimum shear force of approximately 10 dynes/cm<sup>2</sup> is necessary to distract red blood cells from a glass surface. Polyethylene required about 4.6 dynes/cm<sup>2</sup>; siliconized glass required 3.5 dynes/cm<sup>2</sup> and Teflon 2.4 dynes/cm<sup>2</sup>. Not only were the natural surfaces investigated but these surfaces were also coated with various proteins to compare results. Their modification of Weiss's design (4) has the advantage of much higher shear force capability and a higher speed (up to 800 RPM), while maintaining laminar flow.

The use of a rotating shear disc reduces the number of problems encountered in controlling and defining the distractive shear force. Fibroblasts have been primarily used, however, to avoid incorrect conclusions regarding cell adhesion, cell types with different properties should be investigated. The usefulness of synthetic substrates is evident and measurement of adhesion to synthetic substrates can be applied to biological models as well as the materials used in prosthetic devices.

For this work we have attempted to accomplish 4 objectives:

1. To construct a device to easily and accurately measure cell-substrate adhesion.
2. To investigate the importance of proper substrate cleaning and preparation as it relates to cell adhesion.
3. To measure cell adhesion as a function of substrate composition and topography.
4. To measure and compare adhesion of both normal and transformed cells.

Illustrated in Figure 1 is the rotating shear disc equipment used for this work. It is a design somewhat modified from that used by Weiss (4) and also by Mahandas (3). A single rotating disc is spun in a temperature controlled medium of controlled viscosity such as phosphate buffered saline (PBS). A well controlled and defined shear force is produced at the fluid-disc interface, which is a function of the angular velocity of the spinning disc and the viscosity of the shearing medium (3,5).

For laminar boundary flow over the surface of the disc the shear stress ( $\tau_s$ ) produced at the fluid-disc interface is:

$$\tau_s = 0.8 r (\omega/\nu)^{1/2}$$

where  $r$  is the radial distance measured from the center of the disc,  $\omega$  is the angular velocity and  $\nu$  is the kinematic viscosity ( $\mu/\rho$ ). For a rotating disc  $\tau_s$  increases linearly with the distance from the center, assuming laminar flow exists.

To compare substrate preparation, 2 different techniques were utilized. The surfaces considered to be untreated were scrubbed in a dilute Ivory soap solution, rinsed in warm tap water and followed with a distilled water rinse. Samples were then rinsed in absolute ethanol followed by a final rinse in ethyl ether and allowed to air dry in a dust-free hood at least 12 hours. The treated surfaces went through the same treatment prior to their exposure to the radio-frequency glow discharge (RFGD) treatment (see Figure 2.) The plasma was generated with 25 watts of power and maintained at 200  $\mu$ Hg pressure using a purified argon atmosphere. After inserting the samples into the RFGD chamber it was evacuated to 1  $\mu$ Hg and filled with argon to 200  $\mu$ Hg pressure. The plasma treatment proceeded for 2 minutes and the chamber was re-evacuated to 1  $\mu$ Hg; and again backfilled with argon to atmospheric pressure before withdrawing the samples.

Both untreated and RFGD treated surfaces were quenched and stored in Dulbecco's Modified Eagle's Medium (DMEM) containing 10% fetal calf serum two hours prior to their use.

Substrate materials evaluated in this study were:

1. FEP, a fluorinated ethylene/propylene copolymer produced by Du Pont.
2. Glass cover slips, 1 1/2 x 22 mm in diameter manufactured by Corning, Type 0211.
3. Polystyrene, Lux brand cover slips, obtained from Lux Scientific Corporation. They are shipped pre-sterilized and cut into circular sections 1.5 x 25 mm.
4. Silastic rubber, a polydimethyl siloxane polymer. A medical grade, vulcanized, nonreinforced sheet provided by Dow Corning.
5. Polyurethane, block copolyether-urethanes-ureas. The copolyether urethanes, synthesized in Dr. D.J. Lyman's laboratory, are based upon polypropylene glycol, in ethylene-bis (4 phenylisocyanate) and ethylene diamine.



Experimental cell lines used included normal 3T3 fibroblasts a line established by G. Todaro and H. Green (6) in 1962 from Swiss mouse embryos. This cell line retains a high degree of cell contact inhibition and is an excellent cell to represent connective tissue fibroblast. The SV40-transformed 3T3 was developed by transforming a 3T3 cell via infection with an oncogenic virus type SV40. These transformed cells have reduced contact inhibition and demonstrate reduced adhesive properties (7).

The 3T12 fibroblasts are also a transformed version of the 3T3 cell, but exhibit different properties than the SV40-3T3 cells. The transformation process stems from growing 3T3 cells at much higher densities to achieve a cell with reduced contact inhibition properties (8). The normal and BCG activated mouse peritoneal macrophages were harvested directly from the peritoneal cavity of mice. These cells differ extensively from the types of fibroblasts (9,10) listed above. Cell suspensions were prepared and added to the test substrate samples and allowed to settle and attach to the test surface for 30 minutes. The samples were then spun on the shear disc for 2 minutes at controlled speeds, removed and fixed in ethanol followed by staining in 1:10 Giemsa Stain and distilled water. Microscopic examination consisted of counting the number of cells per unit area at different radial positions across the diameter of the circular test sample. These values were then compared to control samples, which were not spun. For each type of cell line and/or surface, a series of 5 separate test runs were performed. The results were then averaged for plotting percent of cells attached versus shear stress.

For brevity the results of only 2 cell types on 3 different surfaces will be illustrated. Figures 3a and 3b demonstrate the increased adhesion of the normal 3T3 fibroblasts to RFGD treated glass, Silastic rubber and FEP. The most dramatic change was observed with the FEP surface. The test samples with 3T3 cells were spun at 682.73 R.P.M. Corresponding with the large increase in cell attachment to FEP was a large increase in surface wettability as measured by contact angle of water. Contact angle of untreated FEP was  $94^\circ$ , after 2 minutes of RFGD treatment the contact angle was  $55^\circ$ . This corresponds to surface tensions of 17 dynes/cm and 34 dynes/cm respectively. Surface topography, when observed at 5300X demonstrated both glass and FEP surfaces to be smooth, while Silastic rubber was rough and irregular. Substrates tested with 3T3 cells including polystyrene (Lux cover slips) and 2 different polyurethanes demonstrated behavior similar to those observed with glass.

Results of adhesion tests performed with the SV40 transformed 3T3 were because of their reduced adhesive properties spun at a lower speed (271 R.P.M.). Illustrated in Figures 4a and 4b are the results of those experiments. Unlike the results with the 3T3 cells, there was very little change in adhesive properties of the transformed cells to the treated and untreated substrates, except with FEP, where a dramatic increase in adhesion was observed. Polystyrene and the polyurethanes exhibited no increase in adhesive properties similar to glass and Silastic rubber.

These few tests' results have just scratched the surface of valuable information that may be closely examined using a simple shear disc. The use of well characterized cell lines have proven a valuable tool to examine changes in adhesive properties of many substrates. The spectacular cell surface adhesive properties observed here may be much different than long-term adhesiveness. With short-term measurements one assumes that we are measuring the adhesive properties of the cell substrate rather than the cohesive strength of the cell. The ease and reproducibility of measuring cell adhesion with this technique could enable many cell-substrate interactions to be more closely and accurately monitored.

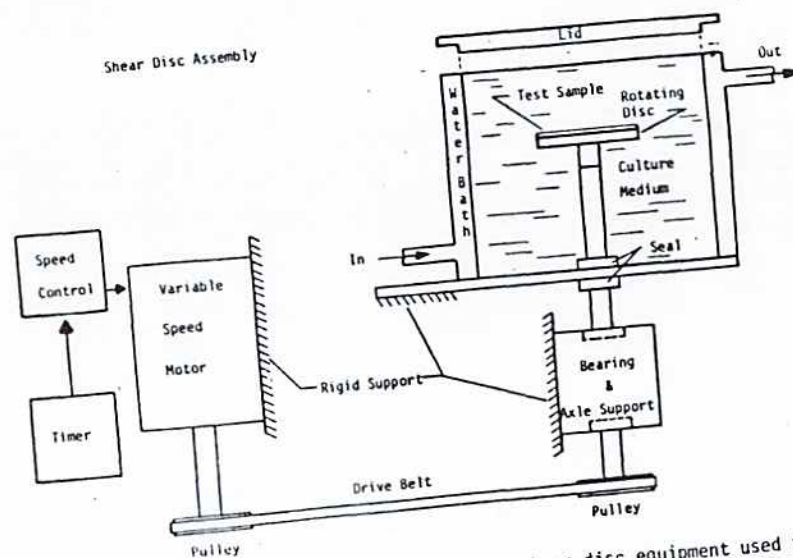


Figure 1. Illustrated above is the rotating shear disc equipment used for measuring cell attachment. The shear disc platform holds circular samples 25 mm in diameter that are spun either in culture media or phosphate buffered saline (PBS) at  $37^\circ\text{C}$ .

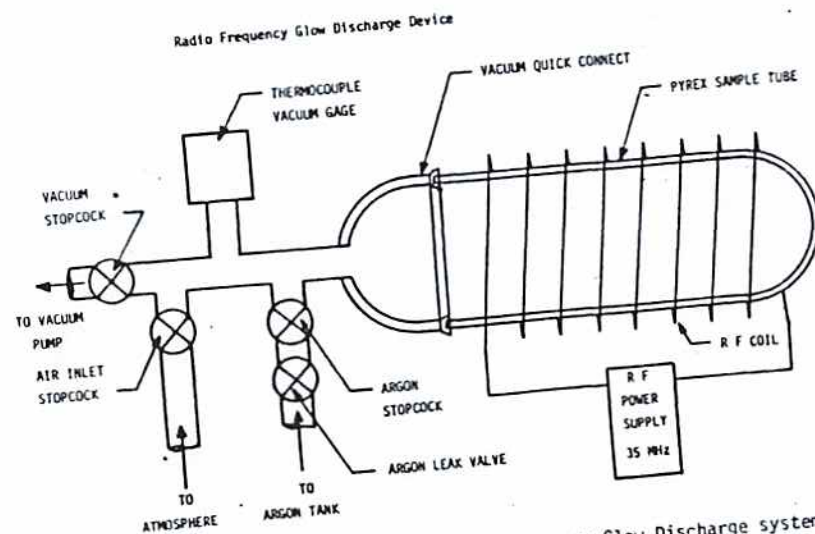


Figure 2. Above is illustrated the radio frequency Glow Discharge system used for treating the test samples to an inert gas plasma.



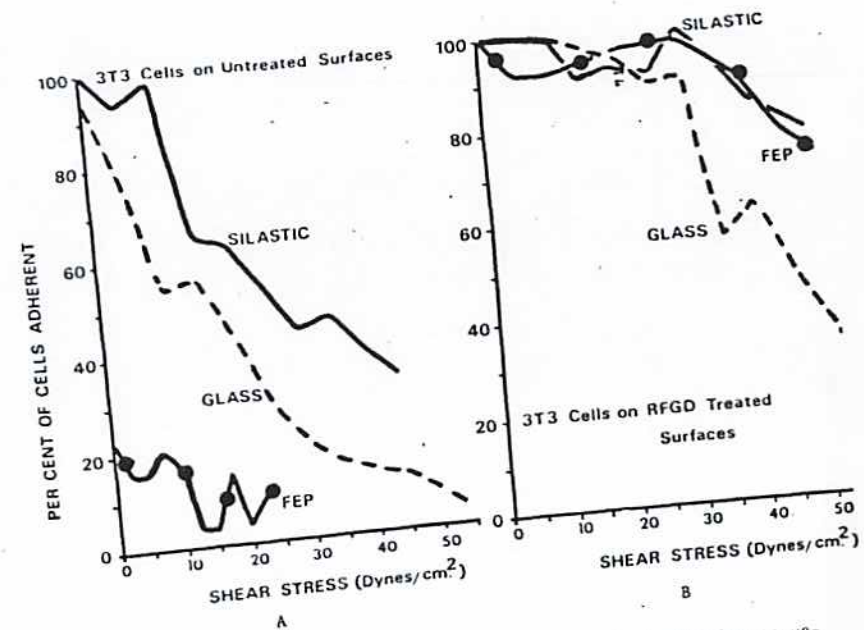


Figure 3a. Demonstrates the results of 3T3 fibroblast adhesion to untreated FEP, glass and Silastic rubber, as measured on the rotating disc equipment.

Figure 3b. Illustrates the adhesive properties of the 3T3 cell to the same substrates after they were treated for 2 minutes with an inert gas plasma.



Proceedings  
~~Abstracts~~, Int. Symp.  
Contact Lenses & Artificial  
Eyes 12-15 JULY, 1982  
Durham, England.

## CONTACT ANGLE ANALYSIS OF HYDRATED CONTACT LENSES

L.M. Smith\*, L. Bowman\*\*, and J.D. Andrade\*

Substrate surface energetics are most readily monitored via contact angle analysis. Unfortunately, contact angle data for ophthalmic lense materials is often misleading because measurements are performed on non-hydrated samples and seldom are both advancing and receding contact angles recorded. Wetting characteristics, incorporating Wilhelmy plate techniques can readily be measured and correlated to lense composition and surface treatment for optimization of wetting characteristics. Routine quality control, hydration changes, surface cleanliness, topography, and surface treatment can be easily monitored.

INTRODUCTION

Over eleven million people now wear contact lenses and sales of ophthalmic devices in 1982 is estimated to reach over 500 million dollars (1). With twenty years of experience and such a large market, it is surprising that so little data exists concerning the surface characteristics of ophthalmic lens materials.

One key element of success for a lens substrate is its degree of wettability (hydrophilicity). Early lens materials were based on hydrogel compositions that exhibited a high degree of water uptake and remained hydrophilic if kept wet (2, 3). For increased strength methacrylate copolymers have been incorporated. With greater consumer emphasis on comfort and ease of use, manufacturers have begun using more oxygen permeable polymers such as silicones and animal collagens. Increased oxygen transport through the lens extends the length of time the lens may be worn (4). Development of newer polymeric formulations and lens pretreatments require improved methods for surface characterization and long term quality assurance.

Hydrophobic and hydrophilic lenses behave differently in their environments. Proteins, lipids, minerals, and bacteria may absorb and adsorb differently depending upon the chemistry and wetting characteristics of the lens substrate (5, 6). Development of lens materials that minimize spot and deposit formation requires reliable wetting characterization. Likewise, quality assurance testing necessitates accurate hydration data, performed in a variety of environments. The analysis of the polymer-aqueous interface by wetting measurements is the focus of this article.

\*Department of Bioengineering, University of Utah, Salt Lake City, Utah  
84112 USA

\*\*Syntex Ophthalmics Inc., 10210 North 25 Avenue, Suite 300, Phoenix, Arizona  
USA



There are many techniques used to measure wetting behavior. We have had experience with two methods that can be applied to fully hydrated surfaces. Contact angles determined on nonhydrated (dry) surfaces are usually easier to obtain but, as we shall see, are not relevant for polymers used in an aqueous environment. One technique (7), uses captive air and octane bubbles measured on polymer samples inverted and submerged in water. The dispersion and polar components of the surface energy of fully hydrated surfaces can be estimated by this technique. Although useful this technique is slow and under normal circumstances only allows measurement of the polymer-water-air receding contact angle (8, 9).

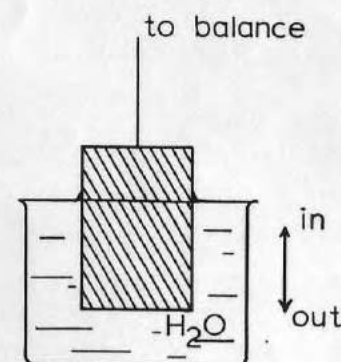
### Theory of Contact Angle Hysteresis

Most polymeric materials have more than one stable contact angle. There are usually two reproducible, stable contact angles: 1) an advancing contact angle measured when an aqueous solution is advanced over a previously unwetted surface; and 2) a receding contact angle observed when water recedes over a previously wet surface. The difference between the two angles is referred to as contact angle hysteresis. There have been several hypotheses offered to explain hysteresis (10). Langmuir (11) and others have suggested that it is due to the overturning of surface molecular groups as the aqueous solution advances and recedes over the polymer surface. At a polymer-water interface there is a thermodynamic driving force to minimize the interfacial tension by orientation of hydrophilic groups and side chains toward the water phase. In air, the driving force is to reduce the polymer-air interfacial tension by orientation of hydrophilic groups and side chains toward the air phase. Even with fairly rigid materials such as polymethylmethacrylate, there is sufficient surface mobility at room temperature to allow for such behavior. With fully hydrated materials, water acts as a plasticizer in the outermost surface region to enhance the surface mobility. Thus, a measure of only one contact angle, the advancing ( $\theta_{adv}$ ) or receding ( $\theta_{rec}$ ), is not sufficient for most polymers.

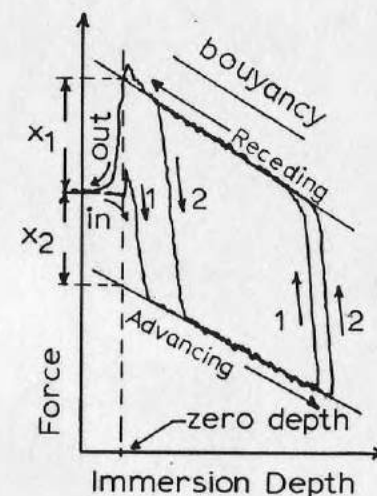
Wilhelmy, in 1863, developed a technique to directly measure the wetting force on surfaces at the solid-water-air interface (12). The Wilhelmy plate technique is simple, reliable, and perhaps "custom made" for use in characterizing the wetting behavior of fully hydrated polymeric materials. Measurements can be made with a variety of sample shapes and with most wetting solutions. Both advancing and receding contact angles are automatically obtained. More importantly, characterization may be made continuously during hydration.

### Techniques

For a detailed description of the equipment and methods, refer to the literature (10, 13). Included here are applications of this technique to the measurement of contact lens materials. The technique consists of suspending a sample (plate) of known dimensions from a balance or force transducer. The suspended sample is immersed into a wetting solution, usually ultraclean water or isotonic saline solution, at a slow controlled rate, i.e., 1 to 10 cm per minute. See Figure 1a and 2a. It is, in general, easier to move the wetting liquid rather than move the sample and balance. When the sample first begins to wet, a large force change is observed. If the sample is hydrophilic, a meniscus begins to advance up the sample perimeter; this is recorded as a positive force. Figure 1b illustrates a typical wetting curve for a thin rectangular hydrophobic sample. The sample will not readily wet and its inherent buoyancy (negative slope) must first be overcome. Continued immersion results in a stable slope that is a measure of the advancing contact ( $\theta_{adv}$ ) angle plus the sample's buoyancy. After a determination has been made for



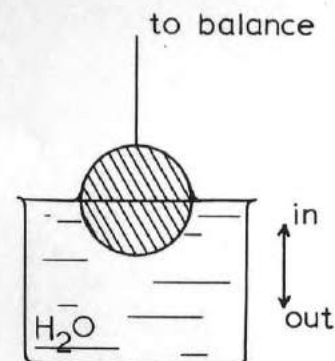
1(a)



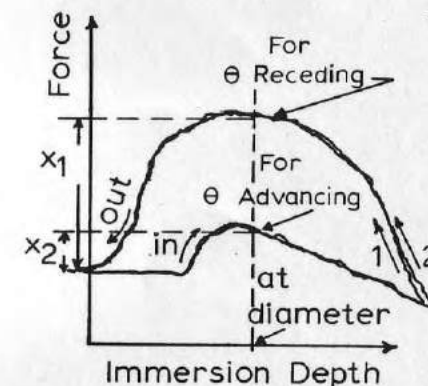
1(b)

Figure 1a. Wilhelmy plate configuration for flat thin plate sample. Fluid is raised and lowered over plate at 4.4 cm/min.

Figure 1b. An advancing and receding contact angle curves showing contact angle hysteresis.  $\theta_{adv} = -x_2/\gamma p$  where  $x_2$  is force,  $p$  = perimeter and  $\gamma$  = surface tension of wetting solution;  $\theta_{rec} = x_1/\gamma p$  where  $\theta_{rec} < 90^\circ$  and  $\theta_{adv} > 90^\circ$ .



2(a)



2(b)

Figure 2a. Wilhelmy plate configuration for round disc.

Figure 2b. Advancing and receding contact angles showing hysteresis of hydrophilic contact lens material. Due to buoyance effect, maximum force does not occur at disc diameter, but appear to the left. Force measurements are determined when disc is one half submerged ( $x_1$  and  $x_2$ ).

② adv, the wetting liquid is lowered to allow the sample to recede. This yields a second stable slope and a measurement of the receding contact angle ( $\theta_{\text{rec}}$ ) plus buoyancy. Repeated immersion and withdrawal cycles should retrace the same hysteresis curve. If the sample is interacting with the wetting solution, cycles will not repeat with time and the observed behavior is not representative of true hysteresis. Extrapolation of the slopes to zero depth of immersion allows calculations of the contact angles without having to consider buoyancy effects, e.g., forces  $x_1$  and  $x_2$ .

Figure 2b is a typical wetting curve for a round hydrophilic sample. Best results are obtained if the sample is thin, exposing more surface area and minimizing edge and buoyancy effects. A curve for a round, perfectly wetting (no hysteresis) disc, submerged half way is illustrated in Figure 3. Due to buoyancy effects, the maximum observed force does not coincide with the wetting force recorded at the disc diameter (f). If the negative force (b), due to buoyancy, is added to the observed force, we obtain the corrected wetting curve. For circular samples, the most accurate wetting determinations are made at the disc diameter, however, the volume of submerged disc needs to be calculated and used to correct for buoyancy at this point. The corrected curve should trace a perfect arc since the wetting force acts only at the perimeter. The buoyancy slope, is a volumetric relationship, is more linear, and thus tends to bend the observed wetting curves from perfect radial arcs. To calculate the advancing and receding contact angles of round discs, we record the forces  $x_1$  and  $x_2$ , occurring when the disc is exactly one half submerged, See Figure 2b. To  $x_1$  and  $x_2$ , we add the buoyancy factor to calculate the receding and advancing contact angles, respectively.

We used the movable cross arm of a mechanical tester to raise and lower the wetting liquid at controlled speeds. The position of the cross arm was fed to a x-y plotter along with the force output from a Cahn-RM2 electrobalance. The balance is vibrationally isolated from the mechanical tester, and all equipment is enclosed to maintain constant temperature (20°C) and humidity (35% RH).

Equation 1 is used to calculate both  $\theta_{adv}$  and  $\theta_{rec}$ .

$$\cos \theta = \frac{mg}{pY} + \frac{V\rho g}{pY} \dots \dots \dots (1)$$

where  $m$  = mass as determined by force transducer [grams]  
 $g$  = local gravitational force 979.3 [dynes/gram]  
 $p$  = perimeter of sample acting on liquid interface [cm]  
 $\gamma$  = surface tension of wetting liquid, for water at 20°C = 72.6 [dynes/cm]  
 $V$  = volume of sample immersed at a particular depth  
 $\rho$  = density of wetting liquid

The second term is the buoyancy factor and can be eliminated when curves are extrapolated to zero depth of immersion. Accurate determinations of  $\gamma$  for a particular wetting liquid can be made by applying the Wilhelmy plate technique to a perfectly wetting surface such as freshly treated radiofrequency glow discharged glass coverslips or fully hydrated agarose coated samples. One assumes the sample is perfectly wetting, then  $\cos \theta = 1$  and we can solve for  $\gamma$ . Samples that are perfectly wetting will generally display no contact angle hysteresis and  $\theta_{adv}$  will equal  $\theta_{rec}$  as shown in Figures 3 and 4.

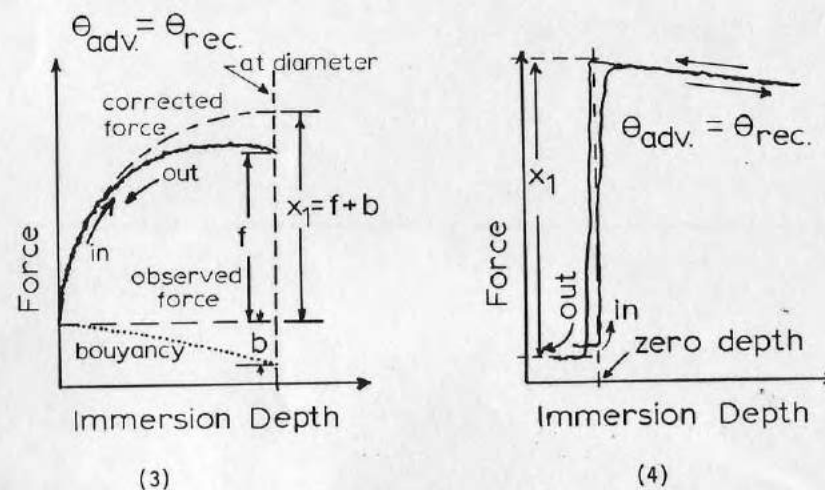


Figure 3. Wilhelmy plate curves for a perfectly wetting round disc, i.e.,  $\theta_{adv} = \theta_{rec}$ . Bouyancy is a function of the disc volume and decreases inversely with the submerged disc segment.  $b \propto 1/(RS - cd)$  where  $R$  = radius,  $S$  = arc length,  $c$  = cord length and  $d = (R - \frac{1}{2} \text{Immersed depth})$ . The force curve corrected for bouyancy is directly proportional to the disc perimeter and traces a perfect arc.  $x_1 \propto 2R \sin S/2R$ . For small round discs, better accuracy is achieved by calculating  $\theta_{adv}$  and  $\theta_{rec}$  at disc diameter.

Figure 4. Contact angle curve typical of perfectly wetting rectangular plate. Curves are extrapolated to zero depth of immersion, and referenced to point where plate first make contact with wetting solution during advancing mode. In withdrawal mode, solution meniscus can rise above wetting solution level making zero depth of immersion difficult to locate. Force determination is referenced to final withdrawal tare weight. Perfectly wetting samples are used in determining ( $\gamma$ ) surface tension of wetting solutions and evaluating the presence of surface active contaminants.

### Methods

Circular 12 mm x 1 mm contact lens disc blanks were examined at 100X for evidence of gross contamination. Samples appearing clean and free from scratches were used for analysis. Three samples were chosen for each material formulation. Wetting solutions were prepared from double distilled water with 50 mg/liter of NaN<sub>3</sub> and 1.5 ppm Cl added/liter to avoid bacterial contamination. Treater water proved to be free from bacteria and pyrogens for greater than 15 days. Surface tension of wetting solution was checked on each batch of prepared water and all contact angle determinations were made in fresh solutions:  $\gamma_{H_2O}$  was  $72.6 \pm .2$  dynes/cm at 20°C.

Many commercial polymers contain extractables that can leach out of the bulk and contaminate the wetting solutions. Many monomers which may be present in residual amounts can be surface active. Low molecular weight, uncrosslinked polymer is often surface active. Various preservatives may also be surface active. This technique was used to measure for extractables during hydration by sampling the surface tension ( $\gamma$ ) of the hydrating solution periodically.

### Results

In Table I are the contact angles and results of hydration effects observed with three different lens formulations. Polycon II and Polycon I are both methacrylate-silicone copolymers with different silicone content. The polymethylmethacrylate (PMMA) is of contact lens grade. All three materials were provided by Syntex Ophthalmics, Phoenix, Arizona.

TABLE I  
Water Contact Angles as a Function of  
Hydration Time of Contact Lenses

Length of Hydration	Polycon II			Polycon I			Polymethylmethacrylate*		
	$\theta^{**}$ adv	$\theta^{**}$ rec	captive bubble	$\theta$ adv	$\theta$ rec	captive bubble	$\theta$ adv	$\theta$ rec	captive bubble
Dry	82	50	61	86	58	67	79	54	63
1 day	69	32		67	34		64	37	
2 days	65	26		52	33		59	33	
3 days	63	21		57	21		56	21	
4 days	64	12		61	20		51	20	
7 days	47	10	19	56	24	34	54	22	35

\* contact lens grade

\*\* tolerance  $\pm 2^\circ$

When measured dry without prior hydration all materials appear hydrophobic (nonwetting), both in the advancing and receding mode. After continued hydration both advancing and receding contact angles decrease. Advancing contact angles are always higher than receding angles, and rarely to both decrease at the same rate. After seven days of hydration all three materials in Table I are considerably more hydrophilic. Included for comparison in Table I are underwater captive air bubble measurements made at one and seven days. The underwater bubble technique, although it provides a measurement approaching the  $\theta$  receding angle, is seldom as low as the dynamic receding angle. Likewise, sessile drop measurement made in the advancing mode will approximate the dynamic advancing angle, but will not be quite as high.

### Conclusions

The Wilhelmy plate technique has proven effective in measuring dynamic water contact angles, both advancing and receding. Measurements can be directly made with most sample configurations. Results given here are for flat plates or round discs. With appropriate mathematical analogs and corrections for buoyancy, wetting curves for converging meniscus lenses may be made directly on lathed samples. The advancing and receding contact angles give a more accurate picture of the dynamic hydration changes observed in contact lens materials. These wetting characteristics are more representative of surface energetics for ophthalmic lenses in situ. To properly understand and perhaps avoid long term lens problems, we must know what wetting changes occur. Polymer-water interactions to a large extent determine which proteins will adsorb and how they adsorb. Optimization of surface wetting characteristics is one possible approach to help avoid long term protein adsorption and deposition problems. To develop optimum polymer surface wetting characteristics, accurate, contact angle data of fully hydrated materials is essential.

### REFERENCES

1. Seligmann, J., and Gosnell, M. 1981, *Newsweek*, Medicine Section.
2. Wichterle, O., and Lim, D., 1960, *Nature*, **185**, 117.
3. Wichterle, O., U.S. Patent #2,976,576, 1961.
4. Hesaka, S., Mori, Y., Kenjo, H., Tanzawa, H., Momose, T., Magatani, H., and Nakajima, A., 1979, *Kobunshi Ronbunsha*, **36**, 265.
5. Freeman, H., and Berta, R., 1977, *Proc. of 35th Annual Meeting Elec. Micro. Sci. Amer.*, 174.
6. Dexter, S.C., 1979, *J. of Colloid and Interface Science*, **70**(2), 346.
7. Andrade, J.D., King, R.N., Gregonis, D.E., and Coleman, D.L., 1979, *J. Colloid Interface Science*, **72**, 488.
8. Smith, L.M., 1979, Ph.D. Thesis, "Cell Adhesion as Influenced by Substrate Surface Properties," Materials Science and Engineering Department, University of Utah.
9. Gregonis, D.E., Hus, R., Buerger, D.E., Smith, L.M., and Andrade, J.D., "Wettability of Polymers and Hydrogels as Determined by Wilhelmy Plate Technique," to be published in *Solvent-Property Relationships in Polymers*, Seymour, R.D., and Stohl, G.A., eds., Pergamon Press, (1982).



10. Johnson, R.E., Jr., and Dettre, R.H., "Wettability and Contact Angles," in Surfaces and Colloid Science, Matijevic, E., Ed., Vol. 2, Wiley, New York (1969), 85.
11. Langmuir, I., 1938, Science, 87, 493.
12. Wilhelmy, L., 1863, Ann. Physik, 119, 177.
13. Smith, L.M., Doyle, C., Gregonis, D.E., and Andrade, J.D., "Surface Oxidation of Cis-Trans Butadiene," J. of Appl. Poly. Sci., (1982), in press.

# Surface Oxidation of Cis-Trans Polybutadiene

L. SMITH,\* C. DOYLE, D. E. GREGONIS, AND J. D. ANDRADE,  
Department of Materials Science and Engineering and Department of  
Bioengineering, University of Utah, Salt Lake City, Utah 84112

## Synopsis

Uncrosslinked cis-trans polybutadiene films were prepared on ultraclean glass microscope slides by uniform dipping. The samples were stored in different environments prior to evaluation of surface oxidation by dynamic contact angle using the Wilhelmy plate method and by X-ray photoelectron spectroscopy (XPS). Storage conditions evaluated were: (1) laboratory air at 20°C and 30% relative humidity; (2) vacuum at 0.1 torr; (3) distilled water equilibrated with air; and (4) degassed distilled water. XPS and contact angle analysis indicate that samples exposed to air undergo significant surface oxidation within 8 h. Exposure of polybutadiene to air-equilibrated water results in slower oxidation. Samples stored in degassed water demonstrated less surface oxidation. Vacuum-stored samples demonstrated the least surface oxidation. Dynamic contact angle measurements demonstrated that receding contact angles are more sensitive to changes in surface oxidation than are advancing contact angles, as expected. Changes in surface wetting characteristics are readily observed after only 1 h in laboratory air, although XPS analysis does not show evidence of oxidation within 4 h of air storage.

## INTRODUCTION

It is well known that butadiene rubbers are susceptible to environmental oxidation by ozone and by thermal and photochemical methods.<sup>1-4</sup> To stabilize these materials, antioxidants of several different types are used.<sup>5</sup> Our interests in the biologic interaction of these polymers required a knowledge of the oxidative stability of additive-free polybutadiene under normal laboratory handling conditions. A recent study showed that the adhesion characteristics of polybutadiene films is dependent upon short exposures to air, indicating that surface oxidation takes place very rapidly.<sup>6</sup> In this report, the surface oxidation of cis-trans polybutadiene exposed to various laboratory handling conditions is measured by Wilhelmy plate dynamic advancing and receding water contact angles and by X-ray photoelectron spectroscopy.<sup>7</sup>

## EXPERIMENTAL

Uncrosslinked cis-trans polybutadiene was obtained from Aldrich Chemical Company, Lot #07. Proton nuclear magnetic resonance (NMR) spectra show the geometry of this polymer to be 39% 1,4-cis, 52% 1,4-trans, and 9% 1,2-configuration. Gel permeation chromatography (GPC) in tetrahydrofuran (THF) using narrow-molecular-weight-distribution polystyrene calibration standards produced the following molecular weights:  $\bar{M}_n = 6.95 \times 10^5$  and  $\bar{M}_w = 1.85 \times 10^6$ . The polymer was purified by dissolving in toluene, extraction with 5% aqueous sodium hydroxide, drying ( $\text{Na}_2\text{SO}_4$ ), and precipitation into 2-propanol.

\* To whom reprint requests should be directed.

These results should also be of significance to the study of butadiene-containing copolymers such as styrene-butadiene random copolymers and various styrene-butadiene di- and triblock copolymers. It is also important to note that the contact angle and XPS methods used are highly sensitive to surface modification and in particular to oxidation. Bulk analysis of such polymer films, such as by transmission infrared or even attenuated total reflectance infrared spectroscopy, would not be expected to show significant evidence of oxidation until much higher levels were reached. It is also important to note that these studies were performed on antioxidant-free material. The surface stability of antioxidant-containing material with respect to surface oxidation remains to be determined.

## CONCLUSIONS

Surface oxidation of cis-trans polybutadiene was determined using both advancing and receding dynamic contact angles as measured by the Wilhelmy plate technique and by X-ray photoelectron spectroscopy. The air-exposed surface undergoes rapid oxidation detectable by water contact angles within 1 to 4 h and by XPS after 4 h. Storage of samples under vacuum or in the absence of oxygen<sup>6</sup> essentially eliminates the surface oxidation. The Wilhelmy plate contact angle technique and X-ray photoelectron spectroscopy are useful tools for evaluating the surface characteristics of polymers. Antioxidant-free cis-trans polybutadiene can be stored under vacuum for up to 120 h without significant surface oxidation. Storage in oxygen-free water results in 2-3% surface oxidation after 24 h. Storage in oxygenated water or in air results in significant oxidation after 4 h.

This work was supported in part by NIH Grant HL26469. The authors are very grateful for the technical assistance of Ms. Diane Cress.

## References

1. S. W. Beavan and D. Phillips, *Eur. Polym. J.*, **10**, 593 (1974).
2. R. L. Pecsok, P. C. Painter, J. R. Shelton, and J. L. Koenig, *Rubber Chem. Technol.*, **49**, 1010 (1976).
3. J. F. Rabek, J. Lucki, and B. Ranby, *Eur. Polym. J.*, **15**, 1089 (1979).
4. J. F. Rabek and B. Ranby, *J. Appl. Polym. Sci.*, **23**, 2481 (1979).
5. *Modern Plastics Encyclopedia*, J. Agranoff, Ed., McGraw-Hill, New York 1979, p. 245.
6. R. K. Chang, A. N. Gent, C. C. Hsu, and K. S. Sehgal, *J. Appl. Polym. Sci.*, **25**, 163 (1980).
7. D. T. Clark, *Adv. Polym. Sci.*, **24**, 126 (1977).
8. S. M. Hall, J. D. Andrade, S. M. Ma, and R. N. King, *J. Electron Spectrosc. Related Phenom.*, **17**, 181 (1979).
9. J. D. Andrade, R. N. King, D. E. Gregonis, and D. L. Coleman, *J. Colloid Interfac. Sci.*, **72**, 488 (1979).
10. L. M. Smith, Ph.D. thesis, University of Utah, Department of Materials Science and Engineering, June 1979.
11. R. E. Johnson and R. H. Dettre, in *Surface and Colloid Science*, Vol. 2, E. Matijevic, Ed., Wiley, New York, 1969, p. 85.
12. R. E. Johnson, R. H. Dettre, and D. A. Brandreth, *J. Colloid Interfac. Sci.*, **62**, 205 (1977).
13. I. Langmuir, *Science*, **87**, 493 (1938).
14. D. E. Gregonis, R. Hsu, D. E. Buerger, L. M. Smith, and J. D. Andrade, in *Solvent-Property Relationships in Polymers*, R. B. Seymour and G. A. Stahl, Eds., Pergamon, New York, 1982.

Received May 14, 1981

Accepted August 25, 1981

The polymer was stored as a 3% solution in toluene under argon until use. Polymer films were prepared by slow, uniform dipping of cleaned glass microscope coverslips and 10 mm × 9 mm × 1 mm glass samples. Film thicknesses produced by this procedure measured approximately 2  $\mu\text{m}$ . The films were dipped and dried in air, a procedure which takes normally 0.5 h, and then vacuum dried at 0.1 torr pressure for 24 h to assure removal of solvent. The 0.5-h air exposure is thus the background level for the oxidation study.

X-Ray photoelectron spectroscopy (XPS) was done with a Hewlett-Packard 5950B instrument using monochromatic Al  $K\alpha_{1,2}$  radiation (1487 eV) with 800 W power at the anode; the spectra were charge referenced to the C-1s alkyl binding energy at 284 eV. Photoelectron spectra were obtained utilizing ten scans over a 20-eV binding energy range. Oxidation was monitored by use of the oxygen-1s peak intensity and by attenuation of the  $\pi-\pi^*$  carbon-1s shakeup satellite due to olefinic bonding<sup>7</sup> as well as from the chemical shift features of the carbon-1s photoelectron peak. The  $\pi-\pi^*$  carbon signal is observed at +7 eV from the main alkyl carbon line at 284 eV. The mean free path of both the C-1s and the O-1s photoelectrons is approximately 60 Å.<sup>8</sup> As the Hewlett-Packard instrument used here has a sample geometry in which the detected electrons are in a path 38.5° from the surface plane, about 63% of the signal detected is from the topmost 40 Å of the sample.

### Wilhelmy Plate Technique

In our laboratory, two techniques have been extensively used for measuring contact angles on fully hydrated surfaces. One technique consists of measuring captive air and octane bubbles on inverted samples submerged in water. The polar and dispersion components of the surface energy of the fully hydrated surface<sup>9</sup> can be estimated by this method. Work by Smith<sup>10</sup> and others has demonstrated good correlation between biologic cell adhesion to surfaces and their captive air and octane contact angle measurements. The captive air and octane contact angle technique, while providing useful information concerning the interface energetics, is rather slow to perform and, under normal circumstances, only provides a measure of the polymer-water-air receding contact angle.<sup>9-12</sup>

Most polymers demonstrate both an advancing and receding stable contact angle. The difference between  $\theta$  advancing and  $\theta$  receding is defined as contact angle hysteresis. Many hypotheses have been presented to explain hysteresis.<sup>11</sup> Langmuir<sup>13</sup> suggested that hysteresis is due to the overturning of molecules as the liquid advances and recedes over the surface.

Since most polymer systems display some form of hysteresis, the more informative Wilhelmy plate technique has been employed in our laboratory for more careful surface evaluation. The technique is simple and requires only a modest investment in equipment. The requisite equipment is already available in most laboratories. For these studies, a standard mechanical testing device (Scotts SRE500 mechanical testing machine) is used to raise and lower a beaker of 2× distilled water at controlled speeds of approximately 40 mm per minute. Situated above the container is a Cahn electrobalance (model RM-2) which supports the test sample on a fine thread. The balance system is mounted separately from the mechanical tester and is vibrationally isolated (see Fig. 1). The mechanical

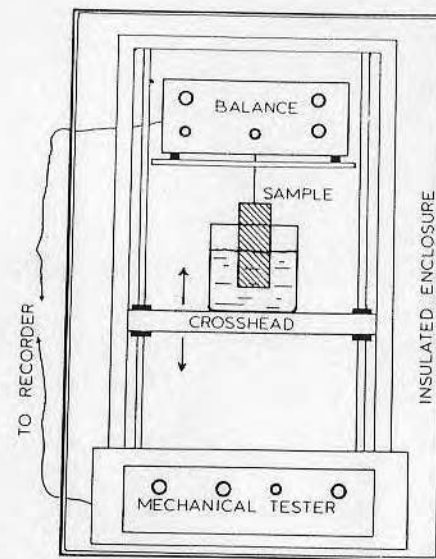


Fig. 1. Schematic of Wilhelmy plate-equipment. A Scotts mechanical tester is used to raise and lower wetting liquid over sample interface at 40 mm/min. Wetting forces are measured on Cahn electrobalance. Equipment is entirely enclosed in temperature-controlled enclosure maintained at 20°C and 30% relative humidity.

tester and balance are contained in an insulated enclosure maintained at constant temperature (20°C) and humidity (30% RH). Various other systems for measuring the wetting force on the test plates have been used by other investigators,<sup>11-13</sup> including chain balances, strain gauges, and linear differential transformers. Electrical signals from the balance and crosshead travel are fed to an X-Y plotter to obtain the wetting curves [see Figs. 2(a), 2(b), and 2(c)]. Routine calibration of the electrobalance is readily performed by the addition of 100 or 200 mg tare weights. With the equipment described, a weight sensitivity of about 3.8 mg/mm is adequate for use with glass coverslips. For very small samples such as fibers and small tubing, a factor-of-10 more sensitivity is required.

As the crosshead is raised, the sample begins its immersion into the test fluid. When the sample first touches the fluid, a meniscus is formed and, as penetration of the sample into the liquid continues, the contact angle levels off, resulting in a constant slope on the X-Y recorder, which is a measure of the advancing angle. After some distance of immersion (2.5–3.0 cm), the process is reversed, the wetting liquid is lowered, and a constant measure of the receding angle is observed. Random vibrations resulting from the movement of the liquid over the sample surface lower the free energy barriers, allowing the advancing angle to more closely approach the maximum theoretical low-energy contact angle. Likewise, the receding angle more closely approaches the maximum high-energy surface contact angle.<sup>11</sup>

A typical curve for cis-trans polybutadiene is illustrated in Figure 2(a). The sample is immersed to a depth of about 2.5 cm (path 1) and then retracted. A second immersion is followed in path 2 that retraces exactly the advancing and



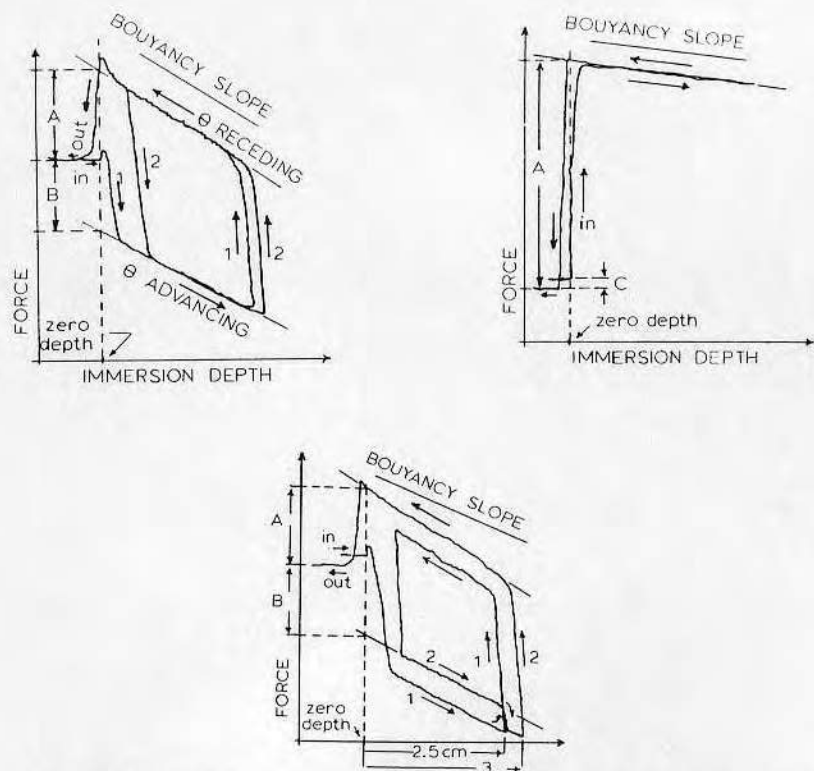


Fig. 2. (a) Typical Wilhelmy plate wetting curve of a polybutadiene sample. The buoyancy slope parallels both advancing and receding contact angles. The sample was taken through two successive dipping cycles to demonstrate reproducibility. Displacement A is used to compute the receding angle, while displacement B is used to compute the advancing angle. Curves are measured at the point of zero depth of immersion so the buoyancy effect can be neglected. (b) Wetting characteristics for hydrated, glow-discharged mica. The advancing curve is identical to the receding curve and parallel to the buoyancy slope. The slope is evaluated at zero depth of immersion. Note that the sample weight coming out of the wetting solution is less than the weight prior to the dipping point. The weight difference  $c$  is due to retained water droplets attached to the sample during hydration. Ultraclean, glow-discharged mica is assumed to be perfectly wetting and is used to measure the surface tension of wetting solutions. (c) Wetting curves of a nonhydrated hydrogel, poly(hydroxyethyl methacrylate). Due to the interaction of water with the nonequilibrated gel, the wetting curves do not parallel the buoyancy slope. Successive wetting cycles demonstrate increased wetting within seconds of a first immersion, demonstrating nonequilibration.

receding curves in path 1. This indicates that no additional equilibration is taking place and that the water is not further interacting with the test sample. The buoyancy slope for the glass coverslip parallels the wetting curve.

Shown in Figure 2(b) are the wetting curves of radiofrequency glow-discharged (RFGD) mica. Freshly cleaved mica is extremely smooth, and, with a 2-min RFGD treatment in helium, it can be made perfectly wetting with no contact angle hysteresis. This also allows for accurate assessment of liquid surface tensions.

For simplification, straight-line approximations of the advancing and receding slopes are made and extrapolated to zero depths of immersion, and the buoyancy factor in eq. (1),  $V\rho g/p\gamma$ , can then be eliminated. Force A [Fig. 2(a)] is used to compute  $\theta$  advancing, and force B [Fig. 2(a)] is used to compute  $\theta$  receding. The basic equation is

$$\cos \theta = \frac{mg}{p\gamma} + \frac{V\rho g}{p\gamma} \quad (1)$$

where  $m$  is mass of the slide (g) as measured via electrobalance;  $g$  is local gravitational force (979.3 dyn/g);  $p$  is perimeter of sample (cm);  $\gamma$  is surface tension of wetting liquid; for water  $\gamma = 72.6$  dyn/cm at 20°C;  $V$  is volume of immersed sample at a particular depth; and  $\rho$  is density of wetting liquid. Zero depth of immersion is more readily observed as the sample first touches the water surface. When the sample is retracted from the water, a meniscus is carried above the water surface for some distance, depending upon the surface tension of the wetting liquid and the wetting characteristics of the sample.

In Figures 2(b) and 2(c), it is observed that the weight of the sample when withdrawn is not necessarily the same as when it is immersed, depending upon whether the sample is hydrated or nonhydrated. The initial weight and final weight may or may not be equal. For calculation purposes, the weight after sample retraction is used for measuring the force displacements. Measurements are frequently made with unequilibrated hydrogel systems, such as poly(hydroxyethyl methacrylate). Illustrated in Figure 2(c) are wetting curves of a nonequilibrated hydrogel surface. Note that the second path, yielding lower angles, does not retrace the first, because water is interacting with the gel surface and, because it interacts longer at the bottom than at the top, the buoyancy slope differs from the sample wetting slope. If the gel sample had been fully equilibrated, the first immersion path would look like Figure 2(a) and succeeding curves would be similar to Figure 2(b), showing no hysteresis.

It has been shown by Johnson et al.<sup>11</sup> that advancing angles are more reproducible on lower-energy (hydrophobic) surfaces, whereas receding angles are more reproducible on higher-energy (hydrophilic) surfaces. The dependence of advancing and receding angle measurements on the speed of immersion and withdrawal of the sample was also demonstrated. Speeds over 100 mm/min seem to influence the advancing angle more than the receding angle and are more noticeable on heterogeneous surfaces as compared to homogeneous surfaces. In general, better measurements are obtained with immersion and withdrawal speeds of less than 50 mm/min.

## Methods

Polymer solutions are prepared as 3 wt % solutions and filtered through 0.1- $\mu$ m filters into precleaned bottles. Ultraclean glass coverslips (Corning Glass), 24 mm by 60 mm, are slowly dipped into the polymer solution to coat both sides uniformly. These samples are air dried for approximately 0.5 h, followed by further drying for solvent removal in a vacuum desiccator (0.1 torr) at 20°C for 24 h. Following desiccation, samples are handled according to their specific protocol prior to measurement.

After 24 h of vacuum drying, the polybutadiene specimens were submitted

to each of the following environments: (1) laboratory air at 20°C and 30% relative humidity, (2) 2× distilled water equilibrated with air, (3) degassed distilled water, and (4) vacuum at 0.1 torr. Water was degassed by boiling and by argon purge. The water-soaked samples were stored in sealed polyethylene slide holders. For the degassed water-equilibrated samples, the slide holders were filled to eliminate any air pockets and then sealed. Samples were tested after exposure periods of 0, 4, 7, 24, and 92 h. For XPS analysis, water-soaked samples were dried for 2 h under vacuum before measurement. The air- and vacuum-stored samples were run immediately. All contact angles were measured immediately after the required time had elapsed. The hydration effect on contact angle is observable; after each measurement the samples were vacuum dried and remeasured dry. A slight increase in hydrophobicity was noted in the dried samples.

## RESULTS AND DISCUSSION

XPS analysis of the oxygen-1s, carbon-1s, and C-1s  $\pi-\pi^*$  satellites shows that exposure to air for times greater than 4 h results in oxidation of the surface of polybutadiene. The air-equilibrated water environment resulted in a much lower rate of oxidation. The desiccator-stored samples showed the least degree of surface oxidation of the storage environments evaluated.

Representative carbon-1s spectra are given in Figure 3. Only the 4 and 24-h storage data are included for the vacuum [Fig. 3(a)], water [Fig. 3(b)], and air

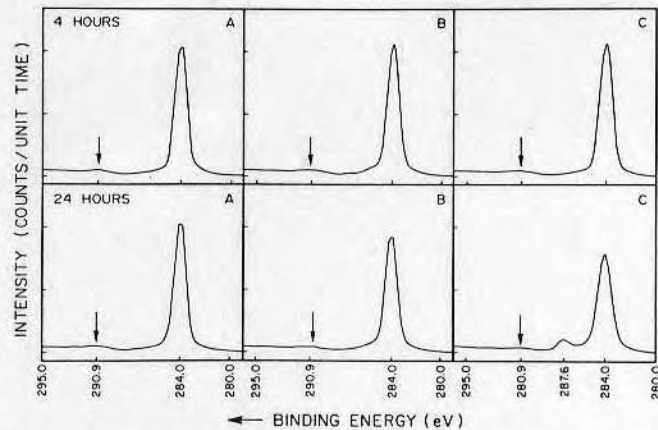


Fig. 3. Carbon-1s X-ray photoelectron spectra of cis-trans polybutadiene surfaces. (a) Samples stored in vacuum desiccator at 0.1 torr pressure, 20°C, for 4 h (top) and 24 h (bottom). (b) Samples stored in deionized/distilled water at 20°C for 4 h (top) and 24 h (bottom). (c) Samples stored in air in a laminar-flow, filtered air bench at 20°C, 30% RH for 4 h (top) and 24 h (bottom). Note the major C-1s peak located at 284.0 eV and the  $\pi-\pi^*$  satellite peak at 290.9 eV. Air-stored samples develop significant surface oxidation at storage times exceeding 4 h. The 24-h air-stored sample (bottom right) shows the presence of an oxidized carbon peak at 287.6 eV (change of 3.6 eV), a characteristic feature for oxidized polybutadiene. The O-1s peak (not shown) analysis confirms the presence of oxidation. Minor differences in peak heights from panel to panel are not necessarily significant. Peak ratios and positions within individual panels are significant. Vertical scale bar represents 50,000 counts/channel.

[Fig. 3(c)] storage environments. The main C-1s line is charge-referenced to 284.0 eV. The  $\pi-\pi^*$  shake-up satellite is present at 6.9 eV higher binding energy (290.9 eV), as expected. No evidence of surface oxidation is present. Such evidence would be an asymmetry in the main C-1s peak resulting in a high binding energy tail or even distinct features. Such features are clearly evident in Figure 3(c), bottom, the 24-h air specimen. The peak at 3.6 eV from the main peak is characteristic of oxidized polybutadiene and could be due to a carbonyl-like carbon-oxygen state. A more detailed XPS study, including detailed analysis of the O-1s spectra, could provide more definitive information on the mechanism of oxidation.

The contact angle data shows comparable results (Fig. 4). The receding contact angle is more sensitive to surface oxidation than is the advancing angle. Both advancing and receding angles are quite stable to vacuum storage, indicating minimum oxidation under vacuum storage conditions. The oxidation of polybutadiene in air is rapid as noted by a decrease in the receding angle after the first hour, although 4 to 10 h of air storage are required before relatively large decreases in the advancing and receding angles (5 and 10° decreases, respectively) are noted. The water-soaked samples were measured as soon as their exposure time was finished. Hydration versus nonhydration of samples affects their contact angles, therefore, typically water-equilibrated materials which are not susceptible to oxidation still result in a decrease in contact angle.<sup>14</sup> To correct for this factor, a few samples were measured wet, then dried in vacuum and remeasured dry. Thus, water-N<sub>2</sub> equilibrated samples at 24 h measured 50° receding angle; after drying, the "dry" remeasured receding angle was 60°. These values correlate quite well with the XPS data which show that vacuum-stored samples undergo minimal or negligible oxidation, degassed water samples show greater oxidation, water equilibrated with air samples show next greatest oxidation, and air-exposed polybutadiene shows rapid surface oxidation. This rapid surface oxidation is also the conclusion derived from the polybutadiene adhesion study.<sup>6</sup>

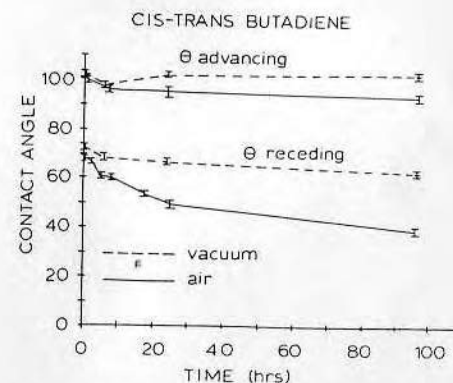


Fig. 4. Surface oxidation and related changes in wetting for cis-trans butadiene are readily apparent as storage conditions change. Wetting continues to change with time for all storage conditions except with vacuum storage. For clarity, only data for vacuum and air storage conditions are illustrated. Contact angle results of samples stored in degassed water and air-equilibrated water are similar to those stored in laboratory air.



## OPTIMIZING BIOSENSOR DESIGN WITH COMPUTER MODELING: A CASE STUDY INVOLVING CREATINE

<sup>1,2</sup>J.W. SMITH, <sup>1</sup>R.H. DAVIES, <sup>1</sup>J.D. ANDRADE, AND <sup>1,2</sup>R.A. VAN WAGENEN

<sup>1</sup>*Department of Bioengineering, University of Utah, Salt Lake City, UT, USA*

<sup>2</sup>*Protein Solutions, Inc., Salt Lake City, Utah, USA*

*E-mail: jws@xmission.com*

### 1. INTRODUCTION

A bioluminescence-based biosensor with the ability to measure several metabolites at once would be a great asset to research as well as to clinical and preventative medicine. One of the advantages of bioluminescence is its sensitivity and ability to measure analytes in the micromolar ( $\mu\text{M}$ ) range. However, to do so, an analytical instrument such as a photomultiplier tube (PMT) based luminometer which can accurately measure light intensity, is typically required. This approach can be too expensive for a home-based monitor; therefore, a hand-held CCD based luminometer is a desirable alternative. Additionally, a CCD has the advantage of being able to easily measure multiple analytes at once compared to a PMT-based luminometer, which is generally limited to only one.

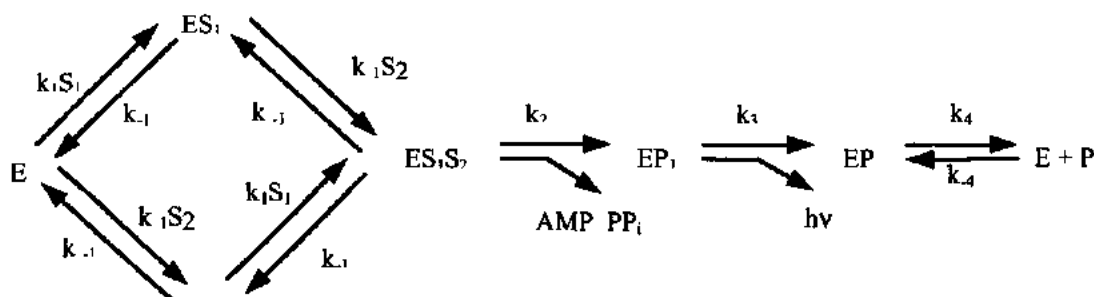
Computer modeling is a useful tool for evaluating the feasibility of various biochemical pathways for measuring a specific metabolite of interest. The parameters of the computer model are governed by the desired detection limits of the metabolite of interest, the reaction kinetics, and the measuring device (in this case a CCD based luminometer). The purpose of this investigation was to apply a computer model of the ATP firefly luciferase reaction, present a case study of a homogeneous, ATP depletion assay for creatine (Cr), and discuss the use of computer modeling for optimizing biosensor design and development.

### 2. FIREFLY LUCIFERASE PLATFORM REACTION

All computer modeling was performed using Gepasi, a program for the simulation and optimization of biochemical reactions.<sup>1</sup> This investigation specifically investigated reactions coupled to firefly luciferase. Thus, the first step was to model the firefly luciferase (FFL) reaction and validate the model results with experimental data. The FFL reaction is shown below (rxn(1)):



The multi-step reaction scheme and kinetic constants used in the computer model were based on Gandelman et al. (1993).<sup>2</sup>



The above reaction scheme was modeled with an initial luciferin ( $\text{LH}_2$ ) concentration of  $30 \mu\text{M}$ , luciferase concentration of  $0.7 \mu\text{M}$ , and ATP concentration ranging from  $0.3 \mu\text{M}$  to  $3.3 \text{ mM}$ . To validate the computer model, experiments were performed using concentrations presented above. A Turner 20/20 luminometer was used to measure the light output as a function of time. The model and experimental results are shown in Figures 1a and 1b.

### 3. COUPLED REACTION SCHEMES

There are two basic types of sensor reactions: ATP depletion and ATP production. This investigation focused on ATP depletion assays ( $\text{rxn}(2)$ ):



An example of an ATP depletion assay is the conversion of Cr to creatine phosphate (CrP) via creatine kinase (CK) (E.C. 2.7.3.2). To quantify Cr using bioluminescence,  $\text{rxn}(2)$  is coupled to the firefly luciferase reaction ( $\text{rxn}(1)$ ). The difference between the ATP consumed by the firefly luciferase reaction alone and the ATP consumed by the coupled reactions is proportional to substrate concentration. This difference can be measured from the light output.

As an example for biosensor design, the creatine assay was modeled to determine feasibility and optimal conditions. The maximum velocity and Michaelis-Menten constants used in the model for the CK reaction were for rabbit muscle and were based on those previously determined by Morrison and James.<sup>3</sup>

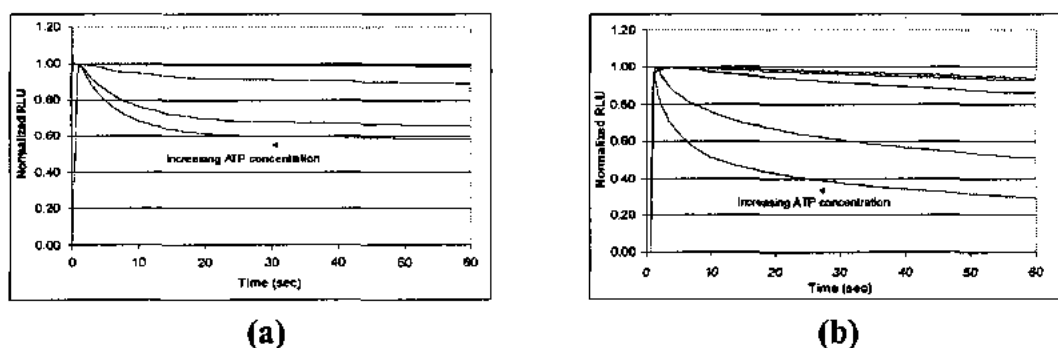


**Fig 1.** Results of the (a) computer model and (b) experiments for the firefly luciferase reaction. Luciferin concentration = 30  $\mu\text{M}$ , luciferase concentration = 0.7  $\mu\text{M}$ , and ATP concentrations of 0.3  $\mu\text{M}$ , 3  $\mu\text{M}$ , 30  $\mu\text{M}$ , .3 mM and 3.33 mM.

#### 4. RESULTS

The computer model was used to optimize the results of the assay by varying the luciferin concentration between 0.01 and 1 mM, the luciferase concentration between  $3 \times 10^{-4}$  and  $3 \times 10^{-3}$  mM, and the ATP concentration between 0.1  $\mu\text{M}$  and 1 mM. The results of the creatine model at varying ATP concentrations and at creatine concentrations between 0 and 300  $\mu\text{M}$  are included in Figures 2a-d.

#### 5. DISCUSSION

The design parameters for a biosensor are based on the required resolution and sensitivity of the assay. For example, a biosensor that measures creatine must be capable of detecting creatine concentrations between 0 and 300  $\mu\text{M}$  with a sensitivity of 10  $\mu\text{M}$  and a precision of  $\pm 5\%$ . To achieve these results, both the reaction kinetics and instrumentation limitations must be considered.

One issue with the CCD is the fact that it is approximately 100-1000x less sensitive than a typical PMT based luminometer and generally requires an integration of light intensity. As a result, it is desirable to maximize the light intensity while maintaining adequate sensitivity. To increase the light intensity, ATP and luciferase concentration can be increased. However, as ATP and luciferase concentrations are increased, the sensitivity of the assay (ability to detect differences between creatine concentrations) decreases. Potential solutions are to manipulate cofactors such as  $\text{Mg}^{2+}$  or to use completely different reaction schemes.

A hand-held CCD analyzer for a multi-channel, multi-analyte biosensor offers unique challenges. Future work will investigate the relationship between the results

of the computer model and the CCD detector output. Ultimately, this will help to maximize the applicability of the computer model and will reduce the need for PMT-based detectors.

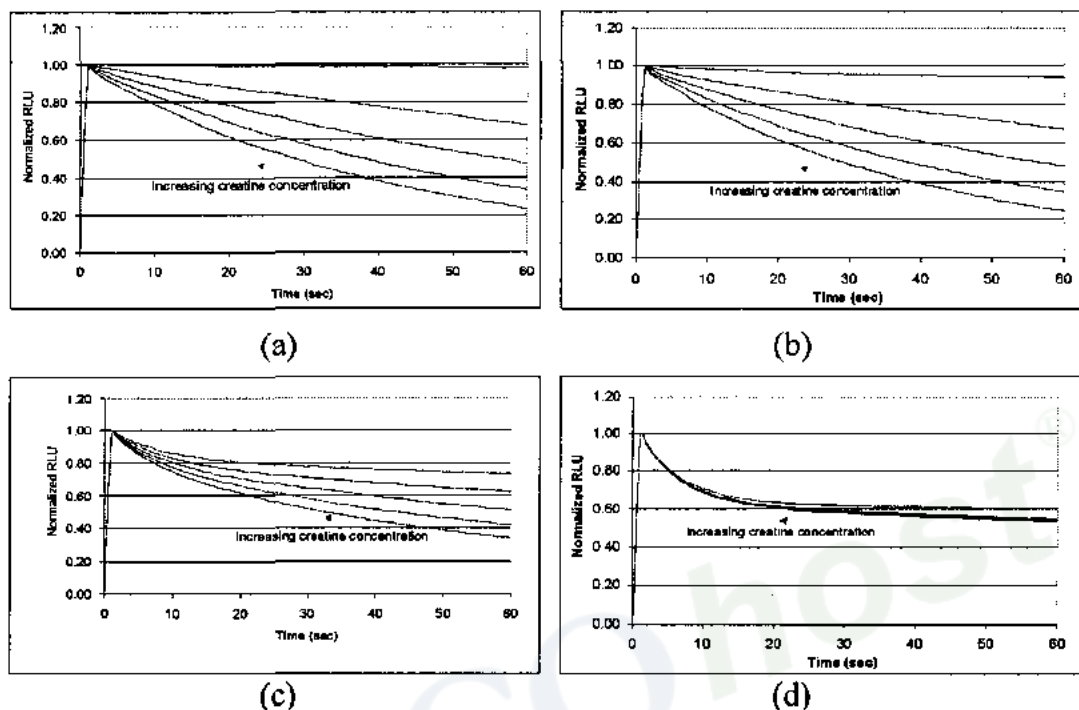


**Fig 2.** Results of computer model of creatine assay with creatine concentrations of 0, 75  $\mu\text{M}$ , 150  $\mu\text{M}$ , 225  $\mu\text{M}$ , and 300  $\mu\text{M}$ ; luciferase concentration = 0.7  $\mu\text{M}$ ; luciferin concentration = 10  $\mu\text{M}$ ; and ATP concentrations of (a) 0.001 mM, (b) 0.01 mM, (c) 0.1 mM, and (d) 1.0 mM.

### Acknowledgements

Financial support was provided by NIH SBIR Grant # 1R43DK5542601.

### References

1. Mendes P. GEPASI: a software package for modeling the dynamics, steady states and control of biochemical and other systems. *Comput Applic Biosci* 1993; **9**: 563-571.
2. Gandelman OA, Brovko LYu, Polenova TE, Ugarova NN. Non-steady state kinetics in bioluminescent firefly luciferase system. *Bioluminescence and Chemiluminescence*, eds., Szalay AA, Kricka LJ, Stanley P. New York: John Wiley & Sons, 1993: 79-83.
3. Morrison JF, James E. The mechanism of the reaction catalyzed by adenosine triphosphate-creatine phosphotransferase *Biochem J* 1965; **97**: 37-52.



E.W. STROUP, A. PUNGOR, A.S. LEA, V. HLADY\*, J.D. ANDRADE  
Department of Bioengineering, University of Utah,  
Salt Lake City, Utah 84112

\*"Ruder Boskovic" Institute, Zagreb, Croatia

# ELASTICITY MAPPING OF POLYMERIC SURFACES WITH SCANNING FORCE MICROSCOPY (SFM)

## 1. Introduction

We have used the SFM to image polymer surfaces producing an "elasticity map". The map image is generated from the differences in surface elasticities, in contrast to a normal topographical image of variances in height. To accomplish this imaging, the SFM is used in force modulation mode (1,2). When activated, the piezoelectric crystal controlling the sample holder moves in the z direction and causes the cantilever to deflect from its original position,  $z_d$ . The deflection,  $\Delta z_d$ , is used in a ratio with the change in height of the piezo,  $\Delta z_m$ , to create an image. This mode allows the SFM to recognize "soft" sections in relation to "hard" sections, since the change in the deflection of the cantilever will be related to the elasticity of the area under the tip (Figure 1) (1). We have used this technique to image the surface of polyurethane films. Polyurethanes are known to phase separate with the domain sizes ranging from 10-350Å (3,4). The contrast in the elasticities of the phases of the polyurethane is revealed through the force modulation method.

## 2. Surface Deformation

The elastic nature of samples is of concern. If the sample is very elastic, it may deform under the force of the tip. This deformation may produce an increase in the contact area between the tip and the sample, thereby creating a convoluted topographical image.

Assuming that the tip is represented by a large nondeformable sphere of radius R interacting with a flat surface, and assuming that the deformation of the surface can be modeled by continuum elastic theory and contact mechanics, then the deformation of the surface can be described by (5,6):

$$D = \left[ \left( \frac{9F^2}{16R} \right) \left( \frac{1-\nu_1^2}{E_1} + \frac{1-\nu_2^2}{E_2} \right) \right]^{\frac{1}{3}}$$

Where D is the surface deformation (meters), F is the applied force (Newtons), R is the tip radius (meters),  $\nu_1$  and  $E_1$  are the Poisson's ratio and Young's modulus for the tip, and  $\nu_2$  and  $E_2$  are the Poisson's ratio and Young's modulus for the sample.

Much work lately has been in an effort to use the SFM in determining the elastic modulus of samples (1,7-10). The strategy is to use the curves that show the deflection of the cantilever in relation to the movement of the sample holder in the Z direction (similar to a force versus distance curve - FvD). After the tip "jumps" into contact with the surface, for a sample with a elastic modulus much greater than the spring constant of the cantilever, the curve will be linear with the cantilever deflecting one unit for every unit the sample moves in the Z direction. Alternatively, for a sample that has a spring constant that is not "much" greater than the cantilever, there will be deformation of the surface as well as deflection of the cantilever. This can be seen as a change in the slope of the FvD curve. The area difference between the curves is related to the elastic energy stored in the sample. Figure 3 shows curves generated using a commercial silicon nitride cantilever with an approximate spring constant of 0.38 N/m<sup>2</sup> (6,11). The differences in slopes for the metal sample and the polycarbonate show that a normal cantilever has enough responsiveness to detect small (or large) elasticity differences.

## 3. Experimental

We have used the SFM to look at the surfaces of polyurethane (PU) film samples. The PU analyzed was a diol extended segmented polyurethane with a PTMO soft segment (Vialon 510x-60, 60% hard segment by weight, Becton Dickinson Co., Franklin Lakes, NJ). The PU was dissolved in N,N-Dimethylformamide at room temperature to create a 1% solution by volume. This solution was spun cast on glass microslips at 4000 rpm for 20 seconds, allowed to air dry and then cast with second and third layers at 4000 rpm for

20 seconds. The PU films were then heat dried in vacuum (70°C, 20mmHg) for 24 hours (3).

## 4. Results and Discussion

The PU samples were imaged using the modulation software (2). The surface was originally imaged at 15,000nm X 15,000nm range, but was found to be very "wavy" at that distance due to the extent of motion by the tip over the sample. The "elasticity" map at this range was inconclusive. The range was reduced to 250nm X 250nm. At this range the surface was much easier to image. Figure 3 is the surface image produced from normal scanning with constant force mode. A nonperiodic surface is shown with surface structures of varying height. Figure 4 illustrates the height of the surface structures; from 1 to 2nm and having a thicknesses of 10 to 40nm. The "elasticity" map of the same area of the surface is shown in Figure 5. Definite differences in the images are noted. Semicontinuous areas of slight height variance are seen. The darker regions indicating a more "elastic" area beneath the tip. Figure 6 shows a profile of the elasticity map. The surface structures show varying widths; from 10 to 50nm. This is in reasonable agreement with the predicted bulk phase domain size of between 5 to 30nm. The PU is known to phase separate and to have a surface composition that is similar to that in the bulk (3,4). The discrepancy can be related to the tip geometry being a limiting factor in the determination of the smaller domains. Also, the phases present are not expected to arrange as simple spheres but as a semicontinuous "blend" of the hard and soft segment. Vialon 510x is known to have a small concentration of soft segment over the surface in air. This may cause the contrast in elasticity of the domains to be lessened. Also, in air the dynamic mobility of the PU surface allows it to reorient to minimize its surface free energy (3,4). To accomplish this minimization the hard segments of the PU will migrate away from the surface. Therefore, there may be a much greater concentration of soft segment at the surface than is expected for the bulk. The presence of impurities, and extractables may also influence the "elastic" effect of the surface.

The "elasticity" map of the surface illustrated very large features at the edges of the images. This is an artifact of the software and scanning mechanism. Further, the Comparison of Figures 3 and 5 as well as 4 and 6 illustrate that the features of the "elasticity" map are not a result of the topography of the sample as may be expected from a purely 2-derivative image.

## 5. Conclusions and Future Work

The advantage of the SFM and similar techniques is based on their ability to image microscale features. This ability is determined by the limitations of the microscope and of the surface to be imaged. Using continuum elasticity concepts a model has been used to estimate the deformation of a system and cantilever deflection due to the force applied by the SFM tip. The results show that estimation of the modulation is possible with knowledge of the cantilevers materials and mechanical properties.

The "elasticity" maps obtained using the force modulation technique also indicate promise for that technique. With the use of cantilevers of varying spring constant, the sensitivity of the modulation images can be enhanced. This technique is also able to produce images in liquid environments, therefore it may be possible to directly study the phase mobility of PU's in different media.

Our efforts to produce "elasticity" maps of the surface have used commercially available cantilevers as well as cantilevers we have modified to increase the spring constant. The cantilevers available on the market have a very small spring constant in relation to the samples of interest, modification will allow for greater contrast in elasticity response.

## 6. References:

1. P. Maivald, et al., Nanotechnology (in press) (1991).
2. The force modulation software provided by Digital Instruments, Inc., Santa Barbara, Ca, (DI) for use with our Nanoscope II Atomic Force Microscope manufactured by DI.
3. K.G. Tingey, Ph.D. Thesis, Department of Materials Science, University of Utah, 1992.
4. K.G. Tingey, et al., in Surface Characterization of Biomaterials, B.D. Ratner ed., Elsevier Science Publishers B. V., Amsterdam, 1988.

5. K.L. Johnson, *Contact Mechanics*, Cambridge University Press, NY, 1985, p92-93.
6. Cantilevers purchased from Park Scientific, Inc. Mt. View Ca.
7. N.A. Burnham, et.al., *Physical Review Letters*, 64(16), 1931 (1990).
8. N.A. Burnham and R.J. Colton, *J. Vac Sci Technol. A7*, 2906 (1989).
9. U. Landman, et.al., *Science*, 248, 454 (1990).
10. J.B. Pethica & W.C. Oliver, *Physica Scripta*, T19, 61 (1987).
11. Computer program for computing the spring constant based on geometry and materials constants was provided by A.L. Wiesenhorn and P.K. Hansma of University of California - Santa Barbara.

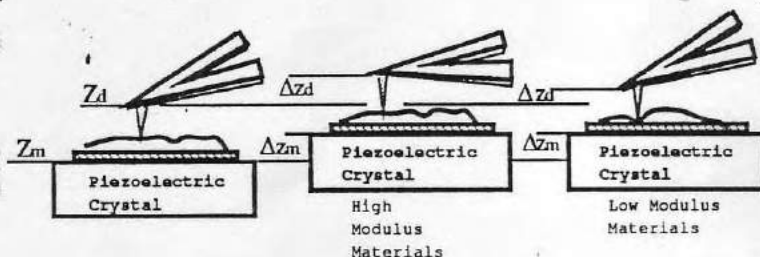


Figure 1. The change in the Z position of the piezo ( $\Delta Z_m$ ) will cause the cantilever to deflect ( $\Delta Z_d$ ). The amount of deflection will depend on the elastic nature of the surface.

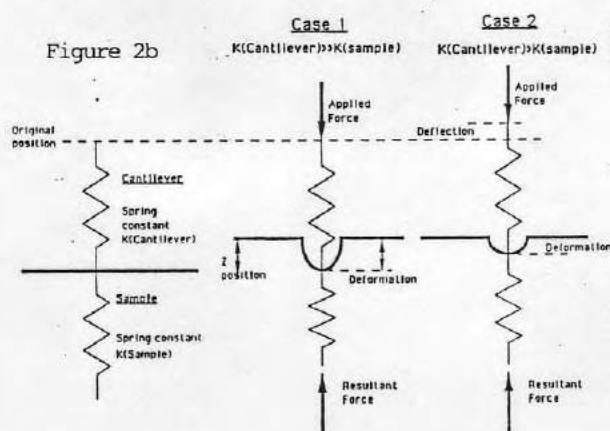
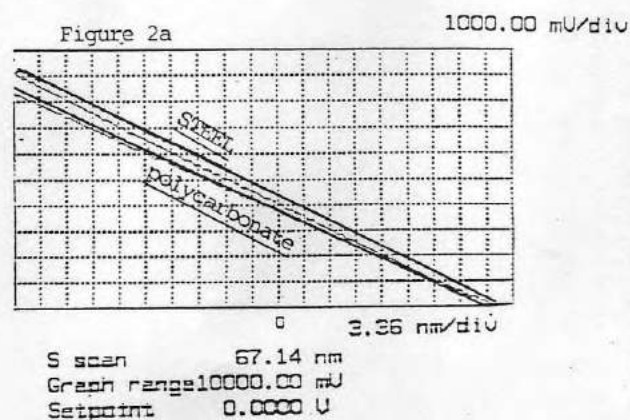


Figure 2a. Graphical representation of the deflection of the cantilever (y-axis) as the sample moves in the Z direction (x-axis). Change in slope of the curves for the samples shows an increase in the elastic energy stored for the samples. 2b. Schematic representation of the deformation of the surface and deflection of the cantilever.



Figure 3. SFM scanned surface view image of segmented polyurethane. Scan size of 250nm X 250nm.

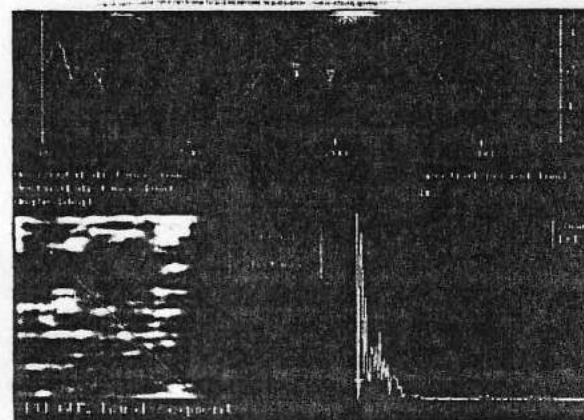


Figure 4. Cross section SFM surface view image of segmented polyurethane.

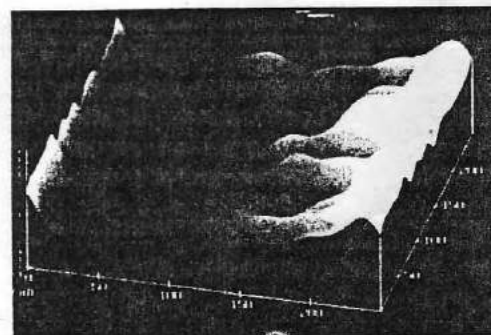


Figure 5. SFM "elasticity" map of segmented polyurethane produced from force modulation.

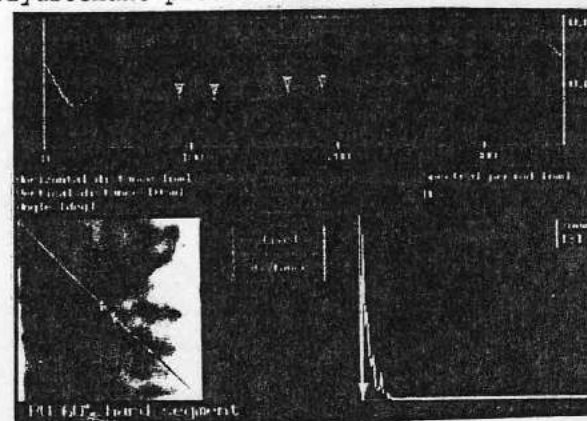


Figure 6. Cross section of SFM "elasticity" map of segmented polyurethane produced from force modulation.



MICRODOMAIN IMAGING OF MODEL COPOLYMERS  
BY SCANNING FORCE MICROSCOPE (SFM)  
ELASTICITY MAPPING

E.W. STROUP\*, A. PUNGOR†, V. HLADY†, J.D. ANDRADE\*†  
Departments of Materials Science\* and Bioengineering†  
University of Utah, Salt Lake City, Utah 84112

Introduction

The SFM senses the forces acting between a surface and a sharp tip. In contrast to the scanning tunneling microscope (STM), the SFM does not require a conductive surface for imaging. This allows the SFM to image polymeric and biological surfaces. The microscopic tip is attached to a small cantilever which deflects in response to the forces between the surface and the tip. The SFM records the deflection of the cantilever.

The SFM can not only be used to obtain topographical images, but also has been used to produce an elasticity map by sensing differences in local surface elasticities using the Force Modulation mode of imaging (1,2). When the Force Modulation mode is activated, the piezoelectric crystal controlling the sample motion oscillates (5 kHz) in the z direction. The sample is scanned below the tip in the x-y direction as the force is kept constant by the system feedback loop. The small movement of the sample in the z direction (approximately 25 nm) causes the cantilever to deflect from its original position,  $z_d$  (Figure 1). The deflection,  $\Delta z_d$ , is used in a ratio with the change in height of the piezo,  $\Delta z_m$ , to create the image. Elastic or soft regions will be penetrated by the tip, whereas hard regions will resist tip motion. This mode allows the SFM images to be formed based on differences between soft sections in relation to hard sections, since the change in the deflection of the cantilever will be related to the elasticity of the area under the tip (Figure 1) (1). The contrast in the elasticities of the components of the samples is revealed through the force modulation method.

In our experiments we have used the SFM to probe the heterogeneous microelasticity of model block copolymer systems in an aqueous media. This is done using the force modulation technique. The samples were viewed in the aqueous environment to provide for more stability in the forces present and to provide the samples with an environment that more closely resembles physiological conditions.

There has been much work lately on the use of the SFM to determine the elastic modulus of a sample (1,3-5). The strategy employed is to analyze the deflection of the cantilever in relation to the movement of the sample holder in the Z direction (this response gives a force versus distance curve - FvD).

The methods used to measure the nanoindentation are significant in that they can provide vital information at the point of interest (5). The single point measurements are highly reproducible and have a great deal of sensitivity. They are limited spatially only by the elastic nature of the sample and the geometry of the scanning probe. These methods are not convenient for samples that have regions of heterogeneous elasticity, particularly if these areas are not distinguishable by differences in topography or by optical methods.

Composites and copolymers are thus extremely difficult to interpret. The force modulation technique allows one to map the surface elasticity of samples that may have a variety of different local elasticities, by comparing the relative elasticities of the area.

Experimental

All SFM experiments were performed using a Digital Instruments Nanoscope II® (2) with an AFM D scanning head providing maximum scanning ranges of 16  $\mu$ m. The experiments were performed in highly purified water (6) using the Nanoscope's flow cell. The cantilevers used in the experiments were microfabricated silicon Ultralevers™ (Park Scientific Instruments, Sunnyvale, Ca.) with reported spring constants ranging from 0.03 to 7.4 N/m. The Ultralevers have a tip radius of approximately 100 Å and an aspect ratio of 3:1 (compared to 1:1 for normal tips).

The model system analyzed was a triblock copolymer of Styrene-Butadiene-Styrene (Kraton D1102, Shell Research Co, Houston Texas) with 29% styrene and 71% butadiene by weight. Films of the copolymer were prepared by spin casting (at 250 rpm for 30 seconds) a 1%(w/v) solution of Kraton in toluene onto plasma cleaned glass microslips (5/8 inch diameter). The samples were air dried in a dust free environment for 30 minutes and then annealed at 100°C for 5 days under vacuum. The samples were quenched to room temperature (in highly purified water), dried under nitrogen and stored at 0°C.

Results and Discussion

The Styrene-Butadiene-Styrene copolymer samples were imaged at 5000 nm X 5000 nm using the constant force mode (normal scanning) (Figure 2). Semicontinuous areas can be seen against the background. These lamella shows an average width of 300nm (Figure3). The copolymer samples were then imaged at 5000 nm X 5000 nm using the modulation software (Figure 4). Semicontinuous areas can again be seen against the background. The darker regions indicate a more elastic area beneath the tip. The phases present are arranged as a semicontinuous blend of the hard and soft segment and not as simple spheres. The surface structures show average widths of approximately 400 nm (Figure 5). The section shows many features similar to the normal scan image, but the differences in width of the features may be attributed to convolution of the elastic response by lamella closely packed.

The scan size and applied force were varied to determine their effect on the surface. By changing their range, it is possible to determine if there has been any damage to the surface as a result of scanning. No plastic deformation of the surfaces was apparent in either case.

Conclusions

The advantage of the SFM and similar techniques is based on their ability to image microscale features. The single point measurements are good for materials of a single type of elasticity, however, PU and other block copolymers have surface elasticities that vary widely. This creates difficulties in applying the this method directly to the deformation seen with these materials. The elasticity maps obtained using the force modulation technique indicate promise for that technique. We can image the microdomains of heterogeneous surfaces on a

level not approached in this degree in a variety of environments.

#### Acknowledgments

Financial support was provided by a fellowship from Becton Dickinson and Co. through the Center for Biopolymers at Interfaces at the University of Utah, and by NIH grant HL44538-03 "Direct Observation of Interfacial Processes - SFM".

#### References

- (3) E.W. Stroup, A. Pungor, A.S. Lea, V. Hlady, J.D. Andrade submitted to Langmuir, 1992.
- (1) P. Maivald, et.al., Nanotechnology, 1991, 2, 103-106.
- (2) Force Modulation software by Digital Instruments, Inc.
- (4) E.W. Stroup, A. Pungor, A.S. Lea, V. Hlady, J.D. Andrade, ACS Polymer Preprints, 1992, 33, 1, 749-750.
- (5) N.A. Burnham and R.J. Colton, J. Vac Sci Technol., 1989, A7, 2906-2913.
- (20) The water used for the experiments was purified by reverse osmosis and further purified by a MilliQ™ system (Millipore).

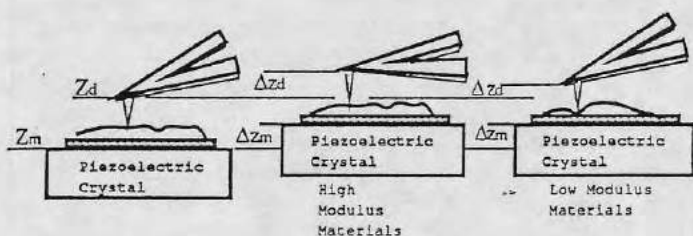


Figure 1: The piezoelectric crystal controlling the sample motion, oscillates (5 kHz) in the z direction as the sample is scanned below the tip as the force is kept constant by the system feedback loop. The small movement of the sample in the z direction (approximately 25 nm) causes the cantilever to deflect from its original position,  $z_d$ . The deflection,  $\Delta z_d$ , is used in a ratio with the change in height of the piezo,  $\Delta z_m$ , to create the image. Elastic or soft regions will be penetrated by the tip, whereas hard regions will resist penetration.

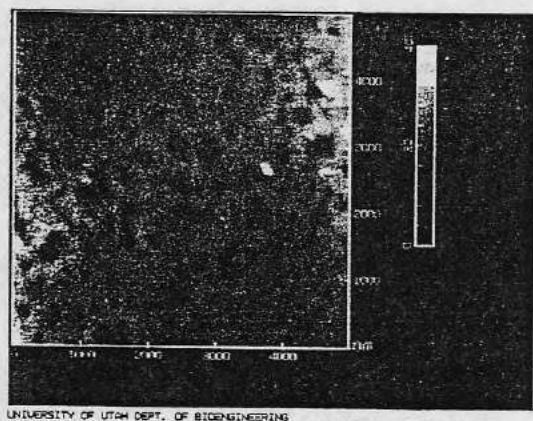


Figure 2 SFM image (constant force) of Styrene-Butadiene-Styrene copolymer. Scan rate 10.7 Hz. This image shows features that indicate a lamellar structure.

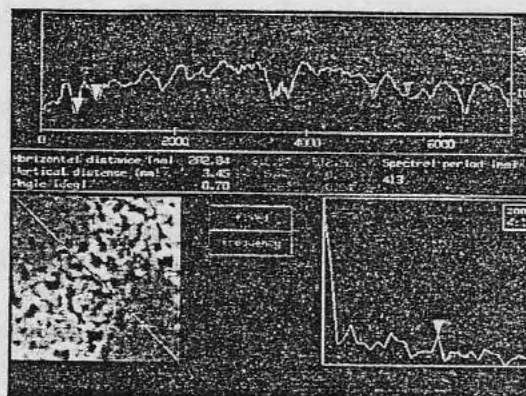


Figure 3 Sectional view of SFM image (constant force) of Styrene-Butadiene-Styrene copolymer. Scan rate 10.7 Hz. This image shows that the lamellar features have an average width of 400Å.

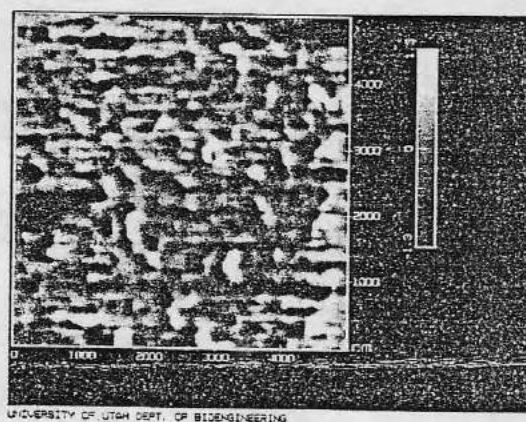


Figure 5. Sectional view of SFM force modulation image of Styrene-Butadiene-Styrene copolymer. This view shows dimensions of the features. Comparison with Figures 3 shows that the resulting images have similar features.

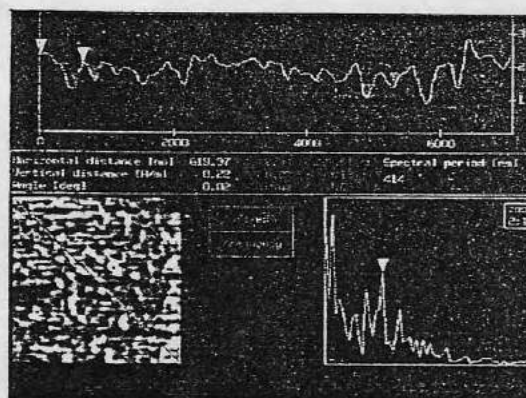


Figure 4. SFM force modulation image of Styrene-Butadiene-Styrene copolymer. Scan rate 12.0 Hz. Semicontinuous areas can be seen against the background. The darker regions indicating a more elastic area beneath the tip. The surface structures show average widths of approximately 400 nm.



[ PP 36(c)-95 ]  
Abst - Stroup - 2

FREQUENCY AND AMPLITUDE EFFECTS OF FORCE  
MODULATION ON SURFACE VISCOELASTICITY ANALYSIS BY  
ATOMIC FORCE MICROSCOPY

E.W. Stroup\*, A. Pungor†, M. Radmacher‡, V. Hlady\*, J.D. Andrade\*\*†

\*Department of Materials Science and Engineering, University of Utah

†Department of Bioengineering, University of Utah

‡Physics Department, University of Santa Barbara

**Introduction:** Elastomers have found wide acceptance in the biomedical industry due in part to their versatile mechanical properties as well as their varied surface properties. Elastomers behave partially as elastic solids and also as viscous liquids. The viscoelastic properties of an elastomer are very dependent on its structure. The glass transition temperature, degree of crystallinity, relaxation spectra, molecular orientation, degree of cross-linking, and morphology all contribute to its viscoelastic properties. This viscoelastic response is a combination of energy stored (related to storage modulus,  $G'$ ) and energy dissipated (loss modulus,  $G''$ ). If a harmonic strain,  $\epsilon$ , is applied to the polymer, the resultant stress,  $\sigma$ , will also be harmonic but will be shifted in phase ( $\delta$  is the phase shift) due to the effect of the viscous nature of the polymer. The energy dissipated by the polymer in the form of mechanical damping (internal friction) is related to loss modulus.

The Atomic Force Microscope (1) is able to image the topographic features of elastomer surfaces and has recently provided information on the viscoelastic properties of these surfaces as well using Force Modulation scanning mode (2-8). In Force Modulation scanning mode a sinusoidal signal added to the feedback signal provides oscillation of the cantilever in the  $z$  direction (Figure 1). When the cantilever tip contacts the sample surface, the amplitude of the cantilever oscillation will change leading to demodulation of the signal. In addition to changes in oscillation amplitude, the viscous properties of the sample surface will introduce a phase shift to the oscillation of the cantilever as compared to the driving signal. The separate detection of the amplitude demodulation and the phase shift enables one to record the sample images that relate to the local storage and loss modulus of the surface.

The frequency at which the Force Modulation scanning mode can operate is limited by the characteristics of the experimental system. The resonance frequency of the scanner and the feedback mechanism provide a low frequency limit (in the range from 1-10 kHz). The resonance frequency ( $\omega_0$ ) of the cantilever changes when it comes into contact with the sample surface. A new effective system spring constant,  $K_{eff}$ , and associated effective mass,  $m_{eff}$ , determine a new resonance frequency,  $\omega$  (equal to  $(K_{eff}/m_{eff})^{1/2}$ ). In practice, the most sensitive operating frequency will be somewhat smaller than the new cantilever resonance frequency. Right there, a first order change in the amplitude of the cantilever will occur for changes in viscoelastic force acting against it (9).

Increasing the amplitude of the driving signal causes a change in the maximum force applied to the sample surface. This will cause an increase in deformation dependent on the elastic properties of the surface.

In our experiments we used Force Modulation to detect the elastic and viscous responses of two different samples: an octanethiol patterned film on a gold substrate and polystyrene latex beads fused on a silicon wafer. The two model samples were chosen for their differences in viscoelastic response.

**Instrument:** A Topometrix TMX 2000 Explorer AFM (Topometrix, Santa Clara, Ca) with a 130  $\mu\text{m}$  scanning head was used in these experiments. Silicon Nitride Microlevers (Park Scientific, Sunnyvale, Ca) with spring constants estimated at 0.05 N/m and tip radius of 20 nm were used. A lock-in amplifier was used to analyze the phase changes in the signal, while an absolute value electronics were used to follow

changes in amplitude. The TMX 2000 simultaneously recorded images based on the feedback current, the demodulation, and phase shift information.

**Materials:** Patterns of octanethiol were made on a gold substrate. The gold was prepared by evaporating a 20 nm layer onto mica. The thiol was stamped onto the gold in a method described by Kumar et al. (10). The stamping was performed by creating a stamp from polydimethylsiloxane molded onto a silicon wafer with a grid pattern. The stamp was "inked" with a 1 mM solution of octanethiol in ethanol and touched lightly to the gold surface to transfer the thiol.

Polystyrene beads (369 nm  $\pm$  12 nm) were attached to a silicon wafer via nitrene groups by UV exposure for 3 min, at 15 mW/cm<sup>2</sup> and then heat cured at 65°C for 2 hours. The nitrene functionalized surface was prepared by submerging a clean silicon wafer into a 2% (v/v) solution of (mercaptopmethyl)-dimethylethoxysilane in trichloroethylene (TCE) for 12 hours followed by rinsing in TCE, acetone, and ethanol, and then submerging the sample in a 10 mM solution of p-azidophenacyl bromide in methanol for 3 hours at 4°C (11).

**Results & Discussion:** AFM images (12 x 12  $\mu\text{m}$ ) of octanethiol on gold in air (Figure 2a) show islands of thiol against the gold background. Force Modulation images of the same area (Figure 2b-c) show the islands as decrease demodulation signal compared to the gold background. This decrease results from the thiol being more elastic than the gold and causing the cantilever oscillation amplitude to become demodulated. Figures 2b and c show the effect of the magnitude of the applied oscillation amplitude on the demodulation. A change of approximately 25% in the demodulation amplitude is found for a change from the 0.5 V to 0.2 V in the driving signal. Different demodulation amplitude indicates the sample is deforming less as the amplitude of the driving signal is decreased.

A light feature in the lower right of figure 2a is apparently a dust particle stuck to the thiol island. It is interesting, however, that the particle caused a dramatic change of the demodulation amplitude (Figures 2b and c). This change is probably due in part from a delay in feedback mechanism and partly because the harness of the particle exceeded the thiol and even the gold.

AFM images (6 x 6  $\mu\text{m}$ ) of polystyrene beads on silicon in air show topographic features that indicate bead aggregates distributed randomly on the silicon surface (Figure 3a). Figures 3b-c are the demodulation and the phase shift images of the same area. Figure 3b shows that the demodulation values for the silicon and latex differ by 25%. The latex value being smaller than the silicon. This indicates that the polystyrene latex aggregates are significantly more elastic than the underlying silicon. The phase shift image (Figure 3c) shows a negative condition for the identical area. It is interesting that the phase shift contrast is also shifted in space compared to the demodulation contrast.

Both images (Figures 2 and 3) clearly show that the viscoelastic properties of a sample surface can be easily detected using the same scanning technique.

**Conclusions:** The topographic, demodulation, and phase images of the two model surfaces have been obtained in the Force Modulation scanning mode of the Atomic Force Microscope. The images illustrate that the local viscoelastic properties of the sample can be used as a contrast mechanism. This method is expected to be a useful tool in the evaluation nanomechanical properties associated with surfaces of elastomers.

**Acknowledgments:** Financial support was provided by a fellowship from Becton Dickinson and Co. through the Center for Biopolymers at Interfaces at the University of Utah, and by NIH grant HL 44538 "Direct Observation of Interfacial Processes - SFM II"

## References:

- (1) G. Binnig, C.F. Quate, C. Gerber, *Phys. Rev. Lett.*, **1986**, 56, 930.
- (2) P. Maivald, et al., *Nanotechnology*, **1991**, 2, 103.
- (3) M. Radmacher, R.W. Tillmann, H.E. Gaub, *Biophys. J.*, **1993**, 64, 735.
- (4) E.-L. Florin, M. Radmacher, B. Fleck, H.E. Gaub, *Rev. Sci. Instrum.*, **1994**, 65, 639.
- (5) D.R. Baselt, S.M. Clark, M.G. Youngquist, C.F. Spence, J.D. Baldeschwieler, *Rev. Sci. Instrum.*, **1986**, 64, 1874.
- (6) E.W. Stroup, A. Pungor, A.S. Lea, V. Hlady, J.D. Andrade, *ACS Polymer Preprints*, **1992**, 33, 1, 749.
- (7) E.W. Stroup, A. Pungor, A.S. Lea, V. Hlady, J.D. Andrade, *ACS Polymer Preprints*, **1993**, 34, 2, 86.
- (8) R.M. Overney, E. Meyer, J. Frommer, H.-J. Guntherodt, M. Fujihira, H. Takano, Y. Gotoh, *Langmuir*, **1994**, 10, 1281.
- (9) D. Sarid, *Scanning Force Microscopy: with applications to electric, magnetic, and atomic forces*, **1991**, Oxford University Press, NY.
- (10) A. Kumar, H.A. Biebuyck, G.M. Whitesides, *Langmuir*, **1994**, 10, 1498.
- (11) A. Martin-Rodriguez, J. Liu, personal communication.

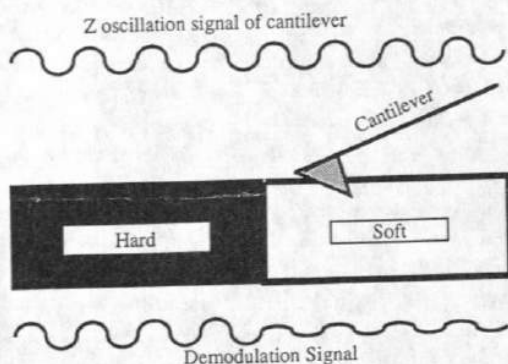
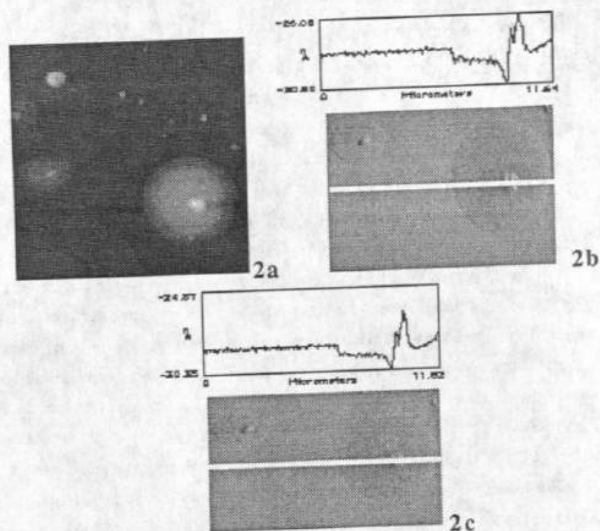


**Figure 1:** The AFM cantilever oscillates in the z direction with a sinusoidal signal, while in contact with the sample. The oscillation's amplitude and phase are affected by the viscoelastic properties of the area beneath the tip. The amplitude will decrease for highly elastic areas. Viscous areas will introduce a phase shift compared to the driving oscillation (not shown here). The detection of the amplitude demodulation and the phase shift enables one to record the sample images that relate to the local viscoelastic properties of the sample surface.



**Figures 2(a-c):** AFM images ( $12 \times 12 \mu\text{m}$ ) of octanethiol on gold in air. a) Topographic image shows islands of thiol. b) The demodulation image was collected at 14 kHz and 0.5 V amplitude of driving signal ( $\sim 0.5 \text{ nm}$ ). The image shows contrast corresponding to the elasticity for the islands of thiol. The islands have a lower signal then the background. c) The demodulation image of amplitude change collected at 14 kHz and 0.2 V amplitude of driving signal ( $\sim 0.2 \text{ nm}$ ). The image again shows the islands with their signal value lower then the background, but the depth is less then the 0.5 V image.

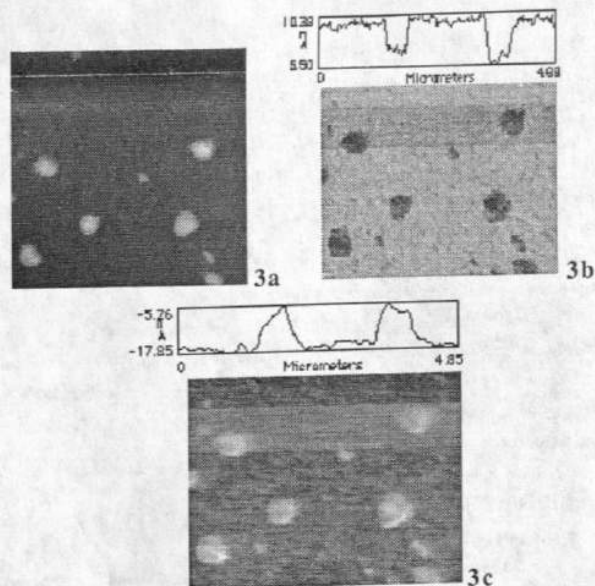


**Figure 3(a-c):** AFM images ( $6 \times 6 \mu\text{m}$ ) of polystyrene beads on silicon. a) Topographic image shows aggregates of beads distributed randomly on the surface. b) Demodulation image collected at 14 kHz and 0.5 V amplitude of driving signal ( $\sim 0.5 \text{ nm}$ ). The image shows the bead aggregates have a demodulation amplitude that is lower than the background by 25%. c) Phase shift image collected at 14 kHz and 0.5 V amplitude of the driving signal. The image shows negative contrast to the demodulation image

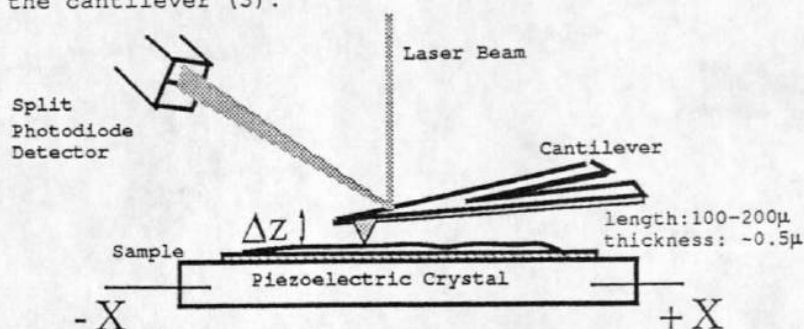
E.W.STROUP, A. PUNGOR, A.S. LEA, V. HLADY, J.D. ANDRADE  
 Department of Bioengineering  
 University of Utah  
 Salt Lake City, Utah 84112

## ATOMIC FORCE MICROSCOPY OF POLYMERIC SURFACES

The Atomic Force Microscope (AFM) has provided the opportunity to image surfaces on atomic resolution. We have shown that the AFM is a powerful tool for the study polymer surfaces, provided that the surface to be imaged does not promote interference from extensive tip-surface interaction. The AFM can also be used to produce images of the contrast in elasticity of regions on the polymer surface. This method provides a means to identify different components within a surface based on their elastic response.

### 1. Introduction

The AFM senses the forces acting between the surface and a sharp tip (1). In contrast to the Scanning Tunneling Microscope (STM) (2), the AFM does not require a conductive surface for imaging. This allows the AFM to image polymeric and biological surfaces. The profiles are obtained from a tip (ideally atomically sharp) that scans across the surface. The AFM records the deflection of the cantilever upon which the tip resides. This is accomplished by a split photodiode detector that records the changes in a laser beam that is reflected off of the back of the cantilever (3).

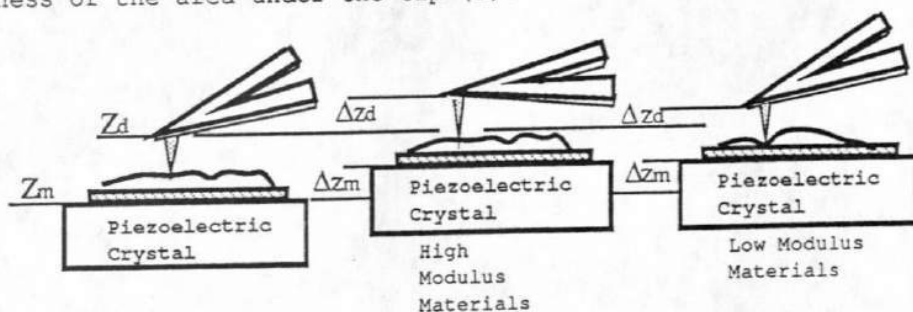


The use of the AFM to image the surface microstructure of polymers has the opportunity to provide valuable information on the surface chemistry, the biological applications, and tribological properties. To date most work on polymers has focused on Langmuir-Blodgett films. These surfaces have been used because they provide uniform surfaces that are relatively free of pinholes (4).

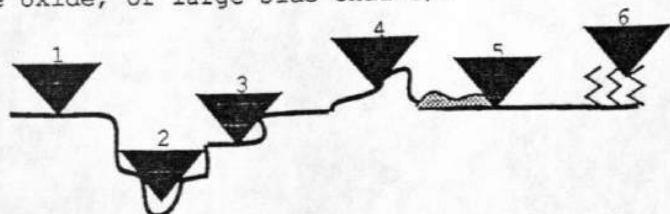
Author	Polymer system	Observations	Reference
M.M. Dovek	Langmuir-Blodgett films	Parallel chains of varying density	J. of Micr., 152, Pt. 1, 229 (1988)
S. Gould	DL-leucine	Methyl peaks in the crystal lattice	Nature, 332, 332 (1988)
O. Marti	n-(2-aminoethyl)-10,12-tricosadiynamide	Parallel rows with 0.55nm spacing	Science, 239, 50 (1988)
B. Drake	Polyaniline	Troughs, and rows	Science, 243, 1586 (1989)
A.L. Weisenhorn	Lipids in air and water	Lattice images	Langmuir, 7, 1, 8 (1991)



One of the more novel uses of the AFM has been to image a surface to produce a "hardness map" from different surface elasticities, in contrast to a topographical image of variances in height. To accomplish this imaging, the AFM is used in force modulation mode. When activated, the piezoelectric crystal controlling the sample holder moves in the  $z$  direction and causes the cantilever to deflect from its original position,  $z_d$ . The deflection,  $\Delta z_d$ , is used in a ratio with the change in height of the piezo,  $\Delta z_m$ , to create an image. This mode allows the AFM to recognize soft sections in relation to hard sections, since the change in the deflection of the cantilever will be a relation of the hardness of the area under the tip (5).

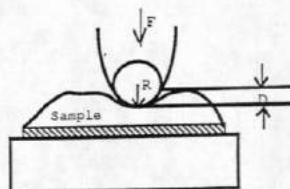


Very little work to date has been done on conventional polymers. There are many problems faced when dealing with conventional polymers. There may be simultaneous imaging from multiple contact points between the tip and the sample, this could be due to extending surface features, impurities (dust), or even portions of the molecule itself protruding from the surface due to natural molecular arrangement. These contacts may cause convoluted images. The tip radius is a limiting factor, since if the sample possesses features that are sharper than the tip itself the image will be of the tip itself. Also, features that are recessed from the scanning surface can only be imaged on the order of the shape of the tip. In the figure below some of the various multicontact problems are illustrated. Tip number 1, represents a tip with a single contact. A tip trying to image a depression that has a pitch of greater degree than the tip's semiaxial angle causes the image to be cut off where the tip cannot enter the depression any further (tip 2), thereby producing multicontacts. Tips numbers three and four show features sharper than the tip. A dust particle is interfering with tip number 5, and tip 6 is coming into contact with polymer bonds (such as grafted polyethylene oxide, or large side chains).



The elastic nature of the sample is also of concern. If the sample is very elastic, it may deform under the force of the tip. This deformation may cause increased surface contact area between the tip and the sample, thereby producing a convoluted topographical image.

Assuming the system of the AFM resembles that of a large sphere of radius  $R$  interacting with a flat surface, that the deformation of the surface can be modeled by continuum elastic theory, and also by contact mechanics, then the deformation can be described by the following (6,7):



F = normal applied force  
R = tip radius  
D = deformation in the z direction  
E = Young's modulus of the sample  
v = Poisson's ratio of sample

$$D = \frac{F^2(1-v^2)}{4E^2R^3}$$

Using this equation we assume that the tip is not deformable, then we can calculate the deformation of various polymer substrates, using a range of Young's modulus values for common polymers and assuming the Poisson's ratio is 0.5. Figure 1 shows the results from calculations for surface deformation involving different radii of curvature for the AFM tip. This figure shows that "hard" materials (those with higher values for modulus) have much less deformation than those for "soft" materials (those with lower values for the modulus) as is expected. It also can be seen that the deformation increases with increasing radius of the tip.

For the AFM to produce micro scale images of a surface it is necessary for it to have limited tip-substrate contact surface area. If the AFM tip has a large radius of curvature, or if the elasticity of the surface allows for such deformation that there is increased area of contact then there may exist convoluted topographical images of the surface. Currently it is very difficult to produce tips with radii of curvature less than 100 Å. The production of the cantilevers on which the tips are mounted has limited the spring constant of the cantilever materials. This, combined with the thermal excitation of the cantilever, has affected the microscope by keeping its range of detectable force to values greater than  $10^{-10}$  N. Using these values as effective constants and referencing the figures presented, it can be seen that it is still not possible to image polymers on an atomic scale. If their material properties allow for limited elastic deformation, such that it does not promote extensive tip-surface interaction, then it may be possible to obtain images with resolution on the order of 100nm.

## 2. Experimental

We have used the AFM to look at the surfaces of several different polymers of varying elasticity. We have been able to image the surface of a Polycarbonate memory storage disk (PC A2700 Mv=26,100 g/mole Idemitsu Petrochemical Co, Inc., Chiba-Ken, Japan). We have also viewed surfaces of Styrenebutadiene block copolymer in force modulation and scanning modes. The copolymer was prepared by dissolving equal parts by weight of styrene (avg MW = 250,000 g/mole Aldrich Chemical Company, Milwaukee, Wisconsin), and cis-Butadiene (average MW= 200,000 to 300,000 g/mole Aldrich Chemical Company, Milwaukee, Wisconsin) in toluene (GC grade, EM Science, Gibbstown, NJ) and then spin casting at 4000 rpm for 20 seconds on glass microslips. The samples were air dried at room temperature (8). A carbon fiber and polycarbonate composite, cut on a

diamond saw and polished with 0.3μ paste, was also imaged using the force modulation technique and normal scanning mode (9).

## 3. Results and Discussion

The polycarbonate disk image showed the laser-etched grooves in the memory storage device, as well as the surface roughness induced by mechanical stamping (Figures 2). The grooves were found to be about 300nm wide and 115nm in depth. The area between the grooves was determined to be approximately 1000nm in width. Scanning Electron Micrographs of the surface verify these dimensional values (Figure 3).

The copolymer of styrene butadiene showed large surface features, on the order of 1000nm. These features may be explained by the spinning technique used to cast the sample, producing a surface that was not uniformly smooth on a small scale. "Ripples" in the image may be due to a "wake" effect produced by the tip as it scanned the image (Figure 4). The sample was also imaged in the force modulation mode. Figure 5 is the surface topographical image in the area which was scanned using force modulation. Figure 6 is the modulation image from the scan area. There are several areas in the modulation image that are shown to have higher degrees of hardness (brighter areas), that do not correspond to surface topographical images on the normal scanned image. These areas may be hard copolymer segments on the surface.

Figure 7 shows a surface view of the graphite fiber polycarbonate matrix composite that was imaged using the normal scanning mode. The apparent matrix fiber interface was aligned with the tip prior to scanning. The image shows a surface discontinuity that may be the fiber matrix interface. Figure 8 shows the area scanned for the force modulation image. Figure 9 is the force modulation image. The lighter zones in figure 9 may be graphite fiber (the reported fiber width is 7μm) (9). It is also significant to note the differences in the apparent hardness of the matrix. The matrix to the outside of the fiber (away from the fiber bundle - right side), is a lighter color and therefore possibly a harder material. This could also be possibly due to the surface topology as indicated by the surface scan images in the figure.

Reviewing the images from the different surface scans, it can be seen that the material with the highest modulus, the polycarbonate disk, produced the sharpest images, and the copolymer sample (having the lowest modulus) was very difficult to image. This result compares well with the expected effects of modulus on the surface scanning.

## 4. Conclusions

The advantage of the AFM and similar techniques is based on their ability to image microscale features with out damaging the surface. This ability is determined by critical parametric considerations of the microscope and of the surface to be imaged. Using continuum elasticity theory arguments and calculations of the intermolecular forces involved, a theory has been presented to describe the deformation of a system due to the force applied by an AFM tip. The results show that atomic resolution of polymeric materials is possible given tips of small radius of curvature, reduced surface forces, or samples of adequate modulus. These constraints are variable considering the tip-cantilever system used, the environment under which the sample is imaged, and the properties of the material itself.

The images obtained using the force modulation technique also indicate promise for that technique. With the use of cantilevers of varying spring constant, the sensitivity of the modulation images can be

enhanced (See figure above). This technique is also able to produce images in liquid environments.

#### 5. Future Work:

The force modulation technique indicates promise in its ability to indicate regions of surface elasticity of a sample. The sensitivity of the technique is highly dependent on the spring constant of the cantilever, where the spring constant will determine the deflection of the cantilever,  $\Delta z_d$ . In order to select a desired sensitivity, cantilevers of varying spring constant need to be built. We are currently making prototype cantilevers that we will be using for force modulation analysis. We would like to image different block systems using the force modulation technique in air and other mediums to identify the different segments. This may allow us to view different processes, such as the mechanochemical transition in polypeptides that may be a result of pH change (10-11), and the surface mobility of segmented polyurethanes (12). The ability to view the polypeptide transition may enable us to confirm the kinetics of the mechanochemical reaction. The structure of polyurethane surfaces in different environments is not widely understood. Specifically, the ability of the segments to reorient in the presence of polar media, such as water, is of great interest. We believe it is possible to use the force modulation method to image the transition in the presence of water.

#### 6. References:

1. G. Binnig, C.F. Quate, C. Gerber, Phys. Rev. Lett., 56, 9, 930 (1986).
2. G. Binnig and H. Rohrer, IBM J. Res. Develop., 30, 4, 355 (1986).
3. P.K. Hansma, V.B. Elings, O. Marti, C.E. Bracker, Science, 242, 209 (1988).
4. M.M. Dovek, et al., J. Microscopy, 152, Pt1, 229 (1988).
5. P. Maivald, et al., unpublished manuscript, 1991.
6. N.A. Burnham & R.J. Colton, J. Vac. Sci. Technol. A, 7(4), 2906 (1989).
7. K.L. Johnson, Contact Mechanics, Cambridge University Press, New York, 1985.
8. J.D. Andrade, D.L. Coleman, D.E. Gregonis, Makromol. Chem., Rapid Commun., 1, 101, 104 (1980).
9. Composite sample provided by Paul Stone, Department of Materials Science, University of Utah, 84112.
10. D.W. Urry, International Journal of Quantum Chemistry: Quantum Biology Symposium, 15, 235 (1988).
11. D.W. Urry, et al., Proc. Natl. Acad. Sci USA, 85, 3407 (1988).
12. K.G. Tingey, J.D. Andrade, R.J. Zdrahala, K.K. Chittur, R. M. Gendreau, "Surface Analysis of Polyether and Polysiloxane soft segment Polyurethanes", in Surface Characterization of Biomaterials, B.D. Ratner ed., Elsevier Science Publishers B. V., Amsterdam 1988.

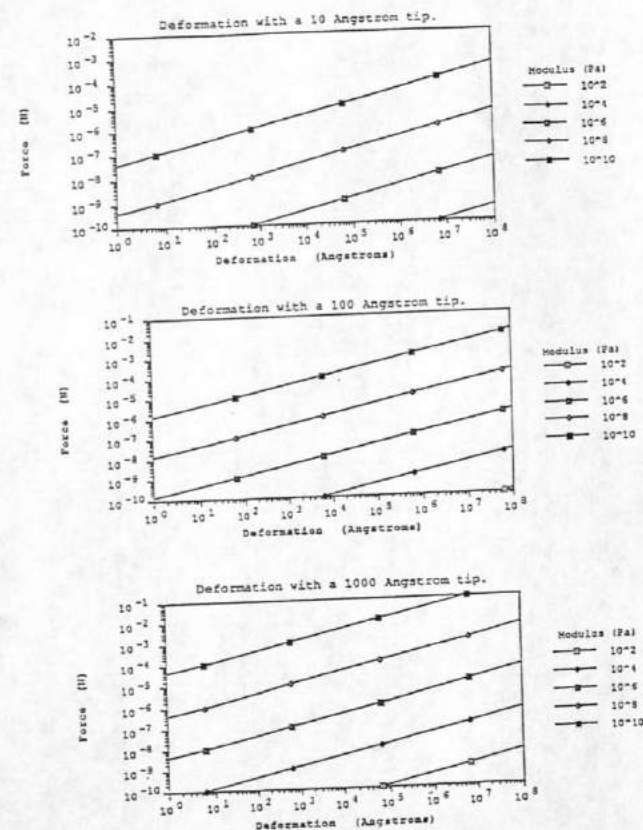
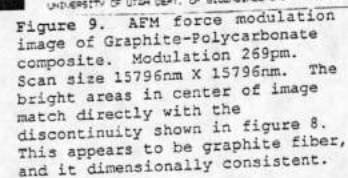
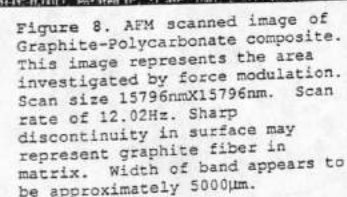
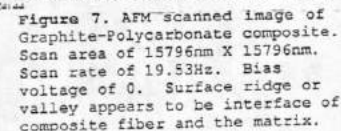
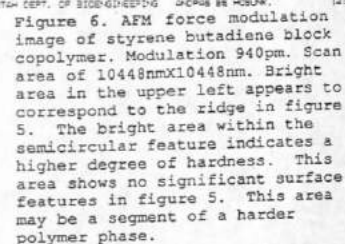
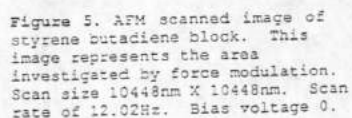
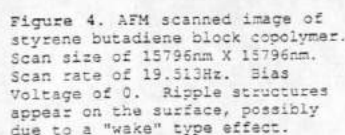
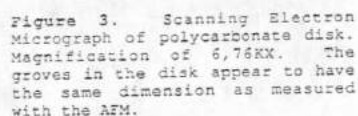
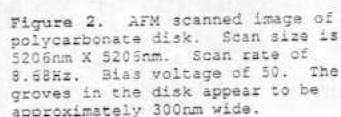


Figure 1. Resulting deformation ( $\text{\AA}$ ), as calculated, versus applied force (N) with changing modulus (Pa), and for three different tip radius values ( $\text{\AA}$ ). From the figures it can be seen that deformations below the detectable range of the AFM (about  $10^2 \text{\AA}$ ) requires a material of high modulus (above  $10^4$ ) for tips of common radius values ( $100 \text{\AA}$ ).





Reprint file  
pdf Stuart - 2 Domain  
1994 AdS Unpubl.

A Structural Domain Approach to Predicting the Adsorption of Albumin

Joan K. Stuart, Joseph D. Andrade and Vladimir Hladky  
Department of Bioengineering, Center for Biopolymers at Interfaces, University of Utah,  
Salt Lake City, UT, 84112, USA

Abstract

Many proteins consist of multiple domains that, while structurally similar, tend to behave autonomously in their electrostatic and thermodynamic properties. It is thought that the microheterogeneity exhibited by these domains can explain why complex proteins adsorb to surfaces with a wide variety of properties. This hypothesis is being applied specifically to albumin, as it has been used extensively as a model for studying complex protein behavior. The X-ray crystal structure for human serum albumin (HSA) has also been recently determined. Using the published two-dimensional images in conjunction with known structural features, a rough computer model has been developed. Electrostatic and hydrophobic properties are simulated using this model, from which adsorption properties can be inferred for each domain and for the molecule as a whole. Using this model and available literature data, the structural domain approach is developed as a basis for studying the adsorption of other complex proteins.

Introduction

The adsorption of proteins at various interfaces is important in a range of medical and biotechnological applications. Protein adsorption is not well understood and thus is not easily controlled.<sup>2</sup> Protein interaction with biomaterial surfaces partially dictates the compatibility of an implant. The events that can occur upon adsorption of blood proteins include: activation of the complement and coagulation cascades, depletion of local regulators or inhibitors of hemostasis or thrombosis,<sup>3</sup> or non-specific binding, in immunoassays and clinical diagnostics.<sup>4</sup> The explanation and prediction of protein behavior at interfaces is thus an important first step in the attempt to manipulate these processes in a beneficial way.

Protein Adsorption

The process of protein adsorption is driven by a reduction in free energy of the surface, solvent and protein.<sup>5</sup> Probably the major interaction parameter that affects free energy minimization is the dehydration of hydrophobic areas. If a protein has exposed hydrophobic patches, their adsorption to a surface will allow for a decrease in the order of the surrounding water molecules, which is highly favorable.

Several techniques have been used to study the hydrophobic interactions at an interface. An "Effective Surface Hydrophobicity" can be determined using fluorescent probe titration or hydrophobic interaction chromatography.<sup>10</sup> If the structure of the surface in question is known, computer graphics packages can be used to visualize and estimate the hydrophobic / hydrophilic ratio. The surface free energy, before and after interaction with proteins, can be estimated using contact angle techniques.<sup>2</sup>

Due to the ionic nature of proteins, the maintenance of electroneutrality is also a driving force for adsorption. The redistribution of charged groups affects the coulombic or electrostatic forces between a protein and a surface.<sup>5,5</sup> As ionized amino acid residues tend to be located at the aqueous interfaces of proteins, there may exist charged patches which will interact with a charged surface. While electrostatic attraction is a major driving force for protein adsorption, electrostatic repulsion has been shown not to prevent adsorption in many cases.<sup>6</sup> It is hypothesized that in this situation, ions are transferred from solution to the adsorbed layer to minimize electrostatic potential and compensate for any contrasts in charge.

Electrostatic properties of biopolymer systems have been well studied.<sup>6,6.5</sup> The isoelectric point of proteins and synthetic polymers can be determined using electrophoretic or chromatofocusing techniques. Norde has demonstrated the effect of pH and ionic strength on adsorption by comparing the electrokinetic charges of proteins and surfaces separately with that of the protein - surface complex.<sup>6</sup> By studying electrophoretic mobilities as well as proton titration profiles, the participation of protons versus other ions in the adsorption process was determined.

For small, compact globular proteins, electrostatic and hydrophobic parameters constitute the major driving forces for protein adsorption. For larger, more flexible multidomain proteins, the problem becomes quite complicated as each major domain can, in principle, interact with the surface semi-independently.<sup>10</sup> In addition, structural rearrangements must be considered as a factor.<sup>7</sup> If a protein's stability is low, hydrophobic regions normally located on the interior of the molecule, such as those of an  $\alpha$ -helix or  $\beta$  sheet, may be able to interact with a sorbent surface in such a way that they are still shielded from contact with water. This may lead to a loss in secondary and tertiary structure, and consequently an increase in conformational entropy of the protein, thus favoring



adsorption. It has been shown that helix amphiphilicity has a large effect on the surface activity and spreading of proteins.<sup>8,9</sup>

An extensive coverage of the important variables considered<sup>2</sup> and techniques used<sup>26,27</sup> in protein adsorption studies has been presented. The energetic nature of the solution, sorbent surface and protein must be well known and properly characterized. Variables such as pH, ionic strength and protein conformation can then be systematically altered to determine protein adsorption parameters.

Although many hypotheses have been developed for "simple" proteins,<sup>28,29</sup> methods to accurately predict the adsorption behavior of multi-domain proteins are not available. A new approach to the definition of protein structure may glean further insight into the interfacial behavior of complex proteins.

#### Rationale for the Domain Approach

The three-dimensional structures and functions of several small proteins are known, and are being used as models to predict the adsorption of simple proteins at simple interfaces.<sup>10</sup> To understand the adsorption behavior of complex systems, such as blood, at complex interfaces, such as those of block copolymers, we must attempt to develop models for predicting the adsorption of proteins for which the 3-D structure may not be known.

According to Privalov, thermal denaturation profiles of large proteins and their proteolytic fragments demonstrated that these proteins are divided into cooperative subsystems, or domains.<sup>11</sup> A cooperative domain consists of a maximum of approximately 200 amino acid residues, its size being dictated by its ability to fold into a discrete structure. Structural domains can be identified as regions of relatively high packing density, which may be highly homologous, usually connected by looser areas of the peptide chain. Independent functional and binding behavior of domains can be deduced by proteolytic fragment studies, due to the fact that interdomain connections are usually the most susceptible to cleavage.<sup>12</sup>

Structural domains have been shown to behave somewhat autonomously in their thermodynamic and electrostatic properties.<sup>13,14</sup> While structurally similar, the

conformational stability of each domain may vary enough to be detected in denaturation studies. Because of the varying amino acid composition of each domain, proteins also appear to exhibit a microheterogeneity, wherein the overall charge of a protein can be broken down to the charges carried by each individual domain. It is proposed that the differences in properties of structural domains can help to explain why complex proteins are capable of adsorbing to surfaces with widely varying characteristics.<sup>10, \*</sup>

Because the X-ray crystal structures of many complex proteins of interest have not yet been resolved, several numerical and empirical methods have been developed to predict protein structure from a known amino acid sequence. One such method, developed by Lim,<sup>15</sup> searches for patterns of polar and non-polar residues in order to identify possible helices and  $\beta$ -sheets. A related method of analysis, developed by Eisenberg and utilized here, calculates the "hydrophobic moment," or magnitude and direction of the hydrophobic "face" of each individual helix and of the molecule as a whole.<sup>16</sup> There are also several powerful homology software packages which compare segments of amino acid sequence against those in proteins of known structure. If the sequences are homologous, it can be deduced that the folding properties are similar. These prediction methods are usually anywhere from 50 to 70% accurate.<sup>15</sup>

#### Case Study: Domain Properties of Albumin

In our efforts to model multi-domain proteins at multidomain interfaces, we have attempted to simulate structural domain properties using available literature data and some of the numerical prediction methods. One of the most commonly studied complex proteins is serum albumin. Because of its importance in blood-material interactions, as well as the fact that it is well characterized and the 2.8 Å resolution X-ray crystal structure of Human Serum Albumin (HSA) was recently published,<sup>17</sup> it is selected as a model complex protein with which to begin application of the domain concept.<sup>14</sup>

As coordinates for HSA are not yet available in the Protein Data Bank, we have utilized the two-dimensional published photographs with relative locations of helices and disulfide bonds,<sup>17</sup> along with the available literature data<sup>12-14,18-21</sup> and amino acid sequence information<sup>18</sup> to create a rough computer model of albumin (see Figure X). This model was built using the Biopolymer module of the INSIGHT / DISCOVER molecular graphics package (BIOSYM Technologies, Inc., San Diego, CA) on a Silicon Graphics Indigo™ workstation. Due to the structural homology of albumin's three

domains, for practical purposes, the structure of one domain was first developed, and then copied and modified as needed for the other two domains. The helical locations were estimated and oriented to maintain a hydrophobic inner core by calculating the hydrophobic moment.<sup>16</sup> This method locates a polar vector every 100° with a magnitude equal to the relative hydrophobicity of each residue, then calculates the overall magnitude and direction of the hydrophobic core for each helix.

As one can see from Figure X, a depiction of the original images from Ref. 17, Human Serum Albumin is a heart shaped three domain protein with sides of approximately 80Å. The arrows point to locations of two main hydrophobic binding pockets known to exist in albumin. The equilateral placement of the three domains is different from the linear "cigar" shape that has been typically considered.<sup>18</sup> Figure Y represents a "cartoon" of the orientation of domains reflected by this structure, adapted from the model previously proposed in Ref. 18. The equal accessibility of each domain should allow albumin to adsorb from any orientation, depending on the properties of the interface.

Studies in the literature have provided strong support for the domain concept as it applies to albumin. Tiktopulo, et. al., used calorimetry to study denaturation curves of intact albumin (HSA and Bovine Serum Albumin, BSA) and of a fragment corresponding to domains II and III, and were able to discriminate three and two (respectively) independent melting temperature peaks, indicating that the three domains of albumin do behave or unfold independently.<sup>13</sup> An alternative theory which supports the domain concept is that of Damodaran's group.<sup>19</sup> This research looks at the refolding of hydrophobic binding regions of albumin, using ANS as a hydrophobic probe. By following helical content, it is demonstrated that the refolding process follows complex kinetics, suggesting cooperativity between domains. It is thought that there are corresponding portions of each domain which have analogous stabilities, and therefore the stepwise refolding reflects first the independent refolding of subdomain regions and reshuffling of disulfide bonds, then the interaction of subdomains to form the three native domains.

With regard to hydrophobic binding sites, Hamilton has looked at the fatty acid binding sites of domain-sized fragments of albumin.<sup>20</sup> While the three domains are known to be structurally similar,<sup>17</sup> their ligand binding capabilities are not equal. Through NMR studies it is recognized that there exist unique "microenvironments" around each binding site, probably due to differences in amino acid composition and stability. They also note

that the binding of one site tends to affect the binding capability of the others. It is interesting to note that two of the three major fatty acid binding sites, known to be located in domains IIA and IIIA, can be seen in Figure X to be in physical proximity and could easily affect the stability of one another.<sup>17</sup>

As noted, the three domains, while structurally quite similar, have slight differences in their properties which could cause them to prefer different surfaces. When exposed to a hydrophobic surface, the domain with least stability would be expected to drive the adsorption in order to dehydrate hydrophobic pockets. It is known that domains II and III each contain six disulfide bonds, while domain I has a free cysteine and only five disulfide bonds.<sup>18</sup> Therefore the stability of subdomain IA would be expected to be slightly lower than the others. It has also been shown by Takeda that the C-terminal helices are the first to denature in surfactant binding studies.<sup>21</sup> It was suggested that Domain III is relatively loosely packed, and it can be seen from the X-ray crystal structure that this is indeed the case.

Surface tension studies have shown that, although albumin contains so many disulfide bonds, it is not especially conformationally stable at the air-water interface, as compared to several other smaller, compact proteins.<sup>8</sup> This is in agreement with the structural rearrangements proposed by Norde for model proteins. With the availability of the crystal structure images, one can see that the inter-subdomain connections, shown in Figure M as our developed computer model for domain II, are flexible extended regions which serve as "hinges" for the opening of the binding pockets and which could easily allow for unfolding and structural rearrangements to occur. Damodaran also notes that the backbone must be flexible and that the intersubdomain connections have no disulfide bonds, in order to facilitate proper refolding.<sup>19</sup>

#### Simulation of Properties

Andrade, et. al., have used the amino acid sequence of each domain to simulate their individual charge characteristics at various pH values.<sup>14</sup> It is possible from this data to begin to predict the behavior of individual domains at various interfaces (see Figure B).

One can imagine that at lower pH values, the more positively charged domains (I and III) would tend to adsorb at a negatively charged surface, while at physiologic pH, the molecule may orient in an end-on fashion, with hydrophobic interactions dominating its adsorption.

Domains with the least charge may tend to adsorb at hydrophobic interfaces. However, the less stable loops in domains I and III may dominate the adsorption in order to dehydrate the hydrophobic residues.

Predictions such as these are being made now to explain the behavior of multidomain proteins at multidomain interfaces. Andrade, et. al., have developed a method for multivariate analysis of protein surface parameters called the Tatra plot.<sup>10</sup> Using this twelve-axis radial plot, one is able to correlate various contributions of charge, hydrophobicity and stability factors to observed adsorption behavior. These plots have been developed for simple proteins, such as lysozyme, myoglobin, etc. It is proposed that the development of a simplified Tatra plot for each domain of albumin, or of other complex proteins, would aid in deducing trends which may not be easy to visualize when looking at the protein as a whole.

Molecular graphics packages provide a powerful tool for simulating and visualizing various surface properties of biomolecules, which could be incorporated into a Tatra plot. Once a relatively realistic model of albumin had been built using this software, it was then possible to simulate the electrostatic and hydrophobic properties of the so-called "native" state. Figure N shows a view of HSA using a van der Waals surface with a probe radius of 4 Å. The amino acid residues are colored according to their properties, with the hydrophobic residues in white. By quantifying the proportion of hydrophobic surface area, one is able to estimate the "effective surface hydrophobicity" of the molecule. The hydrophobic as well as charged patches on the surface of a molecule can give one a good indication of the events upon initial contact between a protein and a surface.

Shown in Figure P is an electrostatic simulation of the albumin model using BIOSYM's DelPhi module. This package utilizes a finite difference method to calculate electrostatic potential with the non-linear Poisson-Boltzmann equation. Positively charged fields are depicted by the blue mesh, and negatively charged with red. The image shows a simulation of the field at 1 kT/e around the molecule, at neutral pH and an ionic strength of .01M. It can be seen that the charge is not distributed evenly around the molecule, but is more positive at domain III and negative at domain I. As depicted in Figure C, initial adsorption onto a surface may depend on the orientation of the molecule and which domains collide with it.

It is also possible to compare the properties of each individual domain with those of the whole protein. [Figure Q (a&b) shows the electrostatic potential of domains II and III, resp. \*\*\*\*] The hydrophobicity and electrostatic field of one domain would be expected to interact with and affect the properties of another domain as much as it would with a surface.

The properties of a sorbent surface have as much of an effect on adsorption as do the biomolecule's surface properties. As discussed earlier, Norde has demonstrated the role of low-molecular-weight counterions in the adsorption of proteins to positively and negatively charged surfaces.<sup>6,23</sup> The anomalous effect of surfaces has been shown.<sup>6,5,30</sup> Bernabeu found that negatively charged proteins at pH 7.4 would adsorb to a negatively charged platinum electrode, while adsorption was charge-independent on a carbon electrode.<sup>6,5</sup> Again ion coadsorption is thought to be a factor. It is also possible, in the case of albumin, that domain III, which is neutrally charged as well as relatively unstable at neutral pH,<sup>14</sup> could aid in driving its adsorption.

Protein interactions have also been analyzed at the interfaces of complex polymers, specifically segmented polyurethanes.<sup>24</sup> Block co-polyurethanes have demonstrated good biocompatibility in blood contacting applications. It is thought that the phase-separated microstructure of these materials, which have surface "domains" ranging from 50-250Å in width,<sup>25</sup> may direct protein adsorption, as many protein domains are of comparable size.

Simulations of polymer surface properties are readily done using Biosym's extensive Polymer module, recently released, or the newly developed Surfaces module. With this software, an extremely intensive simulation of the interactions between multidomain proteins and multidomain surfaces can be performed by associating a surface, protein and solvent, and initiating a free energy minimization.

#### Conclusion

The adsorption properties of individual structural domains can be predicted using a combination of current techniques. Much of the existing literature data, especially that obtained from proteolytic domain-sized fragments, can glean information on independent domain behavior. The electrostatic characteristics can be inferred from the amino acid sequence, as well as from isoelectric or chromato-focusing techniques. Effective surface

hydrophobicity may be qualified using experimental techniques, although often these data are misleading. Advances in numerical prediction methods are allowing accurate and robust models to be developed when the X-ray structure for a protein is not known. Computer software is also now available which will simulate the surface properties of proteins as well as those of synthetic homopolymers or copolymers with great accuracy, thus enhancing the ability to quantitatively determine electrostatic and hydrophobic parameters.

By breaking large proteins down into structural and functional entities, one is able to simplify the understanding of their behavior. By approaching the prediction of the adsorption of multi-domain proteins on to multi-domain surfaces in this simplified manner, we may be better able to resolve seemingly anomalous behavior, and therefore better engineer a more compatible or desirable protein-surface interaction.

#### Acknowledgements

This work was supported by an NIH Biotechnology Training Grant (GM08393) and by the Center for Biopolymers at Interfaces, University of Utah. The authors wish to thank BIOSYM Technologies, Inc., for their generous donation of INSIGHT / DISCOVER computer graphics software and Silicon Graphics, Inc., for computer graphics workstations.

#### References:

- 2) Andrade, JD, "Principles of Protein Adsorption," Protein Adsorption, JD Andrade, ed., Plenum, 1985.
- 3) Brash, JL, "Role of Plasma Protein Adsorption in the Response of Blood to Foreign Surfaces," Blood Compatible Materials and Devices: Perspectives Toward the 21st Century, CP Sharma and M Szycher, eds., Technomic, Lancaster, PA, 1991.
- 4) Lin, J-N, Chang, I-N, Andrade, JD, Herron, JN and Christensen, DA, "Comparison of site-specific coupling chemistry for antibody immobilization on different solid supports," *Journal of Chromatography*, **542** (1991) 41-54.
- 5) Norde, W, "Why Proteins Prefer Interfaces," *J. Biomater. Sci. Polymer Edn.*, Vol. 2(3), 183-202 (1991).
- 5.5) Ho, C-H, Ph.D. Thesis, University of Utah, anticipated 1994.
- 6) Norde, W, "Ion Participation in Protein Adsorption at Solid Surfaces," *Colloids and Surfaces*, **10**, (1984) 21-31.
- 6.5) P. Bernabeu and A. Caprani, "Influence of surface charge on adsorption of fibrinogen and/or albumin on a rotating disc electrode of platinum and carbon," *Biomaterials*, **11**, 1990, 258-264.
- 7) Norde, W, "The Behavior of Proteins at Interfaces, with Special Attention to the Role of the Structure Stability of the Protein Molecule," *Clinical Materials*, **11** (1992) 85-91.
- 8) Tripp, B, Ph.D. Thesis, University of Utah, 1993.
- 9) Krebs, KE and Phillips, MC, "The contribution of  $\alpha$ -helices to the surface activities of proteins," *FEBS Letters*, **175**(2), 263-266.
- 10) Andrade, JD, et al., "Proteins at Interfaces: Principles, Multivariate Aspects, Protein Resistant Surfaces, and Direct Imaging and Manipulation of Adsorbed Proteins," *Clinical Materials*, **11** (1992) 67-84.
- 11) Privalov, P, "Physical Basis of the Stability of the Folded Conformations of Proteins," *Protein Folding*, T. Creighton, ed., WH Freeman, 1992.
- 12) Takeda, K, Wada, A, Nishimura, T, Ueki, T and Aoki, K, "Isolation of Domain-Sized Fragments of Bovine Serum Albumin by Limited Peptic Digestion and Their Secondary Structural Changes in Solution of Urea, Guanidine Hydrochloride and Sodium Dodecyl Sulfate," *Journal of Colloid and Interface Science*, Vol. 133, No.2, 497-504, 1989.
- 13) Tiktopulo, EI, Privalov, PL, Borisenko, SN and Troitskil, GV, "Microcalorimetric Study of Domain Organization of Serum Albumin," translated from *Molekulyarnaya Biologiya*, Vol. 19, No. 4, 1072-1078, 1985.
- 14) Andrade, JD, Hlady, V, Wei, A-P and Golander, C-G, "A Domain Approach to the Adsorption of Complex Proteins: Preliminary Analysis and Application to Albumin," *Croatica Chemica Acta*, **63** (3) 527-538 (1990).
- 15) Argos, P, "Predictions of protein structure from gene and amino acid sequences," *Protein Structure: a practical approach*, T. Creighton, ed., IRL Press, 1989.
- 16) Eisenberg, D, Weiss, RM, Terwilliger, TC and Wilcox, W, "Hydrophobic Moments and Protein Structure," *Faraday Symp. Chem. Soc.*, 1982, **17**, 109-120.
- 17) He, X-M and Carter, DC, "Atomic structure and chemistry of human serum albumin," *Nature*, **358**, (16 July 1992), 209-215.
- 18) Peters, T, "Serum Albumin," *Adv. Prot. Chem.*, **37**, 161-245, 1985.
- 19) Damodaran, S, "Kinetics of formation of hydrophobic regions during refolding of bovine serum albumin," *Int. J. Peptide & Protein Res.*, **27**, 1986, 589-595.



- 20) Hamilton, JA, Era, S, Bhamidipati, SP and Reed, R, "Locations of the three primary binding sites for long-chain fatty acids on bovine serum albumin," *Proc. Natl. Acad. Sci. USA*, **88**, 2051-2054, 1991.
- 21) Takeda, K, Shigeta, M and Aoki, K, "Secondary Structures of Bovine Serum Albumin in Anionic and Cationic Surfactant Solutions," *Journal of Colloid and Interface Science*, **117**, No.1, 1987, 120-126.
- 23) A.V. Elgersma, R.L.J. Zsom, W. Norde and J.Lyklema, "The Adsorption of Bovine Serum Albumin on Positively and Negatively Charged Polystyrene Latices," *Journal of Colloid and Interface Science*, **138**, No. 1, 1990, 145-156.
- 24) S.L. Goodman, S.R. Simmons, S.L. Cooper and R.M. Albrecht, "Preferential Adsorption of Plasma Proteins onto Apolar Polyurethane Microdomains," *Journal of Colloid and Interface Science*, **139**, No. 2, 1990, 561-570.
- 25) K. Tingey and J.D. Andrade, "Probing Surface Microheterogeneity of poly(ether urethanes) in an Aqueous Environment," *Langmuir*, 1991, **7**, 2471-2478.
- 26) Hlady, V, chapter submitted to J. Brash book.
- 27) Horbett, TA, "Techniques for Protein Adsorption Studies," in Techniques of Biocompatibility Testing, Volume II, D.F. Williams, ed., pp. 183-214, CRC Press, Inc., Boca Raton, FL, 1986.
- 28) Hlady, V, Andrade, JD, Ho, C-H, Feng, L, Tingey, K, "Plasma Protein Adsorption on Model Biomaterial Surfaces," submitted to *J. Clin. Materials*, August 1991.
- 29) Dill, KA, "Dominant Forces in Protein Folding," *Biochemistry*, **29**, No. 31 (1990), 7133-7155.
- 30) Feng, L and Andrade, JD, "Protein Adsorption on Low Temperature Isotropic Carbon: II. Effects of Surface Charge of Solids," submitted to *Journal of Colloid and Interface Science*, 1992.

Joe-  
 No it was never submitted  
 (!!!) Sorry about 46.13-  
 I needed to do some more  
 Biosym simulations and  
 kept having technical problems  
 or time problems....  
 Did you want to reference  
 it? I may be able to get  
 it together when we get  
 connected in the new bldg.

- Joan

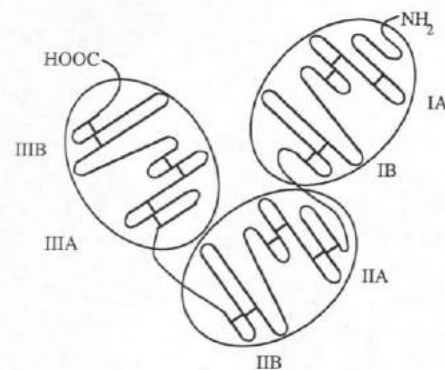
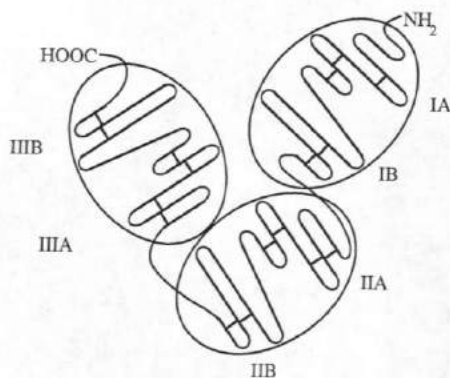


Figure Y.



(4)  
Fig. 2. Cartoon model of serum albumin, modified from Ref. 18 to reflect the recently determined equilateral orientation of the three domains. Subdomains are labeled accordingly (IA, IB, etc.), and disulfide bridges are represented by lines connecting backbone chains.

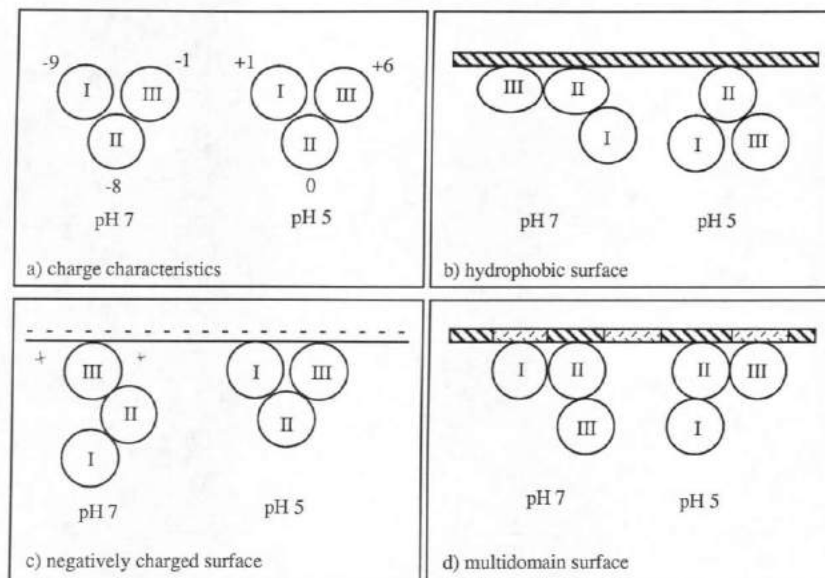


Figure B. Charge characteristics of individual structural domains of BSA (adapted from Ref. 10). a) Charge values for each domain at different pH values, calculated using \_\_\_\_\_ software. b) Possible behavior on a hydrophobic surface. Domains with the least charge, or the least stability in solution, will favor adsorption. Varying degrees of unfolding may also occur. c) Possible behavior on a negatively charged surface. Positively charged domains (I and III) at pH 5 may drive adsorption. At physiologic pH, there will be electrostatic repulsion, somewhat counteracted by hydrophobic interactions. d) Predictions for interactions with multidomain surfaces, the domains of which are of similar size to those of a protein.

opposed by counterions &

# Effect of water and tacticity on the glass transition temperature of poly(2-hydroxyethyl methacrylate)

Y. K. Sung, D. E. Gregonis, G. A. Russell, and J. D. Andrade

Department of Materials Science and Engineering, University of Utah, Salt Lake City, Utah 84112, USA

(Received 4 April 1978; revised 23 June 1978)

Poly(2-hydroxyethyl methacrylate) (PHEMA) and related hydrogels are being studied for a variety of medical applications<sup>1</sup>.

Several conflicting values of the glass transition temperature ( $T_g$ ) of PHEMA have been reported. The range of values quoted are summarized in Table 1. The disagreement between the values quoted may be attributed to the large influence of sorbed moisture due to the hygroscopic nature of the materials<sup>2</sup>. Differences in tacticity may also be expected to affect the  $T_g$ .

In this study the  $T_g$  of PHEMA samples of different tacticities has been determined as a function of sorbed water content. The samples based on PHEMA are: (a) 58% syndiotactic, 42% heterotactic PHEMA containing 1 mol % ethylene glycol dimethacrylate (EGDMA) crosslinker and polymerized at 333K and (b) 80% isotactic, 15% heterotactic, 5% syndiotactic PHEMA polymerized at 263K without added crosslinker (preparation details are given in ref 13). The tacticities of the samples were measured by <sup>13</sup>C n.m.r. spectra<sup>3,4,13</sup>.

The  $T_g$  data were obtained from differential scanning calorimetry (d.s.c.) thermograms using a Dupont 990 thermal analyzer and d.s.c. cell base. The instrument was calibrated with indium, tin, and triple distilled water. The  $T_g$  values measured are shown in Figure 1. Extrapolating linearly the portion of

the graph where water content approaches zero, the  $T_g$  values are:  $393 \pm 2$ K for the 58% syndiotactic sample (a), and  $311 \pm 2$ K for the 80% isotactic sample (b).

The effect of diluents (or plasticizers) on the  $T_g$  of a polymer may, for many systems, be given by<sup>14,16</sup>:

$$\frac{1}{T_g} = \frac{W_1}{T_{g1}} + \frac{W_2}{T_{g2}} \quad (1)$$

where subscripts 1 and 2 refer to polymer and diluent (H<sub>2</sub>O), respectively;  $W_1$  and  $W_2$  are the weight fractions of polymer and water, respectively. Equation (1) may be arranged to a more convenient form by utilizing the identity:

$$W_1 = (1 - W_2) \quad (2)$$

Thus:

$$\frac{1}{T_g} = \frac{1}{T_{g1}} - W_2 \left( \frac{T_{g2} - T_{g1}}{T_{g1} T_{g2}} \right) \quad (3)$$

This equation states that for systems containing no water  $T_g$  is equal to  $T_{g1}$ .

Utilizing equation (3), we can calculate the average  $T_g$  of the system PHEMA-H<sub>2</sub>O since we know the  $T_g$  for 58% syndiotactic PHEMA (393K), for 80% isotactic PHEMA (311K) and for water (139K)<sup>17,18</sup>. The calculated values for PHEMA-H<sub>2</sub>O systems are shown as the broken and full lines in Figure 1.

The results show that the  $T_g$  of PHEMA is markedly affected by the water content and by the stereochemistry of the polymer. This lowering of  $T_g$  is likely due to the removal of barriers to the rotational and translational motions of the PHEMA molecule chain segments due to their interactions with water molecules. The difference between the  $T_g$  of isotactic and syndiotactic PHEMA can be interpreted in terms of structure formation as follows: in the isotactic structure the steric hindrance between the bulky ester side chains can be minimized by coiling the backbone into a helical

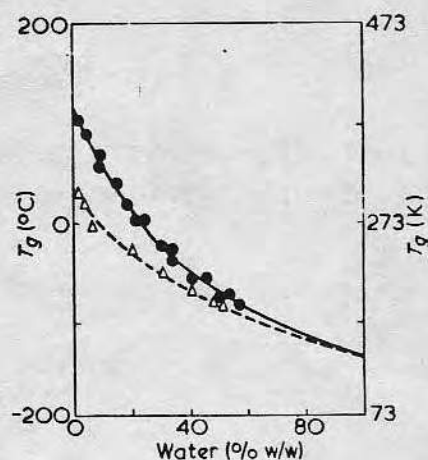


Figure 1 The glass transition temperature as a function of water content in (a) 58% Syndiotactic, 42% Heterotactic PHEMA - 1 mol % EGDMA; (b) 80% Isotactic, 15% Heterotactic, and 5% Syndiotactic PHEMA ( $\Delta$ ). The  $T_g$  of pure water is taken as 139K 139K<sup>17,18</sup>. The dotted and solid lines are the values calculated from equation (3)

structure<sup>3</sup>. The syndiotactic polymer, however, may form much stiffer structures because the side chain impingement cannot be eliminated by helix formation<sup>3</sup>. These results correspond with the data observed for poly(methyl methacrylate) PMMA; i.e.,  $T_g$  of isotactic PMMA is 316K, while that of syndiotactic PMMA is 388K<sup>19</sup>.

## REFERENCES

- 1 Ratner, B. D. and Hoffman, A. S. in 'Hydrogels for Medical and Related Applications', (Ed. J. D. Andrade), ACS Symp. Ser. 1976, 31, pp. 1-36
- 2 Kettle, G. J. *Polymer*, 1977, 18, 742
- 3 Russell, G. A. *PhD Dissertation* University of Utah, Salt Lake City, Utah (1977)
- 4 Russell, G. A., Dalling, D. K., Gregonis, D. E., DeVisser, A. C. and Andrade, J. D. in 'Hydrogels for Medical and Related Applications', (Ed. J. D. Andrade), ACS Symp. Ser. 1976, 31, p 139
- 5 Shen, M. C., Strong, J. D. and Matusik, F. J. *J. Macromol. Sci. (B)* 1967, 1, 15
- 6 Haldon, R. A. and Simha, R. *J. Appl. Phys.* 1968, 39, 1890
- 7 Ilavsky, M. and Prins, W. *Macromolecules* 1970, 3, 415
- 8 Ilavsky, M., Hasa, J. and Janacek, J. *Collect. Czech. Chem. Commun.* 1968, 33, 3197
- 9 Nakamura, K. and Nakagawa, T. *J. Polym. Sci. (Polym. Phys. Edn)* 1975, 13, 2299
- 10 Ilavsky, M. and Hasa, J. *Collect. Czech. Chem. Commun.* 1968, 33, 2142
- 11 Kolarik, J. and Janacek, J. *J. Polym. Sci. (A-2)* 1972, 10, 11

Table 1 Reported glass transition temperatures of PHEMA

$T_g$ (K)	Reference
308*	3
347	4
359	5, 6
363	7
366.5	8, 9
371	10
373	11, 12
382†	3

\* Isotactic PHEMA; † syndiotactic PHEMA

- 12 Kolarik, J., Janacek, J. and Nicolais, L. *J. Appl. Polymer Sci.* 1976, **20**, 841
- 13 Gregonis, D. E., Russell, G. A., de Visser, A. C. and Andrade, J. D. in preparation
- 14 Fox, T. G. *Bull. Am. Phys. Soc.* 1956, **1**, 123
- 15 Miller, M. L. 'The Structure of Polymers', Reinhold, New York, 1966, p 291
- 16 Nielson, L. E. 'Mechanical Properties of Polymers', Reinhold New York, 1962, p 27
- 17 'Water, A Comprehensive Treatise', (Ed. F. Franks), Plenum Press, New York, 1972, Vol 1, pp 116, 127, 407, 408
- 18 Sugisaki, M., Suga, H., and Seki, S. *Bull. Chem. Soc. Jpn* 1968, **41**, 2591
- 19 Fox, T. G., Goode, W. E., Gratch, S. Huggett, C. M., Kincaid, J. F., Spell, A. and Stroupe, J. D. *J. Polym. Sci.* 1958, **31**, 173



# Thermal and Pulse NMR Analysis of Water in Poly(2-hydroxyethyl Methacrylate)

Y. K. SUNG,\* D. E. GREGONIS, M. S. JOHN,<sup>†</sup> and J. D. ANDRADE,  
Department of Materials Science and Engineering and Department of  
Bioengineering, College of Engineering, University of Utah,  
Salt Lake City, Utah 84112

## Synopsis

Hydrophilic three-dimensional methacrylate polymer networks (hydrogels) were prepared from 2-hydroxyethyl methacrylate (HEMA) monomer and tetraethylene glycol dimethacrylate (TEGDMA) as crosslinker. The nature and states of water in these hydrogels were studied by differential thermal analysis and pulse NMR relaxation spectroscopy. The thermal studies showed no endotherm peak for ice melting in the lower water content (bound water region); there are two endotherms peaks for higher water content hydrogels near 0°C. The amounts of bound water, intermediate water, and bulklike (free) water in the hydrogels were determined from a quantitative analysis of the endotherms of the water melting transitions. The water structure ordering in the hydrogels were discussed in terms of the fusion entropy and enthalpy obtained from the endotherm. Nuclear magnetic relaxation spectroscopy was also used to understand the mobilities of the water protons in the hydrogels and the interaction of water molecules with the gel networks. The measured spin-lattice relaxation time ( $T_1$ ) values for water protons in the hydrogels are greatly reduced compared to that of liquid water. The measured values of spin-spin relaxation times ( $T_2$ ) of water protons in the hydrogels are approximately 10 times less than that of  $T_1$  and are almost constant in the region of bound water content. Beyond the bound water content region in the hydrogels, the  $T_2$  values rapidly increase as the water content increases.

## INTRODUCTION

Hydrophilic methacrylate polymers are being considered for biomedical applications.<sup>1-5</sup> These polymers swell in water to become soft crosslinked gels, so-called hydrogels. Synthetic hydrogels have been extensively discussed in the literature.<sup>6-8</sup> The transport characteristics of hydrogel membranes have been examined for a broad range of potential applications, including soft contact lenses,<sup>9</sup> reverse osmosis membranes,<sup>10-12</sup> kidney dialysis membranes,<sup>13-15</sup> and drug delivery systems for antibiotics,<sup>16-18</sup> steroids,<sup>19,20</sup> and enzymes.<sup>21,22</sup>

In order to develop useful synthetic biomedical hydrogels, it is of interest to understand the state and properties of water in such hydrogels. Water in hydrogels has been treated in terms of a three-state model.<sup>23</sup> To test the validity of the model, dilatometry, specific conductivity, and dielectric studies of water in hydrogels have been carried out from -15°C to room temperature for poly(2-hydroxyethyl methacrylate) (pHEMA)<sup>24,25</sup> and poly(2,3-dihydroxypropyl methacrylate) (pDHPMA) gels.<sup>26</sup>

Using the three-state model, we have determined the amounts of bound water, intermediate water, and bulklike (free) water in hydrophilic methacrylate gels

less than 25% water content, the values of  $T_2$  are almost constant. However, beyond this region the  $T_2$  values rapidly increase as the water content gradually increases, indicating the presence of increasing amounts of free and intermediate water. These results are in good agreement with the spin-lattice relaxation results.

## CONCLUSIONS

It is proposed that the interaction of water with hydrophilic methacrylate polymers occurs in three ways: (1) Water molecules are strongly bound to specific sites such as the hydroxyl or ester groups within the polymer network; dynamically and thermodynamically they behave as part of the chains. (2) Water molecules are weakly bound to the hydrophilic sites and/or preferentially structured around the polymer network. (3) Water molecules behave dynamically and thermodynamically as "bulklike" or free water.

The assistance of Dr. D. Dalling and the use of the NMR facilities of the University of Utah Regional Biomedical Resource are gratefully acknowledged. This work was supported by NIH Grant HL16921. We also acknowledge support by the U.S.-Korea Cooperative Science Program, NSF-INT-78-24474. Yong K. Sung thanks Busan National University for a leave of absence to conduct this work.

## References

1. O. Wichterle and D. Lim, *Nature*, **185**, 117 (1960).
2. V. Majkus, Z. Horakova, F. Vymuta, and M. Stol, *J. Biomed. Mater. Res.*, **3**, 443 (1969).
3. M. F. Refojo, *J. Biomed. Mater. Res.*, **3**, 333 (1969).
4. C. R. Taylor, T. C. Warren, D. G. Murray, and W. Prins, *J. Surg. Res.*, **11**, 401 (1971).
5. D. F. Williams and R. Roaf, *Implants in Surgery*, Saunders, London, 1973.
6. O. Wichterle, in *Encyclopedia of Polymer Science and Technology*, Wiley, New York, 1971, Vol. 15, p. 273.
7. S. D. Bruck, *Trans. Am. Soc. Artif. Internal Organs*, **18**, 1 (1972).
8. J. D. Andrade, Ed., *Hydrogels for Medical and Related Applications*, ACS Symposium Series, No. 31, ACS, Washington, D.C., 1976.
9. M. F. Refojo, "Contact Lenses," in *Encyclopedia of Polymer Science and Technology*, Wiley, New York, 1976; Supplement Vol. 1, pp. 195-219.
10. T. A. Jadwin, A. S. Hoffman, and W. R. Vieth, *J. Appl. Polym. Sci.*, **14**, 1339 (1970).
11. J. Kopecek and J. Vacik, *Collection Czechoslov. Chem. Commun.*, **38**, 854 (1973).
12. A. S. Hoffman, M. Modell, and P. Pan, *J. Appl. Polym. Sci.*, **14**, 285 (1970).
13. B. D. Ratner and I. F. Miller, *J. Biomed. Mater. Res.*, **7**, 353 (1973).
14. J. Vacik, M. Czakova, J. Exner, J. Kalal, and J. Kopecek, *Collection Czechoslov. Chem. Commun.*, **42**, 2786 (1977).
15. J. Kopecek, J. Vacik, and D. Lim, *J. Polym. Sci., A-1*, **9**, 2801 (1971).
16. M. Tollar, M. Stol, and K. Kliment, *J. Biomed. Mater. Res.*, **3**, 305 (1969).
17. J. N. LaGuerre, H. Kay, S. M. Lazarus, W. S. Calem, S. R. Weinberg, and B. S. Levowitz, *Surg. Forum*, **19**, 522 (1968).
18. S. M. Lazarus, J. N. LaGuerre, H. Kay, S. R. Weinberg, and B. S. Levowitz, *J. Biomed. Mater. Res.*, **5**, 129 (1971).
19. G. M. Zenter, J. R. Cardinal, and S. W. Kim, *J. Pharm. Sci.*, **67**, 1347 (1978).
20. G. M. Zentner, J. R. Cardinal, and S. W. Kim, *J. Pharm. Sci.*, **67**, 1352 (1978).
21. R. Langer and J. Folkman, *Nature*, **263**, 797 (1976).
22. Y. K. Sung, S. W. Kang, and U. S. Kim, *J. Busan Natl. Univ.*, **29**, 27 (1980).
23. M. S. Jhon and J. D. Andrade, *J. Biomed. Mater. Res.*, **7**, 509 (1973).
24. H. B. Lee, M. S. Jhon, and J. D. Andrade, *J. Colloid Interface Sci.*, **51**, 225 (1975).
25. H. B. Lee, J. D. Andrade, and M. S. Jhon, *Polym. Preprints*, **15**, 391 (1974).
26. S. H. Choi, M. S. Jhon, and J. D. Andrade, *J. Colloid Interface Sci.*, **61**, 1 (1977).
27. J. H. Simpson and H. Y. Carr, *Phys. Rev.*, **11**, 1201 (1958).

\* Department of Chemistry, Busan National University, Busan 607, Korea.

<sup>†</sup> Department of Chemistry, Korea Advanced Institute of Science, Seoul, Korea.

by utilizing differential thermal analysis and nuclear magnetic resonance (NMR) relaxation spectroscopy.

## EXPERIMENTAL

### Preparation of Materials

Purified 2-hydroxyethyl methacrylate (HEMA) was obtained as a gift from Hydro-Med Sciences, Inc., New Brunswick, N.J., containing about 0.2% methacrylic acid, 0.16% diethylene glycol methacrylate, and 0.01% ethylene glycol dimethacrylate. The polymerization of HEMA monomer was initiated by azobis (methyl isobutyrate), 7.84 mmol initiator/mL of HEMA monomer. This ratio is independent of water content in the hydrogels. The other pHEMA copolymers were polymerized with the crosslinking agent tetraethylene glycol dimethacrylate (TEGDMA). The pHEMA of fixed water content was obtained by polymerizing a solution of HEMA with the proper amount of water. The water used in this experiment was distilled three times and exhibited a conductivity of less than  $1.4 \times 10^{-6} (\Omega \text{ cm})^{-1}$ . After degassing the solution, the polymer was prepared by thermal initiation at 60°C for 24 h.

The samples for thermal analysis were sealed in aluminum pans to prevent the evaporation of water during measurements. The exact water content of the hydrogels was obtained by drying to constant weight. The samples for NMR relaxation spectroscopy were prepared by polymerizing in sealed NMR sample tubes after a nitrogen gas purge and freeze-thaw degassing<sup>27,28</sup> to remove the free oxygen. The samples were allowed to stand at room temperature for 60 days to cure completely.

### Measurements and Apparatus

#### Differential Thermal Analysis (DTA)

Differential thermal analysis (DTA) was performed in a Du Pont 990 thermal analyzer and cell base. The temperature scales were calibrated using the melting point of standard pure indium and triple distilled water. The samples sealed in an aluminum pan were weighed before and after DTA runs.

After cooling with liquid nitrogen and allowing to stand at -100°C for 20 min to stabilize, the temperature was raised at a programed rate of 5°C/min under nitrogen gas and the results recorded. The effect of programmed rate at 1, 5, 10, and 20°C/min was tested by detection of the melting transitions of pure water. There was some variation in melting temperature at temperature rates greater than or equal to 10°C/min. The transitions detected at 5°C/min were the same as those measured at slower rates. The heat of fusion of water in the hydrogel was measured from the melting peak area as a function of water content in the samples. The area of the melting peaks were within  $\pm 3\%$  on repeated runs.

#### Nuclear Magnetic Resonance (NMR) Relaxation Spectroscopy

The longitudinal (spin-lattice) and transverse (spin-spin) proton relaxation times were measured by utilizing a pulsed 100-MHz NMR spectrometer (Varian XLFT-100). The spin-lattice relaxation time ( $T_1$ ) measurements were made

using a  $\pi-\tau-\pi/2$  pulse sequence<sup>29,30</sup>;  $T_1$  was determined from the slope of semilogarithmic plots. Spin-spin relaxation times ( $T_2$ ) were obtained from the full width at half maximum absorption following the pulse sequence.<sup>30,31</sup> The temperature was controlled at  $34 \pm 1^\circ\text{C}$  during the measurements.

## RESULTS AND DISCUSSION

### Differential Thermal Analysis

The integral heats of fusion of the water melting transition in hydrogels were measured from the total peak area of the endotherms. Typical melting transition endotherms of water, indium, and water-swollen methacrylate gels are shown in Figure 1. The lower water content (10% H<sub>2</sub>O) pHEMA sample does not show any sharp transition near 0°C (Fig. 1, middle). Double peaks in hydrogel systems are found for the higher water content (40% H<sub>2</sub>O) pHEMA sample, as shown in Figure 1 (top). The shape of the endotherm was somewhat dependent upon the freezing conditions, though the total area of the endotherm was approximately constant. We define the total water transition to consist of both peaks in the vicinity of 0°C. Figure 2 presents the detailed endotherms for the pHEMA—H<sub>2</sub>O samples and Figure 3 for the TEGDMA crosslinked pHEMA—H<sub>2</sub>O samples. The integral heats of fusion of the total water transition for each system were determined from eq. (1) on the basis of the standard indium endotherm. The heat of fusion of sample,  $\Delta H_s$ , is expressed as<sup>32,33</sup>:

$$\Delta H_s = \Delta H_{\text{In}} \cdot \frac{W_{\text{In}} A_s R_s S_{\text{In}}}{W_s A_{\text{In}} R_{\text{In}} S_s} \quad (1)$$

where the subscript *s* refers to sample and In refers to indium.  $\Delta H$ , *W*, *A*, *R*, and *S* are the heat of transition, weight, peak area, range, and chart speed, respectively.

Figures 4 and 5 show the integral heat of fusion of the water melting transition as a function of water content for pHEMA and pHEMA—TEGDMA hydrogels, respectively. In the figures,  $W_{nf}$  represents the nonfreezable water. By similar measurements of the total area under the endothermic curves,<sup>34–36</sup> we have determined the integral heat of fusion of the water melting transition. Extrapolation to  $\Delta H = 0$  intercepts the water content axis at a point which is the total bound water content of the sample, given in Table I.

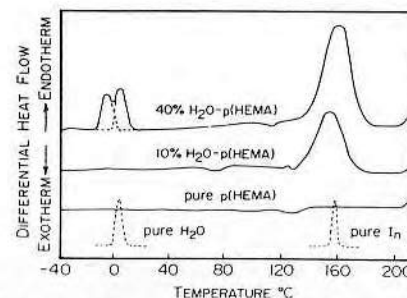


Fig. 1. Endotherms for water, indium, poly(2-hydroxyethyl methacrylate) hydrogels. The program rate is 5°C/min.; flow rate of N<sub>2</sub> gas is 50 mL/min.

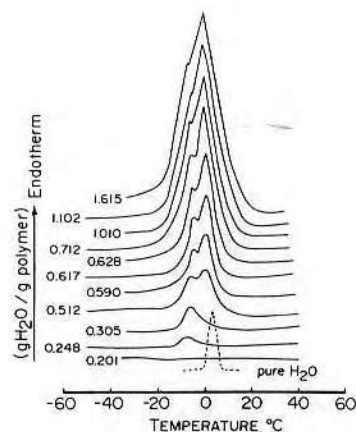


Fig. 2. The endotherms of pHEMA—H<sub>2</sub>O samples. The program rate is 5°C/min.; flow rate of N<sub>2</sub> gas is 50 mL/min.

A plot of the integral heat of fusion versus water content of gels shows approximately a straight line in the measured range.<sup>36</sup> The slope at high water contents is approximately equal to the heat of fusion of bulk water ( $\Delta H_f = 79.7$  cal/g).<sup>37</sup> From the slope of the straight line, the specific heats of water transition in the samples were evaluated as listed in Table I. The values of  $\Delta H_f$  of polymeric systems, such as pHEMA—H<sub>2</sub>O and pHEMA—EGDMA—H<sub>2</sub>O, are less than that of  $\Delta H_f$  of bulk water. The lower  $\Delta H_f$  values may be due to volume shrinkage and structuring of water in the gel network, which can be directly observed by dilatometry.<sup>24</sup> The values of  $\Delta H_f$  obtained for the hydrogel systems based on pHEMA are reasonable and are similar to related systems.<sup>38,39</sup> One can also compare with the reported values of 77.6 cal/g for purified elastin<sup>40</sup> and 77.5 cal/g for native elastin.<sup>40</sup>

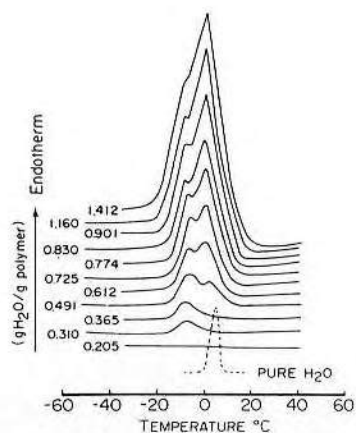


Fig. 3. The endotherms of pHEMA—TEGDMA—H<sub>2</sub>O samples. The program rate is 5°C/min.; flow rate of N<sub>2</sub> gas is 50 mL/min.

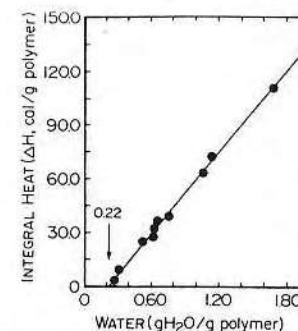


Fig. 4. The integral heat of fusion of the water transition as a function of water content for the pHEMA—H<sub>2</sub>O system.  $W_{nf}$  is 0.22 g H<sub>2</sub>O/g polymer (18.0 wt % H<sub>2</sub>O).

The specific entropies of fusion of the water transition as the melting point were evaluated from the relationship  $\Delta S_f = \Delta H_f/T_m$ , using the  $\Delta H_f$  data listed in Table I. The observed entropy deficit can be interpreted as the ordering of the bulklike water in the hydrogels and is somewhat greater than the ordering of ordinary water and ice, whose specific entropy of fusion is 0.292 eu.<sup>27</sup> It is interesting to compare the specific entropy of fusion of the water transition in

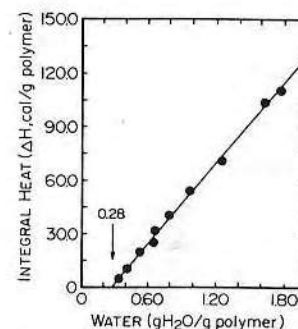


Fig. 5. The integral heat of fusion of the water transition as a function of water content for the pHEMA—TEGDMA—H<sub>2</sub>O system.  $W_{nf}$  is 0.28 g H<sub>2</sub>O/g polymer (21.9 wt % H<sub>2</sub>O).

TABLE I  
Total Bound Water Content and Specific Thermal Parameters of Water Transition in Some Methacrylate Systems

Systems	Bound water content (wt %)	Mole ratio of bound H <sub>2</sub> O/monomer unit	Specific enthalpy of fusion, $\Delta H_f$ (cal/g) <sup>a</sup>	Specific entropy of fusion, $\Delta S_f$ (eu) <sup>a</sup>
Ice	100.0	—	79.7 <sup>b</sup>	0.292 <sup>b</sup>
pHEMA—H <sub>2</sub> O	18.0	1.59	76.3 ± 0.7	0.279 ± 0.003
pHEMA—(1 mol % TEGDMA)—H <sub>2</sub> O	21.9	2.05	75.2 ± 0.7	0.275 ± 0.003

<sup>a</sup> For freezing (intermediate and bulklike) water in the hydrogels.

<sup>b</sup> Data taken from Ref. 37.



pHEMA hydrogels with the values found for various tissues, which range from 0.259 eu to 0.279 eu.<sup>41</sup> Water molecules bound to polymer networks are distinguishable from other water molecules by a higher binding energy, an appreciably lower rotational freedom, and an extended lifetime.

Since the endotherms show two different peaks in higher water content gels,<sup>24,36</sup> an enthalpic heat of fusion can be obtained from each peak. Each peak was manually resolved and the individual peak areas were determined.<sup>36</sup> The water which melts near 0°C is called "bulklike" water; the water which has a lower melting temperature is called "intermediate" water; and the water which does not show any melting transition above -100°C is called "bound" water.<sup>24,36</sup>

Figures 6 and 7 show the partial enthalpic heats of the freezable water as a function of water content in the system pHEMA—H<sub>2</sub>O and pHEMA—TEGDMA—H<sub>2</sub>O, respectively. In Figures 6 and 7,  $W_{f(I)}$  is the "intermediate" (lower melting) water;  $W_{f(F)}$  is the "free" or "bulklike" (0° melting) water in the hydrogels. The slope of bulklike (free) water in the hydrogels is very close to the heat of fusion of bulk water. The amounts of bound water, intermediate water, and bulklike water in each hydrogel system were determined from the data of Figures 4–7 and are presented in Table II for pHEMA hydrogels of different total water contents; Table III gives the data for 1 mol % TEGDMA—pHEMA—H<sub>2</sub>O systems. As seen in Tables II and III, bulklike (free) water in the hydrogels increases only after the bound water and intermediate water are saturated.

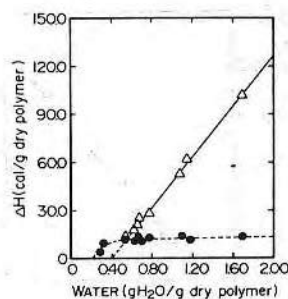


Fig. 6. The heat of fusion of the  $W_{f(I)}$  and  $W_{f(F)}$  transitions as a function of water content for the pHEMA—H<sub>2</sub>O hydrogels; (●)  $W_{f(I)}$ ; (Δ)  $W_{f(F)}$ .

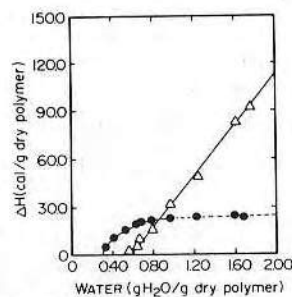


Fig. 7. The heat of fusion of the  $W_{f(I)}$  and  $W_{f(F)}$  transitions as a function of water content for the pHEMA—TEGDMA—H<sub>2</sub>O hydrogels; (●)  $W_{f(I)}$ ; (Δ)  $W_{f(F)}$ .

TABLE II  
Determination of Bound Water, Intermediate Water, and Bulklike Water in pHEMA Hydrogels (Uncrosslinked) of Different Total Water Content

wt % of total water in hydrogels	18.0	20.0	25.0	30.0	35.0	40.0	45.0	50.0
Total water/polymer (g/g)	0.22	0.25	0.33	0.43	0.54	0.67	0.82	1.00
Bound water/polymer (g/g)	0.22	0.22	0.22	0.22	0.22	0.22	0.22	0.22
Intermediate water/polymer (g/g)	0	0.03	0.11	0.16	0.16	0.16	0.16	0.16
Bulklike water/polymer (g/g)	0	0	0	0.05	0.16	0.29	0.44	0.62

The process of water imbibition in the hydrogels may be interpreted in terms of three steps: (1) An amount of water is first bound to the hydrophilic sites; (2) additional water is preferentially oriented around the bound water and the polymer network structure as a secondary or tertiary hydration shell; and (3) any other water is present as free or bulklike water.

### Nuclear Magnetic Relaxation Spectroscopy

Table IV presents the spin-lattice relaxation times ( $T_1$ ) as a function of water content for the pHEMA and pHEMA—TEGDMA systems at 100 MHz and 34°C. Comparing with the  $T_1$  of pure water (4.50 s at 34°C), the average  $T_1$  values for the hydrogel systems are reduced, suggesting that there are considerable interactions between the water molecules and the polymer networks. The short  $T_1$  of water protons in the hydrogel suggests that the water is less mobile than in pure water. This can be interpreted in terms of the structure ordering of water molecules in gel networks. The most probable binding positions of water molecules are the polar sites, such as the hydroxyl and ester groups. The effect of a crosslinking agent, such as TEGDMA, produces rather slight changes in  $T_1$ .

TABLE III  
Determination of Bound Water, Intermediate Water, and Bulklike Water in 1 mol % TEGDMA—pHEMA Hydrogels of Different Total Water Content

wt % of total water in hydrogels	21.9	25.0	30.0	35.0	40.0	45.0	50.0
Total water/polymer (g/g)	0.28	0.33	0.43	0.54	0.67	0.82	1.00
Bound water/polymer (g/g)	0.28	0.28	0.28	0.28	0.28	0.28	0.28
Intermediate water/polymer (g/g)	0	0.05	0.15	0.25	0.29	0.29	0.29
Bulklike water/polymer (g/g)	0	0	0	0.01	0.10	0.25	0.43

TABLE IV  
Proton NMR Spin-Lattice Relaxation Times for Hydrogels Based on pHEMA of Different Total Water Contents at 100 MHz and 34°C (Units: s)

wt % of total water content in the hydrogel	pHEMA—H <sub>2</sub> O		pHEMA—1 mol % TEGDMA—H <sub>2</sub> O	
	$T_1$	$T_{11}$	$T_1$	$T_{11}$
25	0.189	0.272	0.182	0.217
30	0.214	0.298	0.190	0.232
35	0.260	0.311	0.207	0.279
40	0.300	0.337	0.238	0.304
45	0.340	0.336	0.268	0.302

$T_{1F} = 4.50$  s at 34°C.

$T_{1B} = 0.169$  s for 18% H<sub>2</sub>O—pHEMA; 0.178 s for 21.9% H<sub>2</sub>O—pHEMA—TEGDMA.



though the hydrophilic tendency can be seen. The results are in good agreement with the bound water quantities obtained from the differential thermal analysis data.

The measured values of the proton spin-lattice relaxation times,  $T_1$ , can be considered as an average of three states of water in the hydrogels: bound water, intermediate water, and bulklike (free) water,<sup>25</sup>

$$\frac{1}{T_1} = \frac{f_B}{T_{1B}} + \frac{f_I}{T_{1I}} + \frac{f_F}{T_{1F}} \quad (2)$$

where  $f_B$ ,  $f_I$ , and  $f_F$  are the fraction of bound, intermediate, and bulklike water in the hydrogels, and  $T_{1B}$ ,  $T_{1I}$ , and  $T_{1F}$  are the spin-lattice relaxation times for bound, intermediate, and bulklike water in the hydrogels, respectively.  $T_{1F}$  is taken to be that of pure water;  $f_B$ ,  $f_I$ , and  $f_F$  are obtained from the differential thermal analysis data.  $T_{1B}$  corresponds to the measured  $T_1$  for the known content of  $W_H$  in Figures 4 and 5. Hence, one can estimate  $T_{1I}$  for intermediate water in the hydrogels. Table IV gives  $T_{1I}$  determined for pHEMA—H<sub>2</sub>O and 1 mol % crosslinked (TEGDMA)—pHEMA—H<sub>2</sub>O systems.

The  $T_1$  values are inversely proportional to the magnitude of the interactions between water protons and lattice environments, i.e., the lower value of  $T_{1I}$  means a stronger interaction between water molecule and polymer network.

According to the data in Table IV, the spin-lattice relaxation times ( $T_{1B}$ ) of bound water in the hydrogels are about 30 times less than that of water protons in pure liquid water. The values of  $T_{1I}$  of intermediate water in the hydrogels are approximately twice that of  $T_{1B}$  of bound water. The proton spin-lattice relaxation times directly give the mobility of water molecules in the hydrogels. Comparing the data with the  $T_{1F}$  of bulklike (free) water, the mobility of water protons of bound water or intermediate water is less than that of water protons in pure liquid water. This indicates that some water molecules around the polar sites in the gels may be structured and preferentially ordered, probably due to hydrogen bonding or strong polar interactions. That is in line with the specific entropy data obtained from the thermal analysis listed in Table I.

Figure 8 shows the spin-spin relaxation times ( $T_2$ ) of water protons as a function of water content in pHEMA and pHEMA—TEGDMA hydrogel systems. The values of  $T_2$  are approximately 10 times less than those of  $T_1$ , in general agreement with the principles of spin relaxations.<sup>30,31</sup> In the region of

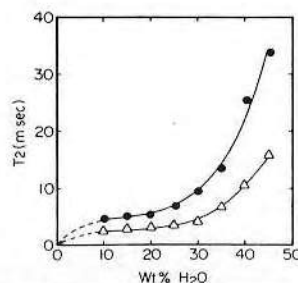


Fig. 8. The spin-spin relaxation times ( $T_2$ ) of water protons as a function of water content in polyhydroxyethyl methacrylate polymers at 34°C and 100 MHz; (●) pHEMA—H<sub>2</sub>O; (Δ) pHEMA—TEGDMA—H<sub>2</sub>O.

28. A. W. Nolle and P. P. Mahendroo, *J. Chem. Phys.*, **33**, 863 (1960).
29. H. Y. Carr and E. M. Purcell, *Phys. Rev.*, **94**, 630 (1954).
30. T. C. Farrar and E. D. Becker, *Pulse and Fourier Transform NMR*, Academic, New York, 1971.
31. H. Eyring, D. Henderson, B. J. Stover, and E. M. Eyring, *Statistical Mechanics and Dynamics*, Wiley, New York, 1964.
32. C. M. Guttman and J. H. Flynn, *Anal. Chem.*, **45**, 408 (1973).
33. I. Buzas, Ed., *Thermal Analysis*, Heyden, London, 1975.
34. Y. Taniguchi and S. Horigone, *J. Appl. Polym. Sci.*, **19**, 2743 (1975).
35. R. A. Nelson, *J. Appl. Polym. Sci.*, **21**, 645 (1977).
36. Y. K. Sung, "Interaction of Water with Hydrophilic Methacrylate Polymers," Ph.D. dissertation, University of Utah, 1978.
37. R. C. Weast, Ed., *Handbook of Chemistry and Physics*, 54th ed., Chemical Rubber Company, Cleveland, Ohio, 1974.
38. H. Shiraishi, A. Hiltner, and E. Baer, *Biopolymers*, **16**, 231 (1977).
39. H. Uasuda, H. G. Olf, B. Crist, C. E. Lamaze, and A. Peterlin, in *Water Structure at the Water-Polymer Interface*, H. H. G. Jellinek, Ed., Plenum, New York, 1972.
40. G. Ceccorulli, M. Scandola, and G. Pezzin, *Biopolymers*, **16**, 1505 (1977).
41. E. L. Andronikashvili, G. M. Mrevlishvili, and P. L. Privalov, in *Water in Biological Systems*, L. P. Kayushin, Ed., Consultants Bureau, New York, 1969, 67.

Received February 19, 1981

Accepted April 20, 1981

# Thermal and Pulse NMR Analysis of Water in Poly(2-hydroxyethyl Methacrylate)

Y. K. SUNG,\* D. E. GREGONIS, M. S. JOHN,<sup>†</sup> and J. D. ANDRADE,  
*Department of Materials Science and Engineering and Department of  
Bioengineering, College of Engineering, University of Utah,  
Salt Lake City, Utah 84112*

## Synopsis

Hydrophilic three-dimensional methacrylate polymer networks (hydrogels) were prepared from 2-hydroxyethyl methacrylate (HEMA) monomer and tetraethylene glycol dimethacrylate (TEGDMA) as crosslinker. The nature and states of water in these hydrogels were studied by differential thermal analysis and pulse NMR relaxation spectroscopy. The thermal studies showed no endotherm peak for ice melting in the lower water content (bound water region); there are two endotherms peaks for higher water content hydrogels near 0°C. The amounts of bound water, intermediate water, and bulklike (free) water in the hydrogels were determined from a quantitative analysis of the endotherms of the water melting transitions. The water structure ordering in the hydrogels were discussed in terms of the fusion entropy and enthalpy obtained from the endotherm. Nuclear magnetic relaxation spectroscopy was also used to understand the mobilities of the water protons in the hydrogels and the interaction of water molecules with the gel networks. The measured spin-lattice relaxation time ( $T_1$ ) values for water protons in the hydrogels are greatly reduced compared to that of liquid water. The measured values of spin-spin relaxation times ( $T_2$ ) of water protons in the hydrogels are approximately 10 times less than that of  $T_1$  and are almost constant in the region of bound water content. Beyond the bound water content region in the hydrogels, the  $T_2$  values rapidly increase as the water content increases.

## INTRODUCTION

Hydrophilic methacrylate polymers are being considered for biomedical applications.<sup>1-5</sup> These polymers swell in water to become soft crosslinked gels, so-called hydrogels. Synthetic hydrogels have been extensively discussed in the literature.<sup>6-8</sup> The transport characteristics of hydrogel membranes have been examined for a broad range of potential applications, including soft contact lenses,<sup>9</sup> reverse osmosis membranes,<sup>10-12</sup> kidney dialysis membranes,<sup>13-15</sup> and drug delivery systems for antibiotics,<sup>16-18</sup> steroids,<sup>19,20</sup> and enzymes.<sup>21,22</sup>

In order to develop useful synthetic biomedical hydrogels, it is of interest to understand the state and properties of water in such hydrogels. Water in hydrogels has been treated in terms of a three-state model.<sup>23</sup> To test the validity of the model, dilatometry, specific conductivity, and dielectric studies of water in hydrogels have been carried out from -15°C to room temperature for poly(2-hydroxyethyl methacrylate) (pHEMA)<sup>24,25</sup> and poly(2,3-dihydroxypropyl methacrylate) (pDHPMA) gels.<sup>26</sup>

Using the three-state model, we have determined the amounts of bound water, intermediate water, and bulklike (free) water in hydrophilic methacrylate gels

\* Department of Chemistry, Busan National University, Busan 607, Korea.

<sup>†</sup> Department of Chemistry, Korea Advanced Institute of Science, Seoul, Korea.

by utilizing differential thermal analysis and nuclear magnetic resonance (NMR) relaxation spectroscopy.

## EXPERIMENTAL

### Preparation of Materials

Purified 2-hydroxyethyl methacrylate (HEMA) was obtained as a gift from Hydro-Med Sciences, Inc., New Brunswick, N.J., containing about 0.2% methacrylic acid, 0.16% diethylene glycol methacrylate, and 0.01% ethylene glycol dimethacrylate. The polymerization of HEMA monomer was initiated by azobis (methyl isobutyrate), 7.84 mmol initiator/mL of HEMA monomer. This ratio is independent of water content in the hydrogels. The other pHEMA copolymers were polymerized with the crosslinking agent tetraethylene glycol dimethacrylate (TEGDMA). The pHEMA of fixed water content was obtained by polymerizing a solution of HEMA with the proper amount of water. The water used in this experiment was distilled three times and exhibited a conductivity of less than  $1.4 \times 10^{-6} (\Omega \text{ cm})^{-1}$ . After degassing the solution, the polymer was prepared by thermal initiation at 60°C for 24 h.

The samples for thermal analysis were sealed in aluminum pans to prevent the evaporation of water during measurements. The exact water content of the hydrogels was obtained by drying to constant weight. The samples for NMR relaxation spectroscopy were prepared by polymerizing in sealed NMR sample tubes after a nitrogen gas purge and freeze-thaw degassing<sup>27,28</sup> to remove the free oxygen. The samples were allowed to stand at room temperature for 60 days to cure completely.

### Measurements and Apparatus

#### *Differential Thermal Analysis (DTA)*

Differential thermal analysis (DTA) was performed in a Du Pont 990 thermal analyzer and cell base. The temperature scales were calibrated using the melting point of standard pure indium and triple distilled water. The samples sealed in an aluminum pan were weighed before and after DTA runs.

After cooling with liquid nitrogen and allowing to stand at -100°C for 20 min to stabilize, the temperature was raised at a programed rate of 5°C/min under nitrogen gas and the results recorded. The effect of programmed rate at 1, 5, 10, and 20°C/min was tested by detection of the melting transitions of pure water. There was some variation in melting temperature at temperature rates greater than or equal to 10°C/min. The transitions detected at 5°C/min were the same as those measured at slower rates. The heat of fusion of water in the hydrogel was measured from the melting peak area as a function of water content in the samples. The area of the melting peaks were within  $\pm 3\%$  on repeated runs.

#### *Nuclear Magnetic Resonance (NMR) Relaxation Spectroscopy*

The longitudinal (spin-lattice) and transverse (spin-spin) proton relaxation times were measured by utilizing a pulsed 100-MHz NMR spectrometer (Varian XLFT-100). The spin-lattice relaxation time ( $T_1$ ) measurements were made

using a  $\pi-\tau-\pi/2$  pulse sequence<sup>29,30</sup>;  $T_1$  was determined from the slope of semilogarithmic plots. Spin-spin relaxation times ( $T_2$ ) were obtained from the full width at half maximum absorption following the pulse sequence.<sup>30,31</sup> The temperature was controlled at  $34 \pm 1^\circ\text{C}$  during the measurements.

## RESULTS AND DISCUSSION

### Differential Thermal Analysis

The integral heats of fusion of the water melting transition in hydrogels were measured from the total peak area of the endotherms. Typical melting transition endotherms of water, indium, and water-swollen methacrylate gels are shown in Figure 1. The lower water content (10%  $\text{H}_2\text{O}$ ) pHEMA sample does not show any sharp transition near  $0^\circ\text{C}$  (Fig. 1, middle). Double peaks in hydrogel systems are found for the higher water content (40%  $\text{H}_2\text{O}$ ) pHEMA sample, as shown in Figure 1 (top). The shape of the endotherm was somewhat dependent upon the freezing conditions, though the total area of the endotherm was approximately constant. We define the total water transition to consist of both peaks in the vicinity of  $0^\circ\text{C}$ . Figure 2 presents the detailed endotherms for the pHEMA— $\text{H}_2\text{O}$  samples and Figure 3 for the TEGDMA crosslinked pHEMA— $\text{H}_2\text{O}$  samples. The integral heats of fusion of the total water transition for each system were determined from eq. (1) on the basis of the standard indium endotherm. The heat of fusion of sample,  $\Delta H_s$ , is expressed as<sup>32,33</sup>:

$$\Delta H_s = \Delta H_{\text{In}} \cdot \frac{W_{\text{In}} A_s R_s S_{\text{In}}}{W_s A_{\text{In}} R_{\text{In}} S_s} \quad (1)$$

where the subscript  $s$  refers to sample and In refers to indium.  $\Delta H$ ,  $W$ ,  $A$ ,  $R$ , and  $S$  are the heat of transition, weight, peak area, range, and chart speed, respectively.

Figures 4 and 5 show the integral heat of fusion of the water melting transition as a function of water content for pHEMA and pHEMA—TEGDMA hydrogels, respectively. In the figures,  $W_{nf}$  represents the nonfreezable water. By similar measurements of the total area under the endothermic curves,<sup>34-36</sup> we have determined the integral heat of fusion of the water melting transition. Extrapolation to  $\Delta H = 0$  intercepts the water content axis at a point which is the total bound water content of the sample, given in Table I.

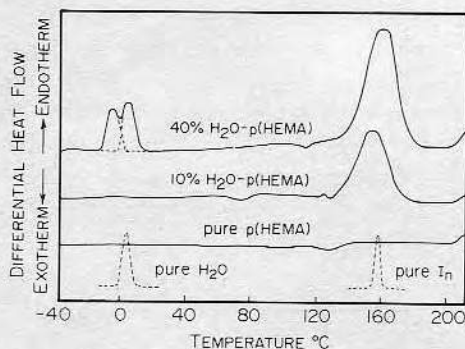


Fig. 1. Endotherms for water, indium, poly(2-hydroxyethyl methacrylate) hydrogels. The program rate is  $5^\circ\text{C}/\text{min}$ ; flow rate of  $\text{N}_2$  gas is  $50 \text{ mL}/\text{min}$ .



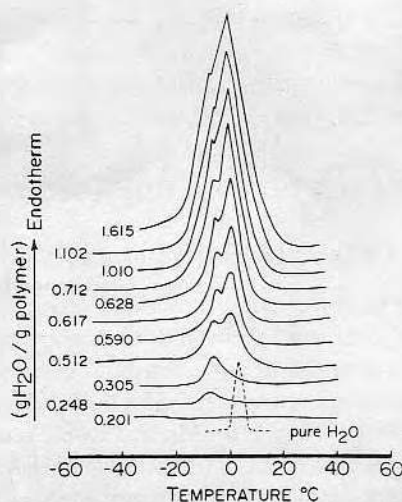


Fig. 2. The endotherms of pHEMA—H<sub>2</sub>O samples. The program rate is 5°C/min.; flow rate of N<sub>2</sub> gas is 50 mL/min.

A plot of the integral heat of fusion versus water content of gels shows approximately a straight line in the measured range.<sup>36</sup> The slope at high water contents is approximately equal to the heat of fusion of bulk water ( $\Delta H_f = 79.7$  cal/g).<sup>37</sup> From the slope of the straight line, the specific heats of water transition in the samples were evaluated as listed in Table I. The values of  $\Delta H_f$  of polymeric systems, such as pHEMA—H<sub>2</sub>O and pHEMA—EGDMA—H<sub>2</sub>O, are less than that of  $\Delta H_f$  of bulk water. The lower  $\Delta H_f$  values may be due to volume shrinkage and structuring of water in the gel network, which can be directly observed by dilatometry.<sup>24</sup> The values of  $\Delta H_f$  obtained for the hydrogel systems based on pHEMA are reasonable and are similar to related systems.<sup>38,39</sup> One can also compare with the reported values of 77.6 cal/g for purified elastin<sup>40</sup> and 77.5 cal/g for native elastin.<sup>40</sup>

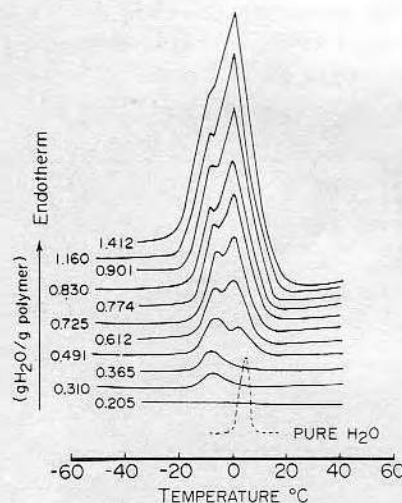


Fig. 3. The endotherms of pHEMA—TEGDMA—H<sub>2</sub>O samples. The program rate is 5°C/min.; flow rate of N<sub>2</sub> gas is 50 mL/min.

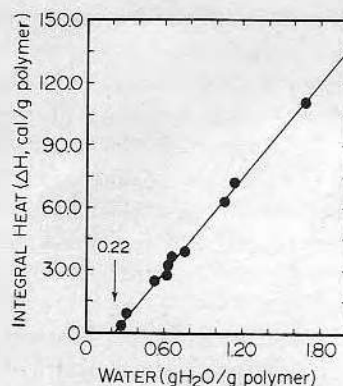


Fig. 4. The integral heat of fusion of the water transition as a function of water content for the pHEMA—H<sub>2</sub>O system.  $W_{nf}$  is 0.22 g H<sub>2</sub>O/g polymer (18.0 wt % H<sub>2</sub>O).

The specific entropies of fusion of the water transition as the melting point were evaluated from the relationship  $\Delta S_f = \Delta H_f/T_m$ , using the  $\Delta H_f$  data listed in Table I. The observed entropy deficit can be interpreted as the ordering of the bulklike water in the hydrogels and is somewhat greater than the ordering of ordinary water and ice, whose specific entropy of fusion is 0.292 eu.<sup>27</sup> It is interesting to compare the specific entropy of fusion of the water transition in

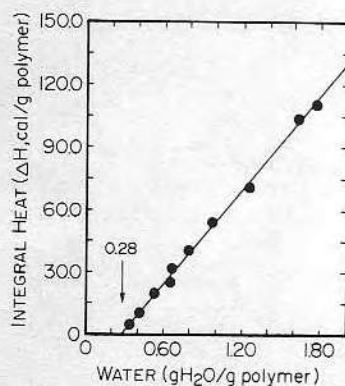


Fig. 5. The integral heat of fusion of the water transition as a function of water content for the pHEMA—TEGDMA—H<sub>2</sub>O system.  $W_{nf}$  is 0.28 g H<sub>2</sub>O/g polymer (21.9 wt % H<sub>2</sub>O).

TABLE I  
Total Bound Water Content and Specific Thermal Parameters of Water Transition in Some Methacrylate Systems

Systems	Bound water content (wt %)	Mole ratio of bound H <sub>2</sub> O/monomer unit	Specific enthalpy of fusion, $\Delta H_f$ (cal/g) <sup>a</sup>	Specific entropy of fusion, $\Delta S_f$ (eu) <sup>a</sup>
Ice	100.0	—	79.7 <sup>b</sup>	0.292 <sup>b</sup>
pHEMA—H <sub>2</sub> O	18.0	1.59	76.3 ± 0.7	0.279 ± 0.003
pHEMA—(1 mol % TEGDMA)—H <sub>2</sub> O	21.9	2.05	75.2 ± 0.7	0.275 ± 0.003

<sup>a</sup> For freezing (intermediate and bulklike) water in the hydrogels.

<sup>b</sup> Data taken from Ref. 37.

pHEMA hydrogels with the values found for various tissues, which range from 0.259 eu to 0.279 eu.<sup>41</sup> Water molecules bound to polymer networks are distinguishable from other water molecules by a higher binding energy, an appreciably lower rotational freedom, and an extended lifetime.

Since the endotherms show two different peaks in higher water content gels,<sup>24,36</sup> an enthalpic heat of fusion can be obtained from each peak. Each peak was manually resolved and the individual peak areas were determined.<sup>36</sup> The water which melts near 0°C is called "bulklike" water; the water which has a lower melting temperature is called "intermediate" water; and the water which does not show any melting transition above -100°C is called "bound" water.<sup>24,36</sup>

Figures 6 and 7 show the partial enthalpic heats of the freezable water as a function of water content in the system pHEMA—H<sub>2</sub>O and pHEMA—TEGDMA—H<sub>2</sub>O, respectively. In Figures 6 and 7,  $W_{f(I)}$  is the "intermediate" (lower melting) water;  $W_{f(F)}$  is the "free" or "bulklike" (0° melting) water in the hydrogels. The slope of bulklike (free) water in the hydrogels is very close to the heat of fusion of bulk water. The amounts of bound water, intermediate water, and bulklike water in each hydrogel system were determined from the data of Figures 4–7 and are presented in Table II for pHEMA hydrogels of different total water contents; Table III gives the data for 1 mol % TEGDMA—pHEMA—H<sub>2</sub>O systems. As seen in Tables II and III, bulklike (free) water in the hydrogels increases only after the bound water and intermediate water are saturated.

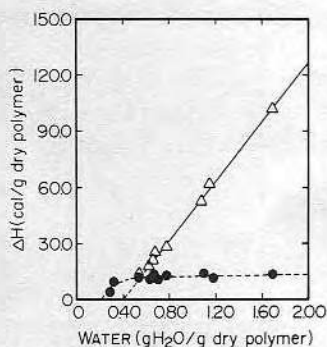


Fig. 6. The heat of fusion of the  $W_{f(I)}$  and  $W_{f(F)}$  transitions as a function of water content for the pHEMA—H<sub>2</sub>O hydrogels; (●)  $W_{f(I)}$ ; (Δ)  $W_{f(F)}$ .

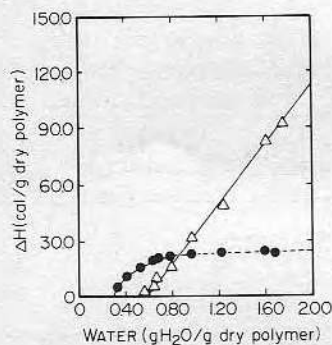


Fig. 7. The heat of fusion of the  $W_{f(I)}$  and  $W_{f(F)}$  transitions as a function of water content for the pHEMA—TEGDMA—H<sub>2</sub>O hydrogels; (●)  $W_{f(I)}$ ; (Δ)  $W_{f(F)}$ .

TABLE II  
Determination of Bound Water, Intermediate Water, and Bulklike Water in pHEMA Hydrogels (Uncrosslinked) of Different Total Water Content

wt % of total water in hydrogels	18.0	20.0	25.0	30.0	35.0	40.0	45.0	50.0
Total water/polymer (g/g)	0.22	0.25	0.33	0.43	0.54	0.67	0.82	1.00
Bound water/polymer (g/g)	0.22	0.22	0.22	0.22	0.22	0.22	0.22	0.22
Intermediate water/polymer (g/g)	0	0.03	0.11	0.16	0.16	0.16	0.16	0.16
Bulklike water/polymer (g/g)	0	0	0	0.05	0.16	0.29	0.44	0.62

The process of water imbibition in the hydrogels may be interpreted in terms of three steps: (1) An amount of water is first bound to the hydrophilic sites; (2) additional water is preferentially oriented around the bound water and the polymer network structure as a secondary or tertiary hydration shell; and (3) any other water is present as free or bulklike water.

### Nuclear Magnetic Relaxation Spectroscopy

Table IV presents the spin-lattice relaxation times ( $T_1$ ) as a function of water content for the pHEMA and pHEMA—TEGDMA systems at 100 MHz and 34°C. Comparing with the  $T_1$  of pure water (4.50 s at 34°C), the average  $T_1$  values for the hydrogel systems are reduced, suggesting that there are considerable interactions between the water molecules and the polymer networks. The short  $T_1$  of water protons in the hydrogel suggests that the water is less mobile than in pure water. This can be interpreted in terms of the structure ordering of water molecules in gel networks. The most probable binding positions of water molecules are the polar sites, such as the hydroxyl and ester groups. The effect of a crosslinking agent, such as TEGDMA, produces rather slight changes in  $T_1$ ,

TABLE III  
Determination of Bound Water, Intermediate Water, and Bulklike Water in 1 mol % TEGDMA—pHEMA Hydrogels of Different Total Water Content

wt % of total water in hydrogels	21.9	25.0	30.0	35.0	40.0	45.0	50.0
Total water/polymer (g/g)	0.28	0.33	0.43	0.54	0.67	0.82	1.00
Bound water/polymer (g/g)	0.28	0.28	0.28	0.28	0.28	0.28	0.28
Intermediate water/polymer (g/g)	0	0.05	0.15	0.25	0.29	0.29	0.29
Bulklike water/polymer (g/g)	0	0	0	0.01	0.10	0.25	0.43

TABLE IV  
Proton NMR Spin-Lattice Relaxation Times for Hydrogels Based on pHEMA of Different Total Water Contents at 100 MHz and 34°C (Units:s)

wt % of total water content in the hydrogel	pHEMA—H <sub>2</sub> O		pHEMA—1 mol % TEGDMA—H <sub>2</sub> O	
	$T_1$	$T_{11}$	$T_1$	$T_{11}$
25	0.189	0.272	0.182	0.217
30	0.214	0.298	0.190	0.232
35	0.260	0.311	0.207	0.279
40	0.300	0.337	0.238	0.304
45	0.340	0.336	0.268	0.302

$T_{1F} = 4.50$  s at 34°C.

$T_{1B} = 0.169$  s for 18% H<sub>2</sub>O—pHEMA; 0.178 s for 21.9% H<sub>2</sub>O—pHEMA—TEGDMA.



though the hydrophilic tendency can be seen. The results are in good agreement with the bound water quantities obtained from the differential thermal analysis data.

The measured values of the proton spin-lattice relaxation times,  $T_1$ , can be considered as an average of three states of water in the hydrogels: bound water, intermediate water, and bulklike (free) water,<sup>25</sup>

$$\frac{1}{T_1} = \frac{f_B}{T_{1B}} + \frac{f_I}{T_{1I}} + \frac{f_F}{T_{1F}} \quad (2)$$

where  $f_B$ ,  $f_I$ , and  $f_F$  are the fraction of bound, intermediate, and bulklike water in the hydrogels, and  $T_{1B}$ ,  $T_{1I}$ , and  $T_{1F}$  are the spin-lattice relaxation times for bound, intermediate, and bulklike water in the hydrogels, respectively.  $T_{1F}$  is taken to be that of pure water;  $f_B$ ,  $f_I$ , and  $f_F$  are obtained from the differential thermal analysis data.  $T_{1B}$  corresponds to the measured  $T_1$  for the known content of  $W_{nf}$  in Figures 4 and 5. Hence, one can estimate  $T_{1I}$  for intermediate water in the hydrogels. Table IV gives  $T_{1I}$  determined for pHEMA—H<sub>2</sub>O and 1 mol % crosslinked (TEGDMA)—pHEMA—H<sub>2</sub>O systems.

The  $T_1$  values are inversely proportional to the magnitude of the interactions between water protons and lattice environments, i.e., the lower value of  $T_{1I}$  means a stronger interaction between water molecule and polymer network.

According to the data in Table IV, the spin-lattice relaxation times ( $T_{1B}$ ) of bound water in the hydrogels are about 30 times less than that of water protons in pure liquid water. The values of  $T_{1I}$  of intermediate water in the hydrogels are approximately twice that of  $T_{1B}$  of bound water. The proton spin-lattice relaxation times directly give the mobility of water molecules in the hydrogels. Comparing the data with the  $T_{1F}$  of bulklike (free) water, the mobility of water protons of bound water or intermediate water is less than that of water protons in pure liquid water. This indicates that some water molecules around the polar sites in the gels may be structured and preferentially ordered, probably due to hydrogen bonding or strong polar interactions. That is in line with the specific entropy data obtained from the thermal analysis listed in Table I.

Figure 8 shows the spin-spin relaxation times ( $T_2$ ) of water protons as a function of water content in pHEMA and pHEMA—TEGDMA hydrogel systems. The values of  $T_2$  are approximately 10 times less than of  $T_1$ , in general agreement with the principles of spin relaxations,<sup>30,31</sup> in the region of

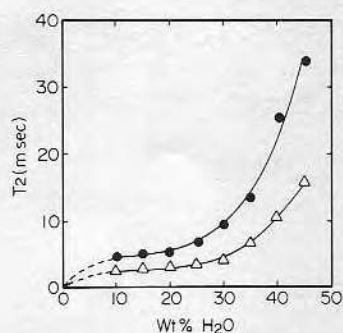


Fig. 8. The spin-spin relaxation times ( $T_2$ ) of water protons as a function of water content in polyhydroxyethyl methacrylate polymers at 34°C and 100 MHz; (●) pHEMA—H<sub>2</sub>O; (Δ) pHEMA—TEGDMA—H<sub>2</sub>O.

less than 25% water content, the values of  $T_2$  are almost constant. However, beyond this region the  $T_2$  values rapidly increase as the water content gradually increases, indicating the presence of increasing amounts of free and intermediate water. These results are in good agreement with the spin-lattice relaxation results.

## CONCLUSIONS

It is proposed that the interaction of water with hydrophilic methacrylate polymers occurs in three ways: (1) Water molecules are strongly bound to specific sites such as the hydroxyl or ester groups within the polymer network; dynamically and thermodynamically they behave as part of the chains. (2) Water molecules are weakly bound to the hydrophilic sites and/or preferentially structured around the polymer network. (3) Water molecules behave dynamically and thermodynamically as "bulklike" or free water.

The assistance of Dr. D. Dalling and the use of the NMR facilities of the University of Utah Regional Biomedical Resource are gratefully acknowledged. This work was supported by NIH Grant HL16921. We also acknowledge support by the U.S.-Korea Cooperative Science Program, NSF-INT-78-24474. Yong K. Sung thanks Busan National University for a leave of absence to conduct this work.

## References

1. O. Wichterle and D. Lim, *Nature*, **185**, 117 (1960).
2. V. Majkus, Z. Horakova, F. Vymuta, and M. Stol, *J. Biomed. Mater. Res.*, **3**, 443 (1969).
3. M. F. Refojo, *J. Biomed. Mater. Res.*, **3**, 333 (1969).
4. C. R. Taylor, T. C. Warren, D. G. Murray, and W. Prins, *J. Surg. Res.*, **11**, 401 (1971).
5. D. F. Williams and R. Roaf, *Implants in Surgery*, Saunders, London, 1973.
6. O. Wichterle, in *Encyclopedia of Polymer Science and Technology*, Wiley, New York, 1971, Vol. 15, p. 273.
7. S. D. Bruck, *Trans. Am. Soc. Artif. Internal Organs*, **18**, 1 (1972).
8. J. D. Andrade, Ed., *Hydrogels for Medical and Related Applications*, ACS Symposium Series, No. 31, ACS, Washington, D.C., 1976.
9. M. F. Refojo, "Contact Lenses," in *Encyclopedia of Polymer Science and Technology*, Wiley, New York, 1976; Supplement Vol. 1, pp. 195-219.
10. T. A. Jadwin, A. S. Hoffman, and W. R. Vieth, *J. Appl. Polym. Sci.*, **14**, 1339 (1970).
11. J. Kopecek and J. Vacik, *Collection Czechoslov. Chem. Commun.*, **38**, 854 (1973).
12. A. S. Hoffman, M. Modell, and P. Pan, *J. Appl. Polym. Sci.*, **14**, 285 (1970).
13. B. D. Ratner and I. F. Miller, *J. Biomed. Mater. Res.*, **7**, 353 (1973).
14. J. Vacik, M. Czakova, J. Exner, J. Kalal, and J. Kopecek, *Collection Czechoslov. Chem. Commun.*, **42**, 2786 (1977).
15. J. Kopecek, J. Vacik, and D. Lim, *J. Polym. Sci., A-1*, **9**, 2801 (1971).
16. M. Tollar, M. Stol, and K. Kliment, *J. Biomed. Mater. Res.*, **3**, 305 (1969).
17. J. N. LaGuerre, H. Kay, S. M. Lazarus, W. S. Calem, S. R. Weinberg, and B. S. Levowitz, *Surg. Forum*, **19**, 522 (1968).
18. S. M. Lazarus, J. N. LaGuerre, H. Kay, S. R. Weinberg, and B. S. Levowitz, *J. Biomed. Mater. Res.*, **5**, 129 (1971).
19. G. M. Zenter, J. R. Cardinal, and S. W. Kim, *J. Pharm. Sci.*, **67**, 1347 (1978).
20. G. M. Zentner, J. R. Cardinal, and S. W. Kim, *J. Pharm. Sci.*, **67**, 1352 (1978).
21. R. Langer and J. Folkman, *Nature*, **263**, 797 (1976).
22. Y. K. Sung, S. W. Kang, and U. S. Kim, *J. Busan Natl. Univ.*, **29**, 27 (1980).
23. M. S. Jhon and J. D. Andrade, *J. Biomed. Mater. Res.*, **7**, 509 (1973).
24. H. B. Lee, M. S. Jhon, and J. D. Andrade, *J. Colloid Interface Sci.*, **51**, 225 (1975).
25. H. B. Lee, J. D. Andrade, and M. S. Jhon, *Polym. Preprints*, **15**, 391 (1974).
26. S. H. Choi, M. S. Jhon, and J. D. Andrade, *J. Colloid Interface Sci.*, **61**, 1 (1977).
27. J. H. Simpson and H. Y. Carr, *Phys. Rev.*, **11**, 1201 (1958).

28. A. W. Nolle and P. P. Mahendroo, *J. Chem. Phys.*, **33**, 863 (1960).
29. H. Y. Carr and E. M. Purcell, *Phys. Rev.*, **94**, 630 (1954).
30. T. C. Farrar and E. D. Becker, *Pulse and Fourier Transform NMR*, Academic, New York, 1971.
31. H. Eyring, D. Henderson, B. J. Stover, and E. M. Eyring, *Statistical Mechanics and Dynamics*, Wiley, New York, 1964.
32. C. M. Guttman and J. H. Flynn, *Anal. Chem.*, **45**, 408 (1973).
33. I. Buzas, Ed., *Thermal Analysis*, Heyden, London, 1975.
34. Y. Taniguchi and S. Horigone, *J. Appl. Polym. Sci.*, **19**, 2743 (1975).
35. R. A. Nelson, *J. Appl. Polym. Sci.*, **21**, 645 (1977).
36. Y. K. Sung, "Interaction of Water with Hydrophilic Methacrylate Polymers," Ph.D. dissertation, University of Utah, 1978.
37. R. C. Weast, Ed., *Handbook of Chemistry and Physics*, 54th ed., Chemical Rubber Company, Cleveland, Ohio, 1974.
38. H. Shiraishi, A. Hiltner, and E. Baer, *Biopolymers*, **16**, 231 (1977).
39. H. Uasuda, H. G. Olf, B. Crist, C. E. Lamaze, and A. Peterlin, in *Water Structure at the Water-Polymer Interface*, H. H. G. Jellinek, Ed., Plenum, New York, 1972.
40. G. Ceccorulli, M. Scandola, and G. Pezzin, *Biopolymers*, **16**, 1505 (1977).
41. E. L. Andronikashvili, G. M. Mrevlishvili, and P. L. Privalov, in *Water in Biological Systems*, L. P. Kayushin, Ed., Consultants Bureau, New York, 1969, 67.

Received February 19, 1981

Accepted April 20, 1981

## Water Vapor Sorption of Stereoregular Poly(2-Hydroxyethyl Methacrylate) and Poly(2,3-Dihydroxypropyl Methacrylate)

Y.K. Sung, M.S. Jhon\*, D.E. Gregonis\*\* and J.D. Andrade\*\*

*Department of Chemistry, Dongguk University, Seoul, Korea*

*\*Department of Chemistry, Korea Advanced Institute of Science and Technology, Seoul, Korea*

*\*\*Department of Materials Science and Engineering, University of Utah, Salt Lake City, Utah 84112, U.S.A.*

(Received March 12, 1984 ; Accepted March 26, 1984)

**Abstract:** Hydrophilic three-dimensional methacrylate polymer networks(hydrogels) were prepared from 2-hydroxyethyl methacrylate and 2,3-dihydroxypropyl methacrylate. Highly isotactic poly(2-hydroxyethyl methacrylate) and highly syndiotactic poly(2-hydroxyethyl methacrylate) were also studied. The sorption of water vapor in the different tactic polymers was measured as a function of water activity. The results were interpreted in terms of Anderson's modified B.E.T. theory and the Hailwood-Horrobin theory of sorption. The former fitting to the experimental isotherms is up to 0.7 equilibrium relative humidity, while the solution theory of Hailwood-Horrobin gives a somewhat better fit to most of the experimental isotherms over the entire range of equilibrium relative humidity. Water vapor sorption by the methacrylate polymers is affected by tacticity and the number of hydrophilic sites in molecules. The amount of water vapor sorbed by isotactic poly(2-hydroxyethyl methacrylate) was found to be greater than that by syndiotactic poly(2-hydroxyethyl methacrylate). Theoretical water sorption models and analysis of the data suggest that isotactic poly(2-hydroxyethyl methacrylate) exists in a surface configuration and structure which provides a larger number of water binding sites in the syndio- or hetero-tactic polymers. Poly(dihydroxypropyl methacrylate) water sorption data and analysis is consistent with its higher hydrophilicity due to the presence of 2-hydroxyl group per repeat unit. These data are also consistent with thermal analysis studies of bound water in fully hydrated systems.

### INTRODUCTION

Some crosslinked hydrophilic polymers have been considered as biomaterials for medical

uses<sup>1,2</sup>. Many of the useful properties of these polymers seem related to their sorption and swelling capacity for water. These polymers become soft hydrogels by the sorption of liquid



and 6 were prepared by solvent casting from a methanol solution. The size of film samples was in 10mm width, 10mm length, and 1mm thickness. The polymers were extracted for seven days with distilled water at room temperature. The conductivity of distilled water used in this study was less than  $1.14 \times 10^{-18} / \Omega \text{cm}$ . The samples were dried to constant weight in a vacuum desiccator before measuring the water vapor sorption.

#### Apparatus and Measurements

Sorption isotherms were measured with a gravimetric sorption apparatus using a Cahn RM-2 electrobalance, recording thermistor, X-Y recorder and humidity meter. The sorption chamber was of height 14cm  $\times$  width 11cm  $\times$  length 27cm. The inside of the sorption chamber was coated with Teflon and was completely isolated from the outside. Standard drying of samples in the chamber was carried out for 48 hours under phosphorous pentoxide as a drying agent. All instruments used were recalibrated for each run.

The graded series of humidities used were obtained by equilibrating the chamber atmosphere with the following pure saturated aqueous salt solutions<sup>20</sup>: LiCl (12.4%),  $\text{MgCl}_2 \cdot 6\text{H}_2\text{O}$  (31.8%),  $\text{K}_2\text{CO}_3 \cdot 2\text{H}_2\text{O}$  (43%),  $\text{NaNO}_2$  (61.3%), NaCl (74.4%),  $\text{ZnSO}_4 \cdot 7\text{H}_2\text{O}$  (90.0%) and  $\text{K}_2\text{SO}_4$  (96.2%). The figures in parentheses refer to the percent relative humidity established over each solution at  $25 \pm 1^\circ \text{C}$ . All humidities were rechecked with a calibrated humidity meter. The system was considered to be in equilibrium after humidity readings had stabilized and had remained constant for two consecutive days. Desorption measurements were carried out at the same conditions. All measurements were carried out at  $25 \pm 1^\circ \text{C}$ .

#### RESULTS and DISCUSSION

Figures 1, 2, 3 and 4 show the water sorption isotherms as a function of water activity for the systems of 40% heterotactic and 60% syndiotactic poly(HEMA); 1 mole % EGDMA-poly(HEMA); 1 mole % TEGDMA-poly(HEMA); 1 mole % HMDIC-poly(HEMA), respectively. In Figures 1 to 4,  $N$  and  $a$  represent moles of sorbed water per mole of monomer unit and the activity of water (equilibrium relative humidity), respectively. The sorption of water vapor in the low water activity region (0-0.5) is almost the same in each of the three systems, but are different in the high water activity region (0.5-1.0). Figure 5 shows the sorption isotherm of water vapor as a function of water activity for the system of 80% isotactic, 14% heterotactic and 6% syndiotactic poly(HEMA). Figure 6 shows the sorption isotherm of water vapor as a function

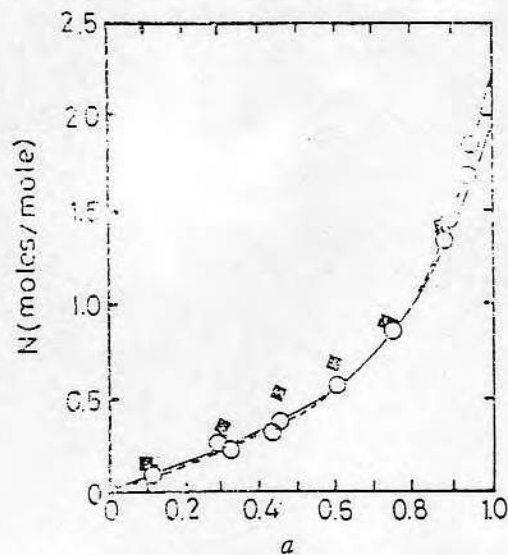


Fig. 1. Sorption Isotherms for Water Vapor in a Sample of 60% Syndiotactic and 40% Heterotactic p(HEMA) at  $25^\circ \text{C}$ .  $a$  = Activity of Water,  $N$  = Amount of Water Sorbed/Monomer Unit of Polymer (Mole/Mole).  $\circ$  = Sorption;  $\square$  = Desorption; ----- Modified B.E.T. Theory; ..... Hailwood-Horrobin Theory.

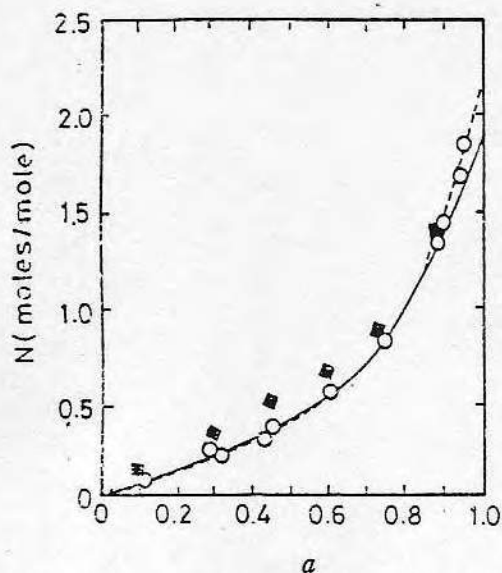


Fig. 4. Sorption Isotherms for Water Vapor in Sample of 1 mole % HMDIC-p(HEMA) at 25°C.  $a$ =Activity of Water;  $N$ =Amount of Water Sorbed/Monomer Unit of Polymer(Mole/Mole).  $\circ$ =Sorption;  $\blacksquare$ =Desorption. — Modified B.E.T. Theory; .....Hailwood-Horrobin Theory.

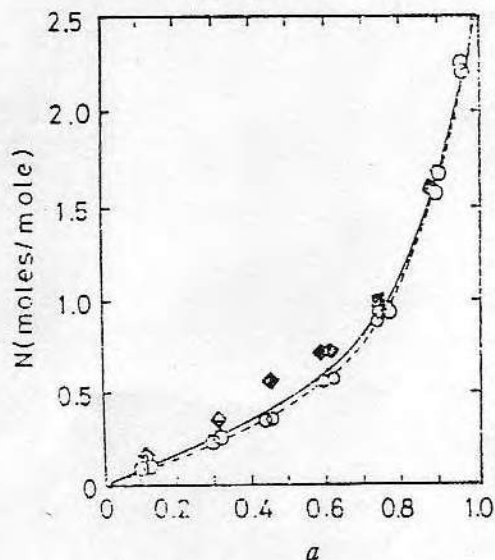


Fig. 5. Sorption Isotherms for Water Vapor in Sample of 80% Isotactic; 14% Heterotactic and 6% Syndiotactic p(HEMA) at 25°C.  $a$ =Activity of Water,  $N$ =Amount of Water Sorbed/Monomer Unit of Polymer(Mole/Mole).  $\circ$ =Sorption;  $\blacksquare$ =Desorption; — Modified B.E.T. Theory; .....Hailwood-Horrobin Theory.

Considering the heat of liquefaction problem, the Anderson-BET equation<sup>16</sup> is

$$\frac{N_t}{M_m} = \frac{c k a}{(1 - k a)[1 + (c - 1)k a]} \quad (1)$$

where  $N_t$  is the amount sorbed per unit of polymer,  $M_m$  is the concentration of sorption sites required for a monomolecular layer,  $a$  is the activity of water,  $c$  is a term related to the binding of a water molecule directly to the site to the indirect binding of water molecules, and  $k$  is the ratio of the affinity of indirect bonding to that of condensation into liquid water. Equation (1) reduces to the BET equation if  $k=1$ .

The parameters  $c$ ,  $k$ , and  $M_m$  can be evaluated from the sorption data by linearizing equation (1) as

$$\frac{a}{N_t(1 - k a)} = \frac{1}{c k M_m} + \frac{(c - 1)a}{c M_m} \quad (2)$$

The best fit values of the parameters were computed and are listed in Table 1. Equation (2) with these sets of parameters fits well at equilibrium relative humidities less than 0.7, but the plots deviate from the experimental values at equilibrium relative humidities greater than 0.7. The parameter  $c$  includes both the net heat of adsorption and the net entropy of adsorption. The constant  $c$  increases considerably from poly(DHPMA) to poly(HEMA). This increment reflects the transition from the convex to the S-shaped sorption isotherm. It seems that the higher hydrophilicity of poly-(DHPMA) is reflected in its stronger affinity towards weakly bound water, but not in a higher sorption ability of the strongly bonding sites. Among these systems, the most hydrophilic material is poly(DHPMA) which has two hydrophilic hydroxyl groups per repeating unit in the molecule.

Since  $k$  is the ratio of the affinity of indi-

This fact can be explained in terms of the configuration of hydroxyl groups in the polymer.

Isotactic poly(HEMA) probably exists in a helical conformation<sup>24</sup>, suggesting that the hydroxyl groups are on the outer surface of the helix. However, some of the hydroxyls in syndiotactic poly(HEMA) are somewhat buried, i.e. the polar side-chains of the polymer may interdisperse into the structure of the molecule. The helical isotactic chains probably have no intrachain hydrogen bonds linking the ester side chains, while the syndiotactic chains probably have intrachain hydrogen bonds between pendant hydroxyl groups. The different stereochemical conformation of the hydroxyl groups may give a different effective surface contact area of sorption sites.

The poly(DHPMA) shows a large effective surface area (273m<sup>2</sup>/g). This can be explained in terms of its structure, which has two hydroxyl groups in the monomer.

#### Interpretation in Terms of the Hailwood-Horrobin Theory

The Hailwood-Horrobin theory<sup>17</sup> has been used extensively for textile and polymer materials. This theory considers sorbed water to exist as an ideal solution of three species, i.e., dissolved water, hydrated water to polymer, and polymer components. This solution model produces a measure of hydrated water, condensed water, and the accessibility of sites for sorption.

Assuming the following two processes<sup>26,27</sup>,

Water vapor (activity,  $a$ )  $\xrightleftharpoons{K_0}$  Dissolved water (activity,  $a_s$ )

and

Dissolved water (activity,  $a_s$ ) + Dry polymer (activity,  $a_d$ )  $\xrightleftharpoons{K_1}$  Hydrated polymer (activity,  $a_h$ ).

Table 2. Parameters Evaluated from the Hailwood-Horrobin Theory for Water Vapor Sorption of Hydrophilic Methacrylate Polymers

No.	Polymer	$K_0$	$K_1$	$M_w$ (g)	$M_r$ (mole / (layer-mole))	$n$
1.	p(HEMA) (60% s, 40% H)	0.672	3.91	74.40	1.75	6.0
2.	p(HEMA)-(1 mole % EGDMA)	0.669	3.89	70.78	1.85	6.0
3.	p(HEMA)-(1 mole % TEGDMA)	0.632	3.80	62.70	2.10	6.5
4.	p(HEMA)-(1 mole % HMDIC)	0.630	3.79	62.68	2.10	6.5
5.	p(HEMA) (80% i, 14% h, 6% s)	0.611	3.59	59.17	2.20	6.0
6.	p(DHPMA)	0.570	2.33	41.28	3.88	8.0

The Hailwood-Horrobin theory<sup>17</sup> gives

$$\frac{mM_w}{18.02} = \frac{K_0 a}{1 - K_0 a} + \frac{K_0 K_1 a}{1 + K_0 K_1 a} \quad (4)$$

where  $m$  is the fractional moisture content,  $M_w$  is the molecular weight of polymer per mole of hydrated water, and  $K_1$  is an equilibrium constant in terms of bound water fractions in the polymers.  $K_0$  is an equilibrium constant related to the different degrees of hydrophilicity of the polymers. Equation (4) can be algebraically transformed to the parabolic relationship

$$\frac{a}{m} = \frac{M_w}{18.02} \left[ \frac{1}{K_0(K_1+1)} + \frac{(K_1-1)}{(K_1+1)} a - \frac{K_0 K_1}{K_1+1} a^2 \right] \quad (5)$$

Utilizing the sorption isotherm data, equation (5) was best fitted empirically and the constants  $K_0$  and  $K_1$  were evaluated (Table 2).

The modified B.E.T. theory predicted a good fit to most of the experimental isotherms up to 0.7 equilibrium relative humidity. However, a somewhat better fit was found with the solution theory of Hailwood-Horrobin over the entire range of equilibrium relative humidities, resulting in the parameters listed in Table 2.



# References

1. O. Wichterle and D. Lim, *Nature*, 185, 117 (1960).
2. J.D. Andrade, ed., "Hydrogels for Medical and Related Applications", ACS Symposium Series 31, Amer. Chem. Soc., Washington D.C., 1976.
3. M. Dole and I. L. Faller, *J. Amer. Chem. Soc.*, 72, 414 (1950).
4. A. D. McLaren and J. A. Cutler, *J. Polymer Sci.*, 3, 792 (1948).
5. R. Puffr and J. Sebenda, *J. Polymer Sci., C* 16, 79 (1967).
6. H. B. Bull and K. Breese, *Archiv. Biochem. Biophys.*, 128, 488 (1968).
7. H. Susi, J. S. Ard, and R. J. Carroll, *Biopolymers*, 11, 1597 (1972).
8. U. Buontempo, G. Careri and P. Fasella, *Biopolymers*, 11, 519 (1972).
9. R. Brodersen, B. J. Haugaard, C. Jacobsen, and A.O. Pedersen *Acta Chem. Scand.*, 27, 573 (1973).
10. I. C. Watt and J. D. Leeder, *Trans. Faraday Soc.*, 60, 1335 (1964).
11. J. D. Leeder, A. J. Pratt, and I. C. Watt, *Textile Inst. J.*, 59, 353 (1968).
12. L. J. Lynch, I. C. Watt and K. H. Marsden, *Kolloid Z.*, 248, 922 (1971).
13. R.W. Green and K.P. Ang, *J. Amer. Chem. Soc.*, 75, 2733 (1953).
14. B. Khaw, B.D. Ratner, and A. S. Hoffman, "The Thermodynamics of Water Sorption in Radiation-Grafted Hydrogels", in J. D. Andrade, ed., "Hydrogels for Medical and Related Applications", ACS Symposium Series 31, Amer. Chem. Soc., Washington, D.C., 1976. p.295.
15. J. Svetlik and J. Pouchly, *European Polymer J.*, 12, 123 (1976).
16. R. B. Anderson, *J. Amer. Chem. Soc.*, 68, 686 (1946).
17. A. J. Hailwood and S. Horrobin, *Trans. Faraday Soc.*, 42B, 84 (1976).
18. D. E. Gregonis, G. A. Russell, J. D. Andrade, and A. C. deVisser, *Polymer*, 19, 1279 (1978).
19. F. A. Bovey, "High Resolution NMR of Macromolecules", Academic Press, N.Y., 1972, p.71.
20. J. R. Kanagy, *J. Amer. Leather Chem. Assoc.*, 42, 98 (1947).
21. G.A. Russell, "Dynamic Relaxation Behavior of Stereoregular Hydrophilic Methacrylate Polymers", Ph.D. Thesis, University of Utah, U.S.A., 1977.
22. W. O. Milligan and H. H. Rachford, Jr., *J. Amer. Chem. Soc.*, 70, 2922 (1948).
23. S. Brunauer, P. H. Emmett, and E. Teller, *J. Amer. Chem. Soc.* 60, 309 (1938).
24. J. Janacek, *J. Macromol. Sci., C* 9, 1 (1973).
25. A.J. Stamm, "Wood and Cellulose Science", Ronald Press Co., New York, 1964, p.161.
26. J. A. Jaroniec, M. Jaroniec, and J. Gawdzik, *J. Appl. Chem. Biotechnol.*, 27, 248(1977).
27. C. Skaar, "Water in Wood", Syracuse University Press, Syracuse, New York, 1972.
28. Y. K. Sung, D. E. Gregonis, M. S. Jhon and J. D. Andrade, *J. Appl. Polymer Sci.*, 26, 3719 (1981).



# References

1. O. Wichterle and D. Lim, *Nature*, 185, 117 (1960).
2. J.D. Andrade, ed., "Hydrogels for Medical and Related Applications", ACS Symposium Series 31, Amer. Chem. Soc., Washington D.C., 1976.
3. M. Dole and I. L. Faller, *J. Amer. Chem. Soc.*, 72, 414 (1950).
4. A. D. McLaren and J. A. Cutler, *J. Polymer Sci.*, 3, 792 (1948).
5. R. Puffr and J. Sebenda, *J. Polymer Sci., C* 16, 79 (1967).
6. H. B. Bull and K. Breese, *Archiv. Biochem. Biophys.*, 128, 488 (1968).
7. H. Susi, J. S. Ard, and R. J. Carroll, *Biopolymers*, 11, 1597 (1972).
8. U. Buontempo, G. Careri and P. Fasella, *Biopolymers*, 11, 519 (1972).
9. R. Brodersen, B. J. Haugaard, C. Jacobsen, and A.O. Pedersen *Acta Chem. Scand.*, 27, 573 (1973).
10. I. C. Watt and J. D. Leeder, *Trans. Faraday Soc.*, 60, 1335 (1964).
11. J. D. Leeder, A. J. Pratt, and I. C. Watt, *Textile Inst. J.*, 59, 353 (1968).
12. L. J. Lynch, I. C. Watt and K. H. Marsden, *Kolloid Z.*, 248, 922 (1971).
13. R.W. Green and K.P. Ang, *J. Amer. Chem. Soc.*, 75, 2733 (1953).
14. B. Khaw, B.D. Ratner, and A. S. Hoffman, "The Thermodynamics of Water Sorption in Radiation-Grafted Hydrogels", in J. D. Andrade, ed., "Hydrogels for Medical and Related Applications", ACS Symposium Series 31, Amer. Chem. Soc., Washington, D.C., 1976. p.295.
15. J. Svetlik and J. Pouchly, *European Polymer J.*, 12, 123 (1976).
16. R. B. Anderson, *J. Amer. Chem. Soc.*, 68, 686 (1946).
17. A. J. Hailwood and S. Horrobin, *Trans. Faraday Soc.*, 42B, 84 (1976).
18. D. E. Gregonis, G. A. Russell, J. D. Andrade, and A. C. deVisser, *Polymer*, 19, 1279 (1978).
19. F. A. Bovey, "High Resolution NMR of Macromolecules", Academic Press, N.Y., 1972, p.71.
20. J. R. Kanagy, *J. Amer. Leather Chem. Assoc.*, 42, 98 (1947).
21. G.A. Russell, "Dynamic Relaxation Behavior of Stereoregular Hydrophilic Methacrylate Polymers", Ph.D. Thesis, University of Utah, U.S.A., 1977.
22. W. O. Milligan and H. H. Rachford, Jr., *J. Amer. Chem. Soc.*, 70, 2922 (1948).
23. S. Brunauer, P. H. Emmett, and E. Teller, *J. Amer. Chem. Soc.* 60, 309 (1938).
24. J. Janacek, *J. Macromol. Sci., C* 9, 1 (1973).
25. A.J. Stamm, "Wood and Cellulose Science", Ronald Press Co., New York, 1964, p.161.
26. J. A. Jaroniec, M. Jaroniec, and J. Gawdzik, *J. Appl. Chem. Biotechnol.*, 27, 248(1977).
27. C. Skaar, "Water in Wood", Syracuse University Press, Syracuse, New York, 1972.
28. Y. K. Sung, D. E. Gregonis, M. S. Jhon and J. D. Andrade, *J. Appl. Polymer Sci.*, 26, 3719 (1981).

## Molecular Monolayers and Films

J. D. Swalen,\* D. L. Allara, J. D. Andrade, E. A. Chandross, S. Garoff,  
J. Israelachvili, T. J. McCarthy, R. Murray, R. F. Pease, J. F. Rabolt, K. J. Wynne,  
and H. Yu

*A Panel Report for the Materials Sciences Division of the Department of Energy*

*Received December 29, 1986*

The considerable activity in the area of organic thin films, involving very thin polymeric films and molecular monolayers and multilayers, led to the formation of a panel, sponsored by the Materials Sciences Division of the Department of Energy, to review this field. Its purpose was to better understand the relevant scientific topics and to suggest suitable areas of research. In particular, a number of potential applications were identified, which require further scientific advances for them to see fruition. These include nonlinear and active optical devices, chemical, biochemical, and physical sensors, protective layers (e.g., for passivation), patternable materials both for resists and for mass information storage, surface modification (e.g., wetting and electrochemical electrode properties), and synthetic biomacromolecules. Studies of these films have the added advantage that they could lead to a better scientific understanding of such subjects as the relationships between the microstructure of ordered molecular arrays and their collective properties, the tailoring of interfaces and surfaces, especially when used to model multibody interactions, and the physical and chemical reactions of films involving phase transitions and intra- and interfilm transport. The areas that appear to require the most attention include the application of new characterization techniques, such as the scanning tunneling microscope, the improvement of mechanical and thermal stability, the identification and characterization of physical and chemical defects, and the effects of internal ordering on macroscopic properties. It is further recommended that strong interdisciplinary efforts be mounted to address and solve these problems.

### Introduction

Molecular films, ordered thin organic films in a thickness range from a few nanometers (a monolayer) to several hundred nanometers, show considerable technological promise, and further scientific investigation could prove to be very fruitful. Electronic and optical devices presently incorporate structures that are in this thickness range or approaching it, and organic thin films have been proposed to replace both passive and active components traditionally fabricated with other materials. Scientific studies of molecular interactions in thin-film structures leading to an understanding of the collective properties of ordered arrays have only recently been possible with organic films, characterized in more detail by a number of the newer surface science techniques. Biological lipid membranes exhibit a variety of different functions, and attempts to produce synthetic thin-film analogues have excited the

imagination of many. For these reasons it was felt that the physical, chemical, biological, and theoretical aspects of thin molecular films should be reviewed and their potential assessed. This report is such a study sponsored by the Materials Sciences Division of the Department of Energy, and it contains our consensus as to the future for this area of investigation.

Chemists have been able to synthesize molecules with many different conformations and chemical structures exhibiting a wide variety of functions. Although collective phenomena have been studied, more emphasis needs to be placed on the design and control of important collective properties so as to make these molecules into useful materials. The future for thin molecular solids lies in designing organized films to perform new and special functions. Of interest are arrays with cooperative properties different from those of the individual molecular components and perhaps possessing some functional enhancement. Liquid crystal displays are a well-known example of a cooperative function, and much interest has focused on the nature of phase transitions and magnetism in two dimensions. The number of possibilities is large, and considerably more research is needed to relate a specific film's structure to its functional properties.

The area of Langmuir-Blodgett films, monolayer structures transferred from a water surface to a substrate, has recently been receiving a great deal of attention.<sup>1-4</sup> These films are appealing for study because of the facile manner in which a single monolayer or multilayers can be

\* Chairman; IBM Almaden Research Center, 650 Harry Road, San Jose, CA 95120. Affiliations of other panel members: Bell Communications Research, 331 Newman Springs Road, Red Bank, NJ 07701, now at Department of Chemistry, Pennsylvania State University, University Park, PA 16802 (D.L.A.); College of Engineering, University of Utah, Salt Lake City, UT 84112 (J.D.A.); AT&T Bell Laboratories, 600 Mountain Ave., Murray Hill, NJ 07974 (E.A.C.); Schlumberger Doll Research, Old Quarry Road, Ridgefield, CT 06877 (S.G.); Department of Chemical Engineering, University of California, Santa Barbara, CA 93106 (J.L.); Polymer Science and Engineering Department, University of Massachusetts, Amherst, MA 01003 (T.J.M.); Department of Chemistry, University of North Carolina, Raleigh, NC 27607 (R.M.); Department of Electrical Engineering, Stanford University, Stanford, CA 94305 (R.F.P.); IBM Almaden Research Center, 650 Harry Road, San Jose, CA 95120 (J.F.R.); Chemistry Division, Office of Naval Research, Arlington, VA 22217 (K.J.W.); Department of Chemistry, University of Wisconsin, Madison, WI 53706 (H.Y.).

(1) *Thin Solid Films* 1980, 68(May 1).  
(2) *Thin Solid Films* 1983, 99(Jan 14).  
(3) *Thin Solid Films* 1980, 132-134(Oct-Dec).  
(4) Roberts, G. G. *Adv. Phys.* 1985, 34, 475.



deposited. Such a capability brings to mind applications as organic superlattices created by the successive deposition of alternating layers of different molecules. Whether these materials could even find use is highly speculative at the present time, but they do serve as good model systems. One could imagine some utilization in a number of areas, including optics, sensors, and barrier films. Electron beam resists<sup>5,6</sup> and "self-healing" capacitor layers<sup>7</sup> have been demonstrated in the laboratory. Functionalized phthalocyanines with attached molecular side groups to change or improve properties, such as solubility, can be used to form LB films,<sup>8</sup> and this is an important advance because they are among the most robust organic molecules known. Topotactic polymerization reactions, dependent on the structural proximity and orientation of reactants, have been used to create poly(diacetylenes) that are crystalline and exhibit nonlinear optical properties.<sup>9-11</sup> Another related topic is that of deposition from solution through a chemical reaction at a surface to give a self-assembled system.<sup>12-16</sup>

The explosive growth of microelectronics technology since 1960 is well chronicled.<sup>17</sup> According to some estimates, the "cost of computing" has decreased by several orders of magnitude during this time. Moreover, the value of the business has greatly increased, making this an attractive area for possible applications of new technology. We know of some specific cases where organic films are being successfully used. Already we have photoresists and electron beam resists for making patterns for very large scale integrated circuits (VLSI), organic photoconductors for printing and copying that compete directly with inorganic photoconductors, liquid crystals for displays, polymer films for insulation and packaging (various layers to encapsulate and protect a VLSI circuit from the environment),<sup>18</sup> and attached molecules and chemically reactive sites to modify surfaces. A classic example of this controlled chemistry is illustrated by color film for photography; films consist of some 20 layers, some as thin as 1  $\mu\text{m}$ , with numerous diffusion barriers.

All of this sounds exciting and promising, but the reader should be aware that there are still many unsolved problems. Organic thin films suffer from fragility, impurities, and defects. Consequently, their use has been limited by the ability to produce films with good integrity, i.e., mechanical, thermal, and chemical stability, as well as with the desired properties. Also, they must be made with few defects, or some mechanism for repair must be found. Efforts to overcome some of these problems, and to find applications that even take advantage of them, are progressing well. For strength, films are being polymerized and

cross-linked. Schemes are being developed to produce them with higher purity and, for polymeric films, with a narrower molecular weight range, and hence more uniformity. Weak interactions, e.g., van der Waals forces, acid-base and charge-transfer interactions, and certain covalent chemical bonding, could be used to modify organic thin films more easily and to make molecular engineering and design changes. That is, there are many ways to modify and make assemblies, but one of the key problems is to make an organized structure whose collective properties can be optimized for a desired goal. Today we have only scratched the surface, and, as stated above, we need more scientific understanding of the relationships not only of the component molecular species but also of the properties of a oriented and arranged array with the desired materials characteristics. This cannot be emphasized enough! If one were asked to make a thin organic film with a particular set of desired physical and chemical properties, generally an empirical approach would be taken. This process must definitely be shortened and put on a more rigorous scientific basis requiring better understanding of preparation and characterization methods.

After discussing a variety of research topics, we agreed that there are some very promising areas and, as a corollary, there are some areas where these materials are likely to remain inferior to others and, as such, should not be pursued with the same vigor. The areas considered to be the most promising for technology are as follows: (1) *thin-film optics*, optical layers and films exhibiting some special optical behavior, such as nonlinear optical effects for second harmonic generation, or switching, amplification, and modulation of optical signals; (2) *sensors and transducers*, thin films for specific sensors, such as biological sensors, as for coupling physical or chemical measurement probes to the film properties, e.g., electrochemical, mass, optical, and conductivity; (3) *protective layers*, thin organic films impervious to deleterious species in the environment so as to prevent some contaminant from disrupting the operation or function of the other layers; (4) *patternable materials*, photoresist and electron beam resists to create patterns at high packing density with greater resolution ( $\ll 1 \mu\text{m}$ ) than heretofore seen; (5) *surface preparation and modification*, surface groups to enhance lubrication, adhesion, wetting, and biological response or to provide new paths for chemical reactions not found in solution or isotropic media; (6) *chemically modified electrodes*, coatings on electrodes to give desired properties for new electrochemical reactions or analyses; and (7) *biomacromolecules*, our understanding of protein films needs to be expanded for more effective utilization. Can we produce or mimic biological effects with artificial films, and how well can we do this?

Besides these technological uses for thin organic films there are also a number of scientific problems which must be addressed:

1. The relationships between structure of oriented and aligned arrays of molecules and their collective properties are not well understood. New chemical designs and unique architecture may be able to create systems capable of exhibiting novel properties.

2. Molecular films can serve as models for the tailoring of interfaces and surfaces. For example, surfactants and modified polymeric surfaces have been used for a long time, but an understanding of them that could lead to new chemistry at a surface or to fabricate a new electronic device without delamination at the interfaces is still in its infancy. Films also can be examples for theoretical models involving several interactions, e.g., more than two-body

(5) Barraud, A.; Rosilio, C.; Ruauel-Teixier, A. *Thin Solid Films* 1980, 68, 99; *Solid State Technol.* 1979, August, 120.

(6) McCord, M. A.; Pease, R. F. W. *J. Vac. Sci. Technol., B* 1986, 4, 86.

(7) Agarwal, D. K.; Srivastava, V. K. *Solid State Commun.* 1972, 11, 1461.

(8) Roberts, G. G.; Petty, M. C.; Baker, S.; Fowler, M. T. Thomas, N. *J. Thin Solid Films* 1985, 132, 113.

(9) Sauteret, C.; Hermann, J. P.; Frey, R.; Pradere, F.; Ducuing, J.; Baughman, R. H.; Chance, R. R. *Phys. Rev. Lett.* 1976, 36, 956.

(10) Kajzar, F.; Messier, J.; Zyss, J.; Ledoux, I. *Opt. Commun.* 1983, 45, 13.

(11) Chollet, P.-A.; Kajzar, F.; Messier, J. *Thin Solid Films* 1985, 132, 1.

(12) Nuzzo, R. G.; Fusco, F.; Allara, D. L. *J. Am. Chem. Soc.* 1987, 109, 2358.

(13) Gun, J.; Iscovici, R.; Sagiv, J. *J. Colloid Interface Sci.* 1984, 101, 201.

(14) Maoz, R.; Sagiv, J. *J. Colloid Interface Sci.* 1984, 100, 465.

(15) Allara, D.; Nuzzo, R. G. *Langmuir* 1985, 1, 45.

(16) Maoz, R.; Sagiv, J. *Thin Solid Films* 1985, 132, 135.

(17) See, for example: *Scientific American* 1977, September.

(18) See, for example: *Proc. IEEE* 1985, 73(September).

interactions and several molecule-molecule interactions, as well as molecule-surface interactions.

3. Thermodynamics and kinetics of films involving phase transitions, viscosity near a surface, elasticity, diffusion, and transport of ions, electrons, and molecular species across them are all important to their properties. The transition from solid to fluidlike behavior, through liquid crystal behavior, is a gradual process and an interesting phenomenon which requires more investigation.

After the panel had identified these key areas of technology and science, it became clear that progress, although good, has been hindered by a number of problems and a certain lack of understanding of some of the key fundamental processes. Problems exist which prevent wide application of molecular monolayers to science and technology. Some of these more important obstacles were identified:

1. Characterization methods and techniques need to be developed further, and existing surface science tools need to be refined and tested on organic films. Clearly we can make and reproduce films of a desired quality only if we can analyze them in detail for their salient structural characteristics. A number of these new and existing methods will be discussed. As an example, scanning tunneling microscopy (STM) has recently been used to observe an organic bilayer. This technique appears to have the potential to observe directly surface topography and morphology. In addition, a number of spectroscopic methods, already applied to the preliminary analyses of thin films, show considerable promise as useful tools for their more detailed characterization.

2. Integrity and stability of films must be improved to overcome some of the problems related to their soft and almost fluidlike behavior. Films are degraded by heat, sunlight, and environmental impurities. Mechanical strength needs to be improved, and dimensional stability is always a problem for any information storage device. Recent results have been reported on thermally stable films with very small in-plane thermal expansion coefficients. Compliance, on the other hand, could be a useful property, if properly combined with other intrinsic properties.

3. Impurities and defects must be identified and the deleterious ones removed. Organic materials are generally harder to purify than other materials, but new methods must be developed and evaluated to produce improved materials. Removal of defects certainly would be an advantage, if such a process could be developed.

4. The question of type and the degree of order needed in a film for a specific function must be addressed. There is fair knowledge of how to make layered structures, but there are few, if any, known ways to produce and measure in-plane ordering for small areas of less than  $1 \mu\text{m}^2$ . This problem, in particular, plagues the biophysicist trying to understand the active sites of a lipid bilayer with a predetermined biological function.

A different type of problem, more of an organizational nature, has also hindered the development of this field of research, and little progress will be made if it is not addressed. Since this is an interdisciplinary field involving physicists, chemists, biologists, electrical engineers, and materials scientists, efforts need to be made at university, industrial, and government laboratories to cross department and divisional lines and boundaries in order to encourage cooperative programs. This may require modifying the promotional system and the methods of funding from government agencies so that collaboration can be encouraged. Researchers should be judged and evaluated on

their joint efforts and not only on their individual accomplishments. An interdisciplinary attack on these problems by our best people is required.

This report will first describe a number of application areas and the scientific research that must be carried out in order to bring about significant progress. Other areas will be identified which are not so attractive at this time either because the material characteristics of organic films and molecular monolayers do not fit the requirements or because there are much better competing materials. Then some related topics, probably best described as scientific endeavors, but which in the future will lead to a much better understanding and consequent utilization of molecular films, will be discussed.

### Thin-Film Optical Materials

The advent of optical fiber communications, generally operating in the  $1.3\text{-}\mu\text{m}$ -wavelength region, has generated a strong need for compact signal-processing units. This includes switches, modulators, and optically driven parametric amplifiers. These devices depend on nonlinear optical effects and a variation of refractive index produced by high optical fields or an external electric field. As a result, nonlinear effects, especially second-harmonic generation (SHG) and third-harmonic generation (THG), have received considerable attention. Four-wave mixing and bistability are two other interesting nonlinear phenomena. Present experimental devices, however, are based on lithium niobate because it is the best available from among a rather unsatisfactory set of inorganic materials. In the last decade, many organic species have been shown to possess much larger interaction cross sections for nonlinear effects,<sup>19</sup> and intensive research is currently underway at British Telecom, CNET (France), several large Japanese firms, Du Pont, Kodak, and AT&T.

Nonlinear phenomena in organic systems depend on the intrinsic nonlinear polarizability of the molecules and on the crystallographic packing. For second-harmonic generation the site and its associated polarizability tensor must not possess a center of symmetry. As a consequence, a Y deposition of an LB film assembly in which the molecules have a head-to-head and tail-to-tail configuration<sup>20</sup> might lead to a reduction in the second-harmonic term in the polarizability tensor expansion. Efforts have recently been directed at depositions with alternating layers of an active dye possessing a strong second-harmonic behavior and an inert layer of spacer molecules, for example, arachidates or stearates.<sup>21-30</sup> Alternatively, the symmetry can be broken by a head-to-tail deposition (called Z deposition).<sup>31,32</sup>

(19) Williams, D. J. *Angew. Chem., Int. Ed. Engl.* 1984, 23, 690.

(20) Gaines, G. L., Jr. *Insoluble Monolayers*; Interscience: New York, 1966.

(21) Girling, I. R.; Cade, N. A.; Kolinsky, P. V.; Montgomery, C. M. *Electron. Lett.* 1985, 21, 169.

(22) Girling, I. R.; Kolinsky, P. V.; Cade, N. A.; Earls, J. D.; Peterson, I. R. *Opt. Commun.* 1985, 55, 289.

(23) Girling, I. R.; Cade, N. A.; Kolinsky, P. V.; Earls, J. D.; Cross, G. H.; Peterson, I. R. *Thin Solid Films* 1985, 132, 101.

(24) Girling, I. R.; Milverton, D. R. Y. *Thin Solid Films* 1984, 115, 85.

(25) Holcroft, B.; Petty, M. C.; Roberts, G. G.; Russell, G. J. *Thin Solid Films* 1985, 134, 83.

(26) Barraud, A.; Leloup, J.; Gouzerh, A.; Palacin, S. *Thin Solid Films* 1985, 133, 117.

(27) Daniel, M. F.; Smith, G. W. *Mol. Cryst. Liq. Cryst.* 1984, 102, 193.

(28) Daniel, M. F.; Dolphin, J. C.; Grant, A. J.; Kerr, K. E. N.; Smith, G. W. *Thin Solid Films* 1985, 133, 235.

(29) Smith, G. W.; Daniel, M. F.; Barton, J. W.; Radcliff, N. *Thin Solid Films* 1985, 132, 125.

(30) Stroeve, P.; Srinivasan, M. P.; Higgins, B. G.; Kowal, S. T. *Thin Solid Films* 1987, 146, 209.



In addition, there is much to be done concerning the fabrication of thin-film wave guides with the incorporation of molecules having large polarizabilities. These are molecules of moderate size which are characterized by both strong intramolecular charge-transfer (CT) electronic transitions and a large excited-state dipole moment. What is needed are methods to incorporate oriented arrays (not necessarily nearest neighbors) of these types of molecules so as to maximize their interaction length with the light. Cyanine dyes, azo compounds, and nitroamino compounds are the molecular types most commonly being investigated because they should have large nonlinearities, but there are many other types of CT complexes and related molecules with high polarizabilities that need to be identified and evaluated.

Polymerized and cross-linked diacetylene films are optically and structurally appealing for third-harmonic generation and other nonlinear phenomena. Researchers at Bell Communication Research Center have recently measured an off-resonance  $\chi^{(3)}$  of  $0.1 \times 10^{-9}$ , which is claimed to be the largest of any known organic material.<sup>33</sup> Work on very thin crystals has been reported by researchers at General Telephone and Electronics Laboratories.<sup>34</sup>

Another new use of SHG is being developed at the University of California at Berkeley for surface analysis (see below under Characterization for more details).<sup>35-40</sup> A surface by its very nature breaks any center of symmetry and can generate, albeit weak, second-harmonic signals. An overcoating can increase or decrease this SHG. It is clear that not only the coating can be detected; properties of the coating, such as its nonlinearity and the elements of the tensor, can be determined. This technique may prove to be very useful in the analyses of surface molecules and thin films.

### Sensors, Transducers, Detectors, and Displays

The rapid decline in the cost of electronic information processing has stimulated a need to interface electronic systems with the real world. Thus, sensors and output transducers should enjoy enormous growth in the market place. It is difficult to estimate the share of the market which those devices based on organic films could capture. Photodetectors and related devices, such as optical image detectors, appear to be well served by inorganic materials. High-frequency loudspeakers and electromechanical actuators have used organic films, and sensors (temperature, pressure, strain, or chemical species) may well be another attractive application. Image displays employ liquid crystals, but a full color, high-contrast, high-definition

display with a lower power requirement than a CRT is probably some years away. However, there are significant advantages for a display whose contrast relies on absorption of ambient light rather than on luminescence stimulated internally; the conversion of electronic watches from light-emitting diode displays to liquid crystal displays has been an obvious example.

Piezoelectric polymers are becoming increasingly well-known and utilized as sensors and transducers. Much work has been done to improve the high-temperature stability of piezoelectric polymers and to maximize the electrical output for a given input of pressure (acoustic wave) or thermal energy. The best known piezoelectric polymer is poly(vinylidene fluoride) (PVF<sub>2</sub>). It has many desirable properties, including insensitivity to water, thermal stability in its piezoelectric behavior to about 100 °C, toughness, and a good impedance match to water (making it a good acoustic sensor in the ocean). However, there are drawbacks which can be significant, depending on the application envisioned. PVF<sub>2</sub> inconveniently crystallizes from the melt in an inactive form ( $\alpha$  or form II). The active form ( $\beta$  or form I) is obtained only by processing, such as with a stretch orientation, which must be subsequently poled under a high electric field to maximize its activity. An advance has been made with copolymers, e.g., poly(trifluoroethylene-1,1-difluoroethylene), which crystallize directly in the  $\beta$  form from the melt. Alternatively, blends (interestingly, poly(methyl methacrylate) (PMMA) forms a compatible blend) have been found to crystallize in the active form. An unfortunate and frequently unmentioned aspect of the utilization of PVF<sub>2</sub> is the fact that, considering the sophisticated electronic applications envisaged, the commercially available polymer is usually obtained in a highly impure form. First, as a consequence of the synthetic method for polymerization, PVF<sub>2</sub> contains a significant fraction (typically 6%) of chain defects, e.g., head-to-head structures. Thus, many would consider PVF<sub>2</sub> to be a random copolymer. Second, with emulsion polymerization the polymer is contaminated with ionic impurities. Both of these problems suggest that further work is needed to optimize PVF<sub>2</sub> or to find new and better materials.

A new approach to piezoelectric materials along this line is the use of molecular/macromolecular blends. These are composed of a molecular component that is compatible with the amorphous phase of a polymer and another component that is compatible with the polymer crystalline phase. Their crystallization in an electric field has led to materials with much improved piezoelectric properties. The component in the amorphous phase acts as a plasticizer to lower the glass transition temperature, thereby improving compliance. For example, a blend of 30% 2-ethyl-1,3-hexanediol and 70% nylon-11 has its piezoelectric coefficient,  $d_{3,1}$ , increased by a factor of 4 and its dielectric constant increased by over a factor of 3 compared to nylon-11 itself.<sup>41,42</sup> Preliminary results<sup>43</sup> also show that a PVF<sub>2</sub> blend may be prepared with a much enhanced dielectric constant, while maintaining an unenhanced (albeit high)  $d_{3,1}$ . These are exciting results and may offer greatly improved capabilities in acoustic sensing.

Sensor response with thin films depends on utilizing any one of a number of effects, such as a change in electrochemical activity, photoconductivity, or mass. The prob-

(31) Ledoux, I.; Vidakovic, P.; Zyss, J.; Hann, R. A.; Gordon, P. F.; Bothwell, B. D.; Gupta, S. K.; Allen, S.; Robin, P.; Chastaing, E.; Dubois, J.-C. *Europhys. Lett.* 1987, 3, 803.

(32) Hayden, M.; Kowel, S. T.; Srinivasan, M. P. *Opt. Commun.* 1987, 61, 351.

(33) Etemad, S., 192nd National Meeting of the American Chemical Society, Anaheim, CA, Sept 7-12 1986.

(34) Carter, G. M.; Chen, Y. J.; Tripathy, S. K. *Opt. Eng.* 1985, 24, 609.

(35) Heinz, T. F.; Tom, H. W. K.; Shen, Y. R. *Phys. Rev. A* 1983, 28, 1883.

(36) Rasing, Th.; Shen, Y. R.; Tom, H. W. K.; Valint, P., Jr.; Bock, J. *Phys. Rev. A* 1985, 31, 537.

(37) Rasing, Th.; Shen, Y. R.; Kim, M. W.; Grubb, S. *Phys. Rev. Lett.* 1985, 55, 2903.

(38) Boyd, G. T.; Shen, Y. R.; Hansch, T. W. *Opt. Lett.* 1985, 11, 97.

(39) Rasing, Th.; Berkovic, G.; Shen, Y. R.; Kim, M. W.; Valint, P., Jr. *Chem. Phys. Lett.* 1986, 130, 1. Berkovic, G.; Rasing, Th.; Shen, Y. R. *J. Chem. Phys.* 1986, 85, 7374.

(40) Shen, Y. R. *New Laser and Optical Investigations on Chemistry and Structure of Interfaces*; Hall, Ellis, Eds.; Verlag-Chemie: Berlin, 1986.

(41) Mathur, S. C.; Scheinbeim, J. I.; Newman, B. A. *J. Appl. Phys.* 1984, 56, 2419.

(42) Scheinbeim, J. I.; Mathur, S. C.; Newman, B. A. *J. Polym. Sci., Polym. Phys. Ed.* 1986, 24, 1791.

(43) Newman, B. A.; Scheinbeim, J. I.; Sen, A. *Ferroelectrics* 1984, 57, 229. (a) *Chem. Eng. News* 1987, 65(Feb 9), 24.

lems are in designing the film for a selective response to a specific species and in coupling the film to an electrode. Recently a neutron detector based on polyacetylene was reported.<sup>43a</sup> Here the neutrons increase the electrical conductivity of the polyacetylene,  $(CH)_x$ . Biosensors depend on binding proteins with the desired characteristics. Immobilized ligands of antibodies can be sensitive to certain antigens. A molecular film can also serve as a barrier to unwanted components in a system, allowing only specific ones to reach the electrode and be detected. The future looks bright for these materials because a very thin coating can turn a rather insensitive device into a very sensitive and specific one. In addition, they can be made inexpensively and extremely small. More details on many of the aspects of sensors are included in the sections on electrodes and biological thin films.

### Packaging and Insulating Layers for Integrated Circuits

Thin films find important uses as insulators in integrated circuits.<sup>18</sup> For those based on silicon, the insulating film immediately on top of the single crystal surface is nearly always thermally grown  $SiO_2$ . However, other semiconductor surfaces are very restricted electrically; for example, only n-channel devices can normally be made of GaAs because uncompensated surface states tend to "pin" the Fermi level outside the bandgap. It may be possible to use thin organic films to fill those states and so allow both n-channel and p-channel devices to be built on the same crystal.<sup>44</sup> Another increasing use of dielectric films is for insulating multiple levels of metal interconnections. The ability to form multiple levels of submicron interconnections is becoming increasingly needed as the degree of integration increases. At present, two levels of metal interconnections are the limit of our technology in manufacturing; in 10 years, four or five levels will be needed. Engineering such a structure may well be facilitated by the ability to incorporate well-characterized and ordered organic films.

Packaging a semiconductor chip consists of mounting it in a small piece of plastic about  $3 \times 15$  mm in size and bringing out the electrical connections to metal pins.<sup>17</sup> Large numbers of interconnections in VLSI structures place increasingly stringent requirements on dielectric polymer films used for encapsulation. The package must also provide adequate protection, electrical connections, and a heat sink. A key requirement for such materials is a minimal thermal coefficient of expansion in the plane of the film. In a system made of many chips, there is often a hierarchy of packaging technologies. The printed circuit board is described as a second-level package, and the assembly of chip and plastic (colloquially called a "dip") is the first level. More complicated chips, which work at high speeds, tend to dissipate more heat, have more off-chip connections, and demand more exotic packaging. Thus thin organic films might well be used for sealing the surface of the chips for chemical protection against, for example, moisture that could stimulate electrolytic corrosion of fine metal interconnections or generate electrolytically metal ions that could degrade the semiconductor. Possibly conducting polymers might be used in the future as mechanically compliant conductors, but at present they lack sufficient stability and conductivity.

One feature that has been clearly identified as affecting the coefficient of expansion is chain ordering. Thus

Kapton as obtained from Du Pont has a coefficient of thermal expansion<sup>45</sup> of  $20 \times 10^{-6} (^\circ C)^{-1}$ , while cast films of this material have twice the expansion. Wide-angle X-ray scattering has shown that the difference is due to substantial in-plane ordering of the rodlike polymer molecules in manufactured films.<sup>45</sup> There is an opportunity for new materials in which orientation effects are optimized. For example, some rodlike liquid crystalline polymers are known to display negative in-plane coefficients of thermal expansion. Polyimides such as Kapton, however, suffer from the fact that the chemical reaction from polyamic acid to polyimide is a condensation reaction with a concomitant release of water, which can cause significant processing difficulties such as corrosion, voids, or film shrinkage. This problem needs to be addressed through the development of polymers which cure via addition polymerization routes or perhaps by the development of thermoplastic polyimides. New results on the liquid crystal behavior in thin-cast films of polyimides have recently emerged showing that films can be constructed<sup>46</sup> with very low thermal expansion coefficients. Understanding gained at the fundamental level will be vitally important for many technologies that rely on high-stability, temperature-resistant polymers. Their application in microelectronics continues to show considerable promise.

### Patternability of Thin Films: Resists and Information Storage

Organic films are already well established as resist materials. They are applied by spin-coating and then exposed with the appropriate pattern of ultraviolet light, X-rays, electrons, or ions. After development, either the exposed or unexposed areas are dissolved away to reveal the underlying circuit material, which can then be etched away either by a wet process or by a reactive plasma. The most complex present-day circuits have  $\sim 1\text{-}\mu\text{m}$  features and a chip size of  $1\text{ cm}^2$ . Moreover, there are between 6 and 12 mask levels for a complete circuit, so the allowed error rate, or defect density per level, must be excruciatingly low. Resolution is expected to drop to about  $0.25\text{ }\mu\text{m}$  by 1995, and chip area is expected to quadruple. Another complication is that the required line width control must be between  $0.025$  and  $0.05\text{ }\mu\text{m}$ , and this is approaching the molecular dimensions of some of the polymers used today. Also, to achieve these narrow lines, films must be much thinner than the present  $1\text{--}2\text{-}\mu\text{m}$  films! Thus, it will be necessary to find new materials with ordering or some other characteristic that allows the formation of thinner films with fewer defects.

The use of thin films for recording information either irreversibly (as in archival memory) or reversibly (as on a magnetic disk) is a related area, but error-correcting codes can be used so that the defect problem may not be too acute. Present-day target densities are about  $10^7$  bits/ $\text{cm}^2$ , but this will probably evolve to  $10^8$  bits/ $\text{cm}^2$ , both for optical and magnetic recording. Another advantage of this application is the wide range of available readout mechanisms. Topographic contrast (as in a resist) may be read capacitively, optically, or by using an electron microscope. Recently, with a focused electron probe, a page of text at a density approaching  $10^{11}$  bits/ $\text{cm}^2$  has been read with a transmission electron microscope (TEM).<sup>47</sup> But naturally, because of the size and expense of the TEM, this technique is impractical. A new much more compact and less expensive instrument, the scanning tunneling

(44) Larkins, G., Case Western Reserve University, unpublished results.

(45) Hofer, D. C., private communication.

(46) Hofer, D. C. *Polym. Mater. Sci. Eng.* 1986, 55, 85.

(47) For a description, see: Newman, T. *Eng. Sci.* 1986, 49(Jan), 24.



microscope (STM), has been used for examining surfaces with atomic resolution and has also been used for writing patterns.<sup>48,49</sup> The STM promises a wide variety of writing and reading mechanisms, so more subtle changes in the film topography may eventually be used for storage. In principle, there is the possibility of improving by 2 orders of magnitude the density of information storage, but molecular films must be developed further in order to meet these needs.

Laser-written metallic patterns on thin organometallic films and photoablative patterning<sup>50</sup> should be mentioned as two other approaches to the patterning of organic films. These are presently being investigated for medical applications but may be useful in other technologies as well, even though they currently are not useful for defining any significantly sized area in production.

### Electronic Circuit Components

Although the use of molecular monolayers for circuit elements seems to be too speculative, some thoughts and ideas regarding these materials will be presented. The resistivity of metals at room temperature is between  $10^{-6}$  and  $10^{-5}$   $\Omega\cdot\text{cm}$  with temperature coefficients between 10 and 1000 ppm/K. Because of these almost optimal properties, it is most unlikely that metal interconnections will be displaced by organic materials! Electrical conduction in organic films is of interest for its scientific value, but existing materials have properties that are already extremely good for practical interconnections.

Conducting polymers can now be made stable in air, insensitive to the presence of water, reasonably stable to thermal excursions, and mechanically compliant. There may, therefore, be special applications where enhanced properties of a conducting organic film could render them attractive. Examples are the use of a conducting polymer as an antistatic material, as in a new line of copiers; self-limiting switches, where the conductivity decreases as temperature increases, thereby providing intrinsic protection; conducting fibers such as Kevlar/phthalocyanine<sup>51</sup> for lightweight composites to shield enclosed electronics from certain damaging radiation; and in the packaging of chips, where resistivity is not critical and a compliant conducting material could allow an increased number of chip-to-substrate contacts. Numerous intrinsically conducting polymers exhibit interesting properties. For example, polypyrrole tosylate<sup>52</sup> is easily made by electropolymerization of the monomer in an aqueous electrolyte under ambient conditions. These black films have stable conductivity in air, though they are moderately hygroscopic, and they are also mechanically tough and thermally stable in air to about 100 °C. Poly(3-alkylthiophenium) salts are new polymers which are soluble in polar organic solvents and are good film-forming materials, provided the alkyl chain is of sufficient length (ca. six carbons).<sup>53,54</sup> Polyanilines are an old class of polymers, but new studies are revealing them to be stable and electronically conducting by unusual "doping" methods. One such method is simple acidification, i.e., "protonic doping".<sup>55</sup>

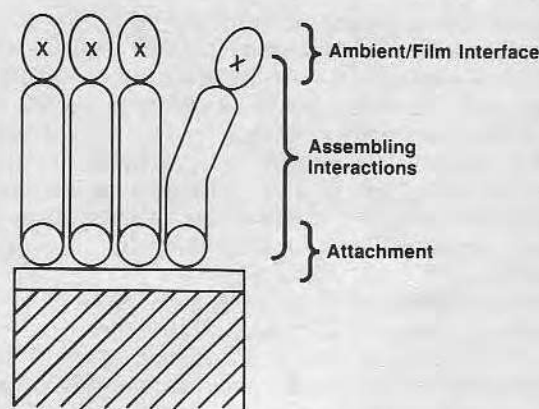


**Figure 1.** Molecules attached to a surface shown schematically. They consist of a head group attached to a substrate, some interior group (most often an alkyl chain) which provides cohesive interactions, and a terminal functional group (X) which interacts with the ambient phase.

Capacitor dielectrics made of organic films may be more likely candidates; they have insulating properties that in many cases rival those of inorganic films. Some circuits require high values of capacitance per unit area, so a high dielectric constant,  $\epsilon$ , is desirable; in other cases, the reverse can be true. It could prove to be very useful for an engineer to have two different values of  $\epsilon$  in similar materials. At the same time, however, the process must still be compatible with the rest of the circuit processing, which can involve temperatures exceeding 1000 °C, and, in addition, the circuit must operate within specifications over a minimum temperature range of -20 to +85 °C.

Semiconductor diodes have outstanding basic properties of low forward resistance and high reverse resistance; silicon transistors have been described as being close to thermodynamically perfect. The members of this panel have some reservations concerning the applicability of organic films to high-speed switching; only with some innovative architecture involving, perhaps, parallel processing could they be made competitive. Applications for organics, therefore, must depend on utilizing some unique or specific property, such as low cost, large areas, or transparency. Thus, again, any amplifying or switching action of organics will have to be combined with some other intrinsic properties for an attractive application to emerge. The possibilities in biomedical instrumentation are discussed in more detail in a later section.

### Functionalization of Surfaces

**Inorganic Surfaces.** A number of useful properties of a solid material depend upon the nature of the ambient surface layer. These include adhesion, wetting, friction, biocompatibility, charge and mass transport, and chemical reactivity. Often these properties can be dramatically altered by the attachment of one or more layers of organic functional groups at the material surface. The variety of possible structures range from random arrangements of attached organic functional groups to highly organized, densely packed, ordered molecular assemblies. An example of the former is organosilane molecules covalently bonded to glass surfaces in order to promote adhesion in glass/polymer composites. An example of the latter is the modification of a semiconductor surface by a physisorbed Langmuir-Blodgett film as part of a metal-insulator-semiconductor (MIS) electronic device. To efficiently

(48) See, for example: *IBM J. Res. Dev.* 1986, 30.

(49) Quate, C. F. *Phys. Today* 1986, 39, 26.

(50) Srinivasan, R.; Braren, B.; Dreyfus, R. W.; Hadel, L.; Seeger, D. E. *J. Opt. Soc. Am. B* 1986, 3, 785.

(51) Inabe, T.; Lomax, J. F.; Marks, T. J.; Tobin, J.; Lyding, J. W.; Kannawurf, C. R.; Wynne, K. J. *Macromolecules* 1984, 17, 260.

(52) Wynne, K. J.; Street, G. B. *Macromolecules* 1985, 18, 2361.

(53) Elsenbaumer, R. L.; Shacklette, L. W. *J. Polym. Sci., Polym. Phys. Ed.* 1982, 20, 1781.

(54) Vardeny, Z.; Ehrenfreund, E.; Brafman, O.; Novak, M.; Schaffer, H.; Heeger, A. J.; Wudl, F. *Phys. Rev. Lett.* 1986, 56, 671.

(55) MacDiarmid, A. G.; Chiang, J. C.; Huang, W.; Humphrey, B. D.; Somasiri, N. L. D. *Mol. Cryst. Liq. Cryst.* 1985, 125, 309.

prepare complex films for specific applications, one must assemble appropriate molecular functionality on a variety of metal, insulator, and semiconductor substrate materials.

The assembling and final structure of a film can be visualized in terms of three overlapping regions of interactions as shown in Figure 1. The molecules in this figure consist of a head group attached to a substrate, some interior moiety (most often an alkyl chain) which exhibits cohesive interactions, and a terminal functional group which interacts with the ambient phase. Variation of the interactions in each of these regions can dramatically alter film properties. The attachment of the film to a solid substrate usually is accomplished by one of three common procedures: spontaneous adsorption of molecules from a vapor environment, spontaneous adsorption of molecules from a solution environment, and forced interfacial transfer processes, such as the LB procedure.

Current and past emphasis has been on the LB technique. While this technique has produced some examples of highly organized monolayer and multilayer films, there are major disadvantages which should prompt serious efforts to develop alternate techniques. These films are not necessarily thermodynamically stable, binding to the surface usually does not occur by strong chemical bonds, and only amphiphilic molecules which form assemblies at the air-water interface are suitable, the most common of which are long-chain fatty acids and closely related structures.

The spontaneous solution-phase process, on the other hand, offers the possibilities of forming layers of multifunctional polar molecules from both aqueous and nonaqueous solvents near or at equilibrium conditions. The reaction of alkyltrichlorosilanes with  $\text{SiO}_2$  to form robust films bonded via silicon-oxygen bonds to the substrate<sup>13,14,56</sup> and the solution reaction of organic thiols or disulfides with gold surfaces<sup>12,57</sup> are two examples that have been shown to be effective in bonding molecules to surfaces. Relatively little work has been done in this area, and new types of attachment chemistry need to be developed, particularly for technologically important substrates such as semiconductors and ceramics.

The vapor-phase process offers possibilities such as the deposition of complex organic assemblies onto ultraclean, single-crystal substrates under ultrahigh vacuum conditions. The possibility of organic "molecular beam epitaxy" (MBE) of crystalline layer growth is thought provoking. Processes for the deposition of conformal thin organic films from the gas phase, such as the formation of poly(*p*-xylylene), have been available for some time. This area offers a challenge to chemists and material scientists. The recent widely publicized plasma-aided deposition of thin diamond films<sup>58,59</sup> being done in Japan and the USSR points to yet another important area in which the U.S. is behind.

The geometrical arrangement and structure of the molecules in the surface-bound film depend upon the geometry of the substrate binding sites, the strength of the substrate-head group bonds, the relative sizes of the head groups compared to the remainder of the molecule, and the intermolecular forces. In principle one can design a specific film architecture for a given substrate if each of these factors is known sufficiently well. However, the task proves to be very difficult or impossible for all but the well-studied system of long-chain alkyl molecules for which a good knowledge of chain-chain interactions exists from

studies of alkane crystals and lipid bilayer systems. Even here, too little is known, particularly in the area of substrate-induced head group arrangements, to allow any but the simplest of guesses as to the general types of structures possible. Aromatic ring compounds are known to assemble spontaneously into ordered films on platinum surfaces.<sup>60,61</sup> However, in general, a great deal of work needs to be done on the effect of molecular structure on film architecture. This issue becomes critically important when functional groups are needed in the film interior for active functions, such as cross-linking and photo- or electroresponse. A body of knowledge is needed about combinations of substrates, head groups, and film interior groups that lead to layers with specifically tailored architecture.

Because of the variety of applications for functionalized surfaces, it is desirable to develop structures which can have a wide variety of exposed organic functional groups (X in Figure 1). These can range from passive low-energy groups, such as  $\text{CH}_3$  and  $\text{CF}_3$ , to highly reactive groups such as  $\text{N}=\text{C}=\text{O}$  or biologically important groups such as phosphatidylcholine. Monolayers spontaneously assembled from  $\omega$ -vinyl-terminated alkylsilanes can undergo smooth, specific cleavage reactions of the olefin group. The resultant functional groups can further react with alkylsilanes to form a multilayer structure.<sup>13,14,56</sup> Adsorption of a wide variety of organodisulfides occurs on gold<sup>12,57</sup> to form monolayers with vastly different wetting properties that depend upon the terminal interface group; these could be  $\text{NO}_2$ ,  $\text{CF}_3$ ,  $\text{CH}_3$ ,  $\text{CO}_2\text{H}$ ,  $\text{OH}$ , or a biological functionality, such as the phosphatidylcholine group. The classic case of adhesion promoters such as  $\omega$ -aminoalkylsilanes is another example. At present, the major problem in creating such structures is that the desired terminal group must exhibit high specificity in the adsorption or chemisorption process and not end up attached to the substrate or buried in the film's interior. As mentioned above, silanes on  $\text{SiO}_2$  and organosulfur compounds on gold are two examples of favorable attachments. However, extensive work is needed in examining relative surface versus ambient interface interactions for other functional groups and substrates in order to find other cases of good film formation. It is possible that the equivalent of a multilayer structure could be achieved by the formation of grafted polymer chains extending outward from a monolayer functionalized substrate. Again, much work is needed in developing films with terminal groups on the surface through appropriate coupling reactions.

**Polymer Surfaces.** Polymer surfaces exhibit unique properties and behaviors different from those of other solid surfaces in that the chains at and near the surface are mobile and can almost be viewed as a viscous liquid. The magnitude of this mobility depends on the temperature relative to the glass transition temperature,  $T_g$ , which spans a range of as much as 400 °C for various common polymers. Therefore, at a given temperature the surface mobility varies greatly from polymer to polymer. Whether or not the outermost polymer chains exhibit a definite glass transition temperature and whether this is the same as the bulk are two separate and important issues. Even polymers with a single bulk composition can display different surface compositions, and block copolymers can concentrate one component at the surface so that some degree of phase separation takes place.<sup>62-71</sup> The structure,

(56) Netzer, L.; Isovici, R.; Sagiv, J. *Thin Solid Films* 1982, 99, 235.

(57) Nuzzo, R. G.; Allara, D. L. *J. Am. Chem. Soc.* 1983, 105, 4481.

(58) See, for example: *The New York Times*; 1986, Sept 14, p 1.

(59) *Industrial Chemical News* 1986, 7,(7), 1.

(60) Soriaga, M. P.; Hubbard, A. T. *J. Am. Chem. Soc.* 1982, 104, 3937.

(61) Hubbard, A. T. *Acc. Chem. Res.* 1980, 13, 177.

(62) Reardon, J. P.; Zisman, W. A. *Macromolecules* 1974, 7, 920.

(63) Clark, D. T.; Peeling, J. J. *Polym. Sci., Polym. Chem. Ed.* 1976, 14, 543.



properties, and reactivities of the polymer surface are very dependent on the environment and its surroundings, which could be another condensed phase (liquid, metal, ceramic, or another polymer). The extent to which interpenetration occurs is also important. Organic polymers, generally, have low surface energies and are more stable in air than other solid surfaces of metals, metal oxides, and inorganic hydrates. This permits relatively easy laboratory manipulation but gives rise to adhesion problems; adhesives often do not function well as binders between two polymer surfaces.

Organic polymer surfaces display a range of functionality and, given the highly developed field of organic chemistry, offer a chemical versatility far surpassing any other class of solid surfaces. To take advantage of this and to control surface structure require a well-characterized polymer surface containing functional groups. These can then be manipulated to a variety of structures, which can be compared to the initial surface. Several key issues must be addressed: What are the three-dimensional locations of the functional groups? What are their mobilities, and what conditions control migration? How does location affect accessibility to reagents in solution? What interactions (reagent-polymer, reagent-solvent, solvent-polymer) and what surface and interface effects, such as geometry or surface energy, affect reactivity? Can well-understood organic chemistry in solution be extrapolated to interface reactions?

The vast literature on polymer surface modification<sup>72,73</sup> includes plasma, corona, flame, chemical, polymer grafting, adsorption, additive, and entrapment treatments. The extent to which these surfaces have been characterized with the criteria mentioned above and understood is, however, meager. Some recent works that have been directed toward the goal of well-characterized surface-modified polymers include chromic acid oxidation of polyethylene,<sup>74</sup> entrapment of functionalized oligomers into polyethylene,<sup>75</sup> and surface-selective modification of fluorinated polymers.<sup>76</sup>

Since the surface of a polymer is complex, a number of questions arise regarding the identity of surface species. It is necessary to know both the concentration of chemical groups at a surface and how that concentration changes as one proceeds into the bulk. This primary structure of the surface will undoubtedly play a major role in determining its secondary or conformational structure. The question of polymer surface structure has not been addressed in both semicrystalline and amorphous polymers. The presence of crystalline material in the vicinity of a

surface may have dramatic effects on both the conformation and orientation of polymer molecules at the surface. In the latter case, the functional properties of a surface may be modified considerably depending on bond orientation at the surface, a fact which will also influence its chemical reactivity.

Perhaps the best approach to these questions is through the use of model systems. With recent successes in the formation and subsequent transfer of a polymer monolayer from a Langmuir-Blodgett trough,<sup>77,78</sup> there are grounds for optimism that some of the previous questions will be addressed. However, substantial progress in understanding structure and orientation in polymer surfaces will come about only with the continued evolution of highly sensitive surface-selective techniques.

### Thin Organic Coatings for Electrodes

Chemically modified electrodes are made by attaching or coating chemicals onto conducting or semiconducting electrodes to give the electrode surfaces some desired property.<sup>79-82</sup> This is important in a number of electrochemically related devices because it is possible to convert, modify, or improve an existing electrode. Ionically conductive coatings are usually polymeric multilayers in the thickness range from monomolecular to  $\sim 5 \mu\text{m}$ . Some examples of their use are fuel cells, chemical sensors, and electrosynthesis. An electrode that reduces dioxygen exclusively and is stable to water at near thermodynamic potential would have a high technological value for energy conversion in a fuel cell, if it has a reasonable lifetime. This has been done for dioxygen with chemisorbed monolayers of cofacial porphyrins, a catalyst designed to accomplish the desired chemistry at an electrode surface.<sup>83</sup>

The use of molecular films to design chemical sensors is an emerging area of high potential (see also the section on sensors). There are important needs for new analytical sensors in the pharmaceutical, environmental, process control, biomedical, and personal diagnostic analysis fields. The sensor response can be based on the current needed to electrolyze a sample via a selective catalytic film or on the detection of a change in mass, work function, or conductivity upon selective adsorption from a liquid or a gas. The measurement of luminescence excited by a chemical reaction between a sample and an electrochemically charged molecular film is another possibility. All these response properties have great sensitivity; in particular, small current, mass, or work function changes in films as thin as a few monomolecular layers can readily be sensed. The challenges in chemical sensors with molecular films are in designing the film for selectivity of response to a particular species and in coupling the film with a sensing electrode or pattern of electrodes. Most of these features are based on particular chemical attributes of the molecular film achieved by the incorporation of either specifically designed or biological catalytic reagents, such as enzymes or antibodies. The recently developed capabilities

(64) Ratner, B. D.; Hoffman, A. S. *Abstracts of Papers*, 177th National Meeting of the American Chemical Society, Honolulu, HI; American Chemical Society: Washington, DC, April 1979; p 156.

(65) Sholtens, B. J. R.; Bijsterbosch, B. H. J. *Colloid Interface Sci.* 1980, 77, 162.

(66) Kamagata, K.; Toyama, M. *J. Appl. Polym. Sci.* 1974, 18, 167.

(67) Schwarcz, A. *J. Polym. Sci., Polym. Phys. Ed.* 1974, 12, 1195.

(68) Pittman, A. G.; Wasley, W. L.; Sharp, D. J. *Polym. Sci., Polym. Chem. Ed.* 1974, 12, 521.

(69) Matsunaga, T.; Tamai, Y. *J. Appl. Polym. Sci.* 1978, 22, 3525.

(70) Yamashita, Y. *J. Macromol. Sci., Chem.* 1979, A13, 401.

(71) Phillips, R. W.; Dettre, R. H. *J. Colloid Interface Sci.* 1976, 56, 251.

(72) Schonhorn, H. "Surface Modification of Polymers for Adhesive Bonding". In *Polymer Surfaces*; Clark, D. T., Feast, W. J., Eds.; Wiley-Interscience: New York, 1978; Chapter 10.

(73) Angier, D. J. In *Chemical Reactions of Polymers*; Fettes, E. M., Ed. (High Polymers, Vol. 19); Interscience: New York, 1964; p 1009.

(74) Holmes-Farley, S. R.; Reamey, R. H.; McCarthy, T. J.; Deutch, J.; Whitesides, G. M. *Langmuir* 1985, 1, 725.

(75) Bergbreiter, D. E.; Chen, Z.; Hu, P. *Macromolecules* 1984, 17, 2111.

(76) Dias, A. J.; McCarthy, T. J. *Polym. Prepr. (Am. Chem. Soc., Div. Polym. Chem.)* 1986, 27(2), 68, 242.

(77) Mumby, S. J.; Rabolt, J. F.; Swalen, J. D. *Macromolecules* 1985, 19, 1054.

(78) Mumby, S. J.; Rabolt, J. F.; Swalen, J. D. *Thin Solid Films* 1985, 133, 161.

(79) Murray, R. W. *Electroanalytical Chemistry*. 13; Bard, A. J., Ed.; Marcel Dekker: New York, 1984.

(80) Murray, R. W. *Annu. Rev. Mater. Sci.* 1984, 14, 145.

(81) Chidsey, C. E. D.; Murray, R. W. *Science (Washington, D.C.)* 1986, 231, 25.

(82) Wrighton, M. S. *Science (Washington, D.C.)* 1986, 231, 32.

(83) Collman, J. P.; Anson, F. C.; Barnes, C. E.; Benscome, C. S.; Geiger, T.; Evitt, E. R.; Kreh, R. P.; Meier, K.; Pettman, R. B. *J. Am. Chem. Soc.* 1983, 105, 2694.



for directly interacting with the electron-transfer groups of enzyme oxidases and reductases and of raising monoclonal antibodies toward a variety of antigens have enormously broadened the possibilities of new sensors. The use of natural materials in molecular films is a very promising subject; however, it is suitable only for situations compatible with enzyme or antibody stability (see the next section on biological thin films for more discussion).

Another emerging subject is the idea of designing a multiplicity of functions into molecular films for sensors. For example, one component of the film may serve as a membrane barrier to exclude unwanted sample constituents, another may serve to selectively bind or complex a desired sample in order to concentrate it prior to measurement, and yet another may serve to aid in its electrocatalytic consumption during measurement. The physical coupling of molecular films with miniaturized sensor electrodes, piezoelectric films, transistor gates, photodiodes, or patterns is another recognized frontier in which lithographic techniques will play a major role. Such sensors can be made very small so as to fit into tight places (biological cells), they can be made very close together so as to utilize relatively poorly conducting films, and they can be replicated on a single device to provide multiplexed sensing. Multiplexed sensing is a potentially important strategy for alleviating problems of response selectivity; an array of sensors with differing films which respond to a sample component in a set of different ways yields a response pattern which can be deconvoluted from that of other sample components. Also, sensors based on a combination of molecular films and lithographically defined electrodes have the potentiality of being mass produced at low cost, making disposable sensors an important possibility.

The needs in electrocatalysis research divide into two areas: immobilization schemes and catalyst design. Among immobilization schemes, the use of chemisorbed monolayers and polymeric films are the most promising approaches. The principal challenge today in electrocatalysis is the design of suitable catalysts that are stable and selective. This includes improved tactics for fast charging of polymeric catalyst films by electrodes and for fast permeation of the substrate into the polymer film. Electron-transfer mediation forms the usual basis for electrocatalysis, and catalyst design then involves selecting reagents that rapidly shuttle electrons (or protons, etc.) between electrode and reaction substrate, often with intermediate formation of an adduct for selectivity reasons.

The general pattern of research for modified electrodes involves chemical synthesis, the preparation of monomolecular layer films, the incorporation of reagents into the film, and the chemistry for making ultrathin polymer films, down to a thickness of several monomers, by using electrochemical deposition or polymerization techniques. Other important factors include details of the structural organization within films, i.e., analytical characterization of the film, and the theory to understand chemical and transport kinetics. The design of films is also important especially in terms of electrons and ion mobilities. The relation of molecular structure to electron mobility in the film is a topic of fundamental and practical importance. Some electroactive films contain the mobile electrons in localized states (redox sites), and the mobility is connected to electron-hopping events. Other films exhibit electronic band structures that are spatially delocalized: the limit of this behavior is an "organic metal", as discussed in the section on electronic circuit components. There has been a great deal of experimental and theoretical work on

transport mechanisms in conducting polymers, but this has been confined to a rather small group of materials.<sup>84</sup> Progress is being made in tailoring monomers in a systematic way to give conducting polymers useful properties. Solubility (for processing purposes) is one such useful property. Also, the molecular criteria that determine when a material with localized states can be transformed into one with delocalized states are relatively unexplored but could facilitate a better understanding of molecular factors necessary for band formation.

Ionic conduction is crucial in the change of oxidation state in an electroactive molecular film, for reasons of electroneutrality. Thus, in the charging of a conducting polymer film in an energy storage application, conduction of electrons throughout the film is necessary for its complete charging, but so also is the conduction (diffusion) of the necessary ions. If the ionic mobility is less than that of the electrons (the usual case), then the rate of battery charge/discharge, for example, may be limited by this ionic diffusion and not the electronic conductivity of the polymer. Much less attention has been given in the study of conducting polymers to ion mobility than to electron mobility; in few cases is the variation in ionic mobility with polymer oxidation state known. In fact, one can estimate that electronic conductivities in excess of  $0.01 (\Omega\text{-cm})^{-1}$  contribute little further to charging rates if the upper limit of ion diffusion coefficients is about  $10^{-5} \text{ cm}^2/\text{s}$ . Studies of ionic mobility and chemical design of polymers that enhance ionic mobility deserve more emphasis than it has thus far received.

In a number of experiments molecular films have been deposited on electrodes in patterned ways. These structures in some respects emulate solid-state electronic functions, such as molecular diodes and transistors, and gates for ions. The research challenges include (1) devising and improving fabrication techniques for stable electroactive polymers and electrodes in spatially controlled ways and in very small dimensions; (2) enhancing the time or frequency response of electrochemically active polymer-electrode structures; (3) patterning electroactive molecular films; and (4) making connections to large, closely spaced arrays of microstructures. Electrodes as devices can have extremely small electrode dimensions and can have contacts on each side or surface of a molecular film. They can have nonlinear current-voltage and ion flux-voltage characteristics leading to rectifying film junctions. In addition, transport rates of ions and electrons can be related to the oxidation state of the film. There are, however, some limitations that arise from the relatively slow switching speeds associated with ion diffusion during changes in oxidation state and from the chemical reactivity (instability) typical of materials with very high or low redox potentials. For example, research is needed to understand molecular geometry changes in film switching and to make films more robust.

Microstructured electrodes are important in fundamental studies of electroactive molecular films, especially their transport properties, as a function of film oxidation state. One bonus emerging from work on electrodes could be new ways to form patterned polymer films; that is, to what extent can a polymer film be deposited on or next to an electrode and not on adjacent areas of the substrate. In contemporary electrochemistry, it is possible for electrodes to have diameters  $\leq 10 \mu\text{m}$ , and electrodes with dimensions 10–100 nm appear possible. These would not only yield important field effects but could also open new

(84) Skotheim, T. A. *Handbook of Conducting Polymers*; Marcel Dekker: New York, 1986; Vol. I, II.



possibilities for arrays that contain a high density of electrodes. The required advances involve electrodeposition or other techniques for making ultrasmall electrodes and for depositing molecular films discretely upon them.

Battery electrochemistry has historically been concerned with electrochemical cells that contain liquids. Elimination of the containment requirement and the ability to design the physical shape of the electrochemical cell are overwhelmingly important reasons to avoid liquids in new batteries. There are numerous additional reasons to conduct electrochemical reactions in the absence of liquids. These include solid-state electron-transfer chemistry, electroanalytical sensors, electrochromics, UHV spectroscopy of functioning electrochemical cells, preparation of novel ions for mass spectrometry, and use of low or high temperatures. Experiments in all of these applications involve use of ultrathin polymer films. The feasibility of each of these solid-state electrochemistries has been demonstrated, but only very recently in every case.

Research needs include (1) the availability of ionically conductive polymers (see the section on sensors for more on conducting polymers) that can be cast as ultrathin molecular films and which are chemically and electrochemically inert and highly conductive in dry, warmed, or plasticized states; (2) electrochemical cells that give access to the powerful repertory of electrochemical voltammetries useful for investigating and characterizing electrochemical reactions; (3) new concepts in electroneutrality and double-layer charging requirements under conditions of low ionic mobility; (4) a range of chemical sensor concepts; (5) an understanding of the coupling of ion and electron motion when mobilities are comparable; and (6) an understanding of the kinetics of mass transport of solutes and ions in polymer films, of transport of electrons there, and of heterogeneous electron transfers at electrode/polymer interfaces. Ionically conductive materials<sup>85-89</sup> include the sodium-doped  $\beta$ -aluminas and their inorganic relatives and newer organic polymers such as poly(ethylene oxide) (PEO) with dissolved alkali metal salts. Organic materials are appealing because they can be processed into very thin films and for their chemical versatility. Ionic conductivities tend to be modest but are amenable to use in thin-film form where the path length is short. These materials are needed to separate the cathode and anode of electrochemical cells (batteries or electrochromic cells) and also as thin-film, physically semirigid "solvents" that can serve as hosts for electroactive solutes and as ionic electrolytes between electrodes bearing electroactive molecular films. So little is known about even the more studied of the organic polymers (such as PEO) however, that electrochemical potential limits are undefined, and even the measurements of ionic conductivity are troublesome. New forms of solid-state electrochemistry will depend mainly on these materials, and continued research into their properties is essential.

### Biological Thin Films of Proteins

Most proteins adsorb readily at solid-aqueous interfaces to form reasonably compact and generally monomolecular films.<sup>90-93</sup> Although no rigorous or quantitative theories

of protein adsorption are available, there is a general qualitative understanding of the process. A number of research groups now working with model proteins, whose structures are well-known, are attempting to develop methods for simulating and predicting the adsorption process for simple systems.<sup>94,95</sup> The Langmuir monolayer trough has been widely used for studies of proteins at air-water interfaces,<sup>20,93,96</sup> and indeed many "rules of thumb" on protein adsorption have been derived from such studies.<sup>97</sup> The transfer of films to solid supports has been accomplished, though the process is difficult and sometimes unpredictable. Recently,<sup>98</sup> specific IgG has been bound to a transferred hapten-phospholipid layer, and it was shown that the close-packed IgG layer assumes a hexagonal structure. This technique may be useful as a means to produce ordered two-dimensional immunoglobulin films.

Adsorbed protein films are used in diagnostic immunoassay with preadsorbed specific immunoglobulins, protein layers or films are used for separation and purification (particularly in the chromatography field), and preadsorbed human plasma albumin is used to improve the blood compatibility of cardiovascular devices. The understanding of protein adsorption with respect to the blood and biocompatibility<sup>91</sup> of medical devices is of considerable interest, including the development of protein-resistant surfaces which actively repel proteins to minimize protein-surface interactions. Such surfaces would have wide application in chromatography, membrane separation processes, and medical devices, including contact lenses.

Specific proteins are routinely bound to chromatographic supports and surfaces by direct coupling<sup>99,100</sup> or affinity methods. If a protein has a specific interaction with a particular ligand, passage of a protein mixture over the immobilized ligand column results in specific binding of the protein of interest to this surface. This is the basis of a popular and commercially important process known as affinity chromatography for separation, purification, and characterization.<sup>101</sup> Often a specific antibody is immobilized to which the protein antigen is readily bound. The complex can then be disrupted by an eluting solution of appropriate pH, ionic strength, etc. Suitable ligands include antibodies (for antigens), sugars (for certain lectins), heparin (for lipoproteins, fibronectin, etc.), collagen (for fibronectin), etc. Certain proteins may also self-aggregate and even self-assemble into complex structures:<sup>102</sup> tubulin self-associates to form microtubules; fibrinogen,<sup>103</sup> after appropriate activation, polymerizes to fibrin.

(90) *Surface and Interfacial Aspects of Biomedical Polymers*; Andrade, J. D., Ed.; Plenum: New York, 1985; Vol. 2 Protein Adsorption.

(91) Andrade, J. D.; Hlady, V. *Adv. Polym. Sci.* 1986, 79, 1.

(92) Lundstrom, I.; Ivarsson, B.; Jonsson, U.; Elwing, H. *Polymer Surfaces and Interfaces*; Feast, W. J., Munro, H. S., Eds.; Wiley: Chichester, Sussex, England, 1987.

(93) MacRitchie, F. *Adv. Protein Chem.* 1978, 32, 283.

(94) Norde, W. *Adv. Colloid Interface Sci.* 1986, 25, 267.

(95) Hansen, J.; Ely, K.; Horsley, D.; Herron, J.; Hlady, V.; Andrade, J. D. *Makromol. Chem., Macromol. Symp.*, in press.

(96) Phillips, M. C. *Chem. Ind. (London)* 1977, 170-176.

(97) Hlady, V.; Van Wagenen, R. A.; Andrade, J. D. In *Protein Adsorption*; Andrade, J. D., Ed.; Plenum: New York, 1985; pp 81-120.

(98) Uzgiris, E. E. *J. Cell. Biochem.* 1985, 29, 239.

(99) *Solid-Phase Biochemistry*; Scouten, W. H., Ed.; Wiley: New York, 1983.

(100) *Affinity Chromatography and Biological Recognition*; Chaiken, I. M., Wilchek, M., Parikh, I., Eds.; Academic: New York, 1983.

(101) Goel, N. S.; Thompson, R. L. *Int. Rev. Cytol.* 1986, 103, 1.

(102) Correia, J. J.; Williams, R. C., Jr. *Annu. Rev. Biophys. Bioeng.* 1983, 12, 211.

(103) Krull V. J.; Thompson, M.; Wong, H. E. In *Fundamentals & Applications of Chemical Sensors*; Schuetzle, D., Hammerle, R., Eds.; ACS Symposium Series 309; American Chemical Society: Washington, DC, 1986; pp 351-362.

(85) Sorenson, P. R.; Jacobsen, T. *Solid State Ionics* 1983, 9/10, 1147.

(86) *Fast Ion Transport in Solids*; Vashishta, P., Mundy, J. N., Shenoy, G. K., Eds.; New York, 1979.

(87) Armand, M. B. *Solid State Ionics* 1983, 9, 745.

(88) Papke, B. L.; Ratner, M. A.; Shriver, D. F. *J. Electrochem. Soc.* 1982, 129, 1694.

(89) Blonsky, P. M.; Shriver, D. F.; Austin, P.; Allcock, H. R. *J. Am. Chem. Soc.* 1984, 106, 6854.



Biosensors are a new area with considerable interest and activity<sup>103-105</sup> (see the sections on sensors and electrodes for related discussions). Most biosensors depend on the specific binding<sup>106</sup> characteristics of proteins or other biological molecules for the specificity and sensitivity of the sensor. For example, receptors embedded in lipid or polymer films are needed for sensing and gating applications.<sup>107</sup> Related is the immobilization of antibodies in order to bind the antigen. Immunoglobulins are of particular interest as they can be used to detect their specific antigen with great selectivity and sensitivity. Immobilized enzymes are widely used in certain biochemical and biotechnological processes.<sup>108</sup> A variety of very complex films, such as real cell membranes, are known to include embedded transmembrane proteins and protein complexes, containing ion channels, receptors, etc. Several groups are attempting to reconstitute purified receptors in organic thin films, mostly lipid bilayers. For example, the acetylcholine receptor (AChR) is being incorporated into bilayers on appropriate microelectronic devices to produce a specific biosensor for nerve agents.

There is some thought that protein films can be used for energy (solar) collection and transfer, such as via chlorophyll-containing and electron transfer/redox enzyme/protein systems. Light detection and transduction is of interest, at least as a model system, such as in rhodopsin. Light emission (bioluminescence) via the luciferase-luciferin or aequorin systems is of great interest, especially for immunoassay applications.<sup>109</sup>

The properties of protein monolayers other than their chemical interactions are not well-known. Certainly, films of proteins containing chromophores such as hemoglobin ( $\text{Fe}^{2+}$ /heme) have the expected optical absorption and resonance Raman properties. The refractive indices of protein monolayers are known by ellipsometry, a technique widely used to study protein adsorption. Crude packing characteristics and surface viscosity data at the air-water interface are available from Langmuir trough studies. As yet, there is very little experience or data on conformation in protein monolayers or on mechanical, optical, or electronic properties. Only in the last few years have research groups begun to apply modern surface analytical techniques to the characterization of protein monolayers.

In order to understand, design, and use protein films, we must understand the forces and interactions responsible for protein structure and function and for their interactions among themselves, with other proteins, and with solid supports. Although the electrostatic, hydrophobic, and hydrogen-bonding interactions are qualitatively understood, better potential functions are needed to effectively model and predict protein folding, denaturation, and adsorption. Direct measurements of such forces and interactions at the protein film-aqueous solution interface are needed.<sup>110,111</sup>

Other methods to characterize and evaluate the properties of protein thin films should be developed, including those to measure electronic, magnetic, optical, and me-

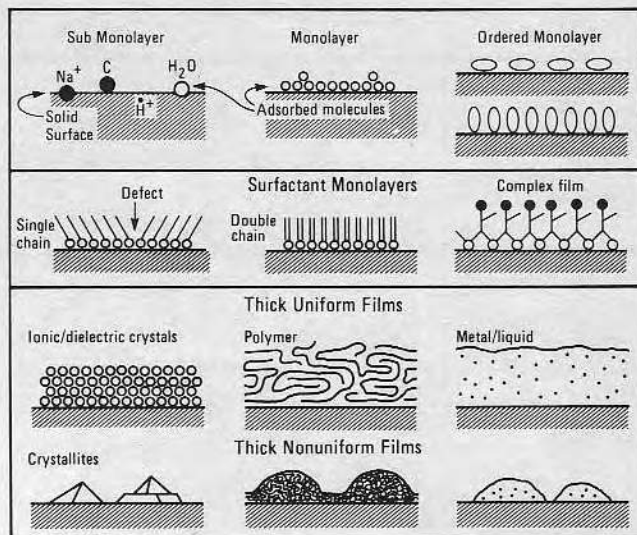


**Figure 2.** Various types of films on solid surfaces shown schematically.

chanical properties. In particular, methods to characterize protein films in situ, i.e., in water, are needed. Although progress has been made in applying reflection fluorescence and infrared methods,<sup>112</sup> more definitive methods are required to probe and characterize packing, orientation, and structure of protein films. Perhaps the most promising approach is direct imaging of LB bilayers<sup>113</sup> and bacteriophage  $\phi 29$ <sup>114</sup> with scanning tunneling microscopy (STM) and even under water.<sup>115</sup> X-ray scattering and diffraction and other means of imaging and characterizing protein films should be encouraged. Fourier transform Raman spectroscopy in the near IR has great potential for characterizing the conformation and orientation of protein thin films (see the section on characterization).

The simulation and modeling of proteins via computer molecular graphics and intermolecular interaction potentials is in its infancy.<sup>116</sup> With better potential functions and with information on the structure of protein films, attempts will undoubtedly be made to model protein interaction and the film-forming process. Useful models will permit the design of structures and the means for self-assembly of films with designed properties. The modeling and simulation of film formation and film properties should include the effects of applied fields.

Proteins are polymers with unique and varied structures and properties. They are beautiful examples of macromolecular engineering for specific purposes. The modeling, preparation, characterization, and application of protein films will lead to a variety of applications. The optimization of enzyme properties is needed for reactions in adverse environments, and modified or synthetic enzymes are needed in other cases. Perhaps most importantly, the study of proteins could aid and simulate materials science to better engineer new macromolecules for applications. There should be attempts to apply the unique properties of certain proteins into mixed films, i.e., together with synthetic polymer films and inorganic films as devices.

(104) Van Brunt, J. *Bio/Technology* 1985, 3, 209.

(105) Haddon, R. C.; Lamola, A. A. *Proc. Natl. Acad. Sci. U.S.A.* 1985, 82, 1874.

(106) Corsel, J. W.; Willems, G. M.; Kop, J. M. M.; Cuypers, P. A.; Hermens, W. T. J. *Colloid Interface Sci.* 1986, 111, 544.

(107) Andrade, J. D.; Van Wagenen, R. A.; Gregonis, D. E.; Newby, K.; Lin, J. N. *IEEE Trans. Electron Devices* 1985, ED-32, 1175.

(108) Needleman, S. L. *Biotechnol. Genetic Eng. Rev.* 1984, 1, 1.

(109) *Alternative Immunoassays*; Collins, W. P., Ed.; Wiley: New York, 1985.

(110) Klein, J.; Luckham, P. *Nature (London)* 1982, 300, 429.

(111) Israelachvili, J. N. *Intermolecular and Surface Forces*; Academic: New York, 1985.

(112) Chittur, K. N.; Fink, D. J.; Leininger, R. I.; Hutson, T. B. *J. Colloid Interface Sci.* 1986, 111, 419.

(113) Smith, D. P. E.; Bryant, A.; Quate, C. F.; Rabe, J. P.; Gerber, Ch.; Swalen, J. D. *Proc. Natl. Acad. Sci. U.S.A.* 1987, 84, 969.

(114) Baro, A. M.; Miranda, R.; Carrascosa, J. L. *IBM J. Res. Dev.* 1986, 30, 380.

(115) Sonnenfeld, R.; Hansma, P. K. *Science (Washington, D.C.)* 1986, April 11, 211.

(116) Venkataraghavan, B.; Feldmann, R. J. (Eds.) *Ann. N. Y. Acad. Sci.* 1985, 439.

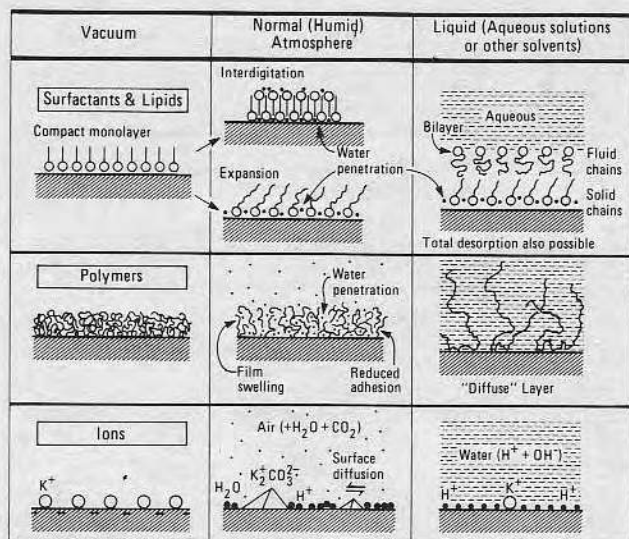


**Figure 3.** Effects of exposure to a vacuum, normal atmosphere, and a liquid shown schematically for surfactants and lipids, polymers, and ions.

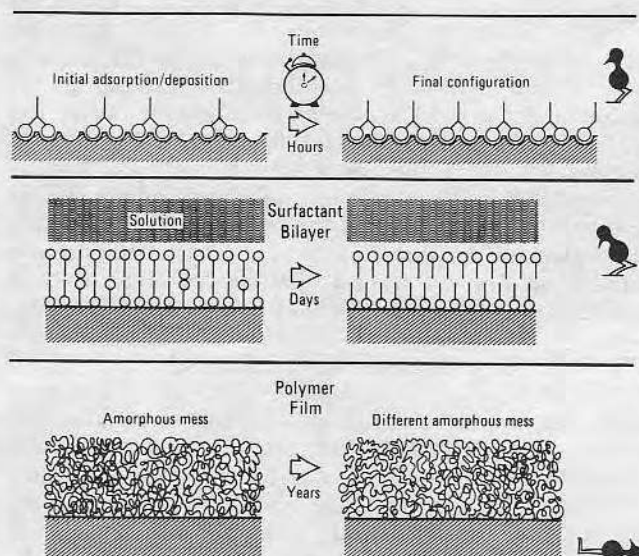


**Figure 4.** Effects of aging on thin films of surfactants and polymers shown schematically.

### Intermolecular Forces

Intermolecular forces in thin surface films determine many of their properties, e.g., structure, stability, etc. In Figure 2 the various types of films, mainly very thin films (<100 nm thick) on solid surfaces, are schematically illustrated. It is important to distinguish those films under vacuum from those exposed to atmospheric air or to bulk liquid. Even in a very rarefied vapor of water,  $CO_2$ ,  $O_2$ , or  $N_2$  a thin surface film may undergo structural, adhesive, and compositional changes, including changes in its dynamics (e.g., lateral diffusion of molecules in the film). Immersion of a surface-supported film in a bulk liquid (solvent) medium will usually further alter a film. The differences of vacuum, vapor, and liquid environments for three types of surface films are illustrated in Figure 3. Most surface layers or films will change slowly with time after they are prepared or after transfer to a different environment (e.g., a different atmosphere or temperature). A number of different relaxation processes may occur in a film at any one time, such as lateral redistribution of binding sites (Figure 4, top), orientational rearrangements of aligned molecules (Figure 4, middle), configurational

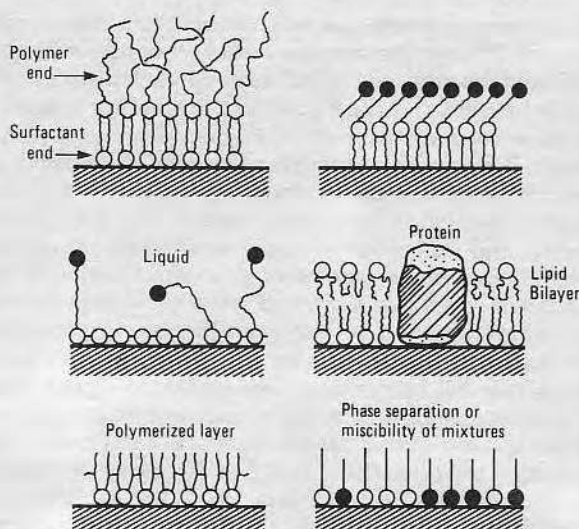


**Figure 5.** Types of thin-film design with multifunctional groups and multicomponent films.

rearrangements in amorphous polymer films (Figure 4, bottom), compositional changes, etc.

Macroscopically, one can also ask whether a thin film differs from a bulk system relative to morphology and structures, in addition to its mechanical, chemical, electric (including dielectric), and optical properties. If so, on what distance scale do they differ from those in bulk relative to the reference plane of the interface? Some properties may not be different from the bulk values even for films as thin as one or two molecular layers. Such properties are usually those that depend on short-range, mainly nearest-neighbor, intermolecular interactions. Some examples are surface energy (or surface tension), fluid viscosity (in thin liquid films), and refractive index. However, those properties that depend on long-range interactions (and that are characterized by long-range order in the bulk) will differ in films at a thickness comparable or less than the range of the order (in the bulk). Such properties include, for example, the density distribution of ions and polymer segments in thick surface layers exposed to liquid solutions. As a rule of thumb a substrate surface could never induce any stable long-range order of some property in a supported film if there were no long-range order of that property in the bulk phase of the film material.

It is worth distinguishing once more between thin-film preparative techniques that occur under vacuum, in a vapor atmosphere, or in solution. Vacuum techniques involve evaporation deposition or sputtering processes. In vapor these involve adsorption, either physisorption or chemisorption, and chemical reaction, and in liquids they involve free adsorption from solution or controlled Langmuir-Blodgett deposition. In the future it should be possible to design and synthesize molecules which could be specifically adsorbed or deposited to produce films with specially desired properties (e.g., hydrophobic, hydrophilic, films with particular surface groups, etc.), as illustrated in Figure 5. A combination of two or more deposition techniques may be needed to build up the desired film, e.g., chemical modification (oxidation) followed by vacuum deposition, followed by Langmuir-Blodgett deposition. Clearly, a multidisciplinary<sup>111,117-124</sup> approach will be called

(117) Israelachvili, J. N.; Adams, G. E. *J. Chem. Soc., Faraday Trans. 1* 1978, 74, 975.

(118) Marra, J. J. *Colloid Interface Sci.* 1985, 107, 446. Marra, J.; Israelachvili, J. *Biochemistry* 1985, 24, 4608.

(119) Pashley, R. M.; McGuigan, P. M.; Ninham, B. W.; Evans, D. F. *Science (Washington, D.C.)* 1985, 229, 1088.



for if such procedures are to be successful, involving physicists, chemists, engineers, surface and colloid scientists, and biologists, with both experimentalists and theoreticians working together.

A number of interfacial situations are possible with thin polymer films located on a solid or liquid substrate or at different interfaces: (1) coatings on a solid substrate; (2) films at a vapor-liquid interface; (3) films at a liquid-liquid interface, (4) films at a liquid-solid interface, (5) boundary layers between vapor and a polymer solution interface, and (6) boundary layers at a polymer-polymer interface. The microscopic properties include the equilibrium chain configuration plus any vicinal anisotropy with respect to the reference plane, both local chain dynamics and cooperative conformational dynamics, and transport properties.

Polar polymer chains at the air-water interface at different number densities can behave as two-dimensional polymer "solutions" by virtue of differing interactions between polar repeating units and substrate water. With the advent of scaling theory of two-dimensional semidilute polymer solutions,<sup>125-129</sup> we can now interpret quantitatively the surface pressure dependence of a polymer monolayer as a function of surface concentration.<sup>130-133</sup> These are just the osmotic expansions in two dimensions where polymer chains do not easily interpenetrate beyond the overlap concentration, in contrast to those in the bulk state. Though it is currently restricted to equilibrium surface pressures, this is truly a breakthrough in polymer physics.

These two-dimensional properties of polymer "solutions" on the air-water and oil-water interfaces are a consequence of the polymer segments in contact with substrate liquids. The polymer chains are not in a pure state, but are rather in "solution". A technological application, of course, is the transfer of polymer films onto solid substrates. The influence of the states of various chain conformations and the dynamics at the transfer step are significant. Whatever subsequent rearrangements and curing may ensue on the solid substrates, the state of a transferred film will be dominantly controlled by chain conformations and dynamics on the liquid surface. In particular, the oil/water interface provides a very different solution condition to polymer chains by having a hydrocarbon layer in contact with chain segments in addition to that of water.

There are a number of intriguing issues and outstanding problems that could be fruitfully addressed with our present knowledge:

1. How is the chain conformation influenced by the hydrophilicity of its segments? Could one induce chain looping and tailing into the aqueous and/or oil layer by

surface pressure before the onset of departure from two-dimensionality for the centers of mass of all chains? What would be the dynamics associated with these configurational changes?

2. Surface viscoelasticity is important for intramolecular conformational and cooperative translational dynamics. Are the interfacial elastic and viscous components of the lateral compressive and shear modes and transverse capillary mode related to the chain dynamics as in three-dimensional cases?

3. What are the phase transitions and the separation kinetics and how are they related? For polymer solutions in two dimensions, there should be conditions for each solution (regardless of whether they can be accessed experimentally) within the range of liquid state of water, and beyond that there should be a critical temperature and associated kinetic behavior of phase separation into high- and low-concentration regimes.

Lateral polymerization<sup>134-138</sup> involving monolayer dynamical behavior during in situ polymerization of monomers should be compared to that of monolayers of polymers synthesized in bulk solution or neat monomer liquids. In addition to the spectroscopy discussed in the Characterization section we have the conventional interfacial techniques of surface tension, surface shear viscosity, and other dynamical methods.<sup>139</sup> Recently developed methods are, however, more intriguing and seem to hold promise for the direct examination of these films. These are surface light scattering (SLS)<sup>140-143</sup> and the measurement of electrocapillary waves (ECW).<sup>144</sup> Both have been applied to amphiphilic monolayers at the air/water interface; however, their application to polymer monolayers has occurred only recently.<sup>145,146</sup>

The surface light-scattering technique relies on spontaneous capillary waves at interfaces induced by density fluctuations while the electrocapillary wave method relies on capillary waves induced by a small inhomogeneous electric field applied to an interface, thereby taking advantage of any difference in dielectric permittivity between the two media. The wave amplitude and phase are detected by optical diffraction of the waves. Since they both deal with capillary waves, either spontaneous or induced, the two methods differ mainly in that the SLS has an inherently fixed small wave amplitude ( $\sim 3$  Å) and is available for a smaller range of accessible independent variables, e.g., scattering wave vector (equal to the spatial wavelength, 1–10  $\mu\text{m}$ , of scattering capillary waves).<sup>147</sup> An additional difference is that SLS probes the propagation rate and temporal damping of capillary waves whereas ECW is used to examine the wavelength and spatial

(120) Israelachvili, J. N. *J. Colloid Sci.* 1986, 110, 263; *Colloid Polym. Sci.* 1986, 264, 1060.

(121) Horn, R. G. *Biochim. Biophys. Acta* 1984, 778, 224.

(122) Christenson, H. K. *J. Phys. Chem.* 1986, 90, 4.

(123) Klein, J. *Nature (London)* 1980, 288, 248; *Adv. Colloid Interface Sci.* 1982, 16, 101; *J. Chem. Soc., Faraday Trans. 1* 1983, 79, 99.

(124) Hadziioannou, G.; Patel, S.; Granick, S.; Tirrell, M. *J. Am. Chem. Soc.* 1986, 108, 2869.

(125) deGennes, P. G. *Scaling Concepts in Polymer Physics*; Cornell University Press: Ithaca, NY, 1979.

(126) Stephen, M. J.; McCauley, J. *Phys. Lett. A* 1973, 44, 89.

(127) Daoud, M.; Jannink, G. *J. Phys. (Paris)* 1976, 37, 973.

(128) Le Guillou, J. C.; Zinn-Justin, J. *Phys. Rev. Lett.* 1977, 39, 95; *Phys. Rev. B* 1980, 21, 3976.

(129) Stephen, M. J. *Phys. Lett. A* 1975, 53, 363.

(130) Vilanova, R.; Rondelez, F. *Phys. Rev. Lett.* 1980, 45, 1502.

(131) Takahashi, A.; Yoshida, A.; Kawaguchi, M. *Macromolecules* 1982, 15, 1196.

(132) Kawaguchi, A.; Yoshida, A.; Takahashi, A. *Macromolecules* 1983, 16, 956.

(133) Douglas, J. F.; Cherayil, B. J.; Freed, K. F. *Macromolecules* 1985, 18, 2455.

(134) Beredjick, N.; Burlant, W. J. *J. Polym. Sci., Polym. Phys. Ed.* 1970, 8, 2807.

(135) Ackermann, R.; Inacker, O.; Ringsdorf, H. *Kolloid-Z.* 1971, 249, 1118.

(136) Day, D. R.; Ringsdorf, H. *J. Polym. Sci., Polym. Lett. Ed.* 1978, 16, 205.

(137) Day, D. R.; Ringsdorf, H. *Makromol. Chem.* 1979, 180, 1059.

(138) Day, D.; Lando, J. B. *Macromolecules* 1980, 13, 1478, 1483.

(139) Adamson, A. W. *Physical Chemistry of Surfaces*, 3rd ed.; Wiley: New York, 1976.

(140) Katyl, R. H.; Ingard, U. *Phys. Rev. Lett.* 1967, 19, 64.

(141) McQueen, D.; Lundström, I. *J. Chem. Soc., Faraday Trans. 1* 1973, 69, 694.

(142) Langevin, D. *J. Chem. Soc., Faraday Trans. 1* 1974, 70, 95.

(143) Hard, S.; Hamerius, Y.; Nilsson, O. *J. Appl. Phys.* 1976, 47, 2433.

(144) Sohl, C. H.; Miyano, K.; Ketterson, J. B. *Rev. Sci. Instrum.* 1978, 49, 1464.

(145) Langevin, D. *J. Colloid Interface Sci.* 1981, 80, 412.

(146) Kawaguchi, M.; Sano, M.; Chen, Y.-L.; Zograf, G.; Yu, H. *Macromolecules* 1986, 19, 2606.

(147) Braslau, A.; Deutsch, M.; Pershan, P. S.; Weiss, A. H.; Als-Nielsen, J.; Bohr, J. *Phys. Rev. Lett.* 1985, 54, 114.



damping of the electrocapillary waves. From the dispersion relation for capillary waves one can extract the longitudinal elasticity and viscosity.

### Intermolecular Order

Intermolecular ordering in mono- and multilayer assemblies of surfactant molecules (molecules composed of a polar "head" group and a hydrocarbon "tail") on solid surfaces is being probed in an effort to answer long-standing questions regarding the relationship between intermolecular ordering and the macroscopic properties of the film. Some of the interfacial properties influenced by ordering are wetting and lubrication, transport properties such as ion diffusion through the layer, and average film properties such as cohesion and stability. From a more fundamental point of view, probes of the intermolecular ordering in these layered assemblies may provide unique insights into the thermodynamics of two-dimensional systems with multiple degrees of freedom and therefore richer phase behavior than exhibited by adsorbed layers of rare gases.<sup>148</sup> Structural information will make it possible to separate the various free energy contributions driving these structures, such as head/surface binding, head/head interactions, entropies and energies of trans/gauche isomerization, and van der Waals interactions between neighboring hydrocarbon chains. A framework can thus be provided for design of the individual moieties in molecules as well as the substrates to enhance particular cooperative properties of the assembly. Conceptual ideas of the intermolecular ordering in surfactant layered systems probably predate Langmuir's pioneering work.<sup>149</sup> Qualitative determinations of intermolecular order by electron diffraction go back as far as 1938,<sup>150</sup> but only recently has a quantitative picture started to emerge. There are hints that these weakly ordered structures, unlike the bulk, are driven by complex competitions between different free energy forces, but understanding and characterization are far from complete.

Both self-assembled (SA) films and Langmuir-Blodgett (LB) films are formed from molecular assemblies: SA films from the surfactant monolayer deposited from solution and LB films from the monolayer at the air/water interface. In both cases the structures of the initial assemblies will affect the final monolayer structures, both enhancing the probability of certain defect structures and predisposing the films to certain types of intermolecular ordering. To date, island growth morphology seems prevalent in SA films.<sup>151,152</sup> Stunning recent results show that LB monolayers at the air/water interface do exhibit some degree of intermolecular order and that order goes through structural phase transitions.<sup>153,154</sup>

Thermodynamics predicts that the positional correlations that can exist in a system depend on the effective dimensionality. In two dimensions, "solid" phases cannot exhibit long-range order, but hexatic phases or phases exhibiting bond-orientational order (with liquidlike correlations of molecular positions but with longer range

correlations of bond directions) can potentially exist.<sup>155</sup> The low-temperature phase of a two-dimensional system, although not literally long-range ordered, can be distinct from the hexatic phase,<sup>155a</sup> but in a finite-sized system it may be very hard to distinguish from a long-range-ordered phase.<sup>155b</sup> Even systems weakly affected by potentials in the third dimension can show interesting types of bond-orientational correlation.<sup>156</sup> Their influence has been seen in magnetic ordering in an LB film<sup>157</sup> and on defect structures in ultrathin free-standing liquid crystal films.<sup>158</sup> Monolayer surfactant assemblies have long been considered as candidates for exhibiting lower than three-dimensional behavior, and this is being pursued in present research. To prove that a structure does have lower dimensional behavior, the nature of the positional and bond-orientational correlations must be measured and shown to be thermodynamic in origin and not the result of frozen-in defect fields, as in a paracrystal.<sup>159</sup> Experiments that measure the structure of monolayers on water,<sup>153,154</sup> on solid hydrophilic substrates,<sup>160</sup> and on solid hydrophobic substrates,<sup>161</sup> each shows certain characteristics of lower dimensional behavior, but the assessment remains incomplete. In addition, the evolving structure seen in LB films, 1–10 layers thick,<sup>162,163</sup> should be compared in the light of a dimensional crossover, as has been observed in freely suspended liquid crystal films.<sup>164</sup>

Even in the densest packed monolayers, small amounts of excess free volume are often available to the carbon chain. The system can minimize its free energy either by trans/gauche isomerization of the carbon chain<sup>165,166</sup> or by a tilting disorder of the all trans chains.<sup>167</sup> Which of these two situations gives the lowest energy depends on the precise mix of entropy and enthalpy each demands. At present, neither theory nor experiment is conclusive; however, Raman<sup>168,169</sup> and infrared<sup>170,171</sup> studies indicate that only a small amount of gauche bonding exists in these monolayers, even close to the melting points. Further quantification of these results will lead to a clearer understanding of the role of trans/gauche isomerization and chain stiffness in the cohesion and stability of surfactant films.

Substrates provide an average potential normal to the surface but may also impose a varying potential in the

(148) Nelson, D. R.; Halperin, B. I. *Phys. Rev. B: Condens. Matter* 1980, 21, 5312.

(149) Langmuir, I. *J. Chem. Phys.* 1933, 1, 756.

(150) Germer, H. L.; Storks, K. H. *J. Chem. Phys.* 1938, 6, 280.

(151) Brockway, L. O.; Jones, R. L. *Adv. Chem.* 1964, 43, 275–294.

(152) Garoff, S.; Hall, R. B.; Deckman, H. W.; Alvarez, M. S. In *Proceedings of Symposium of the Chemistry and Physics of Composite Media*; Electrochemical Society: Pennington, NJ, 1985; Vols. 85–88, p 112.

(153) Dutta, P.; Peng, J. P.; Lin, B.; Ketterson, J. B.; Prakash, M.; Georgopoulos, P.; Ehrlich, S. *Phys. Rev. Lett.* 1987, 58, 2228.

(154) Kjaer, K.; Als-Nielsen, J.; Helm, C. A.; Laxhuber, L. A.; Mohwald, M. *Phys. Rev. Lett.* 1987, 58, 2224.

(155) Pindak, R.; Moncton, D. E. *Phys. Today* 1982, May, 3. (a) Imry, Y. *Crit. Rev. Solid State Mater. Sci.* 1979, 8, 157. (b) Dutta, P.; Sinha, S. K. *Phys. Rev. Lett.* 1981, 47, 50.

(156) Moncton, D. E.; Pindak, R. *Phys. Rev. Lett.* 1978, 43, 701.

(157) Pomerantz, M. In *Molecular Devices*; Carter, F. L., Ed.; Marcel Dekker: New York, 1983; p 279.

(158) Dierker, S.; Pindak, R.; Meyer, R. B. *Phys. Rev. Lett.* 1986, 56, 1819.

(159) Vainshtein, B. K. *Diffraction of X-Rays by Chain Molecules*; Elsevier: New York, 1966; Chapter 6.

(160) Garoff, S.; Deckman, H. W.; Dunsmuir, J. H.; Alvarez, M. S. *J. Phys. (Les Ulis, Fr.)* 1986, 47, 701.

(161) Seul, M.; Eisenberger, P.; McConnell, H. M. *Proc. Natl. Acad. Sci. U.S.A.* 1983, 80, 5795.

(162) Bonnerot, A.; Chollet, P. A.; Frisby, H.; Hoclet, M. *Chem. Phys.* 1985, 97, 365.

(163) Kimura, F.; Umemura, J.; Takenaka, T. *Langmuir* 1986, 2, 96.

(164) Sirota, E. B.; Pershan, P. S.; Sorensen, L. B.; Collett, J. *Phys. Rev. Lett.* 1985, 55, 2039.

(165) Gelbart, W. *J. Chem. Phys.* 1986, 87, 3597.

(166) Dill, K. A. *Macromolecules* 1984, 17, 380, 384.

(167) Safran, S.; Robbins, M. O.; Garoff, S. *Phys. Rev. A* 1986, 33, 2186.

(168) Dierker, S. B.; Murray, C. A.; LeGrange, J. D.; Schlotter, N. E. *Chem. Phys. Lett.*, in press.

(169) Rabe, J. P.; Swalen, J. D.; Rabolt, J. F. *J. Chem. Phys.* 1987, 86, 1601.

(170) Rabolt, J. F.; Burns, F. C.; Schlotter, N. E.; Swalen, J. D. *J. Chem. Phys.* 1983, 78, 946.

(171) Rothberg, L.; Higashi, G. S.; Allara, D. L.; Garoff, S. *Chem. Phys. Lett.* 1987, 133, 67.

plane of the surface and fluctuations normal to the surface. These will act on a monolayer assembly and can alter its structure. Indeed, characteristics of the deposition process and the ultimate structure of the monolayer assemblies vary widely, depending on the nature of these potentials. Hydrophilic and hydrophobic substrates produce different LB film ordering,<sup>172</sup> and even the precise chain ordering on a hydrophobic substrate affects diffusional properties in lipid layers assembled onto these substrates.<sup>173</sup> The strength of the head/surface bond determines the efficacy of a self-assembly route for producing the monolayer assembly. Epitaxial growth of a surfactant monolayer is being attempted in a number of laboratories and the resulting structure verified. The main difficulty with surfactant deposition on a truly ordered substrate is that the substrate must not have any oxide or contaminant overlayers. UHV cleaning of the substrate and in situ doping of surfactant from the gas phase is an obvious route to this end. Even the disordered substrates commonly used provide random field potentials which profoundly affect the monolayer structure. There are suggestions of bond-orientation of the monolayer by step defects on an ordered substrate.<sup>174</sup> Recently, epitaxial growth of lead stearate on mica has been observed by X-ray diffraction.<sup>174a</sup> Theoretical predictions indicate long-range order in overlayers will be broken by such substrates,<sup>175,176</sup> and this could be one origin of the bond-orientational disorder observed in several monolayer systems.<sup>160</sup> The choices in optimizing a monolayer system may be complex, and an understanding of these substrate effects is needed to improve the design of systems.

Ordering in a surfactant film involves the effects of competing length scales: substrate lattice spacing, head/head spacing, and natural chain/chain spacing. Such competing lengths may produce excess free volume for the carbon chains and thus gauche isomerization or splay disorder in the chains. This in turn can cause a chemical heterogeneity and/or slight physical roughening of the surface of the film. The ramifications of this disorder on subsequent layer deposition may seem slight,<sup>177</sup> but its effects on the cohesion and stability are unexplored. Depending on the lateral length scale of the heterogeneity, interfacial properties such as wetting, lubrication, and layer permeability may be affected. In addition, the competing length scales may be responsible for the smeared phase transitions which occur in these films.<sup>160,170,171</sup> Since synthesis gives us so much control over the spacings in organic thin films, their manipulation offers a fascinating avenue for exploring the effects of multiple length scales on the structure, thermodynamics, and physical properties of a system.

The intermolecular ordering in these assemblies should be examined not only in terms of their effective dimensionality but also in terms of the collective degrees of freedom of the film which are frozen out. With structural and elastic measurements, it is possible to determine whether these films are more representative of solids or smectic liquid crystals. The transitions between various phases in the layered assemblies provide a link to the understanding of the fundamental structures for each

phase. Transitions in monolayers at the air/water interface have been studied by several indirect methods, and the first direct study of these structural transitions has been recently reported.<sup>153,154</sup> On substrates, transitions upon heating of mono- and multilayer assemblies have been observed<sup>160,161,168-171</sup> and are believed to be the origin of boundary lubrication failure for surfactant-coated surfaces.<sup>178</sup> Chain disordering, intermolecular disordering, and some degree of desorption are involved, but a good model of the transition does not exist. Further, the melting processes appear to be different for monolayers and multilayers. Other thermal transitions have been observed, but even initial characterizations have not been completed. Not only do studies of these phase transitions illuminate the fundamental statistical mechanics governing the phases but they also may lead to novel applications which utilize these structural transitions in practical situations perhaps involving interfacial properties like passivation or involving new devices such as optical devices.

The measurement of intermolecular structure in ultrathin organic films requires state of the art techniques. While all measurements are difficult, some can be performed on individual laboratory instrumentation while others demand large user facilities. The measurement techniques depend on the aspect of intermolecular order to be measured. Even though defect structures may dominate the behavior and stability of molecular assemblies, the characterization of these defects on a microscopic scale has not occurred. To probe the layering structure normal to the surface, X-ray reflection experiments can be performed with laboratory rotating anode sources. Beginning as early as 1980<sup>179</sup> and continuing in very refined forms, electron density profiling resulting from these measurements has provided information about the interlayer spacing, layer perfection, and surface roughness.<sup>177</sup> New theoretical improvements in the interpretation of X-ray reflection measurements will enhance the value of this technique.<sup>180</sup> Similar reflection measurements have been made on LB films using neutrons<sup>181</sup> where labeling techniques and the penetrating power can greatly enhance the information drawn out of such experiments.<sup>182</sup> The measurement of in-plane ordering on thicker films can be accomplished by using rotating anode sources, but on organic films with a thickness of  $\leq 200$  Å the high fluxes available from synchrotron sources are needed. As mentioned earlier, these measurements are difficult but have been successfully made on monolayers both on liquids<sup>153,154</sup> and on solid surfaces.<sup>173,183,184</sup> Electron-diffraction techniques can provide a very useful alternative to X-rays, particularly for examining in-plane intermolecular ordering. Used for qualitative analysis for many years on surfactant monolayers,<sup>149,178</sup> this technique has recently provided quantitative data on the in-plane intermolecular correlations of an LB monolayer.<sup>160</sup> Particularly because of the difficulty in producing defect-free surfactant films (or in knowing whether or not they are defect free), the ability of the electron microscope beam to diffract from

(172) Blasie, J. K., private communications.

(173) Seul, M.; Subramaniam, S.; McConnell, H. M. *J. Phys. Chem.* 1985, 89, 3592.

(174) Vogel, V.; Woll, C. *J. Chem. Phys.* 1986, 84, 5200. (a) Prakash, M.; Peng, J. B.; Ketterson, J. B.; Dutta, P. *Chem. Phys. Lett.* 1986, 128, 354.

(175) Nelson, D. R. *Phys. Rev. B: Condens. Matter* 1983, 27, 2902.

(176) Sachdev, S.; Nelson, D. R. *J. Phys. C* 1984, 17, 5473.

(177) Skita, V.; Filipkowski, M.; Garito, A.; Blasie, K. *Phys. Rev. B: Condens. Matter* 1986, 34, 5826.

(178) Bowden, F. P.; Tabor, D. *The Friction and Lubrication of Solids*; Clarendon: Oxford, 1968; Part I, Chapter 10; Part II, Chapter 18.

(179) Pomerantz, M. *Thin Solid Films* 1980, 68, 33.

(180) Sinha, S. K., private communications.

(181) Highfield, R. R.; Thomas, R. K.; Cummins, P. G.; Gregory, D. P.; Mingins, J.; Hayter, J. B.; Schaerpf, O. *Thin Solid Films* 1983, 99, 165.

(182) Penfold, J.; Williams, W. G. Report #RAL-85-045, A Pulsed Source Neutron Reflectometer for Surface Studies, Science and Engineering Research Council, Rutherford Appleton Lab., Chilton, Didcot, Oxon, UK.

(183) Prakash, M.; Dutta, P.; Ketterson, J. B.; Abraham, B. M. *Chem. Phys. Lett.* 1984, 111, 395.

(184) Block, J. M., private communications.



small spatial areas which by prior imaging are proven to be defect free is of very great importance. Beam damage of samples does occur but can be mitigated, and even some compromise of the vacuum environment in the microscope can be made.<sup>185</sup> The scanning tunneling microscope provides a very promising new alternative for imaging the in-plane lattices of surfactant films and thus for providing direct measurement of intermolecular ordering. Preliminary work has already succeeded in lattice imaging an LB bilayer,<sup>113</sup> further discussion of STM capabilities and uses appears in the sections on patternability, biological thin films, and characterization. Finally, the usefulness of vibrational spectroscopy to probe trans/gauche conformations in the chain of the surfactants has been well proven.<sup>162,163,168-171</sup> In combination with a diffraction or imaging method for examining intermolecular order it would provide an exceptionally powerful tool for examining the important structural issues discussed above.

### Characterization

Attempts to fabricate new and complex molecular films with novel properties cannot be done efficiently without significant advances in our present analytical capabilities. The detailed structural characterization of subtle molecular features of thin organic films presents new and challenging problems for the field of materials characterization. Because these are organic materials, the methods must not involve any damaging interactions and yet must be capable of determining subtle features such as conformation and orientation of functional groups. The ability to analyze at different depths in the film (depth profiling) is also desirable. In contrast, many of the very useful and sensitive tools for analysis of inorganic surfaces and thin films are largely damaging, insensitive to the subtleties of organic structures, and involve high-vacuum techniques. Complex structures in these organic films are often determined by the environment in which they were designed to operate; analyses done under other conditions may not be meaningful for establishing valid structure-property correlations. Development of in situ analytical techniques is greatly needed for film-vapor and film-solution systems. Excellent examples can be found in biological systems where measurements should be made directly in biological media (in vivo) rather than the standard ultrahigh-vacuum conditions required by many surface analysis techniques. In some cases, such as integrated microcircuit devices, it is also desirable to perform analyses over very small surface regions having submicron dimensions. Few techniques are capable of accomplishing this.

The most useful methods for the analysis of bulk organic materials have proven to be NMR, IR, UV-vis, and Raman spectroscopies, as well as X-ray and neutron scattering. Nonspectroscopic techniques include chromatography and thermal analysis. A major problem arises when the sample becomes a thin, planar film and the thickness is reduced to molecular dimensions; many traditional methods lack the necessary sensitivity for analysis. Refinements and alterations of standard techniques such as IR have made monolayer analysis tractable while continued efforts on Raman spectroscopy and X-ray and neutron scattering have made such analyses appear feasible although difficult.

Some of the newer techniques (discussed below) have been developed specifically with this sensitivity in mind: second-harmonic generation at a surface,<sup>35-40</sup> the near-edge X-ray fine structure (NEXAFS),<sup>185a</sup> the scanning tunneling microscope (STM),<sup>48,49,113-115</sup> the atomic force microscope,<sup>185b-d</sup> and the surface force balance.<sup>111,117,123,124</sup> The latter technique can directly measure various thin-film properties at the molecular level, such as interaction forces in thin films, dynamic and relaxation processes, adhesion, deformation, and surface-induced phase transitions.

The analytical techniques discussed in the remainder of this section are those which are sensitive to microscopic structure and can be viewed in terms of a microscopic input probe, an ensuing physical (and/or chemical) interaction with the film, a resultant microscopic output probe, and a detector system. A large variety of possible combinations exists. The primary probes are photons, electrons, ions, atoms, and neutrons. The interaction mechanisms can include elastic and inelastic scattering, total absorption, sputtering, and other complex processes involving dissimilar ejection, such as X-ray-stimulated photoelectron ejection in X-ray photoelectron spectroscopy. Detector systems range from various semiconductor devices to mass spectrometers and the associated complex digital and analog electronics. Some of these combinations, while potentially quite effective for analyzing certain useful structural features at the monolayer level, are quite costly and difficult, for example, the use of synchrotron X-ray beams for diffraction or mode-locked, pulsed-laser systems for multiphoton spectroscopy. Other useful combinations for analysis, such as infrared absorption spectroscopy (IRAS) and X-ray photoelectron spectroscopy (XPS), can be accomplished by using commercial instrumentation available in many laboratories. Several of these possibilities for studying the structure of thin films in general have been recently reviewed.<sup>186,187</sup>

XPS and IRAS are two spectroscopic techniques that have become standard methods for characterizing organic films and surfaces. While XPS analysis is restricted to vacuum conditions, it has the advantage of sensing the outermost regions ( $\sim 50$  Å) of polymer surfaces for a number of elements and in a variety of chemical bonding situations. On the other hand, IRAS offers the potential for analysis of planar thin films and overlayers under liquids,<sup>188</sup> and recent experiments have shown the feasibility of monolayer studies on traditionally difficult substrates such as carbon.<sup>189</sup> Continued development and application in these tools will promote efficient advances in studies of structure-property correlations in molecular films. An adjunct technique is single-wavelength optical ellipsometry, which has been extremely useful for measuring the thickness of a film. Extensions of this technique to a range of other wavelengths have been extremely useful in characterizing electronic structure in semiconductor films,<sup>190</sup> and similar applications of spectroscopic ellipsometry could prove quite useful in detailed structural analyses of organic films.<sup>191</sup> In addition, optical ellipsometry is compatible with the liquid-solid interface.

One of the important structural features that the above spectroscopies do not directly probe is the precise nature

(185) Hui, S. W. *Ultramicroscopy* 1980, 5, 505. (a) Outka, D. A.; Stöhr, J.; Rabe, J. P.; Swalen, J. D.; Rotermund, H. H. *Phys. Rev. Lett.* 1987, 59, 1321. (b) Binnig, G.; Quate, C. F.; Gerber, Ch. *Phys. Rev. Lett.* 1986, 56, 930. (c) McClelland, G. M.; Erlandsson, R.; Chiang, S. "Atomic Force Microscopy: General Principles and a New Implementation", In *Review of Progress in Quantitative Non-Destructive Evaluation*; Plenum: New York, 1987; p 1307. (d) McClelland, G. M.; Erlandsson, R.; Chiang, S.; Mate, M. *Bull. Am. Phys. Soc.* 1987, 32, 525.

(186) Hayes, M. *Surf. Technol.* 1983, 20, 3-27.

(187) Somorjai, G. A.; Bent, B. E. *Prog. Colloid Polym. Sci.* 1985, 70, 38.

(188) Pons, S.; Davidson, T. J. *Electroanal. Chem.* 1984, 160, 63-71.

(189) Porter, M. D.; Bright, T. B.; Allara, D. L.; Kuwana, T. *Anal. Chem.* 1986, 58, 2461.

(190) Aspnes, D. E.; Schwartz, G. P.; Gualtieri, J. G.; Studna, A. A.; Schwartz, B. J. *Electrochem. Soc.* 1981, 128, 590-597.

(191) Arwin, H.; Aspnes, D. *Thin Solid Films* 1986, 138, 195-207.



of ordering in thin films. Recent experiments (see earlier sections) using synchrotron radiation indicate that diffraction studies on ordered organic monolayers, although arduous, are possible. X-rays also offer other types of useful analysis. X-ray fluorescence has been used to measure concentration gradients (depth profiling) within several hundred angstroms of a liquid-gas interface,<sup>192</sup> and the extension of such studies to the gas-thin film and liquid-thin film interfaces would be quite useful. A further interesting aspect of X-ray technology is the rapid development of X-ray microscopy, which promises analytical capabilities with resolutions in hundreds of angstroms.<sup>193</sup> This capability could be useful in the microelectronics area.

An optical technique based on Raman scattering has been the subject of recent excitement in the materials science community. Although spontaneous Raman scattering has been used to characterize thin organic films and applications to even monolayer sensitivity are beginning to appear, it is virtually impossible to obtain a Raman spectrum from a sample which exhibits considerable fluorescence. Since films and interfaces often contain fluorescent impurities, monolayer level studies may in practice be severely limited by this technique. Fluorescence signals, in principle, can be removed by electronic gating techniques or by excitation at wavelengths outside the fluorescence region. Recently, it has been demonstrated<sup>194</sup> that Raman scattering measurements can be made by using near infrared lasers, such as the Nd:YAG laser with an excitation wavelength of 1.06  $\mu\text{m}$ . The photon energy is low enough that no appreciable fluorescence is excited. Correspondingly, the Raman intensity, which is approximately proportional to the fourth power of the excitation frequency, decreases by a factor of  $\sim 16$ . However, if the advantages associated with Michelson interferometry can be coupled with the excellent detectors developed over the years for IR work, it is readily possible to compensate for the lower scattering intensity. Thus, this FT-Raman technique may provide a way to study thin organic films and interfaces which have intrinsic fluorescence. A related question is whether FT-Raman can be extended to the visible region where spontaneous Raman studies are now made. If improvements in sensitivity are possible in this region, the analytical value of Raman spectroscopy would be enhanced immensely. Thus, developments in FT-Raman over the next 2-3 years warrant careful observation; the evaluation of its potential to characterize thin organic films and surfaces should be encouraged. Raman spectroscopy also has the valuable ability to analyze samples in liquids with the  $\sim 1\text{-}\mu\text{m}$  lateral resolution possible with focused beams. Both variations are now being used on bulk samples, and applications to monolayer and thin films would be of great interest.

Nondestructive analysis is generally preferable, and most methods for organic films are usually selected with this in mind. There are, nevertheless, two techniques which, although destructive, are valuable for other reasons. Secondary ion mass spectrometry (SIMS) can provide an extremely sensitive "fingerprint" of the outermost layers of a given organic surface by the mass analysis of sputtered molecular fragments. Both atomic composition and information on constituent molecular moieties can be obtained on difficult-to-analyze surfaces, such as a polymer.<sup>195</sup>

Recent developments include increased sensitivity, means for reducing total damage to the analysis area, and lateral imaging capabilities that promise to approach hundreds of angstroms.<sup>196</sup> Commercial instruments are now available, and rapid improvements promise an opportunity for interesting applications to organic films. If the kinetic energies of impinging ions on a target material are raised to the million-electronvolt range, the sputtering process becomes less important and simple nuclear elastic collisional processes occur. The technique of Rutherford back-scattering (RBS) utilizes these collisional processes to analyze quantitatively for the atomic compositions and their concentration gradients in solid samples, including organic materials, in depth to  $\sim 10^{-4}$  cm and with depth resolutions possibly less than a hundred angstroms. Applications to diffusing systems and films with compositional gradients open new possibilities.<sup>197</sup>

As mentioned under the section on optical thin-film materials, coherent nonlinear optical techniques show considerable promise for studies at the monomolecular level. One of these is a second-order nonlinear optical process known as surface second-harmonic generation (SHG). It is a highly sensitive method to investigate surfaces even at submonolayer coverages.<sup>35-40</sup> A centrosymmetric molecule which exhibits no nonlinear optical properties will do so when placed on a surface due to the breaking of symmetry. Detailed investigations that include various polarizations of the fundamental laser beam and of the second harmonic can, in principle, lead to a determination of the orientation of the surface second-order nonlinear susceptibility,  $\chi^{(2)}$ . The frequency doubling characteristics of these surface-deposited molecules can also be sampled in time, for example, at picosecond time resolution, and so provide a measure of  $\chi^{(2)}(t)$ . At present there is some, but not yet detailed, microscopic understanding of  $\chi^{(2)}$ . Several theoretical attempts to correlate the microscopic structure with the macroscopic observables are in progress. Nevertheless, SHG remains as a sensitive technique for surface structure investigation and is expected to have a growing impact on our understanding of the structure of organic thin films.

Another technique, in addition to X-ray scattering, for direct measurement of structural ordering in organic materials is neutron scattering. Applications to planar monolayers and thin films are severely hampered by the necessity of conducting analyses at large reactor facilities and by the extremely low-scattering cross sections of these film samples. The technique, nevertheless, has proven to be very powerful for polymer structure analysis, and recent work<sup>198</sup> indicates that the possibility exists to study single-monolayer organic films. An important point is that neutron scattering can be performed in the presence of liquids and that selective deuterium labeling can be used to highlight scattering from selected components in a film.

In general, all spectroscopic and diffraction analyses give information which is averaged over regions large compared to atomic scales. In contrast, scanning tunneling microscopy (STM) is a technique capable of atomic resolution at specific sites that has received considerable attention of late,<sup>48,49</sup> particularly in view of the award of the 1986

(195) Briggs, D.; Hearn, M. J.; Ratner, B. D. *Surf. Interface Anal.* 1984, 6, 184-192 and references therein.

(196) Levi-Setti, R.; Crow, G.; Wang, Y. L.; Parker, N. W.; Mittleman, R.; Hwang, D. M. *Phys. Rev. Lett.* 1985, 54, 2615-2618.

(197) Mills, P. J.; Palmstrom, C. J.; Kramer, E. J. *J. Mater. Sci.* 1986, 21, 1479-1486.

(198) Highfield, R. R. et al. *Thin Solid Films* 1983, 99, 165-72. Penfold, J.; Williams, W. G. Report #RAL-85-045, "A Pulsed Neutron Reflectometer for Surface Studies", Science and Engineering Research Council, Rutherford Appleton Laboratory, Chilton, Didcot, Oxon, U.K.

(192) Bloch, J. M.; Sansone, M.; Rondelez, F.; Peiffer, D. G.; Pincus, P.; Kim, M. W.; Eisenberger, P. M. *Phys. Rev. Lett.* 1985, 54, 1039-1042.

(193) Howells, M.; Kirz, J.; Sayre, D.; Schmahl, G. *Phys. Today* 1985, 38, 22-26.

(194) Hirschfeld, T.; Chase, B. *Appl. Spectrosc.* 1986, 40, 133-137. See also: Zimba, C. G.; Hallmark, V. M.; Swalen, J. D.; Rabolt, J. F. *Appl. Spectrosc.* 1987, 41, 721.

Table I. Some of the Functions of Proteins<sup>204-206</sup>

function	examples	tissue
structural	collagen fibrinogen	bone blood clot
motion	myosin and actin	muscle
optical properties	collagen/crystallin	cornea/lens
recognition	immunoglobulins lectins	blood plants
catalysis	enzymes	all
transport	hemoglobin (O <sub>2</sub> ) transferrin (Fe) lipoproteins (lipids)	red cells blood blood
toxicity	toxic peptides	certain snakes, snails, etc.
regulation	insulin	pancreas blood
transduction	rhodopsin (light) receptors	retina membranes

Nobel prize to Binnig and Rohrer.<sup>199,200</sup> A tunneling technique is limited to dielectric films with thickness in the 1.0–4.0-nm range because anything much thicker than that would prevent tunneling. However, this is exactly the thickness range of interest to many thin-film scientists. Numerous reports of the use of STM to study the surface structure of semiconductors and metals have already appeared in the literature, and some recent efforts have focused on the elucidation of small structures, e.g., LB films<sup>113</sup> and biological proteins<sup>114</sup> on solid surfaces. The possibility also exists for studies in liquid environments.<sup>115,201</sup> The application of STM is thus poised at the threshold of several important research areas, of which one is molecular thin films. In this particular area, questions regarding structural changes of the thin film due to the high tunneling currents between the tip and substrate must first be addressed, but it may be anticipated that as the STM is tailored for the study of thin films, this and related questions will be adequately answered. It is the consensus of this group that developments in STM over the next 3 years will make imaging of surfaces and thin organic films at the molecular level more than just a laboratory curiosity.

One of the most popular and useful analytical techniques for organic materials is NMR. However, the sensitivity of even the best commercial and research instruments is such that monolayers have signals well below instrument noise levels. The use of cryogenically cooled electronics and sensitive superconducting (SQUID) detectors may allow reduction of noise to acceptable levels for these measurements.<sup>202</sup> Dynamic nuclear polarization, where the polarization of an abundant spin can be transferred to weak or few spins of another variety, can lead to a signal enhancement and an improvement of signal-to-noise. Another obvious way to increase the signal strength is to increase the number of spins by sampling a large surface area. This has been done by using particles with a high surface area or by stacking many platelets in the probe. More imaginative approaches are clearly needed. Nevertheless, developments in the directions of reduced noise, enhanced signals, and increased sample volume could be of great help and particularly useful and necessary for observing spins in a film or monolayer.

### Conclusions

A number of points are now clear concerning molecular monolayers and thin organic films.<sup>203</sup> Their use as ordered

arrays of materials with two-dimensional characteristics will increase as we learn the relationships between the structural elements of ordered films and their macroscopic materials properties. New techniques will be required for their synthesis, assembly, and analysis. Imperfections originating in defects and impurities, which can cause a lack of durability, need to be overcome. Can films be made self-annealing or self-repairing? An understanding of the microscopic interfacial interactions will be important to the design of ideal molecular arrangements containing the desired optimal functional groups. Collective properties are the scientific and technical challenges. Can we engineer molecular structures that exhibit new and interesting effects that are much greater or more specific than those of the individual components? Can we make a multimolecular template to sense or detect particular species?

At the present we do not know the answers to these questions. We nevertheless know enough to see clearly the potential of thin molecular films in exciting new applications. Therefore, we recommend that a concerted research effort be directed toward the discovery of new systems, better film preparation methods (with a particular emphasis on the collective behavior), and newer and better methods for their characterization. An understanding of the intermolecular forces, involving mechanical, electronic, chemical, and biological processes, will be the key to progress.

**Acknowledgment.** We thank the Department of Energy for supporting this study. In particular we wish to thank Dr. C. Peter Flynn, Chairman of the Materials Sciences Council, for initiating, supporting and encouraging us. His careful reading of the report and suggesting a number of useful changes and modifications are appreciated. We also appreciate the comments by Drs. Iran Thomas (DOE), Philip Pincus, and Mark Cardillo, of the council, who attended our meeting and offered much guidance.

### Appendix. Biomacromolecules: Mainly Proteins

Nature uses biomacromolecules for a wide range of functions, and the composition and structure of these systems have been optimized over 2 billion years of evolution. The major classes of biomacromolecules are proteins, polysaccharides, and polynucleic acids and also lipid aggregates, such as membranes and vesicles.<sup>204</sup> Various combinations are possible, including lipoproteins (lipid-protein aggregates), glycoproteins (proteins containing oligosaccharide or even polysaccharide components), and others. Polysaccharides perform important mechanical, physical, biochemical, and related functions. Polynucleic acids (DNA and RNA) are key information storage and transfer molecules. Here, due to space and time constraints, we will discuss only proteins.

Proteins are complex copolymers of highly specific sequences consisting of some 20 different amino acids and having molecular weights covering the range of roughly 10<sup>4</sup>–10<sup>6</sup>. A specific protein generally has one or more specific functions and is clearly molecularly engineered to carry out those functions in an efficient, specific, and often unique manner. Table I lists some of the functions of proteins and gives representative examples. Most of these

(199) Binnig, G.; Rohrer, H. *Helv. Phys. Acta* 1982, 55, 726.

(200) Binnig, G.; Rohrer, H. *IBM J. Res. Dev.* 1986, 30, 355.

(201) Hansma, P. K. *IBM J. Res. Dev.* 1986, 40, 370.

(202) Freeman, M. R.; Germain, R. S.; Richardson, R. C.; Roukes, M. L.; Gallagher, W. J.; Ketchen, M. B. *Appl. Phys. Lett.* 1986, 48, 300–302.

(203) The reader is referred to a forthcoming report of an NSF workshop in "The Molecular Engineering of Ultrathin Films: State of the Art and Research Needs"; Stroev, P., Franses, E. I., Eds. (to be published in *Thin Solid Films*).

(204) Stryer, L. *Biochemistry* 1985, 24.

(205) Holzmüller, W. *Information in Biological Systems: The Role of Macromolecules*; Cambridge University Press: Cambridge, 1984.



functions and applications, are discussed briefly in any basic biochemistry textbook.<sup>204</sup>

The primary structure of a protein is its amino acid sequence, which constitutes the primary information and basically controls all properties and functions of the molecule. A secondary level of structure includes associations which result in helix, sheet, and other structures. Globular proteins generally have a complex tertiary structure, which can be directly determined by X-ray diffraction.<sup>206</sup> Finally, two or more polypeptide chains can associate via their tertiary structures to form a quaternary structure. Nearly 200 proteins have been crystallized and their tertiary and/or quaternary structures determined.<sup>207</sup> The atomic coordinates are readily available and can be viewed by using modern molecular graphics on standard computers and via readily available software.

Certain proteins can dimerize and even self-assemble. For example, insulin readily dimerizes and at higher concentrations will form hexamers. Hemoglobin commonly exists as the tetramer. Albumin readily dimerizes and forms higher order oligomers. Fibrinogen, upon the action of the activating proteolytic enzyme thrombin, self-associates and polymerizes to form the fibrin network of blood clotting.<sup>209</sup> Tubulin self-assembles to form the microtubules found within most cells.<sup>210</sup> Actin self-associates and

assembles to form a variety of structures.

The tertiary and quaternary structures of proteins are stabilized by hydrophobic, ionic, and hydrogen-bonding interactions. However, for many proteins, the "native" state is only marginally stable, and the protein can be easily "denatured", i.e., lose part of its biological activity.<sup>211</sup> Proteins are now generally recognized to be dynamic, flexible structures of marginal stability. Changes in pH, temperature, ionic strength, or solute environment can often change the conformation (three-dimensional structure) of a protein. Although there is much activity in trying to predict the tertiary and quaternary structure of proteins from their primary amino acid sequences, the predictions are not usually very good.<sup>207,212</sup> This is partly because many states are only marginally different in overall free energy, so the "true" equilibrium or native state is difficult to find. It is also because intermolecular force functions in ionic solutions are not well understood, including the classical hydrophobic and electrostatic interactions. The interaction potential functions which are available, however, can be incorporated into computer graphics algorithms to yield three-dimensional images of the constituent atoms and their interaction fields, permitting "docking" or interaction studies between two proteins, between a protein and a surface, between an enzyme and its substrate, etc. And through these visual representations, many of the details leading to stable structures are becoming clearer.

(206) Schulz, G. E.; Schirmer, R. H. *Principles of Protein Structure*; Springer-Verlag: New York, 1979.

(207) The Protein Data Bank, Brookhaven National Laboratory.

(208) See, for example: *J. Mol. Graphics*; Molecular Graphics Society, Butterworths: Stoneham, MA.

(209) Doolittle, R. F. *Sci. Amer.* 1981, Dec., 126.

(210) Weber, K.; Osborn, M. *Sci. Amer.* 1985, Oct., 110.

(211) Pace, C. N. *CRC Crit. Rev. Biochem.* 1976, 3, 1.

(212) Wetlaufer, D. B. *The Protein Folding Problem*; AAAS Selected Symposium 89; Amer. Assoc. Adv. Sci.: Washington, D.C., 1984.